Molecular mechanisms of autophagy and the effect of autophagy dysfunction on mitochondrial function

Elsje Gesina (Gisela) Otten

Doctor of Philosophy

Campus for Ageing and Vitality

Institute for Cell and Molecular Biosciences

Newcastle University

December 2017

ABSTRACT

Long lifespan of evolutionary higher organisms including humans is associated with the challenge to maintain viability of post mitotic cells, such as neurons, for decades. Autophagy is increasingly recognized as an important prosurvival pathway in oxidative and proteotoxic stress conditions. Autophagy degrades cytosolic macromolecules in response to starvation and is involved in the selective degradation of damaged/toxic organelles, such as mitochondria. With age autophagy function declines, and is also compromised in several neurodegenerative diseases. We identified a novel role for autophagy in the maintenance of mitochondrial health, specifically respiratory complex I. Intriguingly, galactose-induced cell death of autophagy deficient cells was rescued by preventing ROS production at complex I or bypassing complex I-linked respiration. We propose that aberrant ROS production via complex I in response to autophagy deficiency could be pathogenic and result in neurodegeneration and preventing this could be an interesting therapeutic target.

Furthermore, we found that vertebrates have evolved mechanisms to induce autophagy in response to oxidative stress. This involves the oxidation of the autophagy receptor p62, which promotes autophagy flux and the clearance of autophagy cargo, resulting in increased stress resistance in mammalian cells and survival under stress in flies. In addition, we obtained data revealing an important role for redox-regulated cysteines in NDP52 for the degradation of mitochondria via mitophagy and tools were created to study the role of other autophagy receptors in autophagy initiation and selective autophagy.

ACKNOWLEDGEMENTS

First of all a big thanks to the Biotechnology and Biological Sciences Research Council for funding this project.

I would like to thank everyone who has supported me during my four year period at Newcastle University, starting with my two supervisors. Dr. Viktor Korolchuk has been an amazing supervisor and mentor, who was always available for questions and discussing science. Thanks for your continued support and encouragement and for giving me all the fantastic opportunities during the 4 years in your lab, such as going to two conferences in the USA and a lab visit to Monash University in Melbourne. Also thanks to my second supervisor Dr. Elizabeth Veal for sharing your knowledge about redox signalling and reading my thesis. Unfortunately, we haven't met up as much as we should have, but every time was a pleasure! Your excitement about science is contagious!

I also want to thank everyone from the lab, starting with Diego Manni, it was great to work closely with you on the p62 project. I enjoyed it and I think we were a great team. Also thanks to Lucy and Yoana for contributing to the complex I and NDP52 projects and being fun lab mates! Special thanks for Berni, for helping me out in the lab a lot, and for having me live with you the last year! I hope you've not regretted saying yes to that. Of course, I can't forget Alvaro for having drinks with me and discussing life and Graeme, Rhys and James, who helped me adjust to the British culture when I just arrived to Newcastle and Wouter Huiting for giving me a nice experience in supervising students and celebrating sinterklaas with me.

I also want to thank everyone else who contributed to my projects: Rhoda Stefanatos, Satomi Miwa, Amy Reeve, Diana Jurk, Graham Smith, Glyn Nelson, Agnieszka Bronowska, Joao Passos, Alberto Sanz and Michael Lazarou.

Finally, I want to thank all my Dutch friends, of which many came to visit, which means a lot to me! And the biggest thanks goes to my family, pa & ma, Arjan, Bram and Mannie. I love you and without you I could not have done this!

TABLE OF CONTENTS

LIST OF FIGURES

LIST OF TABLES

LIST OF ABBREVIATIONS

Abbreviation	Explanation
ABIN	A20-Binding Inhibitor of NF-Kβ
AD	Alzheimer's disease
AFG3L2	ATPase Family Gene 3-Like 2
Akt	Protein Kinase B
Alfy	Autophagy-Linked FYVE protein
ALS	Amyotrophic Lateral Sclerosis
AMPK	5' Adenosine Monophosphate-activated Protein Kinase
AO	Antimycin A and oligomycin
aPKC	atypical protein kinase C
APOE	Apolipoprotein E
ASK1	Apoptosis Signalling Kinase 1
ATF5	Activating Transcription Factor 5
ATFS-1	Activating Transcription Factor associated with Stress 1
ATG	autophagy-related genes
Aβ	Amyloid peptide β
β-mE	β-mercaptoethanol
C	Cysteine
C9ORF72	Chromosome 9 Open Reading Frame 72
CASTOR1	Cytosolic arginine sensor for mTORC1 subunit 1
CC	Coiled Coil
CCCH	CysCysCysHis
CHCHD10	Coiled-coil-Helix-Coiled-coil-Helix Domain containing 10
CHMP2B	CHarged Multivesicular body Protein 2B
CHOP	C/EBP-HOmologous Protein
CO2	Carbon diOxide
Complex I	NADH:ubiquinone oxidoreductase
Complex II	Succinate dehydrogenase
Complex III	Cytochrome C oxidoreductase
Complex IV	Cytochrome C oxidase
Complex V	ATP synthase
CoQ	Ubiquinone
COX	Cytochrome C OXidase

CRISPR	Clustered Regularly Interspaced Short Palindromic Repeats
Dcp2	Decapping mRNA 2
DEPTOR	DEP domain containing mTOR-interacting protein
DFCP1	Double FYVE-Containing Protein 1
DLB	Dementia with Lewy Bodies
DLC	Disulphide-Linked Conjugates
DMSO	DiMethyl SulfOxide
DUBs	DeUBiquitylases
Dve1	Defective proVEntriculus in Drosophila
ER	endoplasmic reticulum
ERR-α	Estrogen-Related Receptor α
ETC	Electron Transport Chain
FACS	Fluorescence-Activated Cell Sorting
FADH2	reduced Flavin Adenine Dinucleotide
fALS	Familial ALS
FCCP	Carbonyl Cyanide-4-(triFluoromethoxy)Phenylhydrazone
FIP200	FAK family kinase Interacting Protein of 200 kDa
FMN	Flavin MonoNucleotide
FTD	FrontoTemporal Dementia
FTDP-17	FrontoTemporal Dementia with Parkinsonism-17
FTLD	FrontoTemporal Lobar Degeneration
FUS	FUsed in Sarcoma
GABARAP	γ-AminoButyric Acid Receptor-Associated Protein
GAP	GTPase Activating Protein
Gate-16	Golgi-associated ATPase Enhancer of 16 kDa
GBA	Glucosylceramidase β
GFP	Green Fluorescent Protein
GLUT	GLUcose Transporter
GR	Glutathione Reductase
GRN	proGRaNulin
GSH	Glutathione
H2O2	Hydrogen peroxide
HK2	HexoKinase2
HO-1	Heme Oxygenase 1
HOPS	HOmotypic fusion and Protein Sorting

Hsp	Heat Shock Protein
HTRA2	HTrA serine peptidase 2
HUWE1	HECT, UBA and WWE domain containing 1
IMM	Inner Mitochondrial Membrane
IMS	Inter Membrane Space
INPP5E	INositol Polyphosphate 5-Phosphatase
JNK	c-Jun N-terminal Kinase
K	Lysine
LC3	Microtubule-associated protein 1A/1B-Light Chain 3
LDHA	Lactate DeHydrogenase A
LIR	LC3-binding motifs
LRRK2	Leucine Rich Repeat Kinase 2
LRSAM1	Leucine rich Repeat and Sterile Alpha Motif containing 1
LZ	Leucine-zipper
M	Methionine
MAD	Mitochondrial-Associated Degradation
MAGIC	Mitochondria As Guardian In Cytosol
MAPT	Microtubule-Associated Protein Tau
MEFs	Mouse Embryonic Fibroblasts
MEK5	MAPK/ERK kinase 5
MEKK3	MAPK kinase kinase 3
mES	Mouse Embryonic Stem cells
Mfn	MitoFusin
mLST8	TOR complex subunit LST8 (lethal with SEC13 protein 8)
mtDNA	Mitochondrial DNA
mTORC1	mammalian Target Of Rapamycin Complex 1
NADH	reduced Nicotinamide Adenine Dinucleotide
NBR1	Neighbor Of BRCA1 gene 1 protein
NDP52	nuclear dot protein 52 kDa
NEMO	NF-Kβ Essential Modulator
NF-Kβ	Nuclear Factor kappa-light-chain-enhancer of activated B cells signalling
NOXs	NADPH OXidases
Nrf1	Nuclear Respiratory Factor 1
Nrf2	Nuclear factor (erythroid-devided2)-like 2

OMM	Outer Mitochondrial Membrane
OPTN	optineurin
OXPHOS	OXidative PHOSphorylation
PARIS	PARkin Interacting Substrate
PARL	Presenilins-Associated Rhobiod Like
PAS	phagophore assembly site
PB1	Phox and Bem1
PDB	Paget's Disease of Bone
Pdk1	Pyruvate Dehydrogenase Kinase 1
PE	PhosphatidylEthanolamine
PGAM5	PhosphoGlycerate Mutase family member 5
PGC1	PPARγ (Peroxisome Proliferator-Activated Receptor-γ) Coactivator-1
PI(3,5)P2	Phosphatidylinositol 3,5-bisphosphate
PI3K	Phosphoinositide 3 Kinase
PINK1	PTEN-INduced putative Kinase 1
PKM	Pyruvate Kinase isozyme M
PKR	Protein Kinase R
PLAA	PhosphoLipase A2 Activating protein
PLEKHM1	PLEcKstrin Homology domain containing protein family Member 1
PML	ProMyelocytic Leukaemia
POAG	Primary Open-Angle Glaucoma
POLMRT	Mitochondrial RNA POLymerase
polyQ	Poly-glutamine
PQ	ParaQuat
PRAS40	Proline-Rich Akt Substrate of 40 kDa
Prxs	Peroxiredoxins
PTEN	Phosphatase and TENsin homolog
RA	Retinoic Acid
RCR	Respiratory Control Ratio
Ref(2)P	Refractory to sigma P
RET	Reverse Electron Transport
Rheb	Ras homolog enriched in brain
ROS	Reactive Oxygen Species
S6K1	p70-S6 Kinase 1
sALS	Sporadic ALS

SatB2	Special AT-rich sequence-Binding protein 2
SCARB2	Scavenger Receptor Class B member 2
SFM	Serum Free Medium
SILAC	Stable Isotope Labeling by Amino acids in Cell culture
SKN-1	SKiNhead-1, homolog of Nrf2
SLC38A9	Solute Carrier Family 38 Member 9
SNARE	Soluble NSF Attachment protein Receptor
SNCA	α-SyNuClein
SOD	SuperOxide Dismutase
-SOH	Sulfenic acid
STAT3	Signal Transducer and Activator of Transcription 3
TAFB2M	Mitochondrial Transcription Factor B2
TAX1BP1	Tax1 Binding Protein 1
TBK1	TANK1 Binding Kinase 1
TCA	TriCarboxylic Acid cycle
TDP-43	TAR DNA-binding Protein 43
TFAM	Mitochondrial Transcription Factor A
TFEB	Transcription Factor EB
TRAF6	TNF Receptor Associated Factor 6
Trx	Thioredoxin
TSC	Tuberous Sclerosis Complex
Ub	Ubiquitin
UBA	Ubiquitin associated
UBAN	UBD in Abin proteins and NEMO
UBDs	Ubiquitin binding domains
Ubl5	UBiquitin-Like protein 5
UBZ	ubiquitin-binding ZnF
ULK1/2	Unc-51 Like autophagy activating Kinase 1/2
UPRam	UPR Activated by protein Mistargeting
UPRer	ER Unfolded Protein Response
UPS	Ubiquitin-Proteasome System
USP	Ubiquitin-Specific Protease
UVRAG	UV Radiation Resistance Associated Gene protein
Vps	Vacuolar Protein Sorting
WIPIs	WD repeat domain phosphoinositide-interacting proteins

WT	Wild Type
YFP	Yellow Fluorescent Protein
Z-VAD-FMK	Pan-caspase inhibitor
Δψm	Mitochondrial membrane potential

1 CHAPTER 1: INTRODUCTION

1.1 Autophagy

Autophagy is a broad term referring to different pathways for bulk degradation of cytosolic components and organelles. Three types of autophagy are known: chaperone mediated autophagy, microautophagy and macroautophagy. In chaperone mediated autophagy a chaperone protein binds first to its cytosolic target substrate and then to a receptor on the lysosomal membrane where the unfolding of the protein occurs. The unfolded cytosolic target protein is then translocated directly into the lysosome for its degradation (Massey et al., 2004). Microautophagy translocates cytoplasmic materials into the lysosome or vacuole for degradation by either direct invagination, protrusion, or septation of the lysosomal or vacuolar membrane (Mijaljica et al., 2011). Finally, macroautophagy is characterised by the formation of a cytosolic double-membrane vesicle, the autophagosome. During macroautophagy, cytoplasmic proteins, organelles or other materials are surrounded by phagophores, which expand and close to form autophagosomes. These autophagosomes fuse with lysosomes (or vacuoles) to form autolysosomes, in which the cytoplasmic cargos are degraded by resident hydrolases. The resulting degradation products are then transported back into the cytosol for reuse through the activity of membrane permeases (Figure 1.1) (Klionsky, 2007). Macroautophagy is the most widely studied and best characterised process and is commonly referred to as autophagy (this term will also be used hereafter). Autophagy is orchestrated by a set of autophagy-related (*ATG*) genes, which were originally discovered in yeast, and are conserved in mammals (Inoue and Klionsky, 2010).

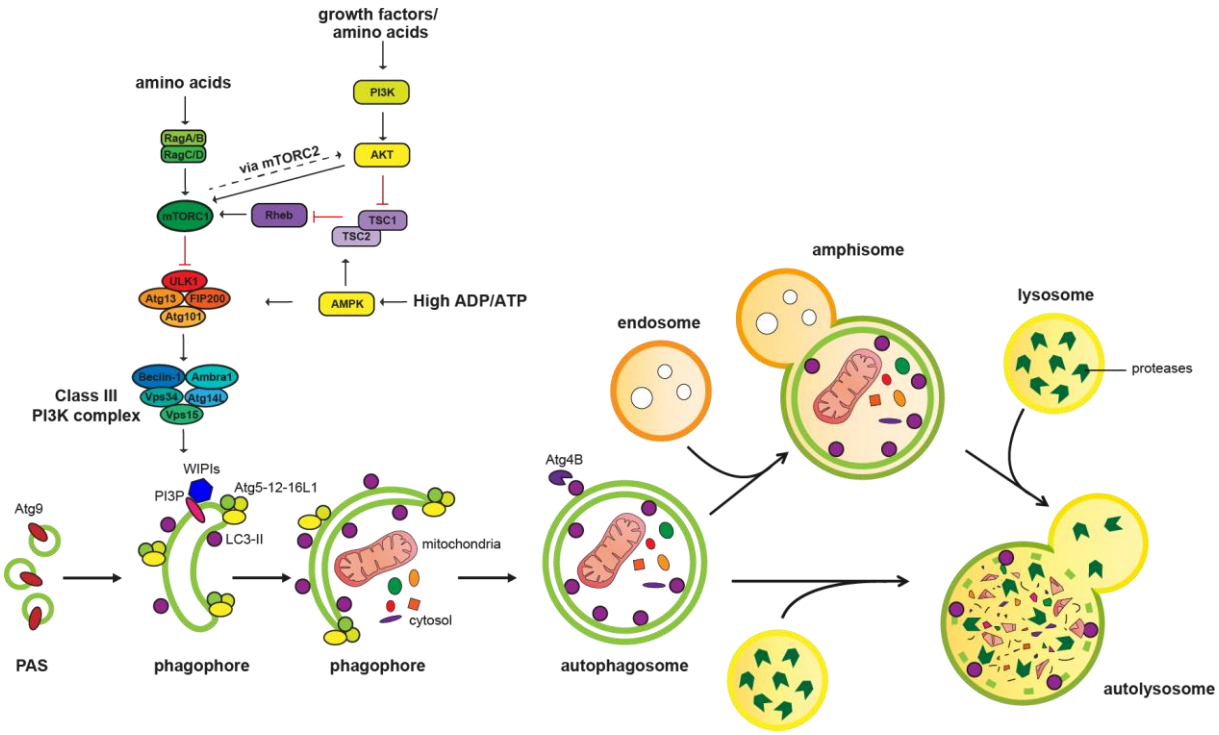

Figure 1 Diagram of the bulk autophagy pathway.

Deprivation of growth promoting stimuli (such as amino acids, growth factors and ATP) activate autophagy via mTORC1 (mammalian Target Of Rapamycin Complex 1) and the ULK1 (Unc-51-Like autophagy activating Kinase 1) complex, which regulate autophagosome biogenesis. The formation of an autophagosome starts with the recruitment of Atg9 positive vesicles to the PAS (Pre-Autophagosomal Structure) and the formation of a phagophore, which surrounds cytosolic cargo. The local production of PI3P (Phosphoinositol 3-Phosphate) by the class III PI3K (Phosphoinositide 3-Kinase) complex promotes the formation of the autophagosomal membrane and the LC3 (Microtubule-associated protein 1A/1B-Light Chain 3) and Atg12-Atg5-Atg16L1 ubiquitin-like conjugation systems is important for elongation of the phagophore. The formed autophagosome matures by fusing with endosomes to form the amphisome and with the lysosome to form the autolysosome. The sequestered cargo is degraded by the lysosomal proteases and recycled.

1.1.1 Autophagy initiation

Autophagosomes are double-membraned vesicles that sequester cytosolic proteins and organelles for lysosomal degradation. Different membrane sources have been proposed to be the origin of the autophagosomal membrane, of which the ER-mitochondrial contact site seems to be one of the main origins of the phagophore, followed by further expansion using membranes from the plasma membrane, endoplasmic reticulum (ER), recycling endosomes, mitochondria and the ER-Golgi intermediate compartment (Lamb et al., 2013, Bento et al., 2016, Yla-Anttila et al., 2009, Hailey et al., 2010, Hamasaki et al., 2013, Ge and Schekman, 2014, Hayashi-Nishino et al., 2009).

Autophagosome biogenesis is initiated by the recruitment of the mATG9 (mammalian Atg9) positive vesicles to the PAS (phagophore assembly site) and the formation of a phagophore (Mari et al., 2010). In yeast, the transmembrane protein Atg9 is a substrate of the kinase Atg1 (mammalian ULK1/2), and in yeast its phosphorylation is essential for the recruitment of Atg18 (mammalian WIPI-1, 2, 3, 4, WD repeat domain phosphoinositide-interacting proteins) and Atg8 (mammalian LC3A, B, C; GABARAPs; Gate-16). Upon autophagy induction, Atg1 and Atg13 assemble with tetrameric Atg17 (mammalian FIP200, FAK family kinase Interacting Protein of 200 kDa) into a complex and this complex promotes the binding of Atg9 to Atg17, which is the first scaffolding protein to arrive at the PAS and was found to have membrane tethering activity (Papinski et al., 2014, Rao et al., 2016, Suzuki et al., 2015).

In mammals, the ULK1 (Unc-51 Like autophagy activating Kinase 1) complex, consisting of the kinase ULK1 (or the orthologue ULK2, which has a redundant function (Lee and Tournier, 2011)), the scaffold FIP200, ATG13 and Atg101 transduces the upstream signals from mTORC1 (mammalian Target Of Rapamycin Complex 1) and AMPK (5' Adenosine Monophosphate-activated Protein Kinase) to initiate autophagy by phosphorylating Beclin1 and Atg14L, which are part of the class III PI3K (PI3 Kinase) complex (Figure 1) (Russell et al., 2013, Park et al., 2016). This complex consists of Beclin 1, the PI (phosphatidylinositol) kinase Vps34 (vacuolar protein sorting 34), Vps15 and Atg14L (Park et al., 2016) and promotes the local production of PI3P (phosphatidylinositol 3-phosphate), thereby promoting the formation of the autophagosomal membrane (Papinski and Kraft, 2016). The PI3P rich membrane patches recruit PI3P-binding proteins, such as WIPI family members and DFCP1 (Double FYVE-Containing Protein 1) (Axe et al., 2008) (Figure 1). Recently, it was shown that WIPI2 interacts with Atg16L1 and recruits the Atg12-Atg5-Atg16L1 to the phagophore (Dooley et al., 2014).

1.1.2 The two ubiquitin-like conjugation systems

The elongation of the phagophore is coordinated by two ubiquitin-like conjugation systems, consisting of an E1-like activating enzyme, an E2-like conjugating enzyme and an E3-like ligase. The first conjugation system involves a group of ubiquitin-like proteins from the mammalian Atg8-like family. The Atg8 family can be subdivided in three families; the LC3 (Microtubule-associated protein 1A/1B-Light Chain 3), GABARAP (γ-aminobutyric acid receptor-associated protein) and GATE-16 (Golgi-associated ATPase enhancer of 16 kDa) family. These ubiquitin-like proteins can be

modified with the lipid PE (phosphatidylethanolamine) and thus exists in two forms, a soluble and membrane bound form (for example LC3-I and II, respectively), of which the membrane bound form can be incorporated into the phagophore- and autophagosomal membrane (Kabeya et al., 2000, Kabeya et al., 2004). For example proLC3, in order to be lipidated needs to be modified by Atg4B to become LC3-I, this is followed by a reaction with Atg7 and the E2-like enzyme Atg3 (Tanida et al., 2004), resulting in the conjugation of LC3-I with PE to form LC3-II (Figure 2) (Kabeya et al., 2000). In mammals, LC3B is the most prevalent form and often used as a marker for autophagosomes. LC3 is mainly cytosolic and nuclear localised, and recently it was found that upon starvation LC3 is redistributed from the nucleus to the cytosol. This redistribution requires deacetylation of LC3 by Sirtuin 1, which promotes the interaction with the nuclear protein DOR and the cytosolic protein Atg7. DOR shuttles LC3 out of the nucleus to the cytosol, where LC3 is able to bind Atg7 (Huang et al., 2015).

The other ubiquitin-like conjugation system involves the E1-like enzyme Atg7 and the E2-like enzyme Atg10, which conjugate the ubiquitin-like protein Atg12 to Atg5. This conjugate then forms a complex with Atg16L1, which acts as an E3-like ligase that promotes the elongation of the phagophore by recruiting Atg3, which is essential for LC3 lipidation (Figure 2) (Hanada et al., 2007). During the entire autophagy cycle, LC3-II remains on the inner autophagosomal membrane, and eventually is degraded in the autolysosome by the lysosomal hydrolases. The LC3-II that is present at the outer membrane is removed by Atg4B (Nakatogawa et al., 2012). On the contrary, as soon as formation of the autophagosome is completed, Atg12-Atg5-Atg16L1 complex is removed from the autophagosomal membrane. Deletion of the essential autophagy gene Atg5 results in a block in autophagy and therefore is often used to model autophagy-deficient conditions (Komatsu et al., 2005, Mizushima et al., 2001).

Till very recently it was thought that the Atg8 family is required for the formation and elongation of autophagosomes and the recruitment of autophagy receptors and their cargo, however Nguyen *et al*. showed that in cells in which all three LC3 isoforms and the three GABARAP isoforms were knocked out, autophagosomes were still formed, (Nguyen et al., 2016b). They convincingly showed that instead of being important for autophagosome formation, the Atg8 proteins have a crucial role in the fusion of autophagosomes with lysosomes. Their results were confirmed in another study where knockout of Atg3, Atg5 and Atg7 blocking conjugation of PE to Atg8 proteins does not prevent formation of autophagosomes (Tsuboyama et al., 2016) (Figure 2).

Another surprising finding was that mitochondria still recruit to the autophagosome in cells lacking the 6 Atg8 proteins, showing that Atg8 family members are not essential for this process either and other proteins can provide a link between the cargo and the autophagosome (Nguyen et al., 2016b).

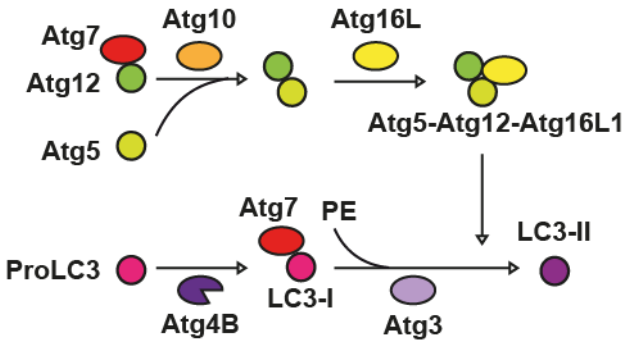

Figure 2 Diagram of the two ubiquitin-like conjugation systems in autophagy.

First Atg4B cleaves ProLC3 to form LC3-I, which reacts with Atg7 and Atg3, resulting in the conjugation to PE (phosphatidylethanolamine) to form LC3-II. Atg7 and Atg10 conjugate Atg12 to Atg5, which forms a complex with Atg16L1. This complex recruits Atg3 to the phagophore and thereby promotes LC3-I lipidation.

1.1.3 Autophagosome maturation

The final step of autophagosome biogenesis is the maturation step, which involves the fusion with endosomes and lysosomes to form amphisomes and autolysosomes respectively. Generally, autophagosomes fuse with endosomes before the final maturation into autolysosomes (Filimonenko et al., 2007). These steps involve several vesicle fusion events, which are mediated by different proteins, such as Rab GTPases, membrane-tethering factors and cytoskeleton-related proteins. The timing of the fusion with lysosomes is of essential importance, for the autophagosome has to be closed. The actual closure of autophagosomes is poorly understood, potentially Atg2A and Atg2B are implicated in this process, because knock-down of these proteins result in the accumulation of unclosed autophagosomes (Velikkakath et al., 2012). At the moment it is not completely clear how the fusion machinery recognises a closed autophagosome. Removal of LC3-II from the outer autophagosomal membrane by Atg4B has been suggested to be a signal (Kirisako et al., 2000). When autophagosomes are closed, using actin filaments and microtubules they move towards the perinuclear region, where the lysosomes reside and there fusion can take place (Fass et al., 2006, Jahreiss et al., 2008, Monastyrska et al., 2009). The Vps34 complex containing UVRAG (UV Radiation Resistance Associated Gene protein) and

Atg14L is directly associated with autophagosome maturation (Zhong et al., 2009, Di Bartolomeo et al., 2010), whilst binding of Rubicon to this complex negatively regulates maturation (Zhong et al., 2009, Kang et al., 2011).

Membrane tethering factors facilitate the docking and fusion process by acting as a bridge between two different membranes. The HOPS (homotypic fusion and protein sorting) complex, consisting of Vps11, Vps6, Vps18, Vps33A, Vps39 and Vps41, via its interaction with the autophagosomal SNARE (Soluble NSF Attachment protein) Receptor) syntaxin 17, promotes the autophagosome-lysosome fusion, together with the GTPase Rab7 (Huotari and Helenius, 2011, Jager et al., 2004, Hyttinen et al., 2013). LC3 recruits PLEKHM1 (Pleckstrin homology domain containing protein family member 1) to the autophagosome, where it interacts with the HOPS complex and Rab7 (Nguyen et al., 2016b, McEwan et al., 2015). PLEKHM1 was suggested to function as an endolysosomal adapter platform that functions in the final maturation of autophagosomes and also mediates autophagosome-lysosome fusion (McEwan and Dikic, 2015, McEwan et al., 2015).

Recently it was shown that lipids also play and essential role in governing autophagosome maturation. It was found that the inositol polyphosphate 5-phosphatase INPP5E regulates the fusion of autophagosomes with lysosomes. At the lysosomes, INPP5E dephosphorylates PI(3,5)P_2 (Phosphatidylinositol 3,5-bisphosphate), which competes with actin filaments for cortactin binding. By decreasing the PI(3,5)P_2 levels, INPP5E promotes actin polymerisation at the lysosome, which allows autophagosome-lysosomes fusion (Hasegawa et al., 2016, Li et al., 2016).

Finally, different membrane anchored snares have been linked to autophagosome maturation, which are reviewed in (Wang et al., 2016d). After this step, the autophagosomal cargo can be degraded by lysosomal hydrolases.

1.1.4 Autophagy regulation via mTORC1 signalling

Autophagy can be highly up-regulated under starvation and is mostly considered nonspecific, thus degrading proteins and other cytosolic macromolecular components that are not specifically targeted for degradation. The nutrient sensor mTORC1, which was first discovered in yeast and later in flies, is one of the key upstream autophagy signalling pathways (Noda and Ohsumi, 1998, Scott et al., 2004). The key mTOR

protein exists in two multimeric complexes, mTORC1 and mTORC2, of which mTORC1 regulates autophagy initiation. The mTORC1 complex consists of 5 subunits, including the scaffold raptor (regulatory associated protein of mTOR), the kinase inhibitors DEPTOR (DEP domain containing mTOR-interacting protein), PRAS40 (Proline-Rich Akt Substrate of 40 kDa), mLST8 (mTOR complex subunit LST8 (Lethal with SEC13 protein 8)) and the protein kinase mTOR (Laplante et al., 2012). mTORC1 integrates a wide variety of anabolic and catabolic signals, such as growth factors, nutrients (amino acids), cellular energy (high AMP/ATP ratio) and oxygen levels to control protein, nucleotide, lipid synthesis, lysosome biogenesis and autophagy (Goberdhan et al., 2016). Growth factor signalling through PI3K and Akt (Protein Kinase B) mainly signal via the TSC (Tuberous Sclerosis Complex)-Rheb (Ras homolog enriched in brain) signalling axis to activate mTORC1 (Petiot et al., 2000, Cantley, 2002, Inoki et al., 2002). Amino acids, mainly leucine, but also arginine, glutamine and serine, regulate mTORC1 activity via different mechanisms. Recently different proteins were identified to be specific amino acids sensors; Sestrin2 as a leucine sensor (Saxton et al., 2016); SLC38A9 (SoLute Carrier family 38 member 9) as a putative arginine sensor (Wang et al., 2015); CASTOR1 (Cytosolic Arginine Sensor for mTORC1 subunit 1) as an arginine sensor (Chantranupong et al., 2016). Arginine was also shown to be able to regulate mTORC1 via the TSC complex (Carroll et al., 2016). The TSC2 subunit of this complex acts as a GAP (GTPase Activating Protein) on the small GTPase Rheb, promoting the hydrolysis of GTP to GDP, resulting in mTORC1 inhibition (Zhang et al., 2003). Finally, low cellular energy levels (low AMP/ATP ratio) can be sensed by AMPK, which negatively regulates mTORC1, but also can promote autophagy directly via the ULK1 and Beclin 1 phosphorylation (Kim et al., 2011, Zhang et al., 2016).

Active mTORC1 results in the phosphorylation of the downstream translation regulators S6K1 (p70-S6 Kinase 1), eIF4E (eukaryotic Initiation Factor 4E) and 4E-BP1 (4E-Binding Protein 1) (Laplante and Sabatini, 2012). In addition to regulation of protein synthesis, mTORC1 regulates autophagy via several mechanisms. Firstly, activated mTORC1 can interact with the ULK1-Atg13-FIP200 complex and phosphorylate ULK1 and Atg13, thereby inhibiting autophagy at an early stage (Hosokawa et al., 2009, Jung et al., 2009, Ganley et al., 2009). Secondly, recently UVRAG was identified as a mTORC1 substrate, its phosphorylation negatively regulates autophagy at a later stage by affecting autophagosome and endosome

maturation (Kim et al., 2016). Thirdly, mTORC1 negatively regulates autophagy at the transcriptional level by phosphorylating TFEB (Transcription Factor EB), which prevents its translocation to the nucleus and inhibits the transcription of autophagy and lysosomal related genes (Martina et al., 2012). Finally, mTOR can regulate autophagy at the post-transcriptional level via Dcp2 (Decapping mRNA 2). In nutrient rich conditions, mTOR phosphorylates Dcp2, allowing the degradation of autophagy related mRNA transcripts (Hu et al., 2015). These different pathways identified to date regulate the autophagy signals downstream of mTORC1.

1.1.5 Autophagy regulation by reactive oxygen species (ROS)

In addition to starvation, several other stressors can activate autophagy. For example, ROS has been shown to modulate autophagy. At high levels ROS are detrimental for the cell, but lower levels have been shown to act as signalling molecules. For example, ROS has been shown to increase Beclin1 expression (Chen et al., 2008), as well as p62 expression via the Nrf2 (Nuclear factor (erythroid-devided2)-like 2) antioxidant pathway (Jain et al., 2010). Also ROS can impinge on the mTOR signalling pathway and thereby indirectly modulate autophagy (Yoshida et al., 2011, Alexander et al., 2010). A more direct regulation of autophagy by ROS was demonstrated by a direct redox regulation of ATG4. It was shown that hydrogen peroxide inactivates ATG4 by oxidising a catalytic cysteine, resulting in the promotion of LC3 lipidation (Scherz-Shouval et al., 2007). So far, ATG4 is the only direct ROS substrate identified in the autophagy pathway and as ROS accumulate with age and in age-related diseases, it would be interesting to investigate if there are more direct targets in the autophagy machinery that can be redox regulated.

1.2 Selective autophagy

In addition to bulk autophagy degradation, selective forms of autophagy have recently been described. Selective autophagy is commonly associated with its housekeeping roles in the maintenance of cellular homeostasis. An important role of selective autophagy is evident in the context of many neurodegenerative diseases for the clearance of aggregate-prone proteins (aggrephagy) and selective degradation of organelles, for example mitochondria (mitophagy). Other targets of selective autophagy include peroxisomes (pexophagy), ER (reticulophagy), ribosomes (ribophagy), bacteria (xenophagy), viruses (virophagy) and nuclear envelope (nucleophagy (Bjorkoy et al., 2005, Kim et al., 2008, Novak and Dikic, 2011, Geisler et al., 2010, Zheng et al., 2009, Orvedahl et al., 2010, Bernales et al., 2006, Mochida et

al., 2015). Growing evidence suggests that adaptor proteins, such as p62, OPTN (optineurin), NDP52 (Nuclear Dot Protein 52 kDa), TAX1BP1 (TAX1 Binding Protein 1) and NBR1 (Neighbor Of BRCA1 gene 1 protein) act as shuttle proteins that transport ubiquitinated proteins to the autophagosome via interactions with both ubiquitin and the autophagic component LC3-II (Johansen and Lamark, 2011, Lazarou et al., 2015).

1.2.1 Ubiquitin as a degradation signal for selective autophagy

Ubiquitin (Ub) has a major role in selective autophagy, as unwanted or aberrantly folded proteins are tagged with Ub signals and are recognised by autophagy receptors. Ubiquitinated proteins can be degraded either by the proteasome or via autophagy depending on the Ub signal. Ub can form a wide variety of homo- and heterotypic Ub-chains on protein substrates, resulting in a distinct cellular responses (Akutsu et al., 2016). Ub is a small protein and can be covalently attached with its C-terminus to a protein substrate or to itself. Three different enzymes are required for this process: an E1 ubiquitin-activating enzyme, an E2 ubiquitin-conjugating enzyme and an E3 ubiquitin-ligating enzyme (Figure 3) (Clague et al., 2015). Ub can be ligated to one or multiple lysines (K) with one Ub molecule (mono-ubiquitination) or Ub chains (polyubiquitination). Ub has 7 lysine residues and in order to form a chain they can be conjugated through different lysines (K6, K11, K27, K29, K33, K48 and K63) or a N-terminal methionine (M1). These options present enormous possibilities to assemble a specific chain. Furthermore, chains can be branched, the length can vary and Ub can be post-translationally modified (acetylation and phosphorylation), giving even more diversity (Akutsu et al., 2016). The fate of ubiquitinated proteins depends on the nature of the Ub modification. Different Ub modifications are specifically recognised by different Ub-binding proteins, resulting in a specific cellular response. Ub modifications can also alter a protein's enzymatic activity, localisation or stability (Husnjak and Dikic, 2012). Most research has been done on K48- and K63-linked Ub chains, however, more recently also other previously considered atypical chains have been studied in more detail (Akutsu et al., 2016). For example, K11-linked poly-Ub chains have been implicated in cell cycle control and Beclin 1 function, whereas linear M1-linked chains have been linked to NF-Kβ (Nuclear Factor kappa-light-chain-enhancer of activated B cells signalling) (Shimizu et al., 2015, Jin et al., 2016, Wickliffe et al., 2011).

K48-poly-Ub chains are the canonical signal for proteasomal degradation, whilst proteins marked with K63-poly-Ub participate in cellular signalling pathways and autophagy (Tan et al., 2008). Recently it has become apparent that autophagy

receptors can recognise different Ub modification, depending on the ubiquitin binding domain, which will be discussed in more detail in section 1.3.1.

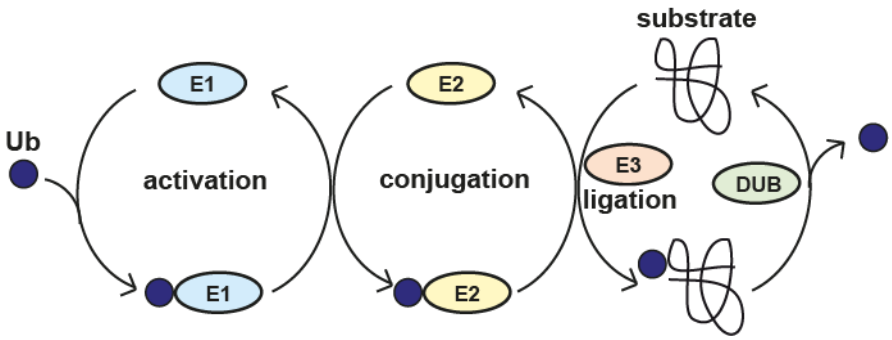

Figure 3 Schematic diagram of the ubiquitin-conjugation system.

The ubiquitination process involves three types of enzymes: ubiquitin-activating (E1), ubiquitin-conjugating (E2) and ubiquitin-ligating (E3) enzymes, which recognises the substrate. Deubiquitinating enzymes (DUBs) can remove the Ub residue from the substrate.

1.3 Autophagy receptors

Autophagy receptors are poorly conserved from yeast to humans, in contrast to the core autophagy machinery, however functional homologs are present. Also as a gene group, autophagy receptors are not very conserved compared to the autophagy genes (Till et al., 2015, Tumbarello et al., 2015). In this section, a subset of autophagy receptors, p62, NBR1, OPTN, NDP52 and TAX1BP1 will be discussed, which all have been implicated in selective autophagy and share structural and functional similarities (Johansen and Lamark, 2011).

In order to bind to ubiquitinated cargo these autophagy receptors contain an ubiquitin binding domain. In addition, some of them have the ability to oligomerise and they all contain LC3-binding motifs that enable them to bind to the autophagosomal machinery (Figure 4).

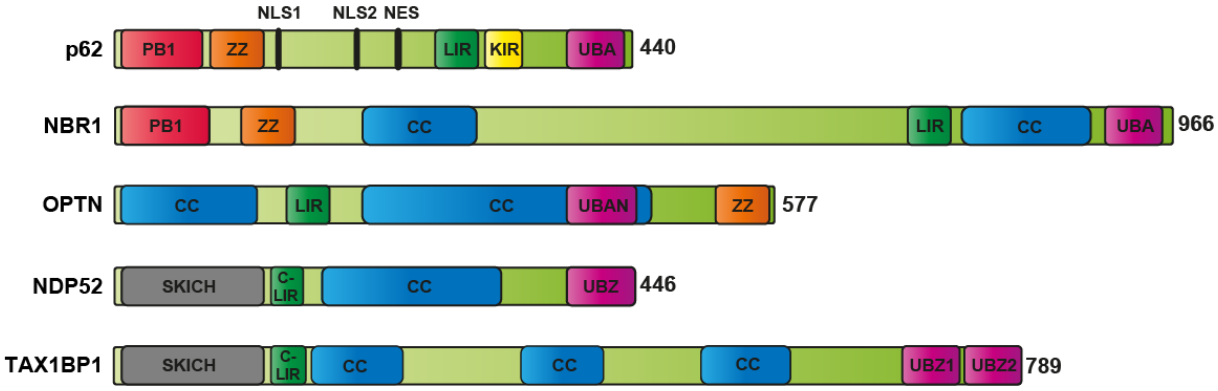

Figure 4 Schematic diagram of the domain structure of p62, NBR1, OPTN, NDP52 and TAX1BP1.

The Ubiquitin binding domains are depicted in purple, PB1 domains in red, CC domains in blue, LC3-binding domains in green, ZZ domain in orange, KIR domain in yellow and the SKICH domain in grey. p62 also contains nuclear localisation signals, depicted in black.

1.3.1 Ubiquitin binding domains (UBDs)

Ub modifications are recognised by a variety of Ub binding domains. These domains are functionally and structurally diverse, reflecting the variation in Ub signals (Rahighi and Dikic, 2012). The most common UBD fold into α-helices, such as the UBA (Ub Associated) and the UBAN (UBD in Abin proteins and NEMO) domain. p62 and NBR1 both contain a UBA domain at the C-terminus. p62 binds mono-and poly-Ub and the UBA-domain of p62 can form homodimers *in vitro* and this inhibits Ub binding. Several mutations in the p62 UBA-domain, resulting in the loss of its ability to bind ubiquitin, have been shown to be to be associated with Paget disease (Section 1.4.1) (Rea et al., 2013). The UBA-domain structure of NBR1 has been solved and has been compared to the p62 UBA-domain. Surprisingly, even though both UBA-domains are very similar, the UBA-domain of NBR1 has a higher affinity for Ub (Walinda et al., 2014). Walinda *et al*. observed that the p62 residue S403 which can be phosphorylated, resulting in an increased affinity for ubiquitin, is replaced by a hydrophobic residue in NBR1, which might increase the affinity for Ub (Walinda et al., 2014, Matsumoto et al., 2011). OPTN contains an UBAN-domain located within the C-terminal CC (Coiled Coil) domain, which is an ubiquitin-binding domain shared among OPTN, NEMO (NF-Kβ Essential Modulator) and ABIN1-3 (A20-Binding Inhibitor of NF-Kβ) (Wagner et al., 2008, Husnjak and Dikic, 2012). In NEMO and ABINs the UBAN-domain has been demonstrated to have an important role in the regulation of NF-Kβ signalling (Wagner et al., 2008). In general, UBAN-domains form a coiled coil, which has specificity for linear Ub chains (Rahighi et al., 2009, Dikic and Dotsch, 2009). Interestingly, a missense mutation in the OPTN UBAN-domain (E478G) has been

associated with ALS (Amyotrophic Lateral Sclerosis) (Maruyama et al., 2010) (Section 1.4.2).

Another group of UBDs contain zinc fingers, such as the UBZ (Ubiquitin-Binding ZnF) domain, which is present in NDP52 and TAX1BP1. In NDP52, the UBZ-domain contains two zinc fingers, which recently have been characterised in more detail. The first ZZ-domain (ZF1) is at amino acid (aa) 392-413, which is an unconventional dynamic CysCysCysHis (CCCH) zinc domain, whereas the second ZZ-domain (ZF2) at amino acid 414-446 is a ubiquitin-binding CCHH zinc finger (Xie et al., 2015). The ZF2 can recognise mono-Ub and different linkage types poly-Ub chains. Both the ZF1 and ZF2 are involved in binding to myosin VI, which has been shown to be important for autophagosome maturation during xenophagy (Verlhac et al., 2015a, Tumbarello et al., 2012, Morriswood et al., 2007, Xie et al., 2015). TAX1BP1 has two C-terminal UBZ-domains, of which the crystal structures have been determined (Ceregido et al., 2014). The second UBZ-domain was shown to be required for Ub binding and binds with high-affinity to K63-linked chains (with a higher affinity than NDP52 and OPTN) and also is able to bind to linear tetra-ubiquitin. Finally, in contrast to NDP52 and OPTN, TAX1BP1 can bind K48-linked chains as well (Tumbarello et al., 2015). A combination of both UBZ1 and UBZ2 domains is important for Myosin VI binding. It was suggested that TAX1BP1 first binds with a lower affinity to ubiquitin, followed by binding to Myosin VI on the out membrane of the autophagosome (Tumbarello et al., 2015).

1.3.2 PB1 domain

p62 and NBR1 contain a PB1 (Phox and Bem1) domain at the N-terminus. The p62 PB1 domain has oppositely charged surfaces and enables p62 to oligomerise. It can oligomerise with itself, and can also form heterodimers with the PB1 domain of other proteins, like aPKCs (atypical Protein Kinase C), MEK5 (MAPK/ERK Kinase 5) and NBR1 (Lamark et al., 2003). The rear end acidic cluster of the p62 PB1 domain interacts with MEKK3 (MAPK Kinase Kinase 3)(Nakamura et al., 2010). All these interactions allow p62 to participate in different signalling pathways. For example, the interaction with aPKCs plays an important role in NF-Kβ signalling (Sanz et al., 2000). Self-oligomerisation of p62 via PB1 domain is also essential for its role in degradation of autophagic substrates (Ichimura et al., 2008). Recently, it was established that the PB1 domain and part of the linker domain between the PB1 and ZZ domains drive the formation of p62 filaments. The PB1 domain functions as a helical scaffold, promoting

oligomerisation. This oligomerisation and formation of p62 filaments is proposed to present multiple LC3 binding sites to promote growth of the phagophore onto the filaments (Ciuffa et al., 2015). The region between the PB1 and ZZ domains is an unstructured region that is rich of basic and acidic residues. A charge-reversal mutant affects p62 aggregation, suggesting that this electrostatic bridge stabilises the PB1 domain (Ciuffa et al., 2015).

In NBR1 the PB1 domain enables NBR1 to interact with p62 and mutation D50R prevents this interaction (Kirkin et al., 2009). Unlike p62, NBR1 does not oligomerise via its PB1 domain, because it lacks the N-terminal basic charge cluster (Kirkin et al., 2009). Therefore, it could be hypothesised that NBR1 binding to p62 inhibits the formation of p62 oligomers.

NBR1 uses the N-terminal CC domain to form oligomers and uses PB1 domain to bind to titin (also known as connectin), which is a very large filamentous protein (about 4000 kDa) found in the striated muscle (Lange et al., 2005; Müller et al., 2006).

In a recently published study, it was shown that autophagy receptors without the ability to oligomerise reside on the outer membrane, whilst oligomerised receptors reside on the inner membrane of the autophagosome, resulting in their degradation. Therefore, not the LC3 binding, but the ability to oligomerise in addition to LC3 binding determines if a protein is an autophagy substrate (Hirano et al., 2016).

1.3.3 CC domain

A coiled coil is a common structural motif in proteins in which 2-7 alpha-helices are coiled together. NBR1 contains two CC domains and the second one is important for dimerisation (Kirkin et al., 2009). It has been hypothesised that the dimerisation via the CC domain is not sufficient to induce formation of large NBR1-positive protein aggregates and that this step thus is dispensable for NBR1-dependent selective autophagy (Shi et al., 2014). OPTN contains two CC domains and its structure is predicted to be over 70% coiled-coiled. A Leucine-zipper (LZ domain) is located within the N-terminal CC domain, and the UBAN-domain is located within the C-terminal CC domain. The N-terminal domain is required for TBK1 (TANK1 Binding Kinase 1) binding, which serves as an important component of multiple signalling pathways, such as NF-Kβ, but also a role for TBK1 in autophagy is emerging. The kinase TBK1 phosphorylates OPTN at S177 (Wild et al., 2011, Lazarou et al., 2015), which promotes

LC3 binding, as well as S473 and S513 which results in an increased selectivity and stronger binding for OPTN to poly-Ub chains (Lazarou et al., 2015).

Leucine zippers consist of a periodic repetition of a leucine residue at every seventh position (heptad repeat) and forms α-helix, which facilitates dimerisation and in some cases higher oligomerisation of proteins. Leucine zippers are known to be sites for protein-DNA or protein-protein interaction. The function of the OPTN LZ domain (aa 143-164) has not been studied in detail, but it was shown to be partially required for Rab8 and transferrin receptor binding (Park et al., 2010). Finally, the C-terminal CC domain of OPTN has been shown to bind to mutant Huntingtin and mutant SOD1 (SuperOxide Dismutase 1) aggregates in an ubiquitin-independent manner (Korac et al., 2013).

The middle region of NDP52 consists of a CC domain, which is important for dimerisation of NDP52 and binding to leucine rich repeat and LRSAM1 (Leucine rich Repeat and Sterile Alpha Motif containing 1), an E3 Ub ligase that has been implicated in xenophagy (Huett et al., 2012). Interestingly, a mutation in the NDP52 CC domain has been linked to Crohn's disease, which is an inflammatory bowel disease that is potentially caused by impaired autophagy (Ellinghaus et al., 2013). TAX1BP1 contains 3 CC domains, of which the second CC domain (aa 320-420) is required for TRAF6 (TNF Receptor Associated Factor 6) binding (Ling and Goeddel, 2000). The role of the other CC domains is not known, but potentially could promote the formation of higher order structures (Woolfson et al., 2012).

1.3.4 LC3-binding motifs

In order to degrade the bound cargo, the autophagy receptors need to bind to LC3-II. The canonical LC3-binding motifs (LIR) consist of a sequence with a core motif corresponding to W/F/Y-XX-L/I/V (where X can be any amino acid). In p62, the LIR motif (amino acid 335-341) is critical for the interaction of p62 with LC3 for autophagic degradation. p62 binds all Atg8 family members: LC3A, B and C and GABARAP, GABARAPL1 and GABARAPL2 (Pankiv et al., 2007, Rogov et al., 2017) in its soluble and insoluble form and the PB1 domain is not essential for this interaction (Kraft et al., 2016, Wurzer et al., 2015). Intriguingly, p62 mutations linked to ALS-FTLD have been mapped to the LIR motif (Rea et al., 2014). OPTN also contains a typical LIR motif (W-V-E-I) similar to p62, and it is required for LC3 recruitment to damaged mitochondria and the degradation of *Salmonella* (Wong and Holzbaur, 2014, Wild et al., 2011).

NBR1 has a non-canonical LIR motif (C-LIR) that consists of 8 amino acids (SEDYIIIL) N-terminal of its C-terminal CC domain (Waters et al., 2009), which binds specifically to GABARAPL1. The structure of the NBR1 LIR motif with GABARAPL1 revealed that the 4 hydrophobic residues (YIII) of NBR1 are important for this interaction (Rozenknop et al., 2011; Klionsky and Schulman, 2014).

NDP52 has a typical LIR motif in the SKICH domain, however, this domain does not mediate NDP52 binding to LC3, because it is not accessible for binding. Instead, a C-LIR motif is present in the linker region between the SKICH and CC domains (von Muhlinen et al., 2012), which binds to LC3C specifically. The C-LIR motif comprises of L-V-V, which is different from the canonical LIR motif, which comprises of W-I-G-I. The main difference between the two motifs is that the C-LIR motif selectively binds to LC3C, whereas the LIR motif interacts with all members of the LC3 family as well as LC3 homologs GABARAP, GABARAPL1, and GABARAPL2 (von Muhlinen et al., 2012). In addition, recently another LIR-like motif was identified, which is present in the CC domain and is essential for NDP52-mediated autophagosome maturation, but not for targeting of bacteria to autophagosomes (Verlhac et al., 2015a). The C-LIR motif of TAX1BP1 can bind to LC3B, LC3C, GABARAPL1 an L2. It was shown that there is no preference in binding to LC3B or LC3C, which is in contrast to NDP52 and OPTN, which both have a higher affinity for LC3C (Tumbarello et al., 2015).

Clearly, some specificity exists in binding to the different Atg8 family members, however the mechanism of this specificity remains to be understood and also the biological and functional significance of binding to these different Atg8 family members is not known.

1.3.5 ZZ domain

ZZ-type zinc finger (ZZ) domain can bind two zinc ions and are thought to be involved in protein-protein interactions. The p62 ZZ domain mediates the interaction with RIP (Receptor-Interacting serine/threonine-Protein Kinase 1, also called, RIP1 or RIPK1), which is implicated in p38MAPK signalling (Festjens et al., 2007; Yu et al., 2009). Through its ZZ domain p62 can also directly interact with AMPA (α-Amino-3-hydroxy-5-Methyl-4-isoxazolePropionic Acid) receptor subunits and thereby recruit the AMPA receptor for phosphorylation by aPKC and thereby regulating synaptic plasticity (Jiang et al., 2009). Recently, the p62 ZZ domain was shown to be required for recognition of N-terminal arginylated ER proteins destined for degradation via autophagy (Cha-

Molstad et al., 2016, Cha-Molstad et al., 2015). OPTN and NBR1 also contain a ZZ domain, however the function remains to be determined.

1.3.6 NLS and NIS signals

Interestingly, p62 and OPTN have been shown to localise to the nucleus in certain conditions. In unstressed cells p62 is primarily found in the cytoplasm, but due to its two nuclear localisation signals and an export signal (NLS1, NLS2 and NES), p62 can shuttle between the nucleus and cytoplasm. This is an active process and happens at a high rate (Pankiv et al., 2010). In the nucleus, p62 is found to localise to PML (ProMyelocytic Leukaemia) bodies and protein aggregates *in vitro* and *in vivo* (Pikkarainen et al., 2011). Furthermore, p62 was found to be dynamically associated with DNA damage foci, where it interacts with filamin A. p62 promotes the proteasomal degradation of filamin A and RAD51 (RAD51 recombinase) in the nucleus, resulting in a slower DNA repair (Hewitt et al., 2016). OPTN migrates to the nucleus upon oxidative stress, however nuclear localisation signals have not been identified (De Marco et al., 2006).

1.3.7 SKICH domain

NDP52 and TAX1BP1 contain an N-terminal SKICH domain, which resembles an IG-fold lacking the 8^{th} β-sheet (Gurung et al., 2003). The NDP52 SKICH domain is responsible for the interaction with Nap1 (Thurston et al., 2009) and phosphorylated tau (Jo et al., 2014). The crystal structure of the TAX1BP1 SKICH domain was determined and revealed that this domain contains some conserved surface exposing aromatic residues, but the function remains unknown (Yang et al., 2014). Thus far, the biological function of the NDP52 and TAX1BP1 SKICH domain remains to be understood.

1.3.8 KIR domain and Nrf2 signalling

In addition to the different domains that have been implicated in the role of these receptors in autophagy, p62 also contains a KIR domain (Keap1 Interaction Region), which is important for the Nrf2 antioxidant pathway. Keap1 is an adaptor of the Cul3-ubiquitin E3 ligase complex responsible for Nrf2 degradation. p62 binds to Keap1 (Kelch-like ECH-associated protein 1) via its KIR domain, targets it for degradation, followed by the translocation of Nrf2 to the nucleus, where it activates genes that are important for the antioxidant response (Komatsu et al., 2010).

The Nrf2/Keap1 pathway is recognised as the main cellular defence mechanism against oxidative and electrophilic stresses. Nrf2 (Nuclear factor erythroid 2-related factor 2) is a transcription factor that mainly regulates the transcription of genes that are known as AREs (antioxidant response element genes) (Chorley et al., 2012), including antioxidant and phase II detoxification genes (Itoh et al., 1997, Thimmulappa et al., 2002). Under normal condition, Nrf2 is constitutively degraded by the UPS, because its binding partner Keap1 recruits the Cullin3 E3 ligase, which ubiquitinates Nrf2 and targets it for degradation by the proteasome (Zhang et al., 2004). In response to electrophiles or ROS Keap1 is inactivated through modification of its cysteines, it changes conformation which disrupts its binding to Nrf2. As a result, Nrf2 is stabilised and translocates to the nucleus, where it activates its target genes (Kobayashi et al., 2006).

p62 is involved in the Nrf2 antioxidant response pathway by facilitating the degradation of Keap1. p62 interacts with the Nrf2 binding site of Keap1, sequesters it and sends it for degradation by autophagy (Taguchi et al., 2012). Accumulated p62, in response to a block in autophagy, competes with the interaction between Nrf2 and Keap1, and enables Nrf2 to translocate to the nucleus and induce gene expression (Komatsu et al., 2010, Kwon et al., 2012). In response to stress serine 351 of the KIR-domain of p62 is phosphorylated, which increases the affinity for Keap1 and activates Nrf2. Interestingly, it was shown that this phosphorylation is mTORC1-dependent, linking the Keap1-Nrf2 system to nutrient signalling and autophagy (Ichimura et al., 2013). Furthermore, p62 contributes to a positive feedback loop, because Nrf2 signalling results in the induction of p62 gene transcription (Jain et al., 2010).

1.4 Autophagy receptors in disease

1.4.1 p62 in disease

In the past years, mutations in p62 have been identified in patients with ALS and FTLD (FrontoTemporal Lobar Degeneration). Before those mutations were identified, p62 was already linked to ALS. p62 was shown to form aggregates in ALS patients as well as in a mutant SOD1 mouse model (Gal et al., 2007, Mizuno et al., 2006). Moreover, p62 colocalises with FUS (FUsed in Sarcoma) and TDP-43 (TAR DNA-binding Protein 43) in ubiquitin-positive inclusions in spinal cords from patients with sporadic and familial ALS (non-SOD1) (Deng et al., 2010) and p62 overexpression prevents TDP-43 aggregation and promotes TDP-43 degradation in an autophagy and proteasomal manner (Brady et al., 2011). p62 promotes SOD1 aggregation in a motoneuron-like

cell line (Gal et al., 2007), where it binds SOD1 directly in an ubiquitin-independent manner. The p62 PB1 domain and a region between the ZZ domain and the TB (TRAF6 Binding) domain are essential for this interaction (Gal et al., 2009).

As mentioned before, mutations in p62 have been identified in both familial and sporadic cases of ALS-FTD (FrontoTemporal Dementia) (Fecto et al., 2011, Rea et al., 2014, Yang et al., 2015). ALS associated mutations in p62 are distributed in different domains throughout the protein (Figure 5) (Rea et al., 2014). A subset of mutations were found in the LIR motif, of which L341V was studied functionally, and it was shown that LC3B binding was impaired (Goode et al., 2016). Another subset of mutations locating to the PB1 domain, could affect p62 oligomerisation and thus possibly LC3 binding. Additionally, many mutations reside in the UBA domain, and all mutants tested had impaired Ub binding (Rea et al., 2009). Interestingly most mutations identified in the UBA domain that are associated with ALS and/or FTLD, have been found in PDB (Paget's Disease of Bone) patients as well (Rea et al., 2014). PDB is a common bone disorder characterised by enhanced resorption of bone as a result of overactivity of osteoclasts. A mouse with the P394L mutation (human P392L equivalent, the most frequent PDB mutation) developed a bone disorder similar to PDB patients (Daroszewska et al., 2011), no ALS or FTD related phenotype was mentioned, but most likely also not studied, because at the time p62 mutations had not been associated with ALS or FTD. The study does suggest that p62 mutations can play a causal role is PDB development and does not necessarily need an environmental trigger. It would be of interest to study the functional effect of all the different p62 mutations. The PB1, LIR and UBA domain mutations have predictable effects on p62 functioning in selective autophagy.

Intriguingly, in addition to mutations in the ZZ, TB, KIR domain and the nuclear export signal, also mutations in unstructured regions and outside the known domain structures have been identified in ALS and/or FTLD (Figure 5). How these mutations effect function and result in the disease phenotype is unknown and of high importance to investigate further.

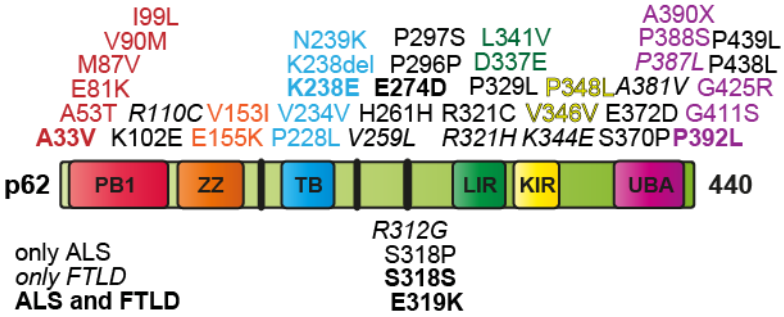

Figure 5 Summary of p62 mutations found in ALS (Amytrophic Lateral Sclerosis) and FTD (Frontotemporal Dementia) patients.

p62 diagram showing all ALS and FTD related p62 mutations identified to date (Rea et al., 2014, Yang et al., 2015). In red, orange, blue, green, yellow and purple are the mutations locating to the PB1, ZZ, TB, LIR, KIR and UBA domain respectively. Mutations R312G, S318P, S318S and E319K occur in the nuclear export signal. Mutations visualised in bold (A33V, K238E, E274D, S318S, E319K and P392L) are mutations found in ALS and FTLD and the mutations in italic (R110C, V259L, R312G, K344E, A381V and P387L) were only found in FTLD cases, but not ALS. Mutations A381V, P387L, A390X, P392L, G411S, G425R have been reported in PDB (Paget's Disease of Bone) previously (Rea et al., 2013).

1.4.2 OPTN in disease

Mutations in OPTN have been associated with the neurodegenerative diseases ALS, FTD and POAG (Primary Open-Angle Glaucoma) (Rollinson et al., 2012, Iguchi et al., 2013, Pottier et al., 2015) (Cirulli et al., 2015, Rezaie et al., 2002). In POAG patients, retinal ganglion cells degenerate, which results in irreversible blindness. The cause of this genetic disease is not clear, several genes have been linked to the disease, however no common pathways were identified (Fingert, 2011). Since mutations in OPTN were identified, and also mutations in TBK1 were linked to the disease, selective autophagy dysfunction could be involved in POAG pathogenesis. Most of the OPTN mutations are missense singly copy mutations, which likely are dominant. One mutation, E50K, was shown to inhibit autophagy and endocytic recycling of the transferrin receptor (Nagabhushana et al., 2010, Chalasani et al., 2014). Furthermore, in neuronal cells differentiated from iPSCs (induced pluripotent stem cells) derived from POAG patients carrying the E50K mutation, revealed that the E50K mutant forms insoluble aggregates, which was suggested to contribute to the pathogenesis (Minegishi et al., 2013). This could potentially explain why the E50K mutant does not translocate to the nucleus upon H_2O_2 induced cell death (De Marco et al., 2006). The E50K mutation also resulted in enhanced TBK1 binding and it was shown that the insolubility of E50K OPTN was dependent of TBK1 (Minegishi et al., 2013). However, POAG associated mutant E50K did not affect mitophagy, suggesting that this is not

involved in the disease pathogenesis (Lazarou et al., 2015). However, more point mutations, distributes throughout the protein, have been identified in POAG patients, and these might have different effects on protein function (Sirohi and Swarup, 2016).

Mutations in OPTN were first shown to cause autosomal recessive ALS, however later also heterozygous mutations were reported in familiar ALS cases (Maruyama et al., 2010, van Blitterswijk et al., 2012). Mutations in OPTN were also associated with FTLD and these mutations were predicted to be highly pathogenic and result in loss of function and reduced protein levels (Pottier et al., 2015). In a minority of sporadic ALS patients, protein inclusions were shown to be positive for OPTN (Osawa et al., 2011, Hortobagyi et al., 2011).

1.4.3 NDP52 in disease

NDP52 is associated with intracellular Aβ (Amyloid peptide β)-plaques and neurofibrillary tangles in an Alzheimer's mouse model (Kim et al., 2014) and has also been associated with hyper-phosphorylated tau in Alzheimer's patients. NDP52 was also suggested to play a role in the degradation of hyper-phosphorylated tau (Jo et al., 2014).

As mentioned before, a mutation in NDP52 was found in Crohn's disease patients. The V248A mutation impairs the regulatory function of NDP52 to inhibit NF-Kβ (Ellinghaus et al., 2013). It would be interesting to assess if the V248 variant also affects autophagy, especially xenophagy. A link between autophagy and Crohn's disease was established previously, as mutations in core autophagy genes, *ATG16L1*, *LRRK2* (Leucine Rich Repeat Kinase 2)*, IRGM* (Immunity-Related GTPase family M protein) and *ULK1* were identified (Massey and Parkes, 2007, Chauhan et al., 2016, Chauhan et al., 2015, Henckaerts et al., 2011).

1.5 Mitophagy

The degradation of mitochondria via autophagy (also called mitophagy) mediates the clearance of damaged mitochondria, as well as mitochondria in a specific context, such as during erythrocyte maturation or to eliminate sperm-derived mitochondria after fertilisation. Mitophagy is one of the most studied selective autophagy pathways in the last years, because of the association of mitochondrial function with the development of neurodegenerative disease. In particular, mutations in two proteins PINK1 (PTEN-INduced putative Kinase 1) and Parkin have been associated with Parkinson's disease (Kitada et al., 1998, Valente et al., 2004), therefore the role of these two proteins have

been investigated in great detail. PINK1 is a serine/threonine kinase, which when the mitochondrial membrane potential (Δψm) is high, binds to PGAM5 (PhosphoGlycerate Mutase family member 5) in the IMM (Inner Mitochondrial Membrane). On the contrary, when mitochondria are damaged and the Δψm is low, PINK1 accumulates on the OMM (Outer Mitochondrial Membrane), where it recruits and phosphorylates Parkin, an E3 ubiquitin-ligating enzyme, resulting in its activation (Figure 6) (Shiba-Fukushima et al., 2014, Kondapalli et al., 2012). PINK1 phosphorylates Ub and Parkin has a high affinity for this pS65-Ub, resulting in recruitment of Parkin to the OMM (Kane et al., 2014, Kazlauskaite et al., 2014, Koyano et al., 2014, Ordureau et al., 2015). Binding of Parkin to pS65-Ub also results in a conformational change, resulting in Parkin activation (Okatsu et al., 2015, Wauer et al., 2015). Parkin then conjugates Ub onto OMM proteins, predominantly K48- and K63-linked chains, which also get phosphorylated by PINK1, thus recruiting more Parkin and resulting in a positive feed-forward loop (Ordureau et al., 2014). Also other Ub chains were identified, including K6- and K11-linked chains, showing the variety of Ub chains on the mitochondria. Recently, two different mitochondrial anchored DUBs (DeUBiquitylases), USP30 (Ubiquitin-Specific Protease 30) and USP15 were found to negatively regulate PINK1/Parkin dependent mitophagy (Bingol et al., 2014, Cunningham et al., 2015, Cornelissen et al., 2014).

The K48-linked chains most likely promote the extraction of OMM proteins and subsequent degradation by the proteasome (Tanaka et al., 2010, Yoshii et al., 2011). The K63-linked Ub chains were found to be mainly important for the recruitment of autophagy receptors to the damaged mitochondrion. p62, NBR1, TAX1BP1, NDP52 and OPTN recruit to mitochondria during PINK1/Parkin induced mitophagy. Making use of HeLa PentaKO cells (CRISPR (Clustered Regularly Interspaced Short Palindromic Repeats) knock-out for OPTN, NDP52, p62, TAX1BP1 and NBR1) and re-expressing the different autophagy receptors showed that primarily OPTN and NPD52 and, to a smaller extent TAX1BP1, are required but functionally redundant for mitophagy (Wong and Holzbaur, 2014, Lazarou et al., 2015, Heo et al., 2015). It was shown that the expression patterns of the different receptors was different. In the brain OPTN is highly expressed, p62 expression is lower, and NDP52 is not detectable. Whilst, for example in the small intestine, moderate to high NDP52 and p62, and undetectable OPTN expression was observed (Lazarou et al., 2015).

Furthermore, it was shown that OPTN and NDP52 have a higher affinity for pS65-Ub chains, however this was not detected *in vitro* suggesting that other factors or

modifications *in vivo* are required (Nguyen et al., 2016a). One of these modifications could be phosphorylation of the receptors, as OPTN, p62, NDP52 and TAX1BP1 can be phosphorylated by TBK1 (Figure 6) during mitophagy, and phosphorylation of OPTN resulted in an increased affinity for all Ub chains (Matsumoto et al., 2015, Heo et al., 2015, Moore and Holzbaur, 2016, Richter et al., 2016). TBK1 depletion or expression of ALS-associated OPTN or TBK1 mutations blocked the efficient degradation of mitochondria, suggesting that phosphorylation of OPTN by TBK1 is essential (Moore and Holzbaur, 2016).

The role of p62 in mitophagy is controversial. Several reports indicate an essential role for p62 (Lee et al., 2010a, Geisler et al., 2010, de Castro et al., 2013, Pimenta de Castro et al., 2012). Others report that p62 is not essential, but has a role in mitochondrial clustering to prepare them for degradation (Lazarou et al., 2015, Narendra et al., 2010). Interestingly, it was thought that autophagy receptors recruit the autophagosomal membrane and machinery to the damaged mitochondrion. However, recently it became apparent that the autophagosomal membrane is built at the OMM upon mitophagy induction (Itakura et al., 2012, Lazarou et al., 2015). ULK1 and Atg9 are recruited to the OMM to initiate the formation of the autophagosome. In HeLa PentaKO cells ULK1, DFCP1 and WIPI1 failed to recruit to the mitochondria, suggesting that these receptors are essential for the recruitment of the key proteins involved in autophagy initiation (Figure 6). Furthermore, NDP52 and OPTN were shown to be essential for ULK1 and DFCP1 recruitment. However, LC3 lipidation was not affected upon mitophagy induction in PentaKO cells, suggesting that the recruitment of key components of autophagy initiation and LC3 lipidation are independently regulated (Lazarou et al., 2015, Nguyen et al., 2016b). After the recruitment of ULK1-, DFCP1- and Atg9- positive vesicles to mitochondria, LC3 is recruited, which promotes fusion of the autophagosome with the lysosome (Figure 6) (Itakura et al., 2012, Nguyen et al., 2016b). It would be interesting to assess if mitophagy makes use of all the other canonical autophagy components in order to complete mitochondrial degradation.

PINK1/Parkin dependent mitophagy has been studied in great detail, because it has been extensively implicated in human disease, especially neurodegeneration. However, alternative mitophagy pathways have been identified as well. Furthermore, it is under debate if mitochondrial defects due to mitophagy dysfunction caused by loss of PINK1 or Parkin are responsible for the loss of dopaminergic neurons in Parkinson's

disease. This is mainly based on the fact that in conditional adult Parkin knockout mice, which show a clear loss of dopaminergic neurons, neither mitophagy defects nor mitochondrial accumulation was observed (Stevens et al., 2015). Instead it was shown that PINK1 and Parkin are involved in the degradation of PARIS, which is a pathogic Parkin substrate. In the case of loss of PINK1 or Parkin, PARIS accumulates and transcriptionally represses PGC1α (PPARγ (Peroxisome Proliferator-Activated Receptor-γ) Coactivator-1α) and this has shown to result in degeneration of dopaminergic neurons (Lee et al., 2017, Shin et al., 2011). Thus, it remains to be determined to what degree PINK1/Parkin-mediated mitophagy is involved in the development of Parkinson's disease.

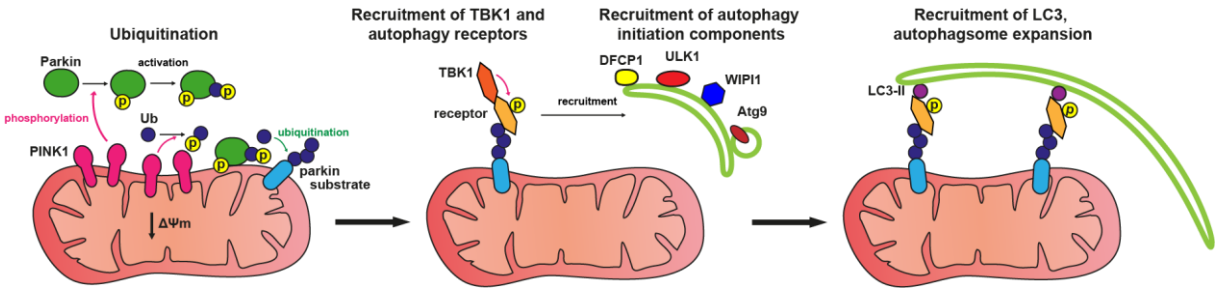

Figure 6 Schematic diagram showing PINK1/Parkin dependent mitophagy.

Upon loss of the mitochondrial membrane potential (Δψm), PINK1 accumulates at the mitochondrial membrane, where it phosphorylates Parkin and ubiquitin (Ub). Parkin ubiquitinates outer mitochondrial membrane proteins, resulting in the recruitment of the kinase TBK1 and autophagy receptors. This is followed by the recruitment of Atg9, ULK1 and WIPI1, promoting the formation of an autophagosomal membrane around the mitochondrion. The autophagy receptors directly bind to LC3, which promotes fusion with lysosomes in order to complete degradation.

1.6 Xenophagy

The degradation of bacteria (xenophagy) is a process that is very similar to the degradation of mitochondria, which can be explained by the fact that mitochondria are of bacterial ancestry. Xenophagy is an innate immune mechanism against bacterial infection and is essential to restrict cytosolic growth of a wide variety of bacteria, like *Salmonella enterica serovar Typhimurium*, *Mycobacterium tuberculosis*, *Listeria monocytogenes* or Group A *Streptococcus* (Gutierrez et al., 2004, Py et al., 2007, Nakagawa et al., 2004, Castrejon-Jimenez et al., 2015, Birmingham et al., 2006). Especially the protection of the gut epithelium against bacteria depends on xenophagy, because mice lacking Atg5 in enterocytes suffer from infections and mutations in NDP52 have been associated with Crohn's disease (an inflammatory bowel disease) (Ellinghaus et al., 2013, Benjamin et al., 2013).

Upon infection, gram-negative bacteria enter epithelial cells via actin-rich membrane ruffles and reside in a vacuole where they are unnoticed by the host defence machinery. In these vacuoles the bacteria do not cause much damage, however occasionally bacteria escape into the cytosol, where they can rapidly proliferate and be detrimental to the cell. As a protective mechanism, upon escaping the vacuole, the bacteria become immediately ubiquitinated, resulting in the recruitment of autophagy receptors p62, OPTN, NDP52, TAX1BP1 and NBR1, which similar to mitophagy result in the recruitment of LC3 and subsequent degradation via autophagy (Randow and Youle, 2014, Gomes and Dikic, 2014).

In case of *Salmonella*, which is the most widely studied pathogen infection, a second “eat me” signals has been reported. In addition to ubiquitination of the bacteria upon escape into the cytosol, damage of the *Salmonella*-containing vacuole can be recognised as well. Galectin 8 binds glycans and provides a signal, which results in the recruitment of NDP52 and TBK1 (Figure 7) (Thurston et al., 2012).

In addition, recently it was found that WIPI1 and WIPI2 are recruited to cytosolic bacteria in a TBK1 dependent manner and that loss of WIPI2, but not WIPI1, restricted xenophagy (Figure 7). This implicates that the autophagosomal membrane is built around the bacteria, similar to what recently was observed during mitophagy. It would be interesting to assess if similar to mitophagy, ULK1 is also recruited to cytosolic *Salmonella* in a TBK1 dependent manner and if other canonical autophagy proteins are required for xenophagy.

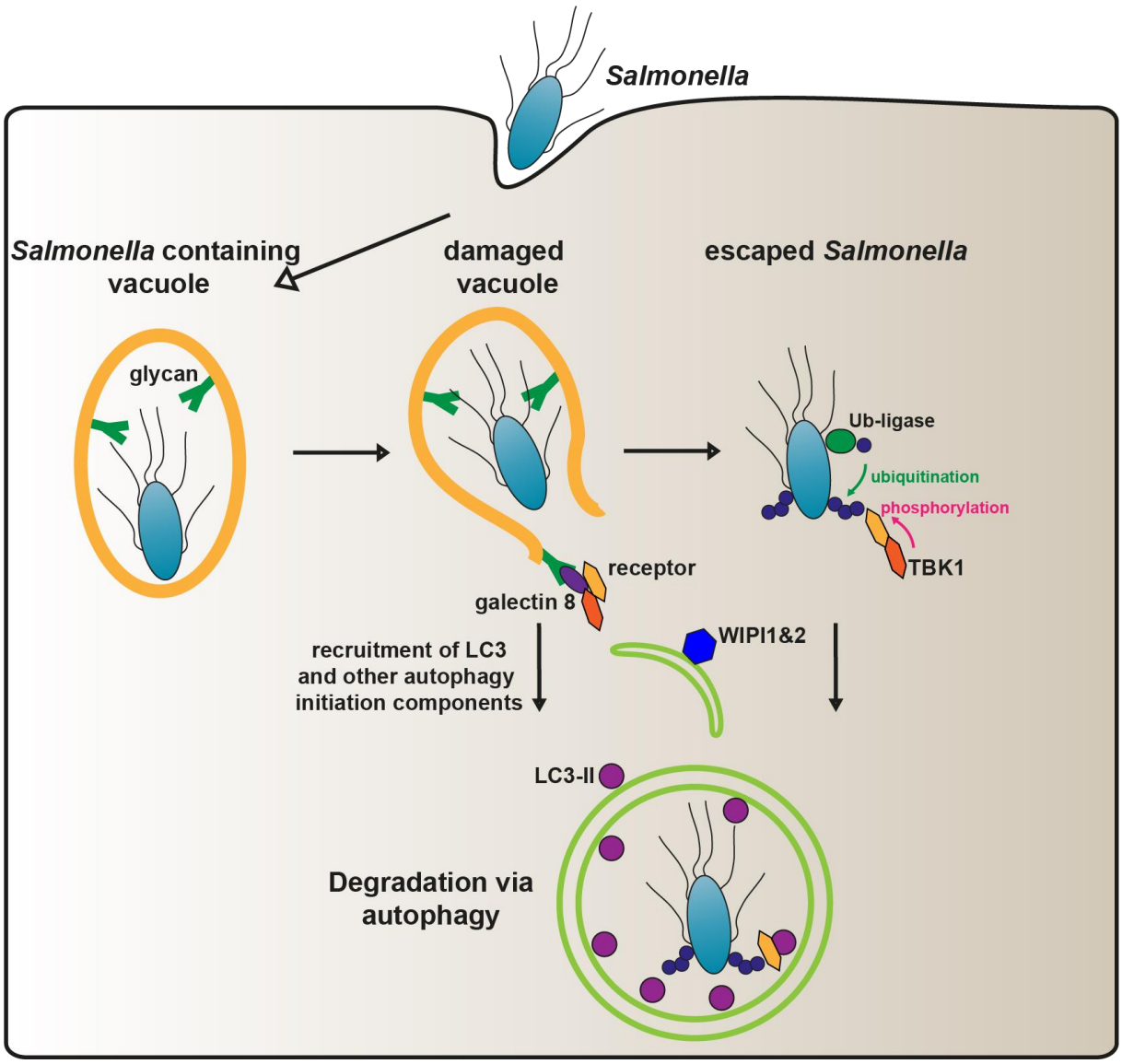

Figure 7 Schematic diagram showing the xenophagy pathway.

Upon infection, *Salmonella* enters the epithelial cell and resides in a vacuole. When the vacuole gets damaged, galectin 8 binds to glycans and the autophagy receptor NDP52 and the kinase TBK1 get recruited. If *Salmonella* escapes the vacuole it gets ubiquitinated by LRSAM1 and Parkin, followed by the recruitment of TBK1 and different autophagy receptors. This is followed by the recruitment of WIPIs and LC3 and subsequent degradation via autophagy.

1.7 Aggregate formation and degradation

Selective autophagy has an essential role in the maintenance of proteostatic balance, because it is involved in the selective degradation of protein aggregates. Protein misfolding and aggregation can be toxic for the cell and can lead to cell death. Molecular chaperones can disentangle protein aggregates and promote correct protein folding (Kim et al., 2013b). In case molecular chaperones are not sufficient to prevent the formation of protein aggregates, soluble smaller aggregates can be cleared via the proteasome, whilst bigger insoluble aggregates or aggresomes are degraded via

autophagy (Kirkin et al., 2009, Stefani and Dobson, 2003, Ravid and Hochstrasser, 2008, Finley, 2009, Piwko and Jentsch, 2006, Hjerpe et al., 2016). Inefficient protein quality control results in the generation of insoluble aggregates, which contribute to many diseases and have also been associated with ageing (Kopito, 2000, Hyttinen et al., 2014). Especially in neurodegenerative diseases protein inclusions are a common feature, for example hyper-phosphorylated tau-containing neurofibrillary tangles and Aβ containing plaques accumulate in Alzheimer's disease, α-synuclein in Lewy bodies in Parkinson's disease, polyQ (poly-glutamine) mutants of huntingtin form aggregates in Huntington's disease and TDP-43 positive aggregates accumulate in FTD and ALS (Winslow et al., 2010, Imarisio et al., 2008, Ravikumar et al., 2002, Hsu et al., 2000, Kuusisto et al., 2001). Suppression of autophagy in neuronal cells in mice causes neurodegeneration in mice, which is associated with an accumulation of Ub positive inclusions (Hara et al., 2006). Autophagy dysfunction in neurodegenerative diseases is discussed in more detail in section 1.12.

1.7.1 The role of p62 in the formation and degradation of protein aggregates

Most neurodegenerative disease-associated protein aggregates are positive for Ub, several heat shock proteins and the autophagy receptor p62 (Zatloukal et al., 2002). p62 has a dual and complicated role in this process, since it is involved in aggregate formation as well as degradation. p62 is an aggregate prone protein by itself, as it has the ability to oligomerize via its PB1 domain and this promotes the formation of p62 positive inclusions (Bjorkoy et al., 2005). In mice, deficient autophagy results in the accumulation of p62 positive aggregates. Interestingly, depletion of p62 in this background dramatically reversed this phenotype in hepatocytes and neurons, showing its opposing role (Komatsu et al., 2007). In *Drosophila melanogaster* it was shown that Ref(2)P (Refractory to sigma P, the fly homolog for p62) was involved in aggregate formation as well (Nezis et al., 2008).

p62 was the first autophagy receptor that was shown to be required for the clearance of Ub positive aggregates (Pankiv et al., 2007) and loss of p62 in mice caused the accumulation of neurofibrillary tangles, resulting in an Alzheimer's disease like phenotype (Wooten et al., 2008). In flies loss of Ref(2)P causes a delay in the autophagy-dependent degradation of polyQ aggregates (Saitoh et al., 2015). Because p62 is involved in aggregate formation and degradation, in some conditions and tissues loss of p62 results in more aggregates as is the case for polyQ proteins in a fly and mouse model for neurodegeneration (Saitoh et al., 2015, Doi et al., 2013) and other

cases p62 depletion results in less aggregates (Bjorkoy et al., 2005, Komatsu et al., 2007).

1.7.2 Molecular mechanism of aggrephagy

In the last decade, a lot of work has been done to identify molecular mechanisms of the clearance of protein aggregates. For example, it has been shown that the formation of K63-linked Ub chains promote the clearance of inclusions associated with neurodegenerative diseases via autophagy (Tan et al., 2008), however not much is known about the role of different Ub-linked chains and Ub-ligating enzymes concerning aggrephagy. Similar to mitophagy and xenophagy, autophagy receptors are recruited to the ubiquitinated aggregates via their ubiquitin binding domains. It was shown that NBR1 and p62 locate in a complex on Ub positive inclusions and both can bind LC3. Furthermore, it was shown that NBR1 can function independently of p62 (Kirkin et al., 2009). OPTN also recruits to p62 positive inclusions via its ubiquitin binding domain. TBK1, which localises to aggregates as well, was shown to phosphorylate OPTN (Korac et al., 2013), which most likely promotes Ub binding, as was shown to happen during mitophagy (Matsumoto et al., 2015, Heo et al., 2015, Moore and Holzbaur, 2016, Richter et al., 2016). Interestingly, OPTN and p62 can also bind to SOD1 aggregates in a ubiquitin-independent manner (Korac et al., 2013, Gal et al., 2009), which is of importance, since in ALS patients SOD1 aggregates negative for ubiquitin were observed (Allen et al., 2003, Osawa et al., 2011).

After autophagy receptors are recruited, it was proposed that Alfy (Autophagy-Linked FYVE protein), by binding to p62 and NBR1, can acts as a scaffold that can recruit the autophagosomal membrane and machinery to p62/NBR1 positive aggregates via a direct interaction with Atg5 and PI3P (via its lipid binding domain called FYVE) (Figure 8). Alfy, which is a large 400 kDa protein, resides in the nucleus, and its translocation to the cytosol depends on p62 (Clausen et al., 2010). Potentially, Alfy binds to p62 and/or NBR1 on aggregates and recruits the Atg5-Atg12-Atg16L1 complex to the aggregate, where it can lipidate LC3, which can be recruited via the LC3 binding domains of p62 and NBR1 (Deretic, 2010). This would promote the fusion with lysosomes in order to degrade the aggregate. Furthermore, it was shown that Alfy does not affect starvation induced bulk autophagy (Clausen et al., 2010), but it would be interesting to asses if it has a role in other selective autophagy pathways.

In addition to the well-known autophagy receptors, recently Tollip was shown to degrade polyQ aggregates in a ubiquitin-dependent manner via a CUE-domain, which has a higher affinity for mono- and poly- Ub chains than the UBA-domain of p62 (Lu et al., 2014). Interestingly, Tollip interacts with p62 and NBR1 and a double knockdown of Tollip and p62 is even more toxic than single knockdowns in response to polyQ expression, suggesting that there is no functional redundancy (Lu et al., 2014).

Since the aggregation of specific proteins is thought to underlie age-related neurodegenerative diseases, elimination of these aggregates via autophagy has been proposed as a strategy to ameliorate these diseases (Eisele et al., 2015, Rubinsztein et al., 2012). Therefore, more research needs to be done in order to identify potential targets for specific intervention.

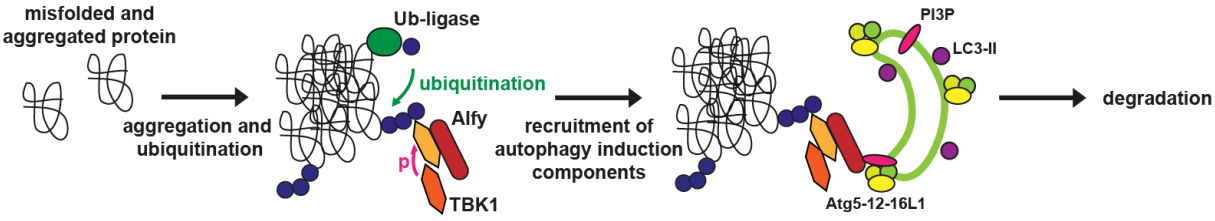

Figure 8 Schematic diagram showing the aggrephagy pathway.

Misfolded and aggregates proteins are ubiquitinated by an unknown Ub-ligase. The formed poly-Ub chains result in the recruitment of autophagy receptors and TBK1. Alfy and LC3 bind to the different autophagy receptors and Alfy binds to Atg5 and PI3P, thereby recruiting the autophagosomal membrane and machinery, and promoting subsequent degradation via autophagy.

To summarise, it is clear that the selective degradation of different cargo via autophagy all have common themes, but there are also distinct differences. It is not clear if the cargo and the use of certain autophagy receptors also result in the usage of different or similar autophagy machinery as in bulk autophagy. Furthermore, still more research needs to be done to identify ligases and deubiquitinating enzymes that are involved in decorating the cargo with different Ub chains and how their activity is regulated. What are the roles of the different autophagy receptors, why do they have redundant functions during mitophagy, but functionally distinct roles in xenophagy? Potentially, the artificial model that has been used in the last decade to study mitophagy is not good enough to detect their specific roles. It would be of interest to study mitophagy in an *in vivo* setting in mice or other organisms using the different tools that have recently become available (McWilliams 2016, Sung 2016, Sun 2016).

1.8 Redox signalling

1.8.1 ROS formation

ROS are a damaging, highly reactive by-product of mitochondrial respiration, oxidative protein folding and other aerobic metabolic reactions, but can also be formed upon exposure of cells to environmental agents such as UV, smoke, drugs (such as paraquat) and xenobiotics (Halliwell and Cross, 1994). In the last years, it has been established that less-reactive ROS, in particular H_2O_2, can act as signalling molecules (Veal and Day, 2011), however when levels are too high they can be damaging to (mitochondrial) DNA, proteins and lipids (Sies, 2017). In the case of ROS produced by mitochondria, it can result in mitochondrial dysfunction and even more ROS generation, resulting in a vicious cycle. Because of their damaging role, but also their role in redox signalling, ROS are implicated in ageing and the pathology of many conditions, such as cancer, inflammatory, cardiovascular and neurodegenerative diseases (Halliwell, 2007, Gutteridge and Halliwell, 2000, Winterbourn, 2008).

In addition to the ROS formed by external cues and internal by-products of inefficient mitochondrial respiration, it has now become clear that cells can generate ROS as a regulated physiological process (Nathan, 2003). In addition to mitochondria, enzymes such as NOXs (NADPH OXidases), xanthine oxidase, nitric oxide synthase and peroxisomal proteins generate ROS (Halliwell, 2007). When these processes are dysregulated aberrant ROS is formed, which causes pathology. Cells have several defensive mechanisms in place to cope with these high ROS levels, these will be discussed in section 1.8.4.

1.8.2 Redox sensitive cysteines

The side chain of a cysteine residue contains a terminal thiol (-SH) group (Figure 9). This thiol group can be a target of oxidation by ROS resulting in different post-translational modifications, among these are reversible S-nitrosylation (SNO), sulfhydration (SSH), S-glutathionylation (RS-SG), disulphide bonds (RS-SR'), sulfenylation (SOH) and largely irreversible modifications such as as sulfinic acid (SO_2H) and sulfonic acid (SO_3H).

Cysteines are the least common amino acid, yet often is found as a highly conserved residue within functional domains and catalytic sites (Marino and Gladyshev, 2010). Not all cysteines are equally sensitive to be oxidised and the formation of one of these post-translational modifications depends on different factors, like the reactivity of the

cysteines (pK_a), the charge of the nearby amino acid residues, hydrogen bonding and steric factors. The pK_a value refers to the tendency of a thiol group to be deprotonated over a range of pH values and the actual pK_a is the pH when 50% of the sites are protonated. For cysteines this value is approximately 8.5, however, reactive cysteines often have a lowered pK_a due to other factors, such as a protein environment (positively charged residues) that stabilises the negatively charged thiol group (Lutolf et al., 2001, Poole, 2015). With a lowered pK_a the thiol group is deprotonated at physiological pH, which enhanced its reactivity. Recently, algorithms have been made to predict which cysteines within a protein are likely to be oxidised, with an accuracy between 70-80% correct predictions (Wang et al., 2016c).

1.8.3 Redox signalling via disulphide bond formation

The oxidation of cysteines can act as a redox switch to modulate cell signalling, protein folding and enzymatic function (Antelmann and Helmann, 2011, Paulsen and Carroll, 2013). The formation of disulphide bonds (also called disulphide bridges or S-S bonds) involves the coupling of two thiol groups and are usually formed from the oxidation of the sulfhydryl (-SH) groups of cysteines (Figure 9). The cysteines can be located within one protein, resulting in an intermolecular disulphide bond, which often attributes to stabilising the secondary structure of a protein. On the other hand, a disulphide bond can be formed between two peptides locating in two different proteins, which is called an intermolecular disulphide bond. Intermolecular disulphide bonds can promote the formation of hetero- or homo- protein dimers or oligomers.

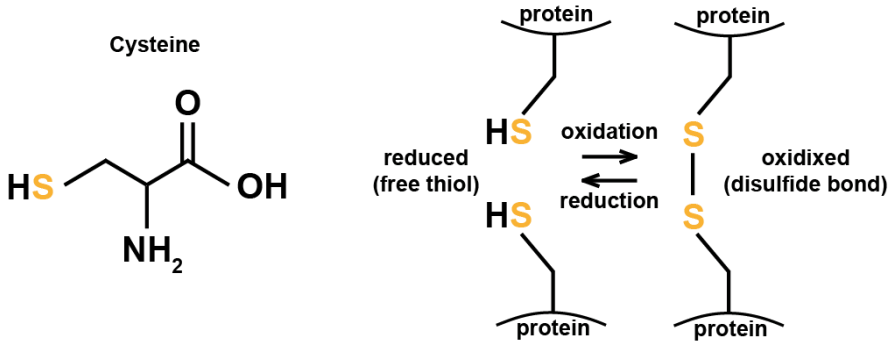

Figure 9 Diagram showing the formation of disulphide bonds between two cysteines.

On the left the structure of the sulphur-containing (yellow) amino acid cysteine is depicted. Cysteines are very reactive and are important for the formation of disulphide bonds, depicted on the right. Free thiols upon oxidation can form disulphide bonds, which are reversible and can be reduced by for example the thioredoxin system.

As mentioned before, not all cysteines are as reactive as others are. H_2O_2 reacts with the thiol groups, but only a minority of proteins have cysteines with low pK_a, and thus are likely to be targets for oxidation. Prxs (Peroxiredoxins) are a family of proteins that contain thiolates with very reactive cysteines and thus reduce H_2O_2. The rate constant of Prxs is very high and they are highly abundant, therefore most H_2O_2 in the cell reacts with these proteins (Wood et al., 2003). GSH (Glutathione) also reacts with a small proportion of H_2O_2 and other proteins are considered non-competitive, based on kinetics and abundance (Winterbourn, 2008). Several mechanisms have been suggested for how redox-regulated proteins can compete with Prx. For example, localisation can play a role, where redox-regulated proteins face extremely high H_2O_2 concentrations, making direct oxidation feasible. Prxs can also be inactivated by a phosphorylation, thereby allowing the accumulation of H_2O_2 and oxidation of redox-regulated proteins (Woo et al., 2010). Another theory (called the floodgate theory) involves the inactivation of Prxs by hyperoxidation to sulfinic acids, which is a mainly irreversible modification, thereby allowing other redox-regulated proteins to be oxidised by H_2O_2 (Wood et al., 2003). Furthermore, redox regulated proteins can be indirectly oxidised by H_2O_2 via Prxs; this mechanism involves a physical interaction between the Prx and the redox regulated protein, for example Prx2 and STAT3 (Signal Transducer and Activator of Transcription 3), which allows the transfer of oxidising equivalents between the two (Sobotta et al., 2015). Interestingly, Prx1 was also shown to interact with several redox-regulated proteins, including PTEN (Phosphatase and TENsin homolog) and ASK1 (Apoptosis Signalling Kinase 1), resulting in thiol-disulphide exchange (Cao et al., 2009, Jarvis et al., 2012, Turner-Ivey et al., 2013), this potentially could be a common redox-signalling pathway, however more research is required (Latimer and Veal, 2016).

1.8.4 The antioxidant system

To prevent that ROS reach damaging levels, ROS can be buffered by the antioxidant system. These antioxidants also serve an essential role in redox signalling, because they can reduce disulphide bonds to a free thiol, which is essential for redox-regulated proteins to function as a switch to regulate protein function.

Primary enzymes, such as glutathione peroxidase, SOD and catalase and Prxs protect the cells against oxygen radicals. SOD is a metalloenzyme that promotes the dismutations of superoxide to oxygen and H_2O_2 (Figure 10). There are three human superoxide dismutases; the cytosolic and mitochondrial SOD1; mitochondrial SOD2

and secretory SOD3. The produced H_2O_2 can be reduced by glutathione peroxidase or catalase.

Glutathione peroxidase, which needs selenium as a cofactor, reduces peroxides to water or alcohol (Figure 10). This reaction involves GSH, which is an abundant tripeptide and upon oxidation forms a disulphide bridge, resulting in dimerization. The oxidised dimer is also called to GSSG (Hansen et al., 2009). The secondary enzymes do not neutralise ROS directly, but play a supportive role. In the case of glutathione peroxidase, GR (Glutathione Reductase) is the secondary enzyme, as it reduces GSSG, which then is ready to react with free radicals again (Figure 10) (Deponte, 2013). Peroxisomal catalase is another enzyme important for the reduction of H_2O_2, which in this case is converted to water and molecular oxygen (Figure 10). The previously mentioned Prxs also scavenge H_2O_2 and thus function as an antioxidant. Humans have 6 Prx isoforms, which have a different cellular distribution (Rhee et al., 2001).

Trx (Thioredoxin) is a highly conserved protein family that reduces target proteins, including Prxs and GSSG. In order to do so, it transfers a disulphide bond to its reactive cysteine pair to form an intermolecular disulphide bond, which then can be reduced by Trx-reductase (Figure 10) (Lee et al., 2013). Humans have two Trx isoforms, a cytosolic expressed Trx 1 and a mitochondrial expressed Trx 2.

These key cellular antioxidants in concert regulate redox homeostasis. Dysregulation of any of these components results in an impaired redox signalling and oxidative stress, which has been implicated in ageing and various diseases, such as cancer, neurodegenerative and immunological diseases (Uttara et al., 2009).

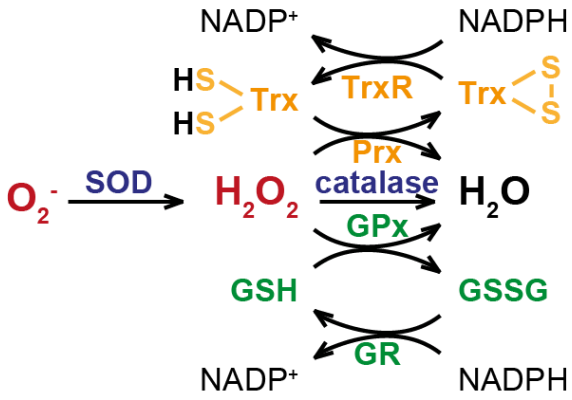

Figure 10 Diagram of the antioxidant system.

Enzymes involved in the first line of defence to protect against oxygen radicals (red). The primary enzymes: SOD (SuperOxide Dismutase), GPx (Glutathione Peroxidase), and Prx (Peroxiredoxin) and catalase converts O_2^- into H_2O. Secondary enzymes involved GR (Glutathione Reductase) and TrxR (Thioredoxin Reductase), which reduce GSSG (oxidised glutathione) and oxidised Trx (S-S) respectively.

1.9 Autophagy deficiency and mitochondrial dysfunction

Mitochondria are known to be the powerhouse of the cell and are responsible for aerobic ATP production. Furthermore, these double-membraned organelles are involved in calcium signalling, cell death and metabolite synthesis. Mitochondrial dysfunction is linked to a range of diseases, including neurodegenerative diseases, cardiomyopathies, cancer, diabetes, muscular diseases and premature ageing (Vafai and Mootha, 2012, Nunnari and Suomalainen, 2012).

The mitochondria are highly dynamic organelles forming a network which depends on the interplay of fusion and fission. Structurally, mitochondria consist of an inner and outer mitochondrial membrane. Energy production via the ETC (Electron Transport Chain) takes place in the IMM. The space between the IMM and OMM is called the intermembrane space. The IMM forms cristae, thereby providing a large surface area to perform electron transport. The matrix contains the mitochondrial enzymes that are responsible for the TCA, (TriCarboxylic Acid cycle, also known as the citric acid cycle or Krebs cycle), which produced NADH (reduced Nicotinamide Adenine Dinucleotide) and $FADH_2$ (reduced Flavin Adenine Dinucleotide), which function as electron carriers. The TCA cycle generates ATP through the oxidation of acetate derived from carbohydrates, fats and proteins into CO_2 (Carbon diOxide) (Watt et al., 2010). During this cycle, NAD^+ and FAD are reduced to NADH and $FADH_2$, which are donated to the ETC. NADH and FADH do not only originate from the TCA cycle, but can also be produced during glycolysis and fatty acid oxidation (Houten and Wanders, 2010).

1.9.1 The electron transport chain

The ETC consists of four complexes (I-IV), which are responsible for the oxidation of NADH and $FADH_2$ (Figure 11). Most enzymes of the ETC are large multi-subunit protein assemblies containing many redox cofactors. This complexity has made it hard to understand how the ETC functions. However, over the last decades the basic functional principles have been elucidated.

NADH enters the ETC through complex I (NADH:ubiquinone oxidoreductase) and $FADH_2$ enters the ETC through complex II (succinate dehydrogenase). The electrons are then transferred to ubiquinone (CoQ, Q, coenzymeQ), followed by complex III (cytochrome C oxidoreductase), cytochrome C and complex IV (Cytochrome c oxidase), which transfers the electrons to oxygen as the final electron acceptor. Membrane-embedded ubiquinone and soluble cytochrome C mediate electron transport between complexes. The oxidation is coupled to the pumping of protons by CI, III and IV from the matrix into the IMS (Inter Membrane Space), creating the $\Delta\Psi m$ for the synthesis of ATP by the ATPase (ATP synthase/ complex V) (Figure 11) (Okuno et al., 2011, Watt et al., 2010, Sazanov, 2015). This respiratory process is called OXPHOS (OXidative PHOSphorylation). OXPHOS complexes function most efficiently in supercomplexes of which the respirasome (Acin-Perez et al., 2008), consisting of complex I, 2x complex III and complex IV is the most common supercomplex, but complex IV copies can vary. Recently, two independent groups determined the structure of the respirasome, which revealed that subunits within the different complexes interact (Gu et al., 2016, Letts et al., 2016). Multiple interactions were especially observed between complex I and III, explaining the increased stability of complex I in the supercomplex (Letts et al., 2016). Furthermore, the tight arrangements are thought to optimize the use of available substrates and the efficiency of electron transfer, but also prevent ROS production (Letts et al., 2016, Maranzana et al., 2013, Lapuente-Brun et al., 2013).

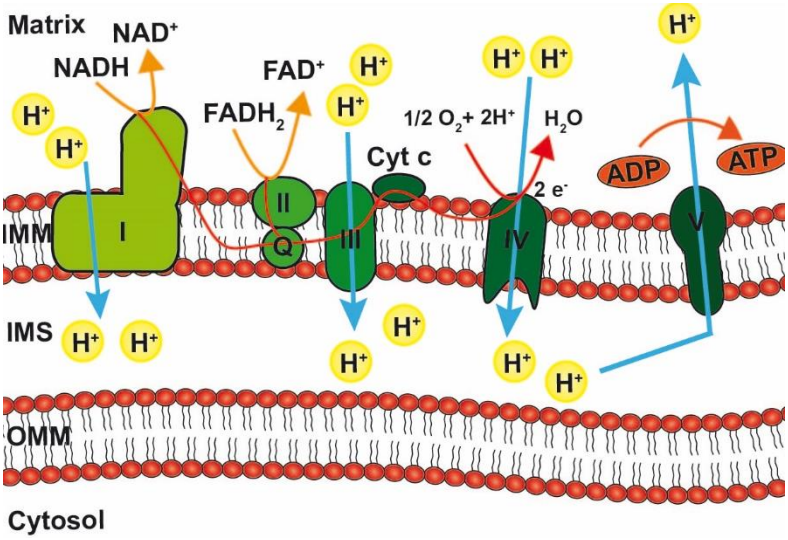

Figure 11 Schematic diagram of the mitochondrial electron transport chain (ETC) and ATP synthase.

The red line shows the path of the electrons and the blue line the path of the protons that are pumped from the matrix into the inter membrane space (IMS). Electrons are transferred from NADH into complex I, and $FADH_2$ into complex II, via complex III, cytochrome c and complex IV, which transfers the electrons to oxygen. During this process, protons are pumped into the IMS, creating a proton gradient. This gradient is used by complex V, the ATP synthase, to phosphorylate ADP, thereby producing ATP.

1.10 Mitochondrial quality control

A decline in mitochondrial quality control has been associated with ageing and correlates with the development of several age-related diseases. For example, ageing is accompanied by a decline in mitochondrial enzyme activity, decreased respiratory capacity per mitochondrion and increased ROS (Sun et al., 2016).

Mitochondrial maintenance is a balance between biogenesis and the different mechanisms that provide quality control, resulting in a healthy functional pool of mitochondria. Because mitochondria produce ROS, resulting in protein damage, the antioxidant system can be seen as the first mechanism to provide mitochondrial quality control (Section 1.8.4), followed by chaperones and proteases that promote protein folding and degradation, respectively. When unfolded, misfolded or unassembled proteins accumulate beyond folding capacity, the UPRmt (Mitochondrial Unfolded Protein Response) can be initiated. This pathway results in transcriptional up-regulation of chaperones and antioxidants, and thereby tries to recover mitochondrial protein homeostasis. When this pathway is not sufficient, proteasomal degradation and autophagy can grant further mitochondrial quality control.

1.10.1 Mitochondrial proteases

Several mitochondrial proteases and antioxidants have been identified. In the mitochondrial matrix, three major ATP-dependent AAA proteases, Lon, ClpXP and the membrane bound m-AAA play a critical role in mitochondrial protein homeostasis (Figure 12) (Voos et al., 2013). The Lon (also known as LON and LON) protease forms a barrel-shaped homo-hexamer and has been shown to play an important role in degrading oxidised proteins, such as aconitase, COX4I1 (Cytochrome C Oxidase Subunit 4I1), Trx2 and TFAM (Bota et al., 2002, Bota and Davies, 2016). Additionally, Lon functions as a chaperone for ETC complex assembly (Bota et al., 2002). The ClpXP complex consists of two hexamer ClpX lids, that is important to unfold target proteins, and two heptamer ClpP barrels that function as proteolytic chambers (Gersch et al., 2016, Voos, 2009). To date only one ClpXP substrate has been identified, being Noa1 (Al-Furoukh 2014). m-AAA is a protease that is anchored in the IMM and faces the matrix. m-AAA consists of either homo-oligomers of AFG3L2 (ATPase Family Gene 3-Like 2) or hetero-oligomers of AFG3L2 and paraplegin (also known as SPG7) (Atorino et al., 2003, Levytskyy et al., 2016) and is primarily involved in the degradation of ETC subunits. m-AAA assembles with prohibitins (Phb 1 and 2) in large supercomplexes in the IMM and modulate the degradation of non-assembled proteins (Steglich et al., 1999). i-AAA is an IMM anchored protease that faces the IMS and functions as a homo-hexamer (Scharfenberg et al., 2015). Substrates of i-AAA include ETC subunits, proteins involved in lipid transport and synthesis and IMM dynamics (Song et al., 2007, Stiburek et al., 2012, Potting et al., 2010). In addition to the ATP-dependent proteases, mitochondria are also equipped with ATP-independent proteases, such as Oma1, PARL (Presenilins-Associated Rhobiod Like) and HTRA2 (HTrA serine peptidase 2, also known as Omi), which reside in the IMM (Levytskyy et al., 2016, Quiros et al., 2015).

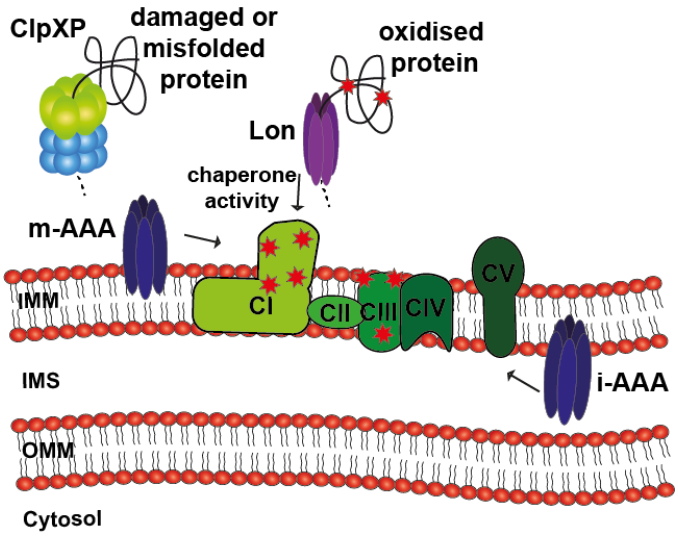

Figure 12 Schematic diagram of the main mitochondrial proteases.

ClpXP, Lon and m-AAA are the proteases that reside in or face the mitochondrial matrix and degrade damaged, misfolded and oxidised proteins, whilst i-AAA faces the IMS. m-AAA and i-AAA are important for the degradation of non-assembled proteins and ETC subunits, respectively. Red stars depict oxidative damage.

1.10.2 Mitochondria As Guardian In Cytosol (MAGIC)

An interesting theory was reported recently involving the degradation of cytosolic aggregate prone proteins by mitochondrial proteases. In yeast, upon a heat shock, aggregates containing cytosolic as well as mitochondrial proteins form. The cytosolic proteins can be co-imported by mitochondrial proteins via the mitochondrial import machinery (Ruan et al., 2017). Hsp104 (Heat Shock Protein 104) , but not Hsp70, is required for this process, potentially to unfold and disaggregate the proteins before mitochondrial import (Ruan et al., 2017). It has to be determined if such a pathway exists in mammalian cells as well. In several neurodegenerative diseases, aggregate prone proteins have been reported to accumulate in mitochondria, resulting in mitochondrial dysfunction (Schapira, 2012, Li et al., 2007, Devi et al., 2008). Thus, this accumulation of disease proteins could be a result of more general cytosolic proteotoxic stress.

1.10.3 Mitochondrial unfolded protein response (UPRmt)

The UPRmt is a recently identified retrograde signalling pathway that is important for the maintenance of mitochondrial quality. This pathway, that is very similar to the extensively studied UPRer (ER Unfolded Protein Response), promotes the recovery of dysfunctional mitochondria. UPRmt has been studied mostly in *C.elegans*, where mitochondrial dysfunction, resulting in increased UPRmt was shown to extend life span

(Dillin et al., 2002, Durieux et al., 2011). It is thought that modest mitochondrial dysfunction leads to life span extension, even though this seems counterintuitive (Yee et al., 2014). Several triggers have been shown to induce the UPRmt pathway in *C.elegans*. For example, inhibition of mitochondrial transcription, which results in an imbalance of mitochondrial and nuclear encoded proteins, and the accumulation of unassembled proteins initiate UPRmt (Yoneda et al., 2004). These accumulated unfolded proteins are digested by ClpP (Clp protease proteolytic subunit) into small peptides, which are actively exported across the IMM and then diffuse through the OMM to the cytosol (Haynes et al., 2007, Haynes and Ron, 2010). The peptides in the cytosol trigger the nuclear translocation of a transcription factor ATFS-1 (Activating Transcription Factor associated with Stress 1), which results in a transcriptional response. This response involves genes that encode for mitochondrial chaperones, antioxidants, but also promotes a rewiring of metabolism by increasing glycolysis and amino acid catabolism genes, whilst repressing TCA cycle and OXPHOS genes (Nargund et al., 2015, Nargund et al., 2012). ATFS-1 is a transcription factor that contains a nuclear and mitochondrial localisation signal. In normal conditions, ATFS-1 it is continuously imported into mitochondria, where it is degraded. However, during mitochondrial stress, a reduced $\Delta\psi M$ prevents the efficient import of ATFS-1 into the mitochondria. Instead, it accumulates in the cytosol, and due to its nuclear localisation signal, it translocates to the nucleus (Nargund et al., 2012). A portion of ATFS-1 also accumulates within mitochondria, where it binds mtDNA and potentially inhibits transcription (Nargund et al., 2015). It is not clear how this is mechanistically regulated and how the accumulation of cytosolic peptides regulates ATFS-1 translocation to the nucleus. Two more transcription factors (Dve1 and Ubl5) were identified to be involved in UPRmt in *C.elegans*. ClpP triggers the activation of Ubl5 (UBiquitin-Like protein 5), which acts as a coactivator of the transcription factor Dve1 (Defective proVEntriculus in *Drosophila*), which bind to the promoters of chaperones, such as Hsp60 (Haynes et al., 2007, Benedetti et al., 2006). Less is known about the UPRmt in mammals; however, some progress has been made in the last years. Evidence suggests that the UPRmt is conserved in mammals, where mitochondrial proteotoxic stress also induces transcription of mitochondrial chaperones and proteases (Zhao et al., 2002, Martinus et al., 1996). Similar triggers were found to induce the UPRmt, such as mitonuclear protein imbalance, which results in the up-regulation of ClpP and heat shock proteins, which are often used as an indicator for the UPRmt induction (Houtkooper et al., 2013). It was shown that ClpXP plays an important role in the UPRmt, indeed overexpression

of ClpX is sufficient to initiates the UPRmt (Al-Furoukh et al., 2015). Peptides produces by ClpP activate two kinases (JNK (c-Jun N-terminal Kinase) and PKR (Protein Kinase R)), which up-regulate the transcription factor CHOP (C/EBP-HOmologous Protein)(Figure 13). CHOP was shown to primarily mediate this ClpX-induced UPRmt and also transcription factors Ubl5, SatB2 (Special AT-rich sequence-Binding protein 2, mammalian homolog of Dve1) and ATF5 (Activating Transcription Factor 5) levels depend on ClpX (Al-Furoukh et al., 2015). Recently, ATF5, which has a lot of homology with ATFS-1, was found to localise to mitochondria, and upon mitochondrial stress ATF5 plays a protective role by inducing the UPRmt (Figure 13) (Fiorese et al., 2016). If misfolded proteins accumulate in the IMS, an alternative UPRmt is induced, involving the protease HTRA2 (also known as Omi) and the transcription factor Nrf1 (Radke et al., 2008, Papa and Germain, 2011).

In addition, it was found that the mammalian UPRmt not only regulates gene expression, but in response to acute folding stress also represses transcription and translation (Munch and Harper, 2016). In yeast another interesting pathway, called UPRam (UPR Activated by protein Mistargeting) was discovered, which acts in response to mistargeted proteins due to mitochondrial import defects. This pathway was shown to up-regulate proteasome activity in response to the amount of mislocalised mitochondrial precursor proteins in the cytosol (Wrobel et al., 2015). This multifaceted response helps to recover the mitochondrial protein homeostasis.

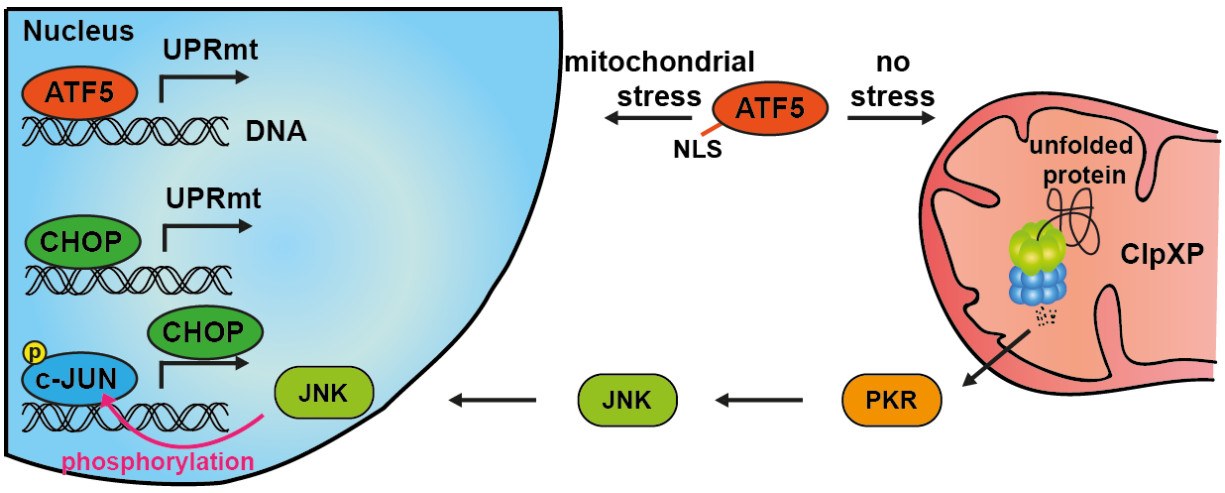

Figure 13 Schematic model of the UPRmt in mammals.

Unfolded proteins in mitochondria are degraded by ClpXP into small peptides, which activate PKR and JNK. JNK phosphorylates c-JUN, resulting in CHOP expression, which induces the UPRmt. ATF5 is an transcription factor, which upon mitochondrial stress was suggested to translocate to the nucleus to induce the UPRmt.

1.10.4 Mitochondrial-associated degradation (MAD)

The ubiquitin-proteasome system (UPS) is responsible for the degradation of misfolded proteins from several cellular compartments to maintain protein homeostasis. Soluble proteins are easily targeted to the proteasome for degradation; however, the degradation of OMM proteins requires an additional step, because they need to be extracted from the membrane.

In yeast, MAD is a UPS (Ubiquitin-Proteasome System) driven pathway responsible for the degradation of OMM proteins via the AAA-ATPase VCP (also known as Cdc48/p97). VCP removes ubiquitinated proteins from the mitochondrial membrane and escort the substrates to the proteasome, where they are degraded to small peptides and this pathway is conserved in mammals.

As discussed previously, mitophagy can be triggered by the loss of ΔψM, which, via the kinase PINK1 and the Ub ligase Parkin, results in the ubiquitination of OMM proteins. These ubiquitinated proteins are recognised by autophagy receptors, followed by the recruitment of the autophagosomal machinery and the formation of the autophagosome around the mitochondrion and subsequent lysosomal degradation. Interestingly, VCP and UPS components, including the E3 ligating-enzyme HUWE1 (HECT, UBA and WWE domain containing 1, E3 ubiquitin ligase) are also recruited to these ubiquitinated mitochondria and target a subset OMM proteins, such as Mfn1 and 2 (MitoFusiN 1 and 2) for degradation by the 26S proteasome (Karbowski and Youle, 2011, Heo et al., 2010, Tanaka et al., 2010, Cohen et al., 2008, Taylor and Rutter, 2011). The recruitment of the highly conserved ubiquitin-directed segregase VCP, which forms a hexameric ring-like structure, depends on Vms1 (Heo et al., 2010, Braun et al., 2015). VCP then extracts proteins from the membrane and recently Doa1 was identified as an adapter that recognises the OMM substrates in yeast (Figure 14) (Wu et al., 2016b). It is not clear if the highly conserved mammalian orthologue PLAA (PhosphoLipase A2 Activating protein) has the same function.

Finally, the proteins are targeted to the 26S proteasome. The 26S proteasome is a barrel-shaped proteolytic organelle that consists of a 20S core particle that can be capped with one or two 19S regulatory particles. Ubiquitinated proteins are recognised by the 19S subunit, followed by deubiquitination, unfolding and translocation to the proteolytic chamber of the 20S core particle (Livneh et al., 2016, Beck et al., 2012). To

date not many MAD substrates have been identified, thus more investigation is needed to identify these.

Interestingly, mitochondrial metabolism has been linked to UPS activity. When mitochondrial respiration was genetically impaired, the cytosolic UPS was less active. This phenotype could be prevented by antioxidants, suggesting that it is ROS dependent (Segref et al., 2014). This correlation seems counterintuitive, as upon mitochondrial stress OMM proteins are degraded via the UPS. However, decreasing the cytosolic UPS activity could tip the balance towards degradation of OMM proteins and strengthen the capacity of the UPS at the OMM.

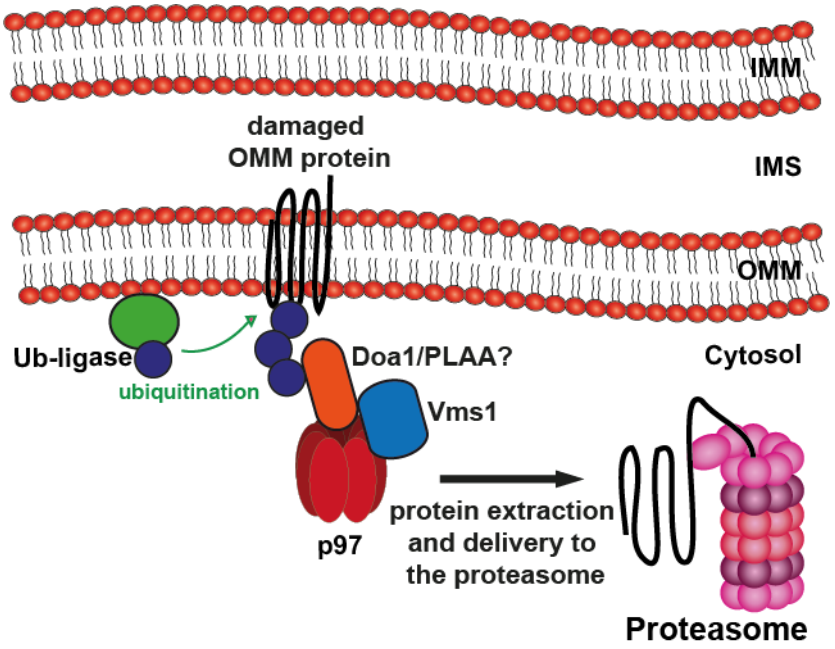

Figure 14 Schematic diagram of mammalian mitochondrial-associated degradation (MAD).

Damaged mitochondrial membrane proteins are presented at the OMM, where they are ubiquitinated by HUWE1 and Parkin. Doa1 in yeast, and potentially PLAA in mammals, binds to the ubiquitinated protein. Vms1 and VCP (p97) are recruited and extract the protein from the OMM, followed by the proteasomal degradation of the OMM protein.

1.10.5 Mitophagy

When the selective removal of damaged oxidised mitochondrial proteins is not sufficient to restore mitochondrial function, cells can use a more robust mechanism to eliminate mitochondria, called mitophagy (Section 1.5). This is a last resort before the cell decides to go into apoptosis.

Many studies revealed crosstalk between these described quality control pathways in maintaining mitochondrial health. For example, it has been suggested that the degradation of OMM proteins via MAD is required for downstream mitophagy (Yoshii et al., 2011, Chan et al., 2011), because the degradation of mitofusins via the MAD pathway facilitates mitochondrial fragmentation and promotes mitophagy (Tanaka et al., 2010). Furthermore, it was shown that among the many Parkin targets, several proteasome subunits and VCP were found (Sarraf et al., 2013). Future research could elucidate the triggers, interdependence and timing of these different mitochondrial quality control events in order to keep a healthy mitochondrial pool that matches the cellular energy demand.

1.11 Mitochondrial complex I

The mitochondrial complex I catalyses the transfer of two electrons from NADH to ubiquinone (Q) to form ubiquinol (QH_2), and simultaneously translocates four protons across the mitochondrial membrane. Complex I is a reversible machine that can also use $\Delta\Psi m$ and ubiquinol to reduce NAD^+.

$NADH + H^+ + Q + 4H^+_{in} \rightarrow NAD^+ + QH_2 + 4H^+_{out}$

1.11.1 Complex I structure

A 5 Å high-resolution X-ray structure of complex I from Bos Taurus (a close relative to the human enzyme) was determined (Vinothkumar et al., 2014), followed up by a 6.8 Å X-ray crystallographic analysis of the membrane bound domain (Zhu et al., 2015). The L-shaped mammalian complex I is a very complex structure containing 44 different subunits, of which 7 of the membrane bound core subunits (ND1-6 and 4L) are mitochondria-encoded, while the others are nuclear-encoded. The complex consists of a membrane bound domain, which comprises the proton-translocating P-module and a mitochondrial matrix-facing arm, containing the NADH-oxidizing dehydrogenase module (N-module) and the Q-module (Figure 15). The N-module provides electrons from the FMN (Flavin MonoNucleotide) into the chain of Fe-S clusters. The Q-module transfers the electrons from the Fe-S clusters to ubiquinone. The P-module is divided into two modules called P_P and P_D (proximal and distal proton pomp) and the P_D contains the proposed proton-translocating subunits ND4 and ND5 (Figure 15) (Hunte et al., 2010). At the moment it is thought that ubiquinone reduction, but not discrete electron transfer steps within the Fe-S clusters, triggers proton pumping (Sazanov, 2015, Wirth et al., 2016).

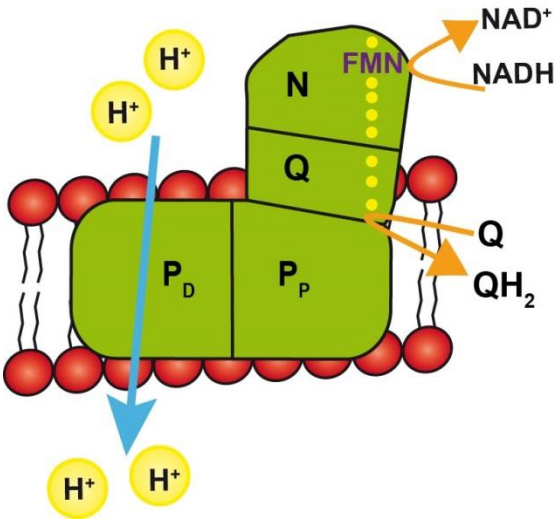

Figure 15 Architecture of mitochondrial complex I.

The matrix arm of complex I consists of the N- and Q-modules. Electrons are transferred from NADH to FMN. Fe-S clusters (yellow circles) transfer electrons from FMN to ubiquinone. The membrane bound core consists of P_P (proximal) and P_D-(distal) modules. P_D contains the proposed proton-translocating subunits (blue arrow). Modified after (Kmita and Zickermann, 2013).

1.11.2 ROS production via complex I

Mitochondrial complex I is a major source of ROS (Murphy, 2009) and these have been implicated in many human diseases, including several neurodegenerative diseases (Viscomi et al., 2015). In the last decade a lot of research has been done to elucidate the exact site of ROS production and how this can modulated. To prevent this excessive ROS leakage, complex I exhibits a regulatory switch between an active and deactive form (A and D-form). When there is a lack of substrate, the complex can convert into the D-form via an S-nitrosation of a cysteine in the ND3 subunit. The A/D transition is a protective mechanism to prevent ROS formation by reverse electron flow of the enzyme during myocardial ischemia/reperfusion in mice (Methner et al., 2014).

Furthermore, the assembly of complex I into respirasomes has been shown to prevent ROS production, due to more efficient transfer of electrons through the complexes. In different cell types with different bioenergetics preferences, the ETC is organized differently. For example, when comparing neurons and astrocytes it became apparent that in neurons, which rely on mitochondrial respiration, complex I was embedded into the respirasome more than in astrocytes, resulting in more efficient respiration and less ROS production (Lopez-Fabuel et al., 2016). On the contrary, astrocytes rely more on glycolysis and these cells have more free complex I, which correlates with more ROS production. NDUFS1 was shown to be essential for the assembly of complex I into the

supercomplex and was more highly expressed in neurons compared to astrocytes (Lopez-Fabuel et al., 2016).

At least 11 ROS producing sites linked to substrate oxidation and respiration have been identified, of which two main sites locate at complex I, being site I_F, which is the Flavin-binding site and I_Q, the Q-binding site (Brand, 2016). Rotenone is a well-known complex I inhibitor and binds to the I_Q site and thereby prevents electrons flowing back from ubiquinone into complex I (Reverse Electron Transport, RET) (Brand, 2016), but more recently also more specific drugs were developed which specifically bind site I_F and I_Q without effecting respiration (Brand et al., 2016). Preventing ROS production at site I_Q by using one of these inhibitors protected against ischemia-reperfusion injury in perfused mouse heart (Brand et al., 2016). This suggests that preventing aberrant ROS production at this site of complex I can be protective, however, it must be noted that ROS also function as an important signalling molecule. Scialò *et al*. elegantly demonstrated that RET, resulting in ROS production specifically through complex I extends fly lifespan (Scialo et al., 2016). Thus, low levels of ROS produced by I_Q can be beneficial for animal lifespan due to its signalling function, whilst ROS produced by I_Q in stress conditions can be highly damaging and result in cell death.

1.11.3 Turnover of complex I

Because complex I is important in redox signalling, but also potentially dangerous for the cells, its quality control is of high importance. Therefore, it is surprising that to date not much is known about how complex I is turned-over. Complex I outside of the respirasome or other supercomplexes is less stable and produces more ROS (Schagger et al., 2004, Guaras et al., 2016). Guaras *et al*. beautifully demonstrate a link between complex I degradation and the ubiquinone redox status. Preventing the binding of ubiquinone and the transfer of electrons from ubiquinone to complex I, restores complex I stability in a complex IV or Cytochrome C knock-out background (Guaras et al., 2016). They found that superoxide produced via RET destabilises complex I by causing oxidative damage to the complex. When cells were switched to hypoxic conditions, complex I was destabilised. The least stable group were the subunits located in the peripheral arm, whilst the membrane arm was more stable, this correlated to the number of cysteines of the different subunits being oxidised. Interestingly, other mitochondrial respiratory complexes were not destabilised, showing that reoxygenation results in an isolated complex I loss (Guaras et al., 2016). Oxidation of cysteines of the different complex I subunits (especially the ones that

stabilise iron-sulfur clusters) could result in the destabilisation of iron-sulfur clusters and trigger the disassembly of complex I, followed by the degradation of the individual subunits (Guaras et al., 2016).

Recently, the first evidence was presented for the selective degradation of the ROS producing N and Q modules of complex I by the mitochondrial matrix localised proteases Lon and ClpP (Pryde et al., 2016). Interestingly, preventing ROS production by I_Q prevented degradation of the N and Q modules (Pryde et al., 2016), suggesting that RET results in oxidative damage in complex I, which could be the trigger for degradation. How Lon and ClpP recognise damaged complex I is not entirely clear, but it was proposed that Lon can specifically recognise oxidised peptides and Fe-S clusters, which could act as ROS sensors (Pryde et al., 2016).

1.11.4 Metabolism and autophagy in neurons

Neurons heavily rely on mitochondrial respiration to meet their extremely high-energy demands, demonstrated by the fact that the brain is responsible for 20% of all oxygen consumption (de Castro et al., 2010). During differentiation from neuronal progenitor cells into neurons, a few rearrangements result in a switch from aerobic glycolysis to mitochondrial respiration (Zheng et al., 2016, Agathocleous et al., 2012). Firstly, LDHA (Lactate DeHydrogenase A) is down-regulated, which is a key switch to turn off aerobic glycolysis. Secondly, there is a shift from PKM2 (Pyruvate Kinase isozyme M2) to PKM1 expression and thirdly, HK2 (HexoKinase2), GLUT1 (GLUcose Transporter 1) and GLUT3 glucose transporters reduce cellular glucose import, thereby reducing glycolysis. Surprisingly, even though mitochondrial mass increases during differentiation, the expression of TCA and mitochondrial respiratory genes do not increase (Zheng et al., 2016). Even though neurons rely heavily on mitochondrial respiration, its ability to withstand oxidative stress is limited. Amongst other things, this is due to relatively low levels of antioxidants and more endogenous ROS generation via specific reactions and high iron levels in certain areas of the brain.

Neurons have highly polarised axons and dendrites in which many macromolecules are synthesised, delivered and degraded for their dynamic functions in synaptic growth and synaptic activity. Since neurons are post-mitotic cells that cannot dilute their toxic waste by cell division, autophagy-dependent cellular quality control is of essential importance. Indeed, autophagy dysfunction is known to cause neurodegeneration in neurons, suggesting that it may regulate neuronal homeostasis (Hara et al., 2006).

1.12 Mitochondrial dysfunction and autophagy deficiency in neurodegeneration

1.12.1 Alzheimer's disease (AD)

AD is the most common form of dementia and affects nearly 44 million people worldwide and is characterised by the progressive loss of cholinergic neurons in the cerebral cortex and accumulation of extracellular amyloid plaques and intracellular neurofibrillary tangles, leading to severe behavioural, motor and cognitive impairment (Salawu et al., 2011). The most common variant of AD usually starts after age 65. Most late onset cases occur sporadically, however some genes have been identified that enhance the risk (Cuyvers and Sleegers, 2016). The most common gene associated with late-onset AD is *APOE* (Apolipoprotein E), which has three forms, being E2, E3 and E4. The *APOE4* form appears to increase the risk to develop AD (Cuyvers and Sleegers, 2016).

Changes in mitochondrial appearance precedes the appearance of neurofibrillary tangles and for that reason mitochondrial dysfunction has been implicated in disease pathogenesis (Hirai et al., 2001, Garcia-Escudero et al., 2013). Overexpression of APP, leading to the accumulation of amyloid plaques, induced a decrease in ATP production, decreased $\Delta\Psi m$, decrease complex IV activity and increased ROS production (Grimm et al., 2016). It is not clear what is the actual causative factor, but recently, it was suggested that ROS can trigger the formation of amyloid plaques (Leuner et al., 2012).

Another AD hallmark are the previously mentioned neurofibrillary tangles that consist of abnormally hyperphosphorylated tau. Mice with a mutation in FTDP-17 (FrontoTemporal Dementia with Parkinsonism-17) leading to the production of abnormally phosphorylated tau, show decreased mitochondrial respiration and ATP levels, decreased complex I activity and increased ROS production (David et al., 2005). In another mouse study, it was confirmed that neurofibrillary tangles are linked to complex I dysfunction, whereas amyloid plaques affect complex IV activity (Rhein et al., 2009).

Impaired autophagy has been linked to AD in AD animal models as well as in AD patients. The consensus now is that in early stages of AD autophagy is induced; the expression of lysosomal proteins is increased which promotes the autophagy flux. This

happens prior to the formation of amyloid plaques and neurofibrillary tangles. However, in later stages of AD autophagy may be blocked (Rubinsztein et al., 2005).

In patients' AD brain neocortical biopsies accumulation of autophagosomes and other prelysosomal autophagic vacuoles was observed, especially in dystrophic neurites, suggesting impaired autophagosome maturation (Nixon et al., 2005). A similar phenotype was observed in PS-1/APP double transgenic mice, an AD mouse model where the accumulation of autophagosomal structures preceded the formation of amyloid plaques (Yu et al., 2005). There are several known causes of the impaired autophagy in AD, including the toxic effects of amyloid plaques on lysosomal function (Lai and McLaurin, 2012). Also the most-common genetic risk factor for late-onset AD links AD to autophagy dysfunction, as the E4 variant of APOE, a neuronal cholesterol transport protein, results in lysosomal membrane disruption and leakage (Ji et al., 2002, Ji et al., 2006). In addition, expression levels of Beclin 1, a protein important for autophagy induction, were found to be decreased in AD-affected brains (Pickford et al., 2008). It is clear that a complex interplay between autophagy deficiency, mitochondrial dysfunction and ROS play an important role in the development of AD.

1.12.2 Dementia with Lewy Bodies (DLB)

DLB is the second most frequent form of dementia and is very similar to Parkinson's disease and AD. Classical DLB is characterised by the presence of Lewy Bodies in the brainstem, limbic region and cortical areas, and the majority of patients have neurofibrillary tangles and amyloid plaques as well (McKeith et al., 2004, Walker et al., 2016). Patients have cognitive and motor symptoms, such as progressive dementia, fluctuations in mental state, visual hallucinations and Parkinsonism (McKeith et al., 2005). Due to the overlap in clinical presentation, neuropathological characteristics and genetic risk factors with AD and Parkinson's disease, DLB is often misdiagnosed, therefore studies of the underlying molecular cause of the pathology have been rare (Guerreiro et al., 2016, McKeith et al., 2005). Mutations in the *SNCA* (α-SyNuClein) were found in DLB patients and α-synuclein is the main component of Lewy bodies (Spillantini et al., 1997). Furthermore, mutations in Parkinson's disease genes *GBA* (Glucosylceramidase β), *LRRK2* and *SCARB2* (Scavenger Receptor Class B member 2) and Alzheimer's disease gene *APOE4* was linked to DLB (Geiger et al., 2016, Bras et al., 2014, Nalls et al., 2013, Berge et al., 2014). Autophagy dysfunction has been implicated in DLB; α-synuclein is a substrate for chaperone mediated autophagy and mutant forms of α-synuclein block autophagy (Cuervo et al., 2004). Overexpression of

α-synuclein impairs autophagy by inhibiting Rab1a, resulting in Atg9 mislocalisation and impaired autophagosome formation (Winslow et al., 2010). LRRK2, GBA and SCARB2 are also involved in the autophagy-lysosome pathway (Schapansky et al., 2014, Schapansky et al., 2015, Maor et al., 2016). Furthermore, as discussed before in the case of AD, DLB patients carrying the *APOE* risk variant exhibit lysosomal dysfunction (Ji et al., 2002, Ji et al., 2006).

1.12.3 Frontotemporal dementia (FTD) and Amyotrophic Lateral Sclerosis (ALS)

FTD and ALS are considered to be part of a disease spectrum. FTD is a common form of dementia and characterised by problems with behaviour, language and motor and cognitive function. Approximately 50% of the FTD cases are familial, with mutations in *GRN* (proGRaNulin), *MAPT* (Microtubule-Associated Protein Tau) and *C9ORF72* (Chromosome 9 Open Reading Frame 72) genes accounting for the majority of cases (Cruts et al., 2006, Baker et al., 2006, DeJesus-Hernandez et al., 2011, Renton et al., 2011, Hutton et al., 1998). ALS is a more progressive motor neuron disorder characterised by muscle wasting. Around 10% of the ALS cases are familial, and mutations in *SOD1* account for 20% of the fALS (Familial ALS) cases (Rosen et al., 1993).

FTD and ALS are two overlapping diseases; 15% of FTD patients develop ALS-like symptoms and 15% of ALS patients develop cognitive abnormalities that are associated with FTD (Lomen-Hoerth et al., 2002). The clinical, genetic and pathological overlap of FTD and ALS is summarised by Ling *et al*. (Ling et al., 2013). Proteins involved in common dysregulated pathways have been identified, including TDP-43, FUS, ubiquilin-2, VCP and C9ORF72 (DeJesus-Hernandez et al., 2011, Renton et al., 2011, Gijselinck et al., 2012, Deng et al., 2011, Watts et al., 2007, Johnson et al., 2010, Wang et al., 2016a). More recently mutations in the autophagy adapter protein p62, OPTN and the kinase TBK1 were identified that underlie FTD and ALS (Borghero et al., 2016, Cirulli et al., 2015, Freischmidt et al., 2015, Gijselinck et al., 2015, Le Ber et al., 2015, Rubino et al., 2012). TBK1 mutations were only associated with FTD patients who were also diagnosed with ALS. The same was observed for p62 mutations, however also a few cases have been identified with pure FTD, without ALS (Miller et al., 2015, Le Ber et al., 2013). ALS-associated p62 mutations have been discusses in more detail in section 1.4.1.

The kinase TBK1 is a key molecule in the NF-Kβ signalling pathway which is also important for autophagosome maturation and has been implicated in different selective autophagy pathways, and has mainly been studied in the context of mitophagy and xenophagy (Section 1.5 & 1.6) (Richter et al., 2016, Heo et al., 2015, Moore and Holzbaur, 2016, Radtke et al., 2007, Thurston et al., 2016, Thurston et al., 2009, Wild et al., 2011, Freischmidt et al., 2015). TBK1 phosphorylates p62 and OPTN, thereby linking these proteins in a common pathway (Richter et al., 2016, Lazarou et al., 2015, Matsumoto et al., 2011).

More genes that have been associated with ALS or ALS-FTD, such as *VCP*, *C9ORF72*, *CHMP2B* (CHarged Multivesicular body Protein 2B) and *ubiquilin-2* are indirectly or directly involved in the autophagy process, making a strong case for autophagy being a potential causative factor in the FTD and ALS pathogenesis (Maruyama et al., 2010, Pottier et al., 2015, DeJesus-Hernandez et al., 2011, Renton et al., 2011, Johnson et al., 2010, Skibinski et al., 2005, Parkinson et al., 2006, Weishaupt et al., 2016).

FTD and ALS have been linked to mitochondrial dysfunction, firstly because the identification of the genes involved in mitophagy. Secondly, based on pathogenic mutations found in the mitochondrial protein CHCHD10 (Coiled-coil-Helix-Coiled-coil-Helix Domain containing 10) (Bannwarth et al., 2014). HeLa cells overexpressing the pathogenic mutant have fragmented mitochondria, disorganised mitochondrial cristae and increased mtDNA deletions (Bannwarth et al., 2014, Genin et al., 2016). In addition to mitochondrial dysfunction, oxidative stress is considered to be a potential causative factor for the disease too. The involvement of oxidative stress is supported by the observed accumulation of oxidative damage to proteins, lipids and DNA in sporadic and familial ALS cases (D'Amico et al., 2013). The involvement of ROS was confirmed by the discovery that mutations in the cytosolic antioxidant SOD1 cause ALS (Rosen et al., 1993). Interestingly, mutant SOD1 localises to the OMM, IMS and matrix, where it forms macromolecular aggregates (Vijayvergiya et al., 2005) (Tafuri et al., 2015), causing mitochondrial toxicity (Vehvilainen et al., 2014). In a SOD1 mouse model, mitochondrial abnormalities appear before the onset on motorneuron degeneration (Kong and Xu, 1998), suggesting that mitochondria are involved in disease initiation. Furthermore, mutant SOD1 interacts with Beclin 1, thereby disrupting autophagy initiation (Nassif et al., 2014). Thus, mutant SOD1 causes oxidative stress, mitochondrial dysfunction, but also autophagy deficiency.

To conclude, according to all these findings, the current dogma is that ALS an FTD are complex multi-factorial syndromes, involving oxidative stress, mitochondrial dysfunction and autophagy deficiency, but also RNA dysregulation (specifically in ALS) (Peters et al., 2015), which is not discussed in this thesis. Furthermore, mutations in certain genes can lead to different disease phenotypes. It is not clear why different mutations in the same gene can result in different disease outcomes and phenotypes. Furthermore, not all carriers of pathogenic *TBK1* loss of function mutations develop ALS or FTD, suggesting that additional genetic variants or external factors play a role and the body has protective mechanisms in place to prevent disease onset. Identifying these protective mechanisms could be ideal therapeutic targets.

1.13 Aims

Despite identification of several genetic hereditary cases, most neurodegenerative cases have an unknown cause and a sporadic onset. Age is one of the risk factors of neurodegeneration and autophagy and mitochondrial function both decrease with age and in age-related neurodegenerative diseases (Wyss-Coray, 2016, Lopez-Otin et al., 2013).To investigate how diminished autophagy can lead to disease the following aims were designed:

Main aim 1: To investigate the interdependence between autophagy and mitochondrial function, especially how autophagy deficiency affects mitochondrial health.

Specific aim 1.1: To investigate mitochondrial function, specifically the respiratory chain, in autophagy deficient cells.

Specific aim 1.2: To prevent or bypass the identified mitochondrial defect in autophagy deficient cells in order to prevent cell death.

Specific aim 1.3: To investigate a potential correlation between autophagy and mitochondrial dysfunction in neurodegeneration.

With age and in neurodegenerative diseases (such as ALS) cells have to cope with increased oxidative and proteotoxic stress conditions. Autophagy is a prosurvival pathways that protects cells against these stress conditions by degrading damaged proteins and organelles, however molecular mechanisms how autophagy is activated in oxidative stress conditions and has a prosurvival role has not been investigated in detail. Data from our laboratory have shown that the autophagy receptor p62 gets oxidised in oxidative stress conditions and cysteine 105 and 113 are essential for its redox-regulation. To investigate what functional significance the oxidation of p62 has the following aims were designed:

Main aim 2: To investigate the importance of oxidation of p62 for cellular homeostasis in oxidative stress conditions with a focus on ageing and ALS.

Specific aim 2.1: To investigate the role of oxidation of p62 on autophagy efficiency.

Specific aim 2.2: To investigate the role of oxidation of p62 on oxidative stress resistance in cells and flies.

Specific aim 2.3: To investigate the effect of the ALS-related K102E mutation on oxidation of p62.

Specific aim 2.4: To investigated if other autophagy receptors (OPTN, NDP52, TAX1BP1 and NBR1) have the same ability as p62 to get oxidised.

Specific aim 2.5: Generate tools to study the role of oxidation of these other autophagy receptors in autophagy and mitophagy.

2 CHAPTER 2: MATERIALS AND METHODS

2.1 Materials

2.1.1 Tissue culture consumables

Table 1: Tissue culture consumables

Consumable	Manufacturer	Catalogue number
0.6 ml 'Crystal Clear' microcentrifuge tube	Starlab	E1405-0600
1.5 ml microcentrifuge tubes	Starlab	S1615-5500
12-well plate	Fisher	TKB-100-110R
15 ml Centrifuge Tube, Conical (Sterile), Loose	Star labs	E1415-0200
175 cm² TC treated flask with filter cap	Greiner-Bio one	661175
2 ml 'Crystal Clear' Microcentrifuge Tube	Starlab	E1420-2000
24-well plates	Fisher	TKB-100-115H
50 ml Centrifuge Tube, Conical (Sterile), Loose	Starlab	E1450-0200
6-well plates	Fisher	11825275
75 cm^2 TC treated flask with filter cap	Greiner-Bio one	658175
Acrodisc® Mini Spike syringe filters	Sigma-Aldrich	Z260444-1PAK
Acryl Aquaclean	WAK-Chemie Medical GmbH	WAK-AQA-250-50L
Bijou sample container, plain label	Sigma-Aldrich	Z645346-700EA
Cell culture dish treated with vents sterile polystyrene non-pyrogenic	Thermo Fisher Scientific	10075371
Coverglass 13 mm/0.16 mm	VWR	631-0150
CryoTube vials	Thermo Fisher Scientific	377267
Glass Pasteur pipettes 230 mm	VWR	612-1702
Mr. Frosty™ freezing container	Thermo Fisher Scientific	5100-0001
Serological pipettes 10 ml	Sarstedt	86.1254.001
Serological pipettes 25 ml	Sarstedt	86.1685.001
Serological pipettes 5 ml	Sarstedt	86.1253.001

2.1.2 Tissue culture reagents

Table 2: Tissue culture reagents

Reagent	Manufacturer	Catalogue number
20x PBS	New England BioLabs	9808
Blasticidin	Thermo Fisher Scientific	R21001
D-Galactose	Sigma-Aldrich	G0750
Dimethyl sulfoxide (DMSO)	Sigma-Aldrich	D2650
DMEM glucose-free medium	Thermo Fisher Scientific	A14430-01
Dulbecco's Modified Eagle's Medium (DMEM), high glucose	Sigma-Aldrich	D5796
Fetal Bovine Serum (FBS), heat inactivated	BioSera	FB1001H
Gelatine	Sigma-Aldrich	G7041
Hepes	Sigma-Aldrich	H0887
Isopropanol	Sigma-Aldrich	278475
Leukaemia inhibitory factor (LIF)	Merck Millipore	ESG1106
L-Glutamine solution	Sigma-Aldrich	G7513
Lipofectamine® 2000	Thermo Fisher Scientific	11668019
MEM Non-essential amino acid solution	Sigma-Aldrich	M7145
Mycoalert Detection Kit	Lonza	LT07-218
Non-essential amino acids	Sigma-Aldrich	M7145
Opti-MEM® I Reduced-Serum Medium, no phenol red	Thermo Fisher Scientific	11058021
Penicillin-Streptomycin	Sigma-Aldrich	P4333
Ready Probes Cell Viability Imaging kit	Thermo Fisher Scientific	R37609
Sodium pyruvate	Sigma-Aldrich	P2256
Trypsin-EDTA solution	Sigma-Aldrich	T3924

2.1.3 Cloning and mutagenesis consumables and reagents

Table 3: Cloning and mutagenesis reagents

Consumable / reagent	Manufacturer	Catalogue number
10-beta Competent E. coli (High Efficiency)	New England BioLabs	C3019
Agarose	Thermo Fisher Scientific	BP1356-500
Ampicillin	Sigma-Aldrich	A5354
Burner Bunsen Natural Gas 13mm	SLS	BUR3000
Calf Intestinal Alkaline Phosphatase	Thermo Fisher Scientific	18009019
Cell culture dish treated with vents sterile polystyrene non-pyrogenic	Thermo Fisher Scientific	10075371
Glass spreaders	Sigma-Aldrich	S4522-6EA
Kanamycin	Sigma-Aldrich	K0254
LB Agar Miller	Thermo Fisher Scientific	10734724
LB Broth Miller Powder	Thermo Fisher Scientific	10638013
Molecular Grade RNase-free water	Thermo Fisher Scientific	B-003000-WB-100
NEB 5-alpha competent E. coli	New England BioLabs	C2987I
NEBuilder HiFi DNA Assembly Cloning Kit	New England BioLabs	E5520S
peqGREEN	Peqlab	37-5000
PfuUltra High-Fidelity DNA Polymerase	Agilent Technologies	600380
PfuUltra II Fusion HS DNA Polymerase	Agilent Technologies	600672
Phusion High Fidelity PCR kit	Thermo Fisher Scientific	F553S
PureYield™ Plasmid Midiprep System	Promega	A2492
Q5 Site-Directed Mutagenesis Kit (Without Competent Cells)	New England BioLabs	E0552S
QIAprep Spin Miniprep Kit	Qiagen	27104
QIAquick Gel Extraction Kit	Qiagen	28704
QuikChange II XL Site-Directed Mutagenesis Kit	Agilent Technologies	200521
S.O.C. Medium	Thermo Fisher Scientific	15544-034
Stable Competent E. coli (High Efficiency)	New England BioLabs	C3040
T4 DNA Ligase	New England BioLabs	M0202S
XL10-Gold® Ultracompetent Cells	Agilent Technologies	200314
α-Select Bronze Competent Cells	Bioline	BIO-85025
α-select Gold Efficiency Competent Cells	Bioline	BIO-85027

2.1.4 Western blot reagents

Table 4: Western blot reagents

Reagent	Manufacturer	Catalogue number
20x PBS	New England Bio	9808
2x Laemmli buffer	Bio-Rad	1610737
Acrylamide/Bis-acrylamide	Severn Biotech	20-2100-10
Ammonium persulphate (APS)	Sigma-Aldrich	A3678
Bovine Serum Albumin (BSA)	Sigma-Aldrich	A2153
Clarity western ECL substrate	Bio-Rad	170-5061
DC Protein Assay Kit	Bio-Rad	500-0112
Gel loading tips	Starlab	1022 0600
GelCode™ Blue stain reagent	Thermo Fisher Scientific	10608494
Glycine	Sigma-Aldrich	G8898
Goat-α-mouse HRP	Sigma-Aldrich	A2554
Goat-α-rabbit HRP	Sigma-Aldrich	A0545
IGEPAL® CA-630 (NP-40)	Sigma-Aldrich	I3021
Immobilon-P polyvinylidene difluoride (PVDF) membrane	Millipore	IPVH00010
Marvel non-fat dry milk powder	Asda	N/A
Methanol	Sigma-Aldrich	32213
N,N,N',N'-Tetramethylethylenediamine (TEMED)	Sigma-Aldrich	T9281
N-ethylmaleimide (NEM)	Sigma-Aldrich	E3876
Phosphatase inhibitor cocktail 100X	Thermo Fisher Scientific	1861280
Polyoxyethylene sorbitan (Tween-20)	Sigma-Aldrich	93774
Precision Plus Protein™ Dual Color Standards	Bio-Rad	610374
Rabbit-α-guinea pig HRP	Dako	P0141
Restore™ PLUS Western Blot Stripping Buffer	Thermo Fisher Scientific	46430
Sodium chloride (NaCl)	Sigma-Aldrich	S7653
Sodium deoxycholate (NaDoC)	Sigma-Aldrich	D6750
Thick blotting paper	VWR	732-0594
Trizma® base (Tris)	Sigma-Aldrich	T1503
β-mercaptoethanol (β-mE)	Sigma-Aldrich	M3148
IGEPAL CA-630 (NP-40)	Sigma-Aldrich	I3021

2.1.5 Blue native page reagents

Table 5: Blue native page reagents and consumables		
Reagent/Consumable	**Manufacturer**	**Catalogue number**
30% Acrylamide/Bis-acrylamide	Severn Biotech	20-2100-10
Ammonium persulphate (APS)	Sigma-Aldrich	A3678
Ammonium persulphate (APS)	Sigma-Aldrich	A3678
Bis-tris	Amresco	715
Bovine Serum Albumin (BSA)	Sigma-Aldrich	A2153
Coomassie blue G	Sigma-Aldrich	B0770
Coomassie Brilliant Blue – R	Sigma-Aldrich	T0377
Digitonin	Santa cruz biotechnology	sc-280675
D-Mannitol	Sigma-Aldrich	M4125
DTT	Thermo Fisher Scientific	R0861
EDTA	Sigma-Aldrich	EDS
Glass homogeniser	Sigma-Aldrich	D8938
Glycerol	Sigma-Aldrich	G5516
Gradient mixer	Thermo Fisher Scientific	11544424
Hepes	Sigma-Aldrich	H3375
N,N,N',N'-Tetramethylethylenediamine (TEMED)	Sigma-Aldrich	T9281
NaCl	Sigma-Aldrich	S7653
PMSF	Sigma-Aldrich	93482
Sucrose	Sigma-Aldrich	S0389
Tricine	Sigma-Aldrich	T0377
Triton X-100	Sigma-Aldrich	X100
ε-amino n-caproic acid	Calbiochem	1381

2.1.6 Immunofluorescence reagents

Table 6: Immunofluorescence reagents		
Reagent	**Manufacturer**	**Catalogue number**
20x PBS	New England Bio	9808
37% Formaldehyde	Sigma-Aldrich	252549
Bovine Serum Albumin (BSA)	Sigma-Aldrich	5482
Microscope slide ground edges, twin frosted	Thermo Fisher Scientific	FB58628
Normal Goat Serum	Plasmid Laboratories	S-1000
Normal Rabbit Serum	Plasmid Laboratories	S-5000
Polyoxyethylene sorbitan (Tween-20)	Sigma-Aldrich	93774
ProLong® Gold Antifade Mountant with DAPI	Thermo Fisher Scientific	P36935
TO-PRO-3 iodide	Thermo Fisher Scientific	T3605
Triton X-100	Sigma-Aldrich	X100

2.1.7 Immunohistochemistry reagents

Table 7: Immunohistochemistry reagents		
Reagent	**Manufacturer**	**Catalogue number**
Microscope slide ground edges, twin frosted	Thermo Fisher Scientific	FB58628
Histoclear	National Diagnostics	HS-200
Ethanol	Thermo Fisher Scientific	E/0650DF/17
Normal Goat Serum	Vector Laboratories	S-1000
VECTASTAIN ABC kit	Vector Laboratories	PK-4000
NovaRED	Vector Laboratories	SK-4800
Haematoxylin	Vector Laboratories	H-3401
DPX mounting medium	Thermo Fisher Scientific	12658646

2.2 Methods

2.2.1 Tissue culture

HeLa, HEK293FT, Atg5 knock-out (*Atg5*$^{-/-}$) and wild-type (*Atg5*$^{+/+}$) mouse embryonic fibroblasts (MEFs), M5-7 MEFs, *p62*$^{-/-}$ and *p62*$^{+/+}$ MEFs (Table 8) were grown in DMEM supplemented with 10% heat-inactivated FCS (Foetal Calf Serum, Biosera), 5% penicillin/streptomycin (Sigma) and 2mM L-glutamine (Sigma) in a humidified atmosphere containing 5% CO_2 at 37°C. Galactose-based medium consisted of DMEM glucose-free medium supplemented with 4mM glutamine (Thermo Fisher Scientific), 10mM galactose (Sigma), 1mM sodium pyruvate (Sigma), MEM nonessential amino acids (Sigma), 10% FCS and 5% penicillin/streptomycin. Control mouse embryonic stem-cell (mES) line ES-I and complex I deficient mES (Cy3-1) (Table 8) were grown in DMEM supplemented with 10% FCS, 2mM L-glutamine, 1mM sodium pyruvate, 100uM 2-mercaptoethanol (Sigma), non-essential amino acids, (Sigma) 1ng/ml LIF (leukaemia inhibitory factor, Merck Millipore) in 0.1% gelatine (Sigma) coated flasks.

Cells were treated different reagent as shown in table 2 at different concentration and time-points in glucose- or galactose-based medium as indicated, all consumables used are listed in table 1.

Table 8: Mouse and human cell lines		
Cell line	**Source**	**reference**
mouse cell lines		
Atg5$^{+/+}$ MEFs	Dr. Noboru Mizushima (Tokyo Medical and Dental University)	(Kuma et al., 2004)
Atg5$^{-/-}$ MEFs	Dr. Noboru Mizushima (Tokyo Medical and Dental University)	(Kuma et al., 2002)
M5-7 MEFs	Dr. Noboru Mizushima (Tokyo Medical and Dental University)	(Hosokawa et al., 2007)
p62$^{+/+}$ MEFs	Dr. Eiji Warabi (University of Tsukuba)	(Komatsu et al., 2007)
p62$^{-/-}$ MEFs	Dr. Eiji Warabi (University of Tsukuba)	(Komatsu et al., 2007)
human cell lines		
HEK293FT	Thermo Fisher Scientific #R700-07	
HeLa cells	ECACC (European Collection of Cell Cultures), Salisbury, UK	
mES ctr	Dr. Amy Reeve (Newcastle University)	(Kirby et al., 2009)
mES CI	Dr. Amy Reeve (Newcastle University)	(Kirby et al., 2009)
HeLa ctr CRISPR	Dr. Michael Lazarou (Monash University, Melbourne)	(Lazarou et al., 2015)
HeLa PentaKO	Dr. Michael Lazarou (Monash University, Melbourne)	(Lazarou et al., 2015)
HeLa PentaKO + YFP-Parkin+ mtKeima	generated by Dr. Michael Lazarou (Monash University, Melbourne)	unpublished

Table 9: Tissue culture treatments				
Reagent	**Manufacturer**	**Catalogue number**	**Stock concentration**	**Final concentration**
Antimycin A	Sigma-Aldrich	A8674	40mM	4µM
Auranofin	Sigma-Aldrich	A6733	1mM	5µM
Bafilomycin A1	Enzo life sciences	BML-CM110-0100	100µM	50 or 400nM
Chloroquine	Sigma-Aldrich	C6628	50mM	50µM
Curcumin	Sigma-Aldrich	C1386	200mM	50µM
Cyclohexamide	Sigma-Aldrich	C7698	20mg/ml	50µg/ml
H_2O_2	Sigma-Aldrich	H1009	1M	1mM-5mM
I-BET 525762A	Insight Biotechnology	HY-13032	1mM	1µM
MG132	Sigma	C2211	40mM	600nm-20µM
MitoQ	Gift Dr. Michael Murphy (MRC Mitochondrial Biology Unit)		20µM	20nM
Oligomycin	Merck Millipore	495455	5mg/ml	10µM
Polybrene	Sigma-Aldrich	107689	5mg/ml	5µg/ml
PR-619	LifeSensors	S19619	10mM	5µM-20µM
S1QEL2.2	Life Chemicals Europe	F2068-0013	500µM	500nM
Tetracycline	Sigma-Aldrich	87128	1mg/ml	1µg/ml
Z-VAD-FMK	Enzo life sciences	ALX-260-02-M001	10mM	20µM

2.2.2 Alignments and *in silico* calculations

p62 protein sequences in 14 organisms were identified by searching UniProt for the gene names SQSTM or Ref(2)P, then removing sequence fragments and choosing the longest isoform from each organism. Multiple Sequence alignment was carried out using the Muscle server at EBI (http://www.ebi.ac.uk/Tools/msa/muscle/) with default parameters. The resulting alignment was visualised using ALINE (Bond and Schuttelkopf, 2009). Conservation is indicated by depth of 10 colour from light to dark red, with conservation below 30% indicated in white. Secondary structure in the PB1 domain was indicated by using the X-ray crystal structure (PDB entry 4MJS chain B), and in the ZZ domain using homology to CBP (PDB entry 1TOT). Alignments were carried out by Dr. Graham Smith.

Table 10: organisms used for multiple protein alignments of p62

Organism	Gene name	Protein ID
Homo sapiens (Human)	SQSTM1	Q13501|SQSTM_HUMAN
Pongo abelii (Sumatran orang-utan)	SQSTM1	Q5RBA5|SQSTM_PONAB
Macaca mulatta (Macaque)	SQSTM1	H9G1C8|H9G1C8_MACMU
Bos taurus (Cow)	SQSTM1	Q32PJ9|Q32PJ9_BOVIN
Mus musculus (Mouse)	Sqstm1	Q64337|SQSTM_MOUSE
Canis familiaris (Dog)	SQSTM1	F1P6L5|F1P6L5_CANFA
Cavia porcellus (Guinea pig)	SQSTM1	H0W6B1|H0W6B1_CAVPO
Gallus gallus (Chicken)	SQSTM1	F1NA86|F1NA86_CHICK
Sarcophilus harrisii (Tasmanian devil)	SQSTM1	G3W939|G3W939_SARHA
Anolis carolinensis (Carolina anole)	SQSTM1	G1KYX2|G1KYX2_ANOCA
Xenopus laevis (African clawed frog)	sqstm1	Q6PGS1|Q6PGS1_XENLA
Latimeria chalumnae (West indian Ocean coelacanth)	SQSTM1	H3AW10|H3AW10_LATCH
Drosophila melanogaster (Common fruit fly)	ref(2)P	P14199|REF2P_DROME
Caenorhabditis elegans (roundworm)	sqst-1	Q22436|Q22436_CAEEL

2.2.3 Structural modelling

To model the p62 linker region (the part between the PB1-domain and the ZZ-domain), which is most likely natively unstructured, the consensus annotation from MobiDB (http://mobidb.bio.unipd.it/entries/Q13501) was used (Potenza et al., 2015). This consensus (amino acids 105-117) was extended slightly to include the ALS-related

K102E mutant. PyMOL (The PyMOL Molecular Graphics System, Version 1.7.0.0 Schrödinger, LLC) was used to build structures of the linker using the wild type sequence and the K102EALS mutant. Electrostatics calculation were carried out with the APBS plug-in for PyMOL (Baker et al., 2001), with PyMOL-generated hydrogens and termini and a concentration of monovalent cations and anions of 0.15 M and the resulting electrostatic potential was mapped to the solvent-accessible surface. Structural modelling was carried out by Dr. Graham Smith.

2.2.4 Modelling of the p62 construct comprising of PB1 and zinc finger domains (residues 3-183)

Prediction of an initial 3D structure of zinc finger domain of p62 (residues 121-183) was performed using MODELLER (Webb and Sali, 2016) using the crystal structure of human MZM-REP domain of Mib E3 ubiquitin ligase (PDB code: 4XI6) as a template. The sequence identity between the template and the target was 38%. The model has been refined by molecular-mechanical energy minimization (50 000 cycles) and 10 ns of unrestrained all-atom MD simulation using Gromacs 5.1.2 (Van Der Spoel et al., 2005) with Amber99SB-ILDN* force field (Lindorff-Larsen et al., 2010) and explicit TIP3P water model. The obtained structure has been fitted on the PB1 domain using protein-protein docking with PatchDock (Schneidman-Duhovny et al., 2005), and the top 5 predicted models were refined by 50 000 cycles of MM minimization and 5 ns of MD simulation. The obtained models were fitted on cryoEM assemblies of p62 PB1 domains (PDB codes 4UF8 and 4UF9), and the final model has been selected using the geometric constraints (relative positions of cysteines, steric clashes overall the model) and energy-minimised with the disulphide bonds introduced. Structural modelling of residues 3-183 was carried out by Dr. Agnieszka Bronowska.

2.2.5 Modelling of the impact of K102E mutation

The mutation has been introduced to the PB1 domain models (residues 3-125) by manual replacement, followed by the conformational using UCSF Chimera (Couch et al., 2006). Then, the whole structure of the mutant (in the monomeric form) has been subjected to 50 000 cycles of MM energy minimization, followed by 10 ns of all-atom MD in Gromacs 5.1.2 with TIP3P explicit water and the Amber99SB-ILDN* force field (Lindorff-Larsen et al., 2010, Van Der Spoel et al., 2005). The wild-type PB1 domains were subjected to the same protocol, as the control group. In the analysis, we focused on the differences between the interactions in the wild-type and the K102E mutant and on the local sampling of the region surrounding the mutated residue. The modelling of the oligomers was done in UCSF Chimera. The positions of the 102-125 loops were refined using FlexPepDock Monte Carlo approach (Alam and Schueler-Furman, 2017). The figure has been generated using UCSF Chimera (Couch et al., 2006). Structural modelling of the K102E mutant was carried out by Dr. Agnieszka Bronowska.

2.2.6 Cloning of His-FLAG-p62 in lentiviral construct (pLENTI6/V5-DEST)

His-FLAG-p62 and His-FLAG-C105,113Ap62 for lentiviral expression were subcloned into the pLENTI6/V5-DEST (Invitrogen, V496-10) using EcoRI and XhoI (ThermoFisher Scientific). His-FLAG-p62 and His-FLAG-C105,113Ap62 inserts were produced using the primers in table 11 which introduce an EcoRI and XhoI restriction site, using His-FLAG-p62 wild-type (pcDNA 3.1, kind gift from Dr. Robert Layfield, University of Nottingham) or C105,113A mutant as templates. PCRs were performed using the Phusion High-Fidelity PCR kit (Thermo Fisher Scientific) and every PCR mixture was prepared according to the provided protocol: 1x Phusion High-Fidelity buffer, 10 ng DNA template, 125 ng oligonucleotide primers (both forward and reverse), 200μM dNTP, Phusion High-Fidelity DNA polymerase (2 U/μl) and H_2O up to final volume of 50 μl. PCR reactions were placed on a Veriti 96-Well Thermal Cycler

(Applied Biosystems) using the provided program: 1 cycle at 98°C for 30 sec, 25 cycles (Denaturation 98°C for 10 sec, Annealing 57°C for 30 sec, Extension 72°C for 1 kb/min) and 1 cycle at 72°C for 5 min. The p62 fragments were then digested with EcoRI and XhoI for 5 min at 37°C and run on 0.8% agarose gel (Thermo Fisher Scientific), which was then gel purified using the QIAquick Gel Extraction Kit (Qiagen). The pLENTI6/V5-DEST plasmid was digested with EcoRI and XhoI and gel purified as well. After the double digestion, the pLENTI6/V5-DEST backbone was dephosphorylated by calf intestinal alkaline phosphatase (Thermo Fisher Scientific) for 50 min at 37°C. The digested p62 fragments were ligated into the double digested pLENTI6/V5-DEST backbone using the T4 DNA Ligase (New England BioLabs) at 16°C overnight. Bacterial transformation was performed using NEB3040 NEB Stable Competent *E. coli* (New England Biolabs) and adding 2µl of ligation mixture to 45µl of cells. Cells were plated on LB agar plates containing 50ng/ml of Ampicillin (Sigma-Aldrich). Colonies were grown for 24 hours at 31 °C the plasmid was extracted using QIAprep Spin Miniprep Kit (Qiagen). To test if the obtained plasmid was correct EcoRV was used as a control digestion, which results in 855 and 8172 bp fragments. The plasmid was sequenced to confirm correct insertion of FLAG-p62 using the UB forward and V5 reverse primers (Table 12) (Eurofins Genomics).

Table 11: Primers used to clone His-FLAGp62 into pLENTI6/V5-DEST	
p62startEcoRI	GGGGGAATTCATGGCGTCGCTCACCG
p62stopXhoI	GGGCTCGAGTCACAACGGCGGGGG

Table 12: Sequencing primers	
LNCX FWD	AGCTCGTTTAGTGAACCGTCAGATC
UB FWS	TCAGTGTTAGACTAGTAAATTG
V5 REV	ACCGAGGAGAGGGTTAGGGAT
T7 REV	GCTAGTTATTGCTCAGCGG

2.2.7 Cloning His-FLAG-NDP52 and His-FLAG-OPTN in lentiviral construct (pLENTI6/V5-DEST)

For cloning of NDP52 and OPTN into pLENTI6/V5-DEST (His-FLAG), Gibson assembly was used. NDP52, OPTN and pLENTI6/V5-DEST (His-FLAG) were PCR amplified using PfuUltra II Fusion HS DNA Polymerase (Agilent) and Gibson assembly primers with 20 bp overhangs (Table 13). As a template FLAG-NDP52 M5P (kindly provided by Dr. Felix Randow), OPTN pDESt26 (Addgene #23050) and the previous generated His-FLAGp62 (pLENTI6/V5-DEST) were used (See appendix for plasmid maps). PCR products were separated by agarose gel electrophoreses, and fragments excised and purified before use in DNA assembly reaction with the NEBuilder HiFi DNA Assembly kit (New England Biolabs) according to the manufacturer's instructions. After the assembly, the reaction mix was transformed into NEB3040 NEB Stable Competent *E. coli* (New England Biolabs) and 2µl of ligation mixture was added to 45µl of cells. Cells were plated on LB agar plates containing 50ng/ml of Ampicillin (Sigma-Aldrich). Colonies were grown for 24 hours at 31 °C and the plasmid was extracted using QIAprep Spin Miniprep Kit (Qiagen). To test if the obtained plasmid was correct, EcoRV and NotI were used for a control digest of the His-FLAG-OPTN and His-FLAG-NDP52 plasmids, resulting in 9403 bp fragment for the OPTN plasmid and 2228 and 6816 bp fragments for the NDP52 plasmid. The plasmids were sequenced to confirm correct insertion of His-FLAG-OPTN and His-FLAG-NDP52 using the UB forward and V5 reverse primers (Table 12)(Eurofins Genomics).

Table 13: Primers used to clone NDP52 and OPTN into pLENTI6/V5-DEST (His-FLAG)	
His-FLAG-pLENTI6 FWD	TCGAGTCTAGAGGGCCCGCGGTT
His-FLAG-pLENTI6 REV	T GCGGCCGCTGCCCATCTTGT
NDP52pLENTI6 FWD	ACAAGATGGGCAGCGGCCGCATGGAGGAGACCATCAAA GATCC
NDP52pLENTI6 REV	CGCGGGCCCTCTAGACTCGATCAGAGAGAGTGGCAGAAC ACG
OPTNpLENTI6 FWD	ACAAGATGGGCAGCGGCCGCTCCCATCAACCTCTCAGCT G
OPTNpLENTI6 REV	CGCGGGCCCTCTAGACTCGATTAAATGATGCAATCCATCA CG

2.2.8 Cloning NDP52 in pDEST26 backbone

To clone FLAG-NDP52 in the mammalian pDEST26 backbone (His) Gibson assembly was used. FLAG-NDP52 and pDEST26 were PCR amplified using PfuUltra II Fusion HS DNA Polymerase (Agilent) and Gibson assembly primers with 20 bp overhangs (Table 14). As a template FLAG-NDP52 M5P (kindly provided by Dr. Felix Randow) and OPTN pDESt26 (Addgene #23050) were used. PCR products were separated by agarose gel electrophoreses, and fragments excised and purified before use in DNA assembly reaction with the NEBuilder HiFi DNA Assembly kit (New England Biolabs) according to the manufacturer's instructions. After the assembly, the reaction mix was transformed into α-select GOLD Efficiency chemically competent cells (Bioline), 2µl of ligation mixture was added to 45µl of cells. Cells were plated on LB agar plates containing 50ng/ml of Ampicillin (Sigma-Aldrich). Colonies were grown overnight at 37 °C and the plasmid was extracted using QIAprep Spin Miniprep Kit (Qiagen). To test if the obtained plasmid was correct, SacI was used for a control digest of the His-FLAG-NDP52 pDEST26 plasmid, resulting in 754 and 6640 bp fragments. The plasmid was sequenced to confirm correct insertion of FLAG-NDP52 using the LNCX forward and T7 reverse primers (Table 12) (Eurofins Genomics).

Table 14: Primers used to clone FLAG-NDP52 into pDEST26 (His)	
His-pDEST26-FLAG-NDP52 FWD	TGTTCTGCCACTCTCTCTGATTGATCGCGTGCATGCGACGTCA
His-pDEST26-FLAG-NDP52 REV	TCGTCGTCCTTGTAGTCGCCGTGATGGTGATGGTGATGGTAGTAC GCCATGGTC
FLAG-NDP52-pDEST26 FWD	ACCATCACCATCACCATCACGGCGACTACAAGGACGACGACGACA
FLAG-NDP52-pDEST26 REV	CGTCGCATGCACGCGATCAATCAGAGA GAGTGGCAGAACACGTGGTCTTC

2.2.9 Mutagenesis

Point mutagenesis of the p62, NDP52 and OPTN genes were carried out using the QuikChange II XL Site-Directed Mutagenesis Kit (Agilent Technologies) or Q5 Site-Directed Mutagenesis Kit (NEB) according to manufacturer's instructions. Mutagenesis primers were designed using the online QuikChange Primer Design program (http://www.genomics.agilent.com/) or the NEB primer design program http://nebasechanger.neb.com (Tables 15, 16 & 17). The GFP-p62 (pEGFP C2, Clontech, 632481), His-FLAG-p62 (pcDNA3.1, Kind gift from Dr. Robert Layfield, University of Nottingham), His-FLAG-NDP52 (pDEST26) and His-FLAG-OPTN (pDEST26, Addgene, 23050) wild-type plasmids were used as templates. PCR reactions were placed on a Veriti 96-Well Thermal Cycler (Applied Biosystems) using the provided program: 1 cycle at 95°C for 1 min, 18 cycles (Denaturation 95°C for 50 sec, Annealing 60°C for 50 sec, Extension 68°C for 7 min) and 1 cycle at 68°C for 6 min. Bacterial transformation was then carried out using 45µl of XL10-Gold® Ultracompetent Cells (Agilent Technologies) and 2µl of β-mE mix provided with the kit, together with 2µl of the DpnI-treated DNA per reaction. Transformation mixtures were incubated on ice for 30 min, heat-pulsed in a 42°C water bath for 30 sec, incubated on ice for 2 min, followed by the addition of 950 µl of S.O.C. medium (Thermo Fisher Scientific). After 1 hour incubation at 37°C with shaking at 220 rpm, 250µl of each transformation reaction were plated on LB agar (Thermo Fisher Scientific) plates containing 100ng/µl of ampicillin (Sigma-Aldrich) and incubated overnight at 37°C.

Then, colonies were picked and grown in 5ml of LB broth (Thermo Fisher Scientific) overnight at 37°C with shaking at 220 rpm. Bacterial DNA was extracted using the QIAprep Spin Miniprep Kit (Qiagen) to a final volume of 50µl and sent for sequencing (Eurofins Genomics).

Table 15: Primers used for p62 mutagenesis

p62 C105A FWD	ACATTAAAGAGAAAAAAGAGGCCCGGCGGGACCACCG
p62 C105A REV	CGGTGGTCCCGCCGGGCCTCTTTTTTCTCTTTAATGT
p62 C113A FWD	CCACCGCCCACCGGCTGCTCAGGAGGCG
p62 C113A REV	CGCCTCCTGAGCAGCCGGTGGGCGGTGG
p62 K102E FWD	CCCGCCGGCACTCTTTCTCCTCTTTAATGTAGATTCGGAA
p62 K102E REV	TTCCGAATCTACATTAAAGAGGAGAAAGAGTGCCGGCGGG
p62 K7A FWD	CGTCGCTCACCGTGGCGGCCTACCTTCTGG
p62 K7A REV	CCAGAAGGTAGGCCGCCACGGTGAGCGACG
p62 D69A FWD	CGCACTACCGCGCTGAGGACGGGGA
p62 D69A REV	TCCCCGTCCTCAGCGCGGTAGTGCG
p62 R106E NEB FWD	AAAAGAGTGCGAGCGGGACCACC
p62 R106E NEB REV	TTCTCTTTAATGTAGATTCGGAAG
p62 R107E NEB FWD	AGAGTGCCGGGAGGACCACCGCC
p62 R107E NEB REV	TTTTTCTCTTTAATGTAGATTCGGAAGATGTC
p62 H109A NEB FWD	CCGGCGGGACGCCCGCCCACCGT
p62 H109A NEB REV	CACTCTTTTTTCTCTTTAATGTAGATTCGGAAGATGTCATC
p62 D108A NEB FWD	GTGCCGGCGGGCCCACCGCCCAC
p62 D108A NEB REV	TCTTTTTTCTCTTTAATGTAGATTCGGAAGATGTCATCCTTCA CGTAGGACATGGCC
p62 E104K NEB FWD	AGAGAAAAAAAAGTGCCGGCGGG
p62 E104K NEB REV	TTAATGTAGATTCGGAAGATGTCATCCTTC

Table 16: Primers used for OPTN mutagenesis	
OPTN C8A FWD	CCCATCAACCTCTCAGCGCCCTCACTGAAAAGGAGG
OPTN C8A REV	CCTCCTTTTCAGTGAGGGCGCTGAGAGGTTGATGGG
OPTN C239A NEB FWD	GCTCCTGCTGGCCCTAAGGGAAG
OPTN C239A NEB REV	TGGCTCACAGTTAACTCC
OPTN C334A FWD	TAATGAAGAAGAGACTTCAAGAAAAGGCTCAGGCCCTTGAAAGG
OPTN C334A REV	CCTTTCAAGGGCCTGAGCCTTTTCTTGAAGTCTCTTCTTCATTA
OPTN C472A FWD	CTTTCAGCATGAAAATCAGAAGCGTAAACTTCCATCTGAGCCCT
OPTN C472A REV	AGGGCTCAGATGGAAGTTTACGCTTCTGATTTTCATGCTGAAAG

Table 17: Primers used for NDP52 mutagenesis	
NDP52 C18A FWD	AGCTGTCTTGCTGGATCACGCTCATTTCTCTCAGGTCATC
NDP52 C18A REV	GATGACCTGAGAGAAATGAGCGTGATCCAGCAAGACAGCT
NDP52 C40A FWD	GTGAAGGTATAATGAGCTGTGACGTCCCCTCCAGGGATG
NDP52 C40A REV	CATCCCTGGAGGGGACGTCACAGCTCATTATACCTTCAC
NDP52 C108A FWD	CACCATCCTCATCCACATAGGCGAACTGGTAATACTCATCAT
NDP52 C108A REV	ATGATGAGTATTACCAGTTCGCCTATGTGGATGAGGATGGTG
NDP52 C153A FWD	CAGCTCCTGGTTTTCTTTGGCAAGCTCCTTGTTGTGCTGC
NDP52 C153A REV	GCAGCACAACAAGGAGCTTGCCAAAGAAAACCAGGAGCTG
NDP52 C163A FWD	CTTCTGGAGGCTGATAGCGCTGTCCTTCAGCTCC
NDP52 C163A REV	GGAGCTGAAGGACAGCGCTATCAGCCTCCAGAAG
NDP52 C321A FWD	GTCTCTGCAGAGCATTAGCTATAATTTCGTTCTCACTCAGTCTTTTTGA
NDP52 C321A REV	TCAAAAAGACTGAGTGAGAACGAAATTATAGCTAATGCTCTGCAGAGAC
NDP52 C397A FWD	CTTTGCAGATAGGGGCTTTCTTGATGGAGAGCGGGCT
NDP52 C397A REV	AGCCCGCTCTCCATCAAGAAAGCCCCTATCTGCAAAG
NDP52 C400A FWD	ATCACAAATATCATCTGCTTTGGCGATAGGGCATTTCTTGATGGAG
NDP52 C400A REV	CTCCATCAAGAAATGCCCTATCGCCAAAGCAGATGATATTTGTGAT
NDP52 C406A FWD	CCAAGGTGTGATCAGCAATATCATCTGCTTTGCAGATAGGGCA
NDP52 C406A REV	TGCCCTATCTGCAAAGCAGATGATATTGCTGATCACACCTTGG
NDP52 C419A FWD	CACAAATTGGACAATTGAAAGCAAGGGGCTGCATCTGCTGT
NDP52 C419A REV	ACAGCAGATGCAGCCCCTTGCTTTCAATTGTCCAATTTGTG

2.2.10 DNA transfections

HeLa cells and MEFs were seeded in either 6- or 12-well plates, cultured for 24 (HeLa) or 48 (MEFs) hours and transfected with Lipofectamine 2000 (Thermo Fisher Scientific) according to the manufacturer's instructions for 24 hours prior to lysis. For each transfection in 6-well plates, 1µg DNA, 3µl of transfection reagent and 100µl Opti-MEM I Reduced-Serum Medium (Thermo Fisher Scientific) was used per well.

2.2.11 SiRNA transfection

ON-TARGETplus SMARTpool siRNA against mouse VCP (L-057592-00), ClpP (L-044020-01), Lon (L-054897-01), Afg3L2 (L-056354-01) and non-targeting SMARTpool siRNA (D-001810-04) were purchased from Dharmacon. *p62*$^{+/+}$ and *p62*$^{-/-}$ MEFs were seeded in 6-plates, 90% confluent cells were transfected with 100ng siRNA using Lipofectamine 2000 according to the manufacturer's instructions for 24 hours. The following day, cells were split and seeded in 6 well plate and the next day 70% confluent cells were transfected again with 30ng siRNA using the same procedure 24 hours prior to lysis.

2.2.12 Generating stable cell lines by lentiviral transductions

Stable expression of FLAG-p62 and FLAG-C105A-C113Ap62 in *p62*$^{-/-}$ MEFs was generated via lentiviral transductions. HEK293FT cells were seeded in antibiotic-free medium supplemented with 0.1mM MEM non-essential amino acids (Gibco) and then cotransfected with either empty or p62 lentiviral expression vectors and 3rd generation packaging system plasmids (Thermo Fisher Scientific). After 24 hours, media was replaced with fresh media without antibiotics. 48 hours after transfection, viral transduction was performed by transferring media from HEK293FT cells to 70% confluent *p62*$^{-/-}$ MEFs in the presence of 5µg/ml Polybrene (Sigma-Aldrich). Media containing virus was replaced after 24 hours with fresh media containing 8µg/ml of blasticidin (Thermo Fisher Scientific) for selection of transduced cells. Media was replaced every 2-3 days for 10-12 days by keeping the antibiotic selection. Stable cell lines were maintained in lower levels of blasticidin (4µg/ml) until seeding for experimental purposes.

2.2.13 Generating stable cell lines via DNA transfections

To generate HeLa PentaKO or HeLa PentaKO + YFP-Parkin + mtKeima cells stably expressing His-FLAG-NDP52, His-FLAG-OPTN or the respective oxidation mutants, HeLa PentaKO were seeded into 6-well plates and 70% confluent cells were

transfected with 1µg of DNA (receptors in pLENTI6/V5-DEST constructs) using Lipofectamine 2000 (Thermo Fisher Scientific) according to the manufacturer's instructions for 24 hours. Cells that incorporated the plasmid into their genome were selected with Blasticidin (8µg/ml), media was replaced every 2-3 days for 3 weeks, after which the expression levels were tested by western blot. Stable cell lines were maintained in lower levels of blasticidin (4µg/ml) until seeding for experimental purposes.

2.2.14 Generation of 'humanised' D. melanogaster Ref(2)P

CRISPR/Cas9-Mediated Genome Editing (homology-dependent repair (HDR) using one guide RNA and a dsDNA plasmid donor) was utilised to generate a humanised Ref(2)P (*CG10360)* (WellGenetics, Taiwan). Amino acids 91-116 of *Drosophila* (knock-in strain w^{1118}) Ref(2)P were replaced with amino acids 100-118 of human p62/SQSTM1 peptide. Guide RNA primers: sense 5'-CTTCGACAGAAGGAGCTTCAGCGT-3'; antisense 5'-AAACACGCTGAAGCTCCTTCTGTC-3'.

2.2.15 Fly husbandry

Flies were crossed and maintained on standard media (Table 18) at 25°C in a controlled 12 hr light: dark cycle. Male flies were used in all experiments. Survival graphs were created using Graphpad Prism software and log rank statistics applied. 60 flies were used for each experimental group and 3 replicate experiments were performed. Graphs presented depict pooled results. All fly work was carried by Dr. Rhoda Stefanatos.

Table 18: Fly food recipe		
%(w/v)	**Ingredient**	**Catalogue number**
1	Drosophila agar Type II	Dutscher Scientific #789150
1.5	Saccharose (sucrose)	VWR #27480.294
3	D-(+)-Glucose	VWR #101176K
3.5	Active Dried Yeast	Dutscher Scientific #789093
1.5	Maize meal	Supermarket
1	Wheat germ	MP biomedicals #0290328805 - 5 lb
1	Soybean flour	Santa Cruz Biotechnology #sc-215897A
3	Treacle	Bidvest #90028S

2.2.16 Paraquat Survival

Two days old males (20 flies/vial) were starved overnight on 5ml 1% agar at 25°C. Flies were transferred to vials containing filter paper soaked in 150µl of a 5% Sucrose solution with 20mM paraquat (Sigma) and maintained at 25°C. Dead flies were counted at 12 hr intervals and media changed daily.

2.2.17 32°C Survival

2 day old males (20 flies/vial) were transferred to 32°C. Media was changed every 1-2 days and dead flies were counted.

2.2.18 Chloroquine feeding

Two days old males (20 flies/vial) were transferred to standard media containing 2.5mg/ml chloroquine (Sigma). Flies were maintained at 25°C for 2 days and then transferred to 32°C for 2 days. Media was changed every 1-2 days and dead flies were counted.

2.2.19 Preparing fly western blot samples

10-20 flies were crushed (using homogeniser) in 200-300µl 1x homogenising buffer, containing 0.2% Triton X-100 (w/v, Promega, H5141), complete mini EDTA-free Protease Inhibitor (Sigma, 000000004693159001) and 1x PBS and left on ice for 10 min, followed by a 15 min spin at 13,000 rpm at 4°C, the supernatant was analysed by western blot analysis described in section 2.2.21.

2.2.20 Cell survival assay

MEFs were seeded 24 hours prior to treatments in 12-well plate. After treatments, cells viability was assessed using Ready Probes Cell Viability Imaging kit (Thermo Fisher Scientific) according to the manufacturer's instructions. Briefly, NucBlue Live reagent (Hoechst 33342) and NucGreen Dead reagent (FITC/GFP) were added to the media for 10 min after treatments to determine cell viability. Cells were imaged on inverted DM IL LED Leica microscope equipped with an Invenio 3SII digital camera (3.1 Mpix Colour CMOS; DeltaPix). Images were analysed using ImageJ and the percentage of cell death was quantified. The cell death analysis using the Ready Probes Cell Viability was done in collaboration with Dr. Bernadette Carroll. Alternatively, bright field images were taken in combination with western blot analysis for apoptotic cell death markers cleaved caspase 3 and Parp-1.

2.2.21 Western blot analysis

MEFs, mES or HeLa cells were seeded in 6-plates 24 hours prior to treatments. After treatments, cells were washed in ice-cold 1x PBS then lysed in RIPA buffer (150 mM NaCl, 1% NP-40, 0.5% NaDoC, 0.1% SDS, 50 mM Tris pH 7.4, supplemented with 1X Halt Protease & Phosphatase inhibitor cocktail in ddH_2O). Cell lysates were then centrifuged at 4°C at 13,000 rpm for 10 min. Protein concentration was measured by Bradford assay using the DC Protein Assay (Bio-Rad) and a FLUOstar Omega plate reader (BMG Labtech). Samples were prepared by boiling in SDS-Loading buffer (Bio-Rad) containing 2.5% β-mE at 100°C for 5 min. 20-40 µg protein was run on 10, 12 or 15% Tris-Glycine SDS-PAGE gels and transferred to Immobilon-P PVDF membranes using a Trans-Blot SD Semi-Dry Transfer Cell (Bio-Rad). Blots were incubated with a blocking solution (PBS containing 5% fat-free dry milk and 0.1% Tween-20) for 1 hour, followed by a wash with PBS. Blots were incubated with primary antibodies (Table 19) diluted in blocking solution at 4˚C overnight, followed by three washes, 10 min each: one time with PBS, once in PBS with 0.1% Tween-20 and one more time in PBS. Then, blots were incubated with secondary HRP-conjugated antibodies α-mouse, α-rabbit or α-guinea pig (1:5000) in blocking solution for 1 hour at room temperature, followed by three washes as described above. Blots were incubated for 5 min with the Clarity Western ECL Substrate (Bio-Rad) and signals were detected by chemiluminescence using a LAS-4000 CCD camera system (Fujifilm).

Table 19: Antibodies used for western blot analysis					
Antibody	**species**	**predicted band (kDa)**	**observed band**	**Manufacturer**	**Catalogue number**
p-AMPK	rb	62		New England Bio	2535
AMPK	rb	62		New England Bio	2603
PKM1/2	rb	60		New England Bio	3190
ATG5	rb	56		Sigma-Aldrich	A0856
NDUFA9	ms	40	36	Abcam	ab14713
NDUFB8	rb	22		Abcam	ab110242
NDUFB9	rb	22		Abcam	ab106699
NDUFS3	ms	30		Abcam	ab110246
NDUFV2	rb	27	24	proteintech,	15301-1-AP
SDHA	rb	70		New England Bio	11998
UQCRC2	ms	49.5		Abcam	ab14745
MT-CO1	rb	57	40	Abcam	ab14705
TOMM20	ms	16		Abcam	ab56783
Mfn2	ms	86	75	Sigma-Aldrich	WH0009927M3
GAPDH	rb	37		New England Bio	3868
p62	gp	62		Progen	GP62-C
LC3B	rb	14-16		New England bio	ALX-803-081-C100
ATP5A	ms	53		Abcam	ab14748
Actin	rb	45	42	New England Bio	4970
Cleaved caspase 3	rb	17-19		New England Bio	9661S
Parp	rb	89, 116		New England Bio	9542P
ClpP	rb	27		Abcam	ab124822
Tubulin	ms	50		Hybridoma Bank	12G10
Ubiquitin	ms			LifeSensors	VU101
Prx-SO_3	rb	22		Abcam	ab16830
Prx 3	rb	20		(Olahova et al., 2008)	
Ref(2)p	rb	92		Abcam	ab178440
Tubulin (α-Drosophila)	rb	50		Abcam	ab179513
Atg8	rb	14-16		Kind gift from Ivana Bjedov, UCL	
FLAG	ms			Sigma-Aldrich	F3165
GFP	ms			Santa Cruz Biotechnology	sc-9996
NDP52	rb	52		New England Bio	9036S
OPTN	rb	66	74	Abcam	ab23666
NBR1	ms	120		Abnova	H00004077-MOI
TAX1BP1	rb	92		New England Bio	5105

2.2.22 Mitochondrial isolation and Blue native page

Atg5$^{+/+}$ and *ATG5*$^{-/-}$ MEFs were seeded in 10cm dishes and collected in 5ml cold PBS and transferred to a 15ml falcon. Cells were centrifuged for 5 min at 800g at 4°C and washed in cold PBS, followed by another round of centrifugation to pellet the cells. Cells were resuspended in solution A (20mM Hepes-KOH pH 7.6 (Sigma), 220mM mannitol (Sigma), 70mM sucrose (Sigma), 1mM EDTA (Sigma), 2mg/ml BSA (Sigma), 2mM DTT (Thermo Fisher Scientific) and 0.5mM PMSF (Sigma)) and homogenised

with 30 stroking using a glass homogeniser and a drill. Cells were centrifuged for 5 min at 800g at 4°C and the supernatant (containing the mitochondria) was collected and aliquoted into 1.5ml tubes, centrifuged for 10 min at 10,000g at 4°C. The supernatant (cytosolic fraction) was removed and the pellet (crude mitochondria) was resuspended in solution B (20mM Hepes-KOH pH 7.6, 220mM mannitol, 70mM sucrose, 1mM EDTA) and centrifuged again for 10 min at 10,000g at 4°C. The pellet was resuspended in 100µl solution B and protein concentration was determined using a BCA kit.

30µg pellet of isolated mitochondria were centrifuged for 10 min at 10,000g at 4°C and resuspenden in 30µl 1% digitonin or 30µl 1% triton X-100 buffer (1% digitonin or 1% Triton X-100, 20mM Bis-Tris pH 7, 50mM NaCl, 10% glycerol and 1mM DTT) and titrated 20x without making bubbles and incubated on ice for 20 min. Detergent-solubilised samples were centrifuged for 10 min at 16,000g at 4°C to remove insoluble material. 10x blue native page loading dye (5% Coomassie blue G (Sigma), 500mM ε-amino n-caproic acid (Calbiochem), 100mM Bis-Tris pH 7.0 (Amresco)) was added and ran on a 4 to 13% acrylamide–bisacrylamide BN–PAGE gel (in 70mM ε-amino n-caproic acid and 50mM bis-Tris pH 7) using an SE600 Electrophoresis Unit (Hoefer). For separation, cathode buffer (15mM bis-Tris pH 7 and 50mM tricine (Amresco)) containing 0.02% (w/v) Coomassie Blue G was used until the dye front had reached approximately one-third of the way through the gel before exchange with cathode buffer lacking Coomassie Blue G. Anode buffer contained 50 mM bis-Tris (pH 7.0). Native complexes were separated at 100V/10mA for 30 min at 4 °C, then 400V/15mA for 45-60 min and 400V/20mA for approximately 1 hour (till the blue front runs out of the gel into the anode buffer). Thyroglobulin (669 kDa), ferritin (440 kDa), and bovine serum albumin (BSA, 140 and 67 kDa) were used as markers. The gel was transferred to PVDF membranes (400 mA for 1.5 hour) and Coomassie stained (40% Ethanol, 7% Acetic acid 0.2% Coomassie Brilliant Blue – R (Sigma)) and destained with 20% Ethanol, 7% Acetic acid, further destained with 90% methanol, 10% acetic acid. Membranes were blocked in blocking solution as described in section 2.2.21. Primary antibodies used were Ndufa9 (Kindly provided by Dr. Michael Ryan (Johnston et al., 2002)), Sdha and Actin. The catalogue numbers for all reagents are listed in table 5.

2.2.23 Nuclear fractionation

Nuclear fractionation was carried out as in (Suzuki et al., 2010). Briefly, $1.8x10^5$ MEFs were seeded 6-well plates 48 hours prior to collection. Cells were washed in ice-cold PBS, scrapped in 1 ml ice-cold PBS and centrifuged for 10 sec at 13,000 rpm at 4˚C. The pellet was carefully resuspended in 1 ml ice-cold 0.1% NP40 in PBS. 50µL was collected in a fresh tube (whole cell sample). Samples were centrifuged again for 10 sec at 13,000 rpm at 4˚C and supernatant, which represents the cytoplasmic fraction, was discarded. The pellet was resuspended in 1 ml ice-cold 0.1% NP40 in PBS. Samples were centrifuged for 10 sec at 13,000 rpm at 4˚C, supernatant was discarded and the nuclear pellet and the earlier collected whole cell lysates were prepared for western blot analysis. The whole cell lysate was mixed 3:1 with 4x Laemmli sample buffer with 10% β-mE (2.5% final concentration) and boiled at 100°C for 10 min on a thermomixer, shaking at 200 rpm. Nuclear pellets were resuspended in 200µL 1x Laemmli sample buffer with 2.5% β-mE and boiled at 100°C for 10 min on a thermomixer, shaking at 200 rpm. Samples were ran on a 12% agarose gel as described in section 2.2.21.

2.2.24 ROS Measurements

MEFs were seeded in a 12-well plate and grown in glucose- or galactose-based medium. Cells were then washed with PBS and trypsinised. Cells were then transferred to a 15 ml falcon tube and centrifuged for 3 min at 1600 rpm. The pellet was resuspended in 200µl SFM containing MitoSOX (5µM, Thermo Fisher Scientific) and incubated at 37˚C for 10 min. Cells were centrifuged again for 5 min at 900 rpm and the pellet was resuspended in 5ml SFM. Cells were analysed by fluorescence-activated flow cytometry (FACS, Partec) and mean fluorescence values were obtained.

2.2.25 qPCR

RNA from *Atg5*$^{+/+}$ and *Atg5*$^{-/-}$ MEFs or *p62*$^{-/-}$ MEFs stably expressing FLAG-tagged wild type, C105A,C113A or K7A,D69A PB1 domain mutant p62 was isolated using the RNeasy minikit (Qiagen) and cDNA was made using the Omniscript RT Kit (Qiagen, #205111) according to the manufacturer's instructions. qPCR was performed using the Power Syber Green PCR Master Mix (Thermo Fisher Scientific, #4368706) in a C1000TM Thermal Cycler, using CFX96TM Real-Time System (Bio-Rad) and Bio-Rad CXF Manager software using the primers in table 20. Expression was normalised to actin.

Table 20: Primers against mouse genes	
Atp5ase FWD	CTGCCACTCAACAGCTCTTG
Atp5ase REV	GGCTGATAACGTGAGACAAG
Mt-co1 FWD	CTGAGCGGGAATAGTGGGTA
Mt-co1 REV	TGGGGCTCCGATTATTAGTG
Ndufa9 FWD	GTCCGCTTTCGGGTTGTTAGA
Ndufa9 REV	CCTCCTTTCCCGTGAGGTA
Ndufb8 FWD	CAAGAAGTATAACATGCGAGTGGAA
Ndufb8 REV	CCATACCCCATGCCATCATC
Ndufb9 FWD	GCATCCCTCTGAGAAAGCAA
Ndufb9 REV	CATCAGGTGATGTTTCCTCCTG
Ndufs3 FWD	TGGCAGCACGTAAGAAGGG
Ndufs3 REV	CTTGGGTAAGATTTCAGCCACAT
Ndufv2 FWD	CGTTCCCTGTCAGCCTAGAG
Ndufv2 REV	TGCACTGCTGTCTTATGCAA
Sdha FWD	GGAACACTCCAAAAACAGACCT
Sdha REV	CCACCACTGGGTATTGAGTAGAA
Uqcrc2 FWD	CCCATCTTGCTTTGCTGTCTG
Uqcrc2 REV	AATAAAATCTCGAGAAGGACCCG
Pdk1 FWD	ACAAGGAGAGCTTCGGGGTGGATC
Pdk1 REV	CCACGTCGCAGTTTGGATTTATGC
Pkm2 FWD	TCGCATGCAGCACCTGATT
Pkm2 REV	CCTCGAATAGCTGCAAGTGGTA
Atf5 FWD	TTGTTGGTGCAGCCTCCATT
Atf5 REV	ATCAGAGAAGCCGTCACCTGC
Chop-10 FWD	CCTGAGGAGAGAGTGTTCCAG
Chop-10 REV	CCTCTTCGTTTCCTGGGGAT
ClpP FWD	TGGGCCCGATTGACGACAGTG
ClpP REV	TAGATGGCCAGGCCCGCAGT
ClpX FWD	TGTTGTTGGCCAGTCGTTTG
ClpX REV	AGCGATCTGAAGGAACTCTCT
Hsp70 FWD	TGCCTCCAATGGTGATGCTT
Hsp70 REV	CAGCATCCTTAGTGGCCTGT
Hspd1 FWD	CCCGCAGAAATGCTTCGACT
Hspd1 REV	ACTTTGCAACAGTGACCCCA
SatB2 FWD	GTCTCCAAATCGGAGCAGCA
SatB2 REV	GAATCATCAAACCTCCCACGG
Ubl5 FWD	TGCGCAACAGAATCGCAAAT
Ubl5 REV	GTGTCATCGGTGTTGCACTT
Actin FWD	TAAGGCCAACCGTGAAAAG
Actin REV	ACCAGAGGCATACAGGGACA
Ho-1 FWD	GGTCAGGTGTCCAGAGAAGG
Ho-1 REV	CTTCCAGGGCCGTGTAGATA

2.2.26 Human brain samples and spinal cord tissue from the Newcastle Brain Tissue Resource Bank

Frozen brain and spinal cord tissue were obtained from the Newcastle Brain Tissue Resource bank. Frozen tissue from Alzheimer's disease (AD, temporal cortex), frontotemporal dementia (FTD, temporal cortex), dementia with Lewy bodies (DLB, cingulate cortex), Parkinson's disease (PD, substantia nigra), sporadic amyotrophic lateral sclerosis (SALS, spinal cord), and matched controls (Table 21 & 22) were

homogenised using a Ultra-Turrax T10 (IKA) in homogenisation buffer (0.1M Tris pH 7.4, 0.5% Triton X-100, 50mM NEM supplemented with 1X Halt protease & phosphatase inhibitor cocktail (Thermo Fisher Scientific) in ddH_2O) in a 1:10 ratio (e.g. 50mg of tissue in 500 µl of buffer). Homogenised samples were centrifuged (13,000 rpm for 10 min at 4°C), protein concentration in supernatants was measured as described previously and samples were made by adding 2x Laemmli sample buffer to supernatants in the presence or absence of 2.5% β-mE. Samples were then analysed by immunoblot analysis.

Table 21: Frozen brain tissues

Case ID	Diagnosis	Area (Cortex)	Hemisphere	Age	Sex	PM delay (h)
205	AD	Temporal	Left	86	F	5
26	AD	Temporal	Left	83	M	12
83	AD	Temporal	Left	63	F	11
378	FTD	Temporal	Left	88	M	42
51	FTD	Temporal	Left	73	F	47
85	FTD	Temporal	Left	83	F	39
932	DLB	Cingulate	Left	78	M	8
310	DLB	Cingulate	Left	91	F	10
17	DLB	Cingulate	Left	77	M	8
115	Control	Cingulate/Temporal	Left	82	F	12
1035	Control	Cingulate/Temporal	Right	66	M	9
102	Control	Cingulate/Temporal	Left	72	M	17

Table 22: Frozen spinal cord tissues

Case ID	Diagnosis	Area of Onset	Age	Sex	PM delay (h)
768	ALS	Limbs	75	F	26
219	ALS	Limbs	72	F	52
1913	ALS	Limbs	80	F	26
496	Control	N/A	80	F	31
1016	Control	N/A	74	F	49
891	Control	N/A	73	M	25

2.2.27 ALS spinal cord tissue from the tissue bank of the Pitié-Salpêtrière hospital Neuropathology Department

Transversal sections (2µm of thickness) of lumbar spinal cords (Table 23) were homogenized in 50mM Tris-HCl pH 8, 150mM NaCl, protease inhibitors (Complete mini tablets, Roche) and 0.5U/µl benzonase endonuclease (Merck Millipore). The samples were incubated at 37°C during 30 min SDS was then added at a final concentration of 2%. Tissue extracts were centrifuged at 13,000 rpm for 10 min and protein concentration of supernatants was estimated by the bicinchoninic acid assay

(Sigma Aldrich). Samples were made by adding 2x Laemmli sample buffer to supernatants in the presence or absence of 2.5% β-mE. Samples were then analysed by immunoblot analysis.

Table 23: Lumbar spinal cord tissues					
case ID	**site of ALS onset**	**Mutation**	**Sex**	**age of death (years)**	**disease duration (months)**
768	Limbs	SALS	F	75	72
219	Limbs	SALS	F	72	60
1913	Limbs	SALS1	F	80	36
A42	Bulbar	SALS2	F	74	9
A40	Bulbar	SALS3	M	71	22
A43	Bulbar	K102E	F	82	10
496	Control	n/a	F	80	n/a
1016	Control	n/a	F	74	n/a
891	Control	n/a	M	73	n/a

2.2.28 Histochemistry of mouse tissues

Mice were housed in same-sex cages in groups of 4 to 6 (56×38×18 cm, North Kent Plastics, Kent, UK) and individually identified by an ear notch. Mice were housed at 20 ± 2°C under a 12 hours light/12 hours dark photoperiod with lights on at 7.00 am. The diet used was standard rodent pelleted chow (CRM (P); Special Diets Services, Witham, UK). Paraffin sections were deparaffinised with Histo-Clear (National Diagnostics) and ethanol, antigen was retrieved by incubation in 0.01M pH 6.0 citrate buffer at 95°C for 20 min. Slides were incubated in 0.9% H_2O_2 for 30 min and afterwards placed in blocking buffer (normal goat serum, Vector Lab) for 30 min at room temperature. Primary antibody (guinea pig α-p62) was applied overnight at 4°C. Slides were washed three times with PBS and incubated for 30 min with secondary antibody (Vector Lab). Antibodies were detected using peroxidase VECTASTAIN ABC kit (Vector Lab) according to the manufacturer's instructions. Substrate was developed using NovaRED (Vector Lab). Sections were counterstained with haematoxylin and mounted with DPX (Thermo Fisher Scientific). This experiment was carried out in collaboration with Dr. Diana Jurk.

2.2.29 Immunofluorescence microscopy

HeLa cells and MEFs were seeded on coverslips in 12-well plates. After treatments, cells were fixed in 3.7% formaldehyde in PBS for 5 min at room temperature. Cells were permeabilised with 0.5% Triton X-100 for 5 min at room temperature (or in methanol at -20°C for LC3 staining). Coverslips were blocked for one hour in 5% normal goat or rabbit serum in PBS 0.05% Tween-20 (for LC3 staining, the Tween-20

was omitted from all steps). Cells were incubated with primary antibodies (Table 24) overnight at 4°C. Cells were washed three times and incubated with the appropriate secondary antibodies for one hour at room temperature (Thermo Fisher Scientific, 1:5000). Cells were washed and nuclear DNA was stained by incubation with TO-PRO-3 iodide (Thermo Fisher Scientific, 1:3000) for 10 min at room temperature. Coverslips were mounted on slides with Prolong Gold Antifade (Thermo Fisher Scientific) and imaged with an LSM 510 META Confocal Microscope (Zeiss) using a 63X Plan-Apo/1.4 NA Oil objective. Images were analysed using ImageJ software (NIH).

Table 24: Antibodies used for immunofluorescence microscopy

Antibody	species	Dilution	Manufacturer	Catalogue number
p62	ms	1/200	BD Bioscience	610832
LC3	rb	1/200	New England BioLabs	3868

2.2.30 Immunofluorescence labelling of mouse intestine

To deparaffinise and rehydrate, paraffin-fixed mouse intestine were incubated at 65°C for 25 min, followed by sequential washing steps in Histoclear (5 min, 10min) (National Diagnostics), and a graded ethanol series (2x100%, 95%, 70%, 5 min each). Next, sections were washed in distilled water and antigen retrieval was performed in 1 mM EDTA, pH 8, in a pressure cooker for 40 min followed by a wash in distilled water and PBS (5 min each). Sections were blocked in 1% NGS (normal goat serum) in PBS for 30 min at room temperature. Ndufb8 (IgG subtype 1, Abcam, ab110242) and the mitochondrial mass marker Vdac (IgG subtype 2b, Abcam, ab14734) were used at a concentration of 1/100 and 1/400 respectively overnight at 4°C. This was followed by three wash steps for 5 min in PBS followed by incubation with secondary anti-mouse conjugated with Alexa Fluor 488 antibodies IgG subtype 1 (Thermo Fisher Scientific, A-21121) and Alexa Fluor 546 IgG subtype 2b (Thermo Fisher Scientific, A-21143) for 30 min at room temperature followed by a three times wash of 5 min in PBS. Nuclei were stained with Hoechst (1/200, Thermo Fisher Scientific) for 30 min at room temperature. Finally sections were washed three times for 5 min in PBS and incubated in Sudan black solution for 10 min, washed again three times with PBS and counted in Prolong Gold (Thermo Fisher Scientific). This experiment was carried out in collaboration with Dr. Amy Reeve.

2.2.31 Live cell imaging to monitor mitophagy

HeLa wild type or PentaKO cells expressing His-FLAG-NDP52 wild type or His-FLAG C153,163,321A-NDP52 were seeded 2 days prior the imaging in glass bottom dishes, 70% confluent cells were treated with 4µM antimycin A (Merck Millipore) and 10µM oligomycin (Merck Millipore) for 3 hours. Imaging was performed using a spinning disk confocal head (CSU-X1, Yokogawa, Japan) mounted on an Axiovert 200M equipped with a 20x NA 0.8 objective driven by Axiovision software (v4.8.1, Zeiss, Cambridge, UK). Mt-Keima was excited with a 458 nm Argon laser (to excite at pH 7.2) and a 561 nm solid-state laser (to excite mtKeima at pH 4.8). Emission was collected using a 630/30 nm filter. YFP-Parkin was excited with a 488 nm Argon laser and 535/30 nm emission filter was used.

2.2.32 OCR and ECAR measurements using Seahorse analysis

Cellular oxygen consumption rates (OCR) and extracellular acidification rate (ECAR) in *Atg5*$^{+/+}$ and *Atg5*$^{-/-}$ MEFs were measured in parallel using a Seahorse XF24 analyser according to the manufacturer's instructions in unbuffered basic medium supplemented with 5mM glucose, 1mM sodium pyruvate, 2mM L-glutamine and 3% FCS or for galactose-based medium with 10mM galactose, 1mM sodium pyruvate, 4mM L-glutamate and 3% FCS. During analysis the following compounds were added to test mitochondrial activity and cellular bioenergetics flux: 0.5µM oligomycin to inhibit complex V, 2.5µM FCCP to stimulate mitochondrial oxygen consumption to maximum capacity, 80mM 2-deoxyglucose (2-DG) to inhibit glycolytic flux and 0.5µM rotenone and 2.5µM antimycin A to inhibit complex I and III respectively. Calculation of ATP production was carried out as described in (Mookerjee et al., 2015).

2.2.33 Complex I- and II-linked respiration measurements using Seahorse analysis

To measure complex I and II-linked respiration cells were permeabilised using Seahorse XF Plasma Membrane Permeabilizer (Agilent Technologies) and OCR was measured in the assay buffer (115 mM KCl, 10 mM KH_2PO_4, 2 mM $MgCl_2$, 3 mM HEPES, 1 mM EGTA and 0.2% fatty acid-free BSA, pH 7.2, at 37 °C) with complex I substrates (10 mM pyruvate and 1 mM malate) or complex II substrate (4mM succinate) in the presence of 0.5µM rotenone to prevent respiration via complex I. State 3 oxygen consumption rates were obtained by adding 4 mM ADP.

Table 25: Reagents used for Seahorse analysis				
Reagent	Manufacturer	Catalogue number	Stock concentration	final concentration
Oligomycin	Sigma-Aldrich	O4876	5mM	0.5µM
FCCP	Sigma-Aldrich	C2920	20mM	2.5µM
Antimycin A	Sigma-Aldrich	A8674	25mM	2.5µM
ADP	Sigma-Aldrich	A5285	100mM	4mM
2-deoxyglucose	Sigma-Aldrich	D8375	-	80mM
Rotenone	Sigma-Aldrich	R8875	5mM	0.5µM
Pyruvate	Sigma-Aldrich	P5280	1M	5mM
Malate	Sigma-Aldrich	M6413	1M	5mM

2.2.34 Quantifications and Statistical Analysis

Quantification of cells was performed by blind scoring of slides as described previously (Korolchuk et al., 2011). More than 200 cells were counted per slide and quantification was based on at least three independent experiments. Quantification of immunoblots was carried out using ImageJ software (National Institutes of Health) by measuring the integrated density from each band after background subtraction. Two-tailed, unpaired Student's t-tests were carried out on experimental data from at least three individual experiments. Unpaired Student's t-tests were used on Seahorse data from at least three individual experiments.

For the quantification of mitophagy events, the ratio (550/438) images of mtKeima were created and analyzed using ImageJ software. High ratio (550/438) regions were automatically segmented, and their areas were calculated. The whole cell region was delineated manually on a fluorescent image to facilitate area calculation. The ratio (high ratio [550/438] area/total cell area) was used as an index of mitophagy. Quantifications were carried about by Dr. Yoana Rabanal Ruiz.

3 CHAPTER 3: AUTOPHAGY DEFICIENCY AND MITOCHONDRIAL DYSFUNCTION

3.1 Introduction

Many neurodegenerative diseases, such as Alzheimer's disease (AD), frontotemporal dementia (FTD) and dementia with Lewy bodies (DLB), have been associated with autophagy dysfunction (Section 1.12). Different genes associated with these diseases, directly or indirectly point to autophagy as the common pathway affected (Frake et al., 2015).

Mutations in core autophagy genes, such as *ATG4D*, cause neurodegeneration (Kyostila et al., 2015) and in mice loss of core autophagy genes specifically in neurons result in neurodegenerative phenotypes as well (Komatsu et al., 2006). Thus, impaired autophagy function has been shown to be an important contributor to neurodegenerative diseases (Menzies et al., 2017). Neurons seemed to be particularly susceptible for autophagy dysfunction, which is thought to be due to their post-mitotic nature and highly polarised cell shape. The long axons and dendrites are especially very susceptible to the accumulation of protein aggregates and damaged organelles, when not cleared efficiently by autophagy. More work needs to be done to investigate the involvement of autophagy in neuropathic mechanisms. How does autophagy dysfunction result in neurodegeneration? The accumulation of toxic protein aggregates in neurons is a common hallmark of neurodegenerative diseases and has been suggested to be pathogenic (Williams et al., 2006), even though this is under debate. These protein aggregates have also been suggested to be protective, whilst the damaged misfolded proteins are pathogenic (Ross and Poirier, 2005). As extensively discussed in section 1.12 mitochondrial dysfunction has been associated with AD, FTD and DLB. Despite identification of several genetic hereditary cases, most neurodegenerative cases have an unknown cause and a sporadic onset. As age is one of the risk factors of neurodegeneration and autophagy and mitochondrial function both decrease with age and in age-related neurodegenerative diseases (Wyss-Coray, 2016, Lopez-Otin et al., 2013), we were interested to study the interdependence in more detail.

Whilst the molecular mechanisms of autophagy are currently an area of intense research, very little is known how autophagy (or its deficiency) affects mitochondrial function. Furthermore, the interdependence has not been studied in great detail, especially the effect of defective autophagy on mitochondrial function. In this results chapter, we aimed to understand if autophagy dysfunction affects mitochondrial function and if mitochondrial dysfunction is the cause of cell death in neurodegeneration. We found that autophagy deficient cells have an isolated complex I dysfunction and preventing ROS production via complex I or bypassing complex I respiration rescues galactose-induced cell death. These results imply that associated with autophagy dysfunction aberrant ROS production via complex I is pathogenic for neurodegenerative diseases and this could be an interesting target for treatment.

3.1.1 A switch to galactose-based medium induces cell death in autophagy deficient MEFs

Culturing cells in galactose- instead of the standard glucose-based medium initially causes energy stress, because of the lack of glucose no energy can be produced via glycolysis, however after longer time periods, the cells adapt and up-regulate mitochondrial respiration (Rossignol et al., 2004). In glucose-free medium containing galactose, cells are forced to rely predominantly on mitochondrial respiration for ATP production because galactose as a carbon source feeds the glycolytic pathway with a low efficiency. It has been shown previously that cells with mitochondrial deficiency do not survive in galactose-based medium (Robinson et al., 1992). To test if autophagy deficient cells have a mitochondrial deficiency, *Atg5*$^{-/-}$ and wild type MEFs were switched to galactose-based medium. Atg5 is an E3 ubiquitin-like ligase, which is required for autophagy, thus loss of this protein results in a complete block of autophagy (Mizushima et al., 2001). Western blot analysis was performed and blots were probed for cleaved caspase 3 and cleaved Parp-1, which are both markers for cell death via apoptosis. After culturing *Atg5*$^{-/-}$ MEFs in galactose-based medium for 24 hours, cleaved caspase 3 was increased, which was significant after 48 hours compared to *Atg5*$^{+/+}$ MEFs (Figure 16A). Parp-1 showed the same trend, however this was not significant. This increased cell death was confirmed by bright field microscopy (Figure 16B). Importantly, re-expressing Atg5 rescued cell death as was shown by bright field microscopy and western blot of cleaved caspase (Figure 16C&D).

Furthermore, to confirm that the cell death was via apoptosis, cells were treated with Z-VAD-FMK. This pan-caspase inhibitor binds to caspase proteases and thereby inhibits apoptosis. Treating cells with Z-VAD-FMK prevented galactose-induced cell death in *Atg5*$^{-/-}$ MEFs, showing that cell death is induced via apoptosis (Figure 16E). Thus, *Atg5*$^{-/-}$ MEFs do not survive in galactose-based medium, suggesting that these cells might have a mitochondrial defect.

This experiment was repeated in M5-7 MEFs, which is an inducible *Atg5* knock-out cell line, which showed a similar phenotype. Removing Tetracycline and thus allowing the cells to re-express Atg5 rescued cell death (Figure 16F). Interestingly, M5-7 cells have to grow in tetracycline for at least 5 weeks in order to observe the phenotype. This suggests that autophagy deficiency could results in a build-up of dysfunctional mitochondria in time (potentially due to a lack of mitophagy), but also suggests that the cell death is not caused by starvation as a result of less recycling of nutrients via autophagy.

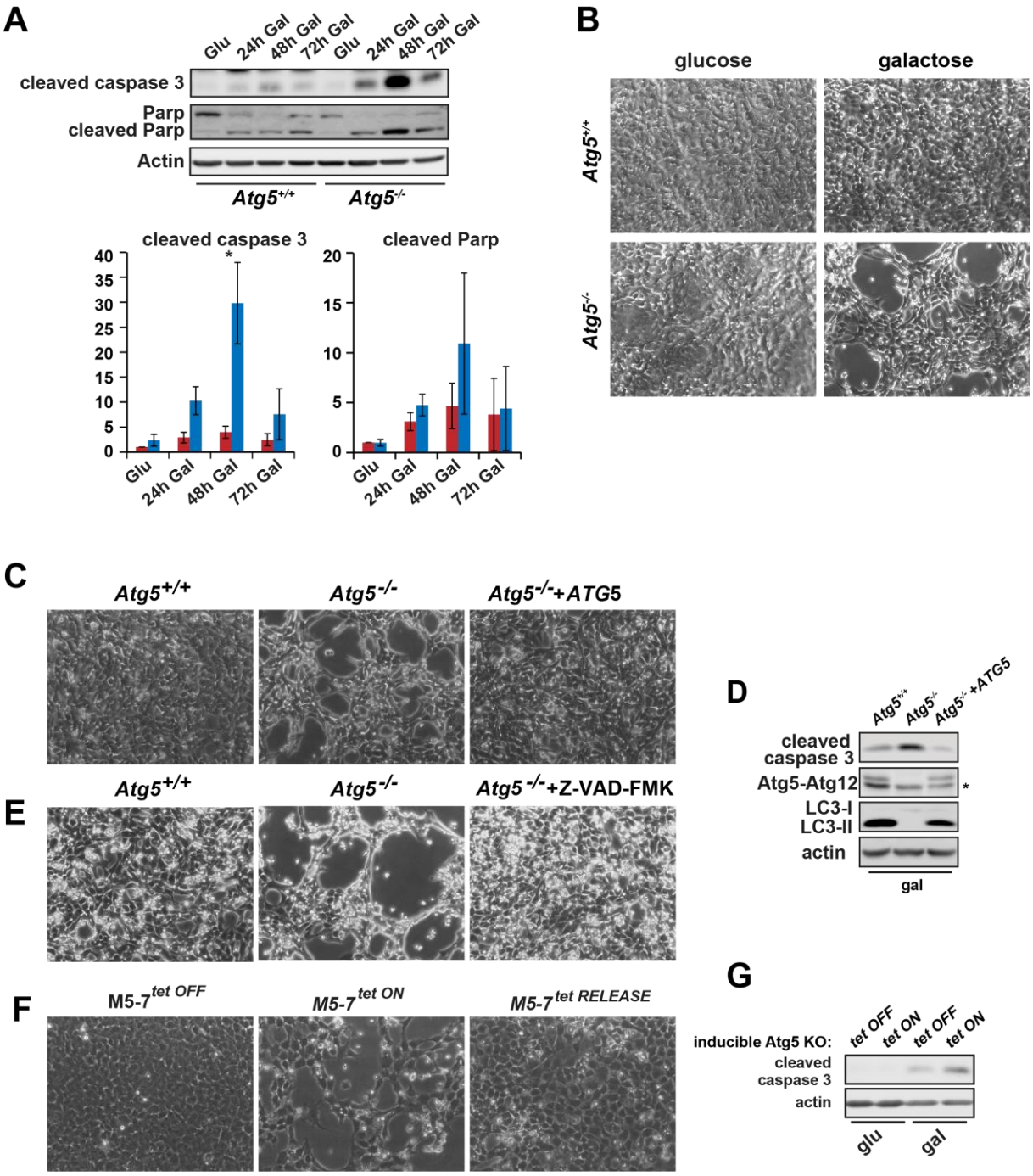

Figure 16 Apoptotic cell death in *Atg5*$^{-/-}$ MEFs upon a switch to galactose-based medium.

(A) Western blot analysis of markers for apoptosis; cleaved caspase and cleaved Parp-1 in *Atg5*$^{+/+}$ and *Atg5*$^{-/-}$ MEFs upon a 24, 48 or 72 hours switch to galactose-based medium. The ratio to actin was normalised to *Atg5*$^{+/+}$ MEFs. Error bars represent s.e.m., *P<0.05 (n=3). (B) Bright field microscopy images of *Atg5*$^{+/+}$ and *Atg5*$^{-/-}$ MEFs grown in glucose- or in galactose-based medium for 72 hours. (C) Bright field microscopy images of *Atg5*$^{+/+}$, *Atg5*$^{-/-}$ or *Atg5*$^{-/-}$ stably expressing *ATG5* or (E) *Atg5*$^{-/-}$ MEFs treated with Z-VAD-FMK grown in galactose-based medium for 48 hours, after 24 hours Z-VAD-FMK (20μM) was added to the cells. (D) Western blot analysis of *Atg5*$^{+/+}$, *Atg5*$^{-/-}$, *Atg5*$^{-/-}$ MEFs re-expressing *ATG5* grown in galactose-based

medium for 48 hours. Blots were probed for cleaved caspase 3, Atg5 and LC3. (F) Bright field microscopy images of M5-7 (inducible *ATG5* KO MEFs) grown in galactose-based medium for 5 days. Before switching to galactose, cells were grown in the presence of tetracycline for 5 weeks and release was for 5 weeks. (G) Western blot analysis of inducible ATG5 KO MEFs grown in glucose- or galactose-based medium for 5 days. Blots were probed for cleaved caspase 3.

3.1.2 *Atg5*$^{-/-}$ MEFs are characterised by the reduced oxygen consumption rate and increased glycolysis

To assess if loss of autophagy influences cellular bioenergetics characteristics through mitochondrial function, cellular oxygen consumption rates (OCR) and extracellular acidification rates (ECAR) were measured in intact *Atg5*$^{+/+}$ and *Atg5*$^{-/-}$ MEFs using a Seahorse XF24 analyzer (Agilent technologies). First the basal oxygen consumption is measured, then the ATP synthase inhibitor oligomycin A is added, which gives information about the proton leak as well as the OCR that is being used for ATP synthesis by calculating the difference. Addition of the mitochondrial uncoupler FCCP (Carbonyl Cyanide-4-(triFluoromethoxy)Phenylhydrazone) results in stimulation of electron transport chain, resulting in maximal OCR. Finally, Antimycin A inhibits the electron flux through complex III, resulting in a block in oxygen consumption (Figure 17). The remaining OCR determined after Antimycin A treatment is non-mitochondrial respiration (www.seahorsebio.com).

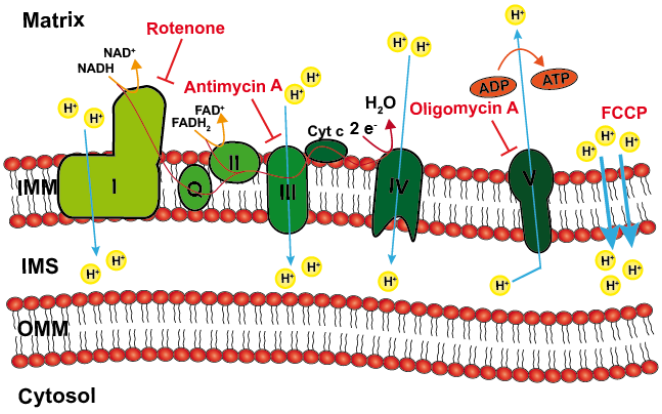

Figure 17 Inhibitors used for Seahorse analysis.

To measure the OCR, first oligomycin A is used to inhibit complex V, giving information about the proton leak from the IMS. FFCP is added to dissipate the ΔψM, resulting in maximum respiration and finally, Antimycin A and rotenone, which inhibits complex III and complex I, resulting in a block in electron flow and thus oxygen consumption. To measure ECAR oligomycin A is added to prevent ATP production via respiration and thus shifts the energy production to glycolysis, the resulting slope gives information about the glycolytic capacity and 2-DG (2-Deoxy-Glucose), a glucose analogue, is added to inhibit glycolysis.

As shown in Figure 18A, *Atg5*$^{-/-}$ MEFs have a reduced basal and maximum OCR. This suggests that when the cells have an increased ATP demand, the reduced maximal respiratory capacity may lead to an energetic crisis for the cells. Therefore, the ECAR (Extracellular ACidification Rate) was determined as well, which is an indirect measure for glycolysis, after corrected for the contribution by CO_2 produced by mitochondrial respiration through TCA cycle to the ECAR (Mookerjee et al., 2015). Because respiration was less efficient in *Atg5*$^{-/-}$ MEFs, we expected the cells to compensate by increasing glycolysis in order to prevent a shortage of energy. To measure ECAR, oligomycin A, FCCP, 2-DG and antimycin A and rotenone were sequentially used, as described in Figure 17. When we calculate the ATP production via OXPHOS and glycolysis, we observed that in *Atg5*$^{-/-}$ MEFs significantly less ATP is produced via mitochondrial respiration and more ATP is produced via glycolysis (Figure 18C). The total ATP production seems to be decreased as well, however this is not significant (Figure 18C). In *Atg5*$^{+/+}$ MEFs approximately 95% of the ATP is produced via OXPHOS and only 5% via glycolysis (Figure 18C). Most likely, pyruvate produced via glycolysis enters the TCA cycle and produces ATP via OXPHOS, whilst in *Atg5*$^{-/-}$ MEFs pyruvate is diverted towards lactate production to produce ATP, potentially because of their mitochondria being dysfunctional. In cells grown on galactose-based medium no ATP production via glycolysis was observed as expected and a clear reduction in total ATP production in *Atg5*$^{-/-}$ MEFs was observed (Figure 18D).

Furthermore, western blot analysis showed increased Ampk phosphorylation in *Atg5*$^{-/-}$ MEFs (Figure 18E). Phosphorylation of this energy sensor indicates that there is energy stress. Ampk gets activated by an increased AMP/ATP ratio and needs to be phosphorylated at Thr172 for its activity (Gowans et al., 2013).

In addition, the glycolytic enzyme Pkm1/2 protein levels were increased in *Atg5*$^{-/-}$ MEFs. Pkm1 is expressed in most adult tissues, whereas Pkm2 is a splice variant that is shown to be essential for aerobic glycolysis in cancers. qPCR revealed that mRNA levels of Pdk1 (Pyruvate Dehydrogenase Kinase 1), another glycolytic enzyme, that has been implicated in the Warburg effect, was significantly increased and Pkm2 mRNA levels showed a trend to be increased too (Figure 18F). From these results, we

conclude that *Atg5*$^{-/-}$ MEFs respire less efficiently and to compensate for the loss of mitochondrial respiratory function, up-regulate glycolysis.

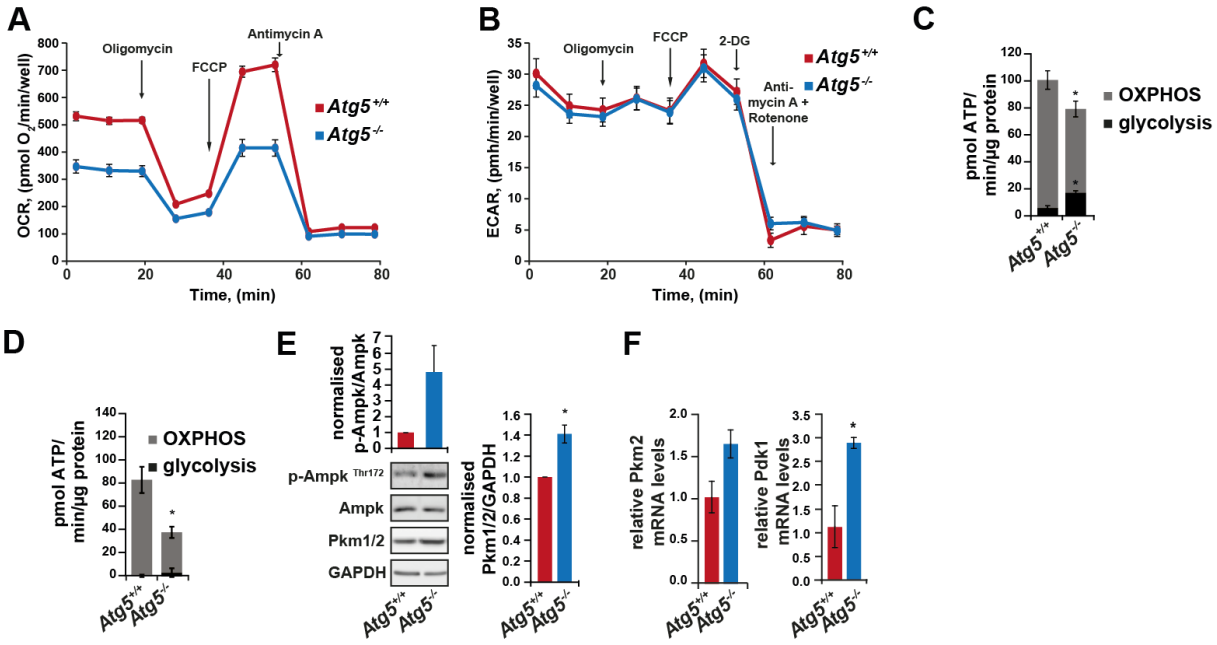

Figure 18 Bioenergetic analysis of *Atg5*$^{+/+}$ and *Atg5*$^{-/-}$ MEFs.

(A) Seahorse analysis of oxygen consumption rate (OCR) in *Atg5*$^{+/+}$ and *Atg5*$^{-/-}$ MEFs in glucose-based medium under basal conditions or following the addition of oligomycin A, FCCP or Antimycin A (n = 3). (B) Seahorse analysis of the extracellular acidification rate (ECAR) in *Atg5*$^{+/+}$ and *Atg5*$^{-/-}$ MEFs under basal conditions or following the addition of oligomycin A, FCCP, 2-DG, antimycin A and rotenone (n = 3). (C) ATP production by glycolysis (black) and OXPHOS (grey) calculated based on the Seahorse results in A and B in *Atg5*$^{+/+}$ and *Atg5*$^{-/-}$ MEFs (n=3). (D) ATP production in in *Atg5*$^{+/+}$ and *Atg5*$^{-/-}$ MEFs in galactose-based medium by glycolysis (black) and OXPHOS (grey) calculated based on the Seahorse results (n=3). (E) Western blot analysis of phospho-Ampk, Ampk, Pkm1/2 and Gapdh in *Atg5*$^{+/+}$ and *Atg5*$^{-/-}$ MEFs. The ratio of phospho-Ampk to total Ampk and Pkm1/2 to GAPDH was quantified and normalised to the *Atg5*$^{+/+}$ MEFs. (n=3) (F) mRNA expression of the glycolytic enzymes Pkm2 and Pdk1 in *Atg5*$^{+/+}$ and *Atg5*$^{-/-}$ MEFs, mRNA levels were normalised to the *Atg5*$^{+/+}$ MEFs. (n=6) Error bars represent s.e.m., *P<0.05. Seahorse experiments were carried out by Dr. Satomi Miwa.

3.1.3 *Atg5*$^{-/-}$ MEFs have an isolated complex I defect

Intact cellular bioenergetics assessment using Seahorse analyzer does not give any information about what the site of mitochondrial dysfunction is, causing the lower maximal respiratory capacity. Therefore, Seahorse analysis was performed in permeabilised cells, using complex I and complex II substrates (pyruvate and malate or succinate, respectively) to assess mitochondrial functional property in more depth

(Figure 19). Firstly ADP, a complex V substrate, was added to stimulate state 3 respiration. Secondly, oligomycin A was added to inhibit complex V to bring the state 4 respiration rate. Thirdly, FCCP was added to stimulate the electron transport chain without coupling and finally the complex III inhibitor antimycin A was added to inhibit the respiratory chain.

Mitochondrial function could be assessed by the RCR (Respiratory Control Ratio), which is state 3 divided by state 4. This ratio indicates the coupling between the ETC and ATP production and the greater the RCR, the better the mitochondrial coupling is. State 3 was initiated with ADP, state 4 induced with oligomycin A. In *Atg5*$^{-/-}$ MEFs the RCR for complex I-linked respiration was lower, meaning that complex I linked respiration is less coupled to ATP production (Figure 19A&B). This indicates that mitochondria are less functional in *Atg5*$^{-/-}$ MEFs and that complex I is the main site of dysfunction. Complex II-linked respiration was not impaired in these cells, showing that complex II, III, IV and V function are not affected (Figure 19C&D). The complex-II linked RCR was even higher in *Atg5*$^{-/-}$ MEFs, suggesting that there is a compensatory mechanism to bypass complex I-linked respiration. This data show that *Atg5*$^{-/-}$ MEFs have an isolated complex I defect.

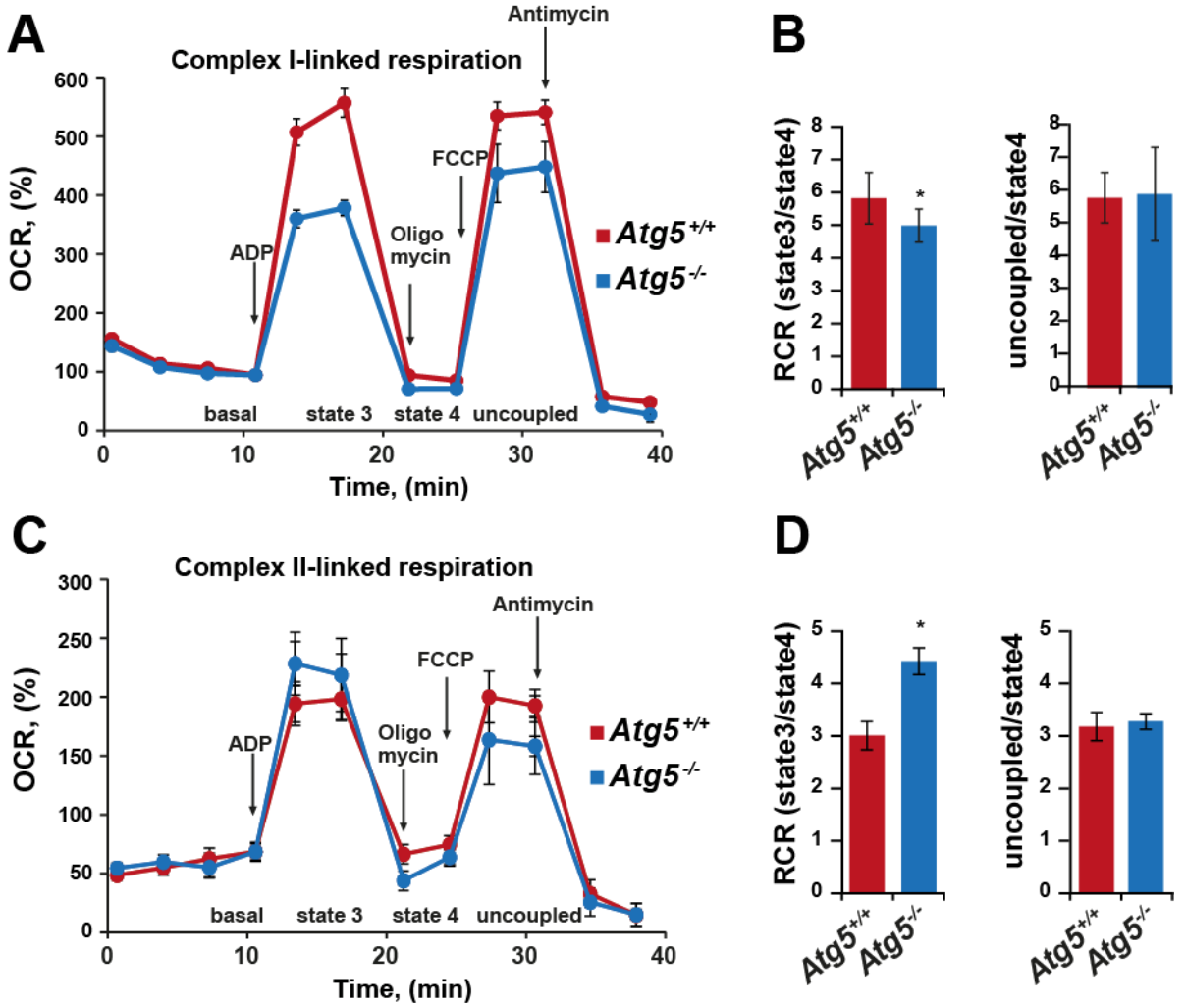

Figure 19 *ATG5*$^{-/-}$ MEFs have reduced complex I-linked respiration.

(A) Seahorse analysis of complex I-linked respiration in permeabilised *Atg5*$^{+/+}$ and *Atg5*$^{-/-}$ MEFs. Media contained pyruvate and malate as a complex I substrate. Sequential measurement of basal, state3, state 4 and uncoupled state were performed through the sequential injections of ADP, oligomyin, FCCP and antimycin. (B) Quantification of the respiratory control ratio (RCR; state 3/state 4 respiration) in *Atg5*$^{+/+}$ and *Atg5*$^{-/-}$ MEFs. (C) Seahorse analysis of complex II-linked respiration, using succinate as a substrate. (D) Quantification of the RCR calculated based on the data in C. Error bars represent s.e.m., *P<0.05, (n=3). Seahorse experiments were carried out by Dr. Satomi Miwa.

To characterise the mitochondrial complex I phenotype we observed via Seahorse in more detail, we performed western blot analysis of mitochondrial ETC complexes. We used set of antibodies recognising subunits in different modules of complex I. Ndufb8 and Ndufb9 are accessory subunits residing in the membrane bound core. Ndufb8 and Ndufb9 were shown to be important for the interaction between complex I to complex III within the respirasome (Wu et al., 2016a, Letts et al., 2016). Ndufs3 is a core subunit

of the matrix arm, which contains three FeS clusters and Ndufa9 has not been allocated to one module, but probably resides in a module interface, between module Q and P_P (Wu et al., 2016a, Stroud et al., 2016) and finally Ndufv2 is a core subunit of the distal matrix arm (module N) (Wu et al., 2016a) (Figure 20C).

To our surprise, we observed a substantial loss of all the nuclear encoded mitochondrial complex I subunits, Ndufb8, Ndufs3, Ndufa9 and Ndufv2, but not Ndufb9 in *Atg5*$^{-/-}$ MEFs, whilst complex II (Sdha), III (Uqcrc2), complex IV (Mt-co1) subunits were unaltered (Figure 20A&B). As a control, complex I deficient mES (mouse Embryonic Stem cells) were used. These cells have mutations in ND5/ND6, which are mitochondrial encoded complex I core subunits, resulting in a severe complex I defect (7% complex I activity) (Kirby et al., 2009). In these cells all complex I subunits tested were decreased (Figure 20A&B). Complex II (Sdha), III (Uqcrc2), complex IV (Mt-co1) and Mfn2 protein levels were unaffected in *Atg5*$^{-/-}$ MEFs and mES cells (Figure 20A). To exclude genetic drift, the M5-7 MEFs (inducible Atg5 knock-out) were used again and these cells displayed the same loss of complex I subunits Ndufb8, Ndufs3, Ndufa9 and Ndufv2 (Figure 20A).

An even more striking phenotype was observed in *Npc1*$^{-/-}$ MEFs, this cell line has a defect in amphisome maturation, resulting in accumulation of immature autophagosomes (Sarkar et al., 2013). In these cells Ndufb8, Ndufs3, Ndufa9 and Ndufv2 protein levels were reduced even more than in *Atg5*$^{-/-}$ MEFs, whilst Ndufb9 and other ETC complexes were unaffected (Lucy Sedlackova, data not shown), suggesting that this isolated loss of complex I is a common feature of autophagy deficient cells and this rules out that complex I is degraded via an Atg5-independent autophagy (Ma et al., 2015).

In literature it has been established that in *Atg5*$^{-/-}$ MEFs mitochondria accumulate (Komatsu et al., 2005, Nakai et al., 2007), however we observed that certain complex I subunits are selectively down-regulated, which suggests that that their protein levels are regulated via a different mechanism in autophagy deficiency. These subunits locate to the different modules of complex I, Ndufs3 (Q module) and Ndufv2 (N module) being in the matrix arm, Ndufa9 has not been allocated to any module, but reside in either the Q or P_P module. Ndufb8 is part of the P_D module in the membrane bound

core (Figure 20C) (Stroud et al., 2016), suggesting that most of the complex is down-regulated.

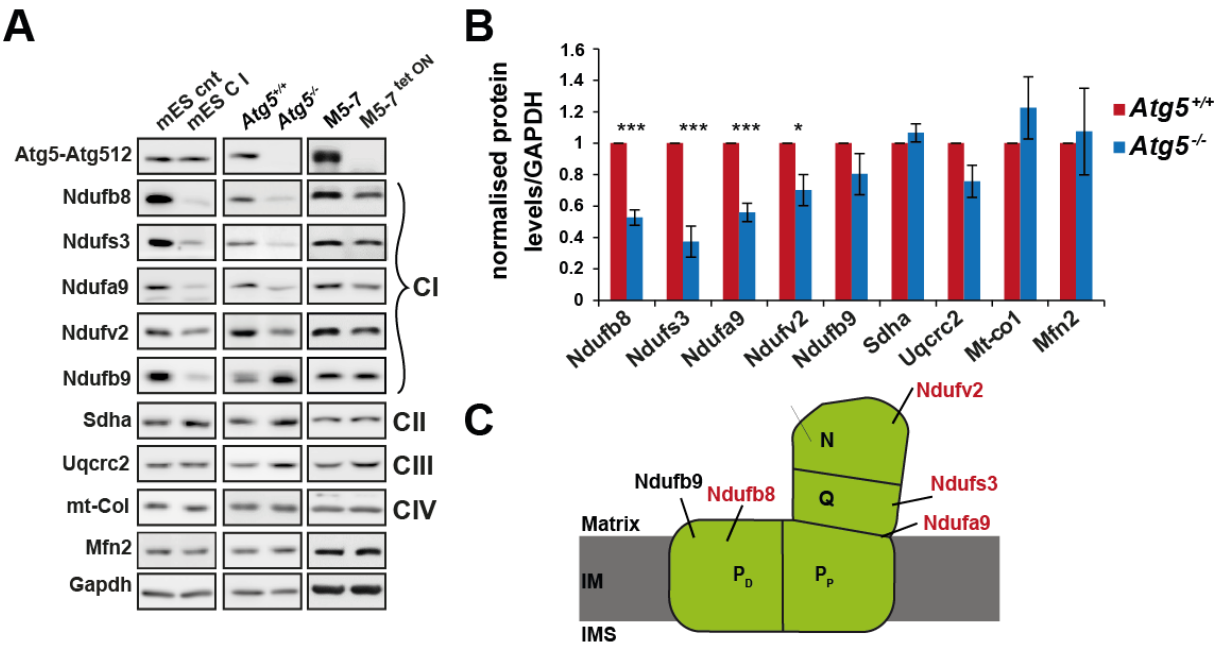

Figure 20 *ATG5*$^{-/-}$ MEFs have reduced complex I protein levels.

(A) Western blot analysis of complex I subunits: Ndufb8, Ndufs3, Ndufa9, Ndufv2, Ndufb9, complex II: Sdha, complex III: Uqcrc2, complex IV: Mt-co1, Tomm20 and Mfn2 in *Atg5*$^{+/+}$, *Atg5*$^{-/-}$ MEFs and inducible *Atg5*$^{-/-}$ MEFs (M5-7). As a positive control for complex I deficient cells, complex I deficient mouse embryonic stem cells (mES) were subjected to the same procedure. (B) Quantification of A. The ratio of the different proteins to Gapdh was normalised to *Atg5*$^{+/+}$ MEFs. Error bars represent s.e.m., *P<0.05, **P<0.01 (n=3). (C) Schematic diagram of mitochondrial complex I and the location of the different subunits used in this results chapter. The matrix arm consists of the N- and Q-model. The membrane bound core consists of P_P (proximal) and P_D-(distal) modules. P_D contains the proposed proton-translocating subunits. The affected complex I subunits are depicted in red. Modified after (Kmita and Zickermann, 2013).

3.1.4 Complex I subunits are not down-regulated in autophagy deficient mouse tissues

Next, we were investigated if the observed loss of complex I subunits in *Atg5*$^{-/-}$ MEFs could also be observed *in vivo*. *Atg5*$^{+/+}$ and *Atg5*$^{-/-}$ mouse intestine sections were subjected to an Ndufb8 and Vdac immunofluorescence staining. Ndufb8 was used as the marker for complex I and Vdac was used as a marker for total mitochondrial mass. No difference in the Ndufb8/Vdac ratio was observed between *Atg5*$^{+/+}$ and *Atg5*$^{-/-}$ mouse intestine (Figure 21A&B). In addition, mitochondrial ETC composition was assessed in autophagy deficient (*Atg7*$^{-/-}$) and wild type (*Atg7*$^{+/+}$) mouse brains by

western blot analysis. All mitochondrial proteins showed a trend to be increased and no loss of complex I subunits was observed (Figure 21C&D). Thus, *in vivo* we did not observe a down-regulation of complex I in response to an autophagy defect.

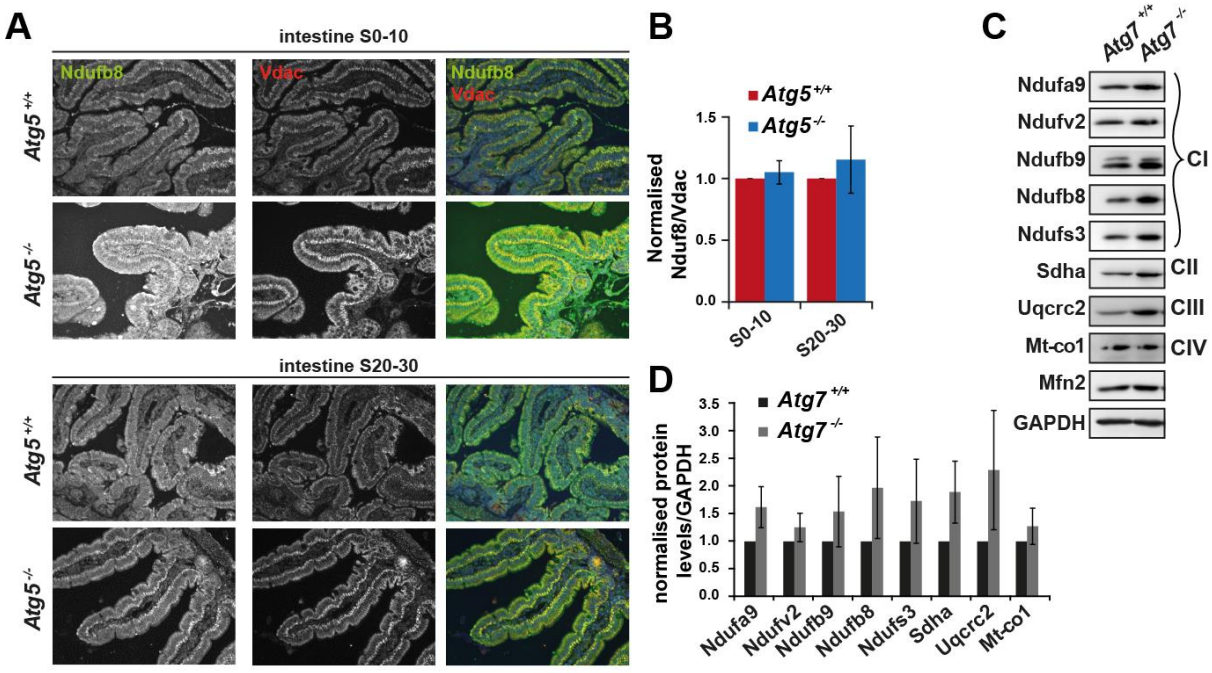

Figure 21 No difference in ETC composition in autophagy deficient mouse intestine and brain.

(A) Immunohistochemistry labelling of intestine from *Atg5*$^{+/+}$ and *Atg5*$^{-/-}$ mice. S0-10 and S20-30 are different sections from a 10 cm length small intestine. Paraffin embedded sections were stained for NDUFB8 (complex I) and VDAC (total mitochondria). This experiment was performed in collaboration with Dr. Amy Reeve. (B) Quantification of A. The Ndufb8/Vdac ratio was normalised to *Atg5*$^{+/+}$ intestine. Error bars represent standard deviation, (n=2). (C) Western blot analysis of complex I subunits: Ndufa9, Ndufv2, Ndufb9, Ndufb8, Ndufs3, complex II: Sdha, complex III: Uqcrc2, complex IV: Mt-co1 and Mfn2 in *Atg7*$^{+/+}$ and *Atg7*$^{-/-}$ MEFs. (D) Quantification of C. Ratio to Gapdh was normalised to *Atg7*$^{+/+}$. Error bars represent standard deviation, (n=2).

3.1.5 Switching cells from glucose to galactose-based media results in the recovery of respiratory complex I subunits in *Atg5*$^{-/-}$ MEFs

Thus far we only observed down-regulation of mitochondrial complex I subunits in autophagy deficient cell lines, but not *in vivo*. Cells in tissue culture are grown in glucose rich medium and therefore have the ability to use glycolysis, in addition to mitochondrial respiration. On the contrary, *in vivo* tissues such as mouse intestine and brain rely mainly on mitochondrial respiration (Bolanos and Almeida, 2010). Interestingly, in glucose-based medium *Atg5*$^{-/-}$ MEFs no cell death is observed, whilst

in mice loss of Atg5 in neurons, results in neurodegeneration and apoptotic granular cells were observed (Hara et al., 2006). In *Atg5*$^{-/-}$ MEFs in galactose-based medium we previously observed cell death, similar to the *in vivo* phenotype in mice (Figure 21). Therefore, we hypothesised that when mitochondrial respiration is enforced by galactose-based medium, complex I levels are maintained, similar to what we see *in vivo*.

To test this *Atg5*$^{+/+}$ and *Atg5*$^{-/-}$ MEFs were switched to galactose-based medium for 24, 48 and 72 hours and protein levels of the different mitochondrial ETC complexes were determined (Figure 22). The subunits that were down-regulated in *Atg5*$^{-/-}$ MEFs (Ndufb8, Ndufs3, Ndufa9 and Ndufv2) in glycolytic media were up-regulated to the levels comparable to those in *Atg5*$^{+/+}$ MEFs after being cultured for 24 hours in galactose-based medium, this increase in protein levels continued after 48 and 72 hours. The other complex I subunits (Ndufb9) were also up-regulated, as well as complex III (Uqcrc2) and complex V (Atp5a). Complex II (Sdha) showed a slightly different behaviour, protein levels increased after 24 hours, followed by a decrease after being cultured in galactose-based medium for 48 and 72 hours (Figure 22). As an indication of total mitochondrial mass, Mfn2 and Tomm20 protein levels were assessed too. These showed a similar behaviour as mitochondrial complex II, being up-regulated after 24 hours, followed by a down-regulation after 48 and 72 hours of galactose-based medium (Figure 22). Thus, cells up-regulate mitochondrial respiratory complexes in galactose-based medium and this was observed in *Atg5*$^{+/+}$ and *Atg5*$^{-/-}$ MEFs.

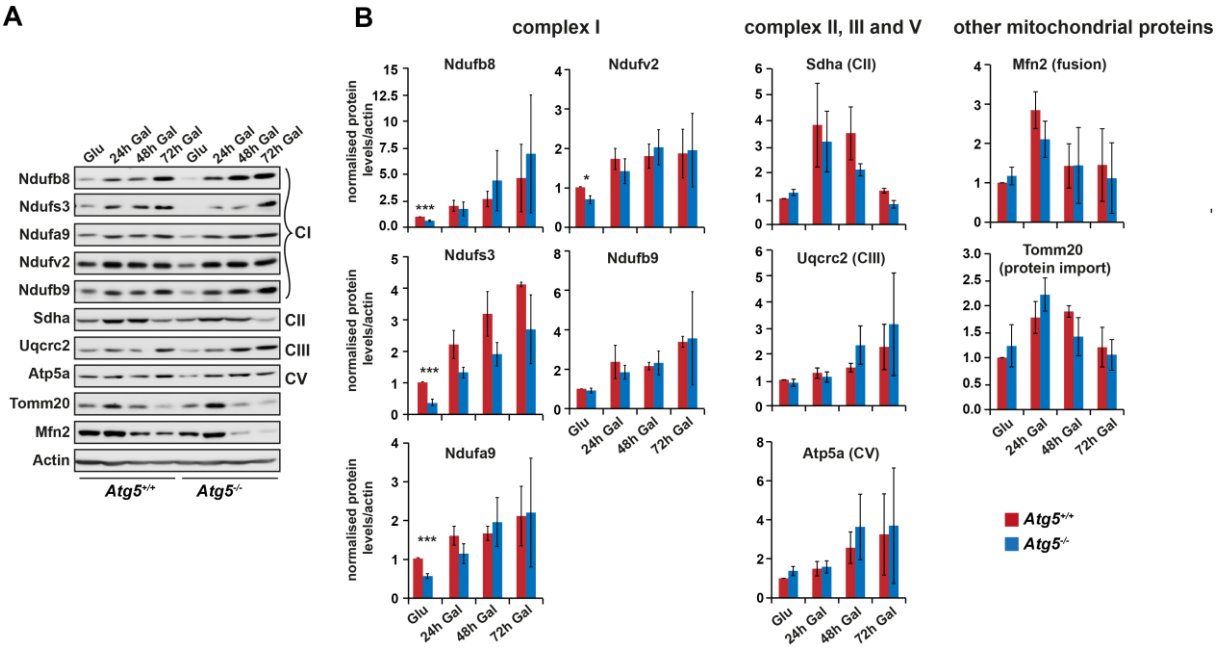

Figure 22 Switching MEFs to galactose-based medium results in up-regulation of ETC complexes in *Atg5*$^{+/+}$ and *Atg5*$^{-/-}$ MEFs.

(A) Western blot analysis of complex I subunits: Ndufb8, Ndufs3, Ndufa9, Ndufv2, Ndufb9, complex II: Sdha, complex III: Uqcrc2, complex IV: Mt-co1, complex V: Atp5a, Tomm20 and Mfn2 in *Atg5*$^{+/+}$ and *Atg5*$^{-/-}$ MEFs upon a 24, 48 or 72 hours switch to galactose-based medium. (B) Quantification the different mitochondrial proteins in A. The ratio to actin was normalised to *Atg5*$^{+/+}$ MEFs. Error bars represent s.e.m., **P<0.01 (n=3).

3.1.6 *Atg5*$^{-/-}$ MEFs incorporate less complex I into higher-order supercomplexes

The individual complex I subunits assemble into the holo-complex I, which is a tightly regulated process. ETC complexes then assemble in supercomplexes (CI-III$_2$-IV) to allow the efficient transfer of electrons through the different complexes (Section 1.11). It has been shown that high ROS levels results in the dissociation of complex I from complex III and this disruption results in less complex I dependent respiration and instability of the complex (Schagger et al., 2004). It could be speculated that these disassembled subunits are then targeted for degradation. We tested the assembly state of complex I and its assembly into supercomplexes in autophagy deficient cells using blue native page electrophoreses. Digitonin is a mild detergent that results in the solubilisation of mitochondrial membranes, whilst mitochondrial supercomplexes remain intact. On the contrary, Triton X-100 is a stronger detergent and disrupts the supercomplexes and is used to assess the assembly state of individual holo-

complexes. In glucose-rich medium we observe less of the holo-complex I in *Atg5*$^{-/-}$ MEFs as we expected based on our western blot results and it is also assembled less into the respirasome (CI-III$_2$-IV) (Figure 20 & 23). Upon a switch to galactose-based medium we previously observed the recovery of complex I subunits (Figure 22). We wanted to test if these newly produced subunits assembled efficiently into the holo-complex and if this holo-complex is incorporated into supercomplexes. Interestingly, we did observe the recovery of the respirasome in *Atg5*$^{-/-}$ MEFs upon a switch to galactose-based media. However, a band on top of the respirasome did not recover. These higher bands are thought to be higher-order supercomplexes that have not been studied in great detail, but have been observed by others as well (Gu et al., 2016).

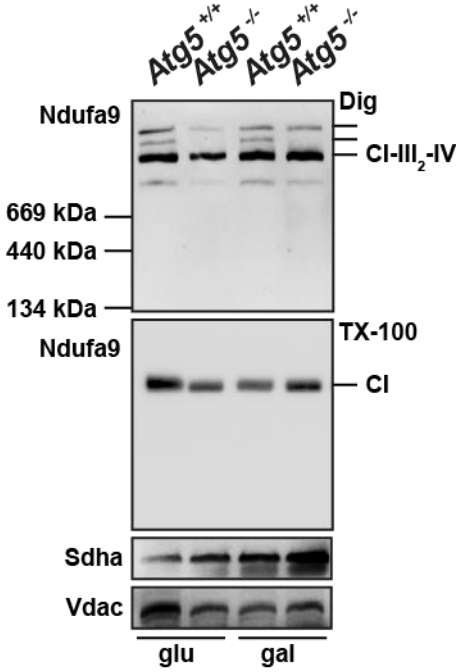

Figure 23 *Atg5*$^{-/-}$ MEFs incorporate less complex I into higher-order supercomplexes.

Blue native page analysis of digitonin or Triton X-100 solubilised mitochondria isolated from *Atg5*$^{+/+}$ and *Atg5*$^{-/-}$ MEFs grown in glucose-based or galactose-based medium for 24 hours. Complex I was analysed by Ndufa9, complex II by Sdha and Vdac was used as a loading control. (n=2)

3.1.7 Antioxidants and bypass of complex I-linked respiration rescue galactose-induced cell death in *Atg5*$^{-/-}$ MEFs

Complex I is known as the main source for ROS production (Section 1.11.2) and we observed a clear complex I deficiency in *Atg5*$^{-/-}$ MEFs in glycolytic conditions (e.g. less respiration (Figure 19) and down-regulation of subunits (Figure 20)). However, in

galactose-based medium and *in vivo* complex I is not down-regulated (Figure 21 & 22), potentially because the cells rely too much on complex I-dependent mitochondrial respiration and cannot afford it. Furthermore, we observed less complex I incorporated into respiratory supercomplexes in *Atg5*$^{-/-}$ MEFs (Figure 23). Therefore, we hypothesised that the down-regulation of complex I in glycolytic conditions is a protective mechanism to prevent aberrant ROS production via complex I. To test this hypothesis, *Atg5*$^{-/-}$ MEFs were switched to galactose-based medium and mitochondrial ROS was measured using mitoSOX as a dye to detect superoxide. In glucose-based medium not much mitochondrial superoxide was produced in *Atg5*$^{+/+}$ nor *Atg5*$^{-/-}$ MEFs, however upon a switch to galactose-based medium a striking increase in mitochondrial superoxide was observed (Figure 24A). Scavenging this mitochondrial ROS by using a mitochondrial targeted antioxidant (mitoQ) (Kelso et al., 2001), partially prevented galactose-induced cell death in *Atg5*$^{-/-}$ MEFs (Figure 24B). These antioxidants are not specifically targeting ROS produced by complex I, therefore S1QEL2.2 was used (Brand et al., 2016). This drug specifically prevents ROS production at site Q of complex I. This inhibitor prevents electrons flowing back from complex III, via Q, and thus limits RET (Reverse Electron Transport). Intriguingly, treating *Atg5*$^{-/-}$ MEFs with S1QEL2.2 fully prevents galactose-induced cell death (Figure 24C). This suggests that cell death in these cells is caused by ROS produced at complex I.

Another way to determine if dysfunctional complex I is the cause of galactose-induced cell death in *Atg5*$^{-/-}$ MEFs is by bypassing respiration via complex I and rewiring respiration towards complex II, which can be accomplished with a drug (I-BET 762) recently published (Barrow et al., 2016). I-BET 762 is a chemical inhibitor of BRD4 (Bromodomain-containing protein 4) and prevents binding of BRD4 to promotors of nuclear-encoded mitochondrial genes and its inhibition results in the rewiring of respiration via complex II and IV (Barrow et al., 2016). Barrow *et al.* convincingly show that cell death caused by chemically inhibition or mutations in complex I could be rescued by I-BET 762. Similar to treating *Atg5*$^{-/-}$ MEFs with S1QEL2.2, treating with I-BET762 also fully prevented galactose-induced cell death (Figure 24C). This suggests that cell death in these cells is indeed caused by dysfunctional complex I.

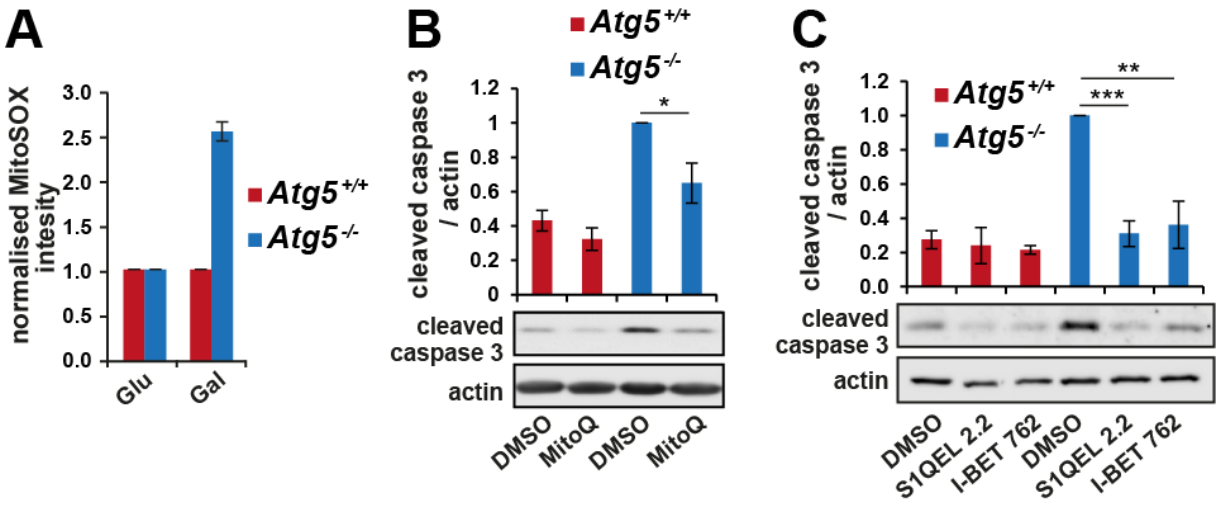

Figure 24 ROS produced by complex I causes galactose-induced cell death in *Atg5*$^{-/-}$ MEFs.

(A) Mitochondrial superoxide production was measured using mitoSOX in *Atg5*$^{+/+}$ and *Atg5*$^{-/-}$ MEFs in glucose-based medium and upon a 24 switch to galactose-based medium. mitoSOX intensity was analysed by FACS (Fluorescence-Activated Cell Sorting). Data were normalised to *Atg5*$^{+/+}$ MEFs, error bars represent standard deviation (n=2). (B) Western blot analysis of *Atg5*$^{+/+}$ and *Atg5*$^{-/-}$ MEFs switched to galactose-based medium for 48 hours in the absence or presence of mitoQ (20nM), or (C) S1QEL 2.2 (500nM) and I-BET 762 (1μM). All drugs were re-fed after 24 hours. Blots were probed for cleaved caspase 3. Error bars represent s.e.m., *P<0.05, **P<0.01, ***P<0.05, (n=3).

3.1.8 Mitochondrial respiratory complexes are transcriptionally up-regulated in galactose-based medium

Based on the timeframe, it is not likely that the increase of respiratory complexes upon a switch to galactose-based medium is caused by stabilisation of the complexes or less degradation. The half-lives of mitochondrial proteins are longer than half-lives on non-mitochondrial proteins and has been estimated to be approximately 400 hours in *D. melanogaster* (Vincow et al., 2013). Hence, we assumed that mitochondrial respiratory complexes were transcriptionally up-regulated. mRNA levels of the complex I subunits *Ndufa9*, *Ndufb8* and *Ndufs3*, complex II (*Sdha*), complex III (*Uqcrc2*) and complex V (*Atp5a*) were measured by qPCR in glycolytic and 24 galactose-based medium in *Atg5*$^{+/+}$ and *Atg5*$^{-/-}$ MEFs. mRNA levels of these subunits all tended to be increased upon a switch to galactose-based medium in *Atg5*$^{+/+}$ as well as *Atg5*$^{-/-}$ MEFs (Figure 25). In galactose-based medium *Ndufb8*, *Ndufs3* and *Atp5a* mRNA levels were even further increased in *Atg5*$^{-/-}$ MEFs compared to *Atg5*$^{+/+}$ MEFs. Interestingly, there were no differences in mRNA levels of *Ndufa9*, *Ndufb8* and *Ndufs3* between *Atg5*$^{+/+}$ and *Atg5*$^{-/-}$ MEFs in glycolytic conditions (Figure 25). Therefore, the

decrease in protein levels of mitochondrial complex I subunits in *Atg5*$^{-/-}$ MEFs in glycolytic conditions cannot be explained by a reduced transcription, but the recovery of subunits can be explained by transcriptional up-regulation.

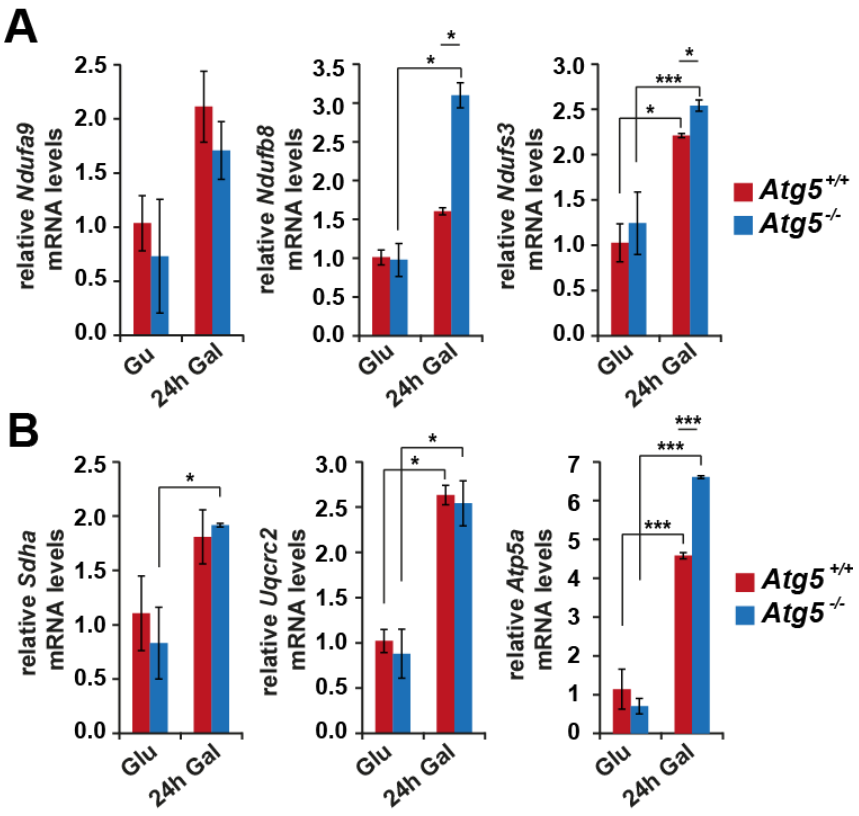

Figure 25 Mitochondrial respiratory complexes are transcriptionally up-regulated in galactose-based medium.

(A) mRNA expression of mitochondrial complex I subunits *Ndufa9*, *Ndufb8* and *Ndufs3* in *Atg5*$^{+/+}$ and *Atg5*$^{-/-}$ MEFs in glycolytic conditions or after being cultured in galactose-based medium for 24 hours. (B) mRNA expression of mitochondrial complex II, III and V subunits *Sdha*, *Uqcrc2* and *Atp5a* in *Atg5*$^{+/+}$ and *Atg5*$^{-/-}$ MEFs in glycolytic conditions or after being cultured in galactose-based medium for 24 hours. Error bars represent s.e.m., *P<0.05, ***P<0.005 (n=6).

3.1.9 UPRmt related genes *ClpX*, *ClpP* and *Ubl5* expression is increased in *Atg5*$^{-/-}$ MEFs

It is not clear how complex I is down-regulated in *Atg5*$^{-/-}$ MEFs in glucose-based medium. We hypothesised that the increased mitochondrial stress in autophagy deficient cells activates the UPRmt pathway, and the up-regulating of mitochondrial proteases could result in the loss of complex I subunits and to a metabolic switch towards glycolysis. To assess the UPRmt, expression levels of several genes involved

in the UPRmt were determined. In *Atg5*$^{-/-}$ MEFs mRNA levels of *ClpX*, *ClpP* and *Ubl5* were increased (Figure 26A), expression levels of these three genes tightly correlate with the UPRmt, suggesting that the UPRmt is induced in these autophagy deficient cells. However, expression levels of *Chop10*, a transcription factor downstream of ClpX (Al-Furoukh et al., 2015), was not affected. Furthermore, *Hsp60* and *Hsp70* mRNA levels were not changed (Figure 26B). Therefore, we conclude that the canonical UPRmt is not activated, however an UPRmt-like pathway may be induced. In addition to the increased *ClpP* mRNA levels, also protein levels were increased in *Atg5*$^{-/-}$ MEFs (Figure 26C). ClpP is a protease that is part of the ClpXP complex, and has been suggested to be involved in the degradation of unfolded and disassembled respiratory subunits, therefore we hypothesised that increased ClpP expression could be responsible for the down-regulation of complex I subunits.

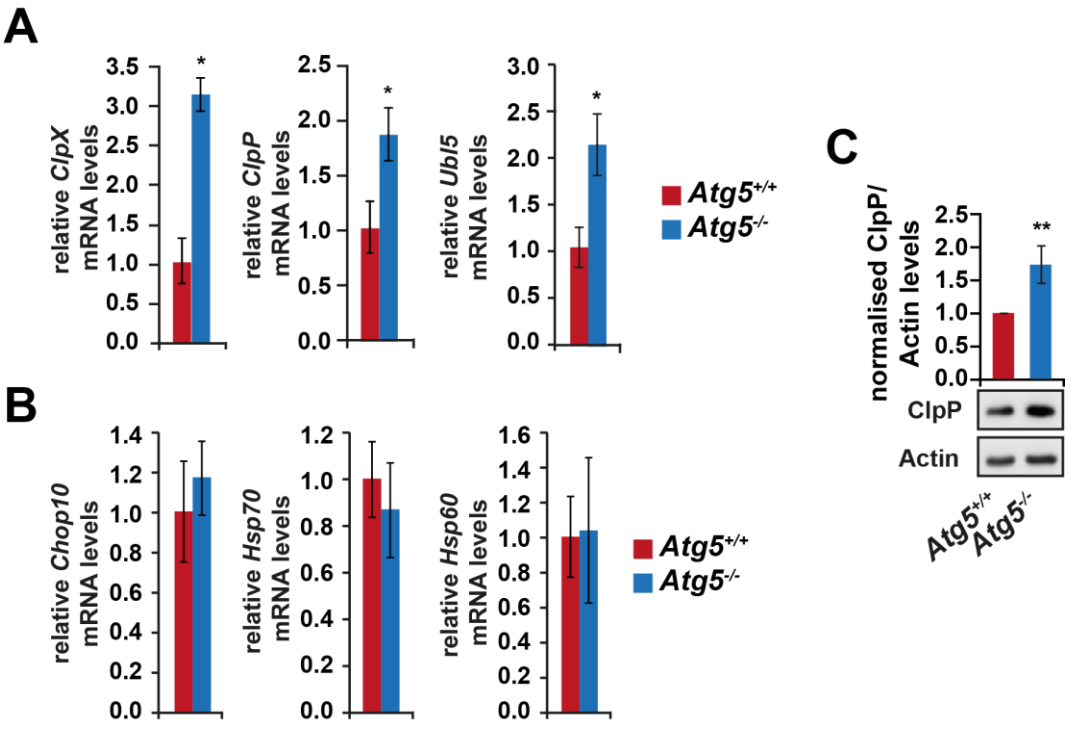

Figure 26 ClpP mRNA and protein levels are increased *Atg5*$^{-/-}$ MEFs.

(A) mRNA expression of UPRmt markers *ClpX*, *ClpP* and *Ubl5* in *Atg5*$^{+/+}$ and *Atg5*$^{-/-}$ MEFs. mRNA levels were normalised to the *Atg5*$^{+/+}$ MEFs in glycolytic conditions. (B) mRNA expression of UPRmt markers *Chop10*, *Hsp70* and *Hsp60* in *Atg5*$^{+/+}$ and *Atg5*$^{-/-}$ MEFs. mRNA levels were normalised to the *Atg5*$^{+/+}$ MEFs in glycolytic conditions. Error bars represent s.e.m., *P<0.05 (n=6) (C) Western blot analysis of ClpP in *Atg5*$^{+/+}$ and *Atg5*$^{-/-}$ MEFs. The ratio to actin was normalised to *Atg5*$^{+/+}$ MEFs. Error bars represent s.e.m., *P<0.05, **P<0.01 (n=3).

3.1.10 Down-regulation of the mitochondrial proteases ClpP, Lon or Afg3L2 with siRNA or inhibiting the MAD pathway does not prevent loss of complex I

To test if ClpP or other mitochondrial proteases (Section 1.10.1) degrade complex I and are responsible for the down-regulation of complex I in glucose-based medium, ClpP, Lon and Afg3L2 were down-regulated using siRNA in *Atg5*$^{-/-}$ MEFs and western blot analysis of complex I subunits was performed. Down-regulation of these proteases did not recover the loss of complex I, which could suggest that loss of complex I is not due to degradation via these mitochondrial proteases. (Figure 27A&B)

Azzu and Brand showed previously that IMM proteins can be degraded by the cytosolic proteasome and potentially this degradation happens via the MAD pathway (Section 1.10.4) (Azzu and Brand, 2010). To study this pathway, we first used MG132 to inhibit the proteasome. This led to a mild recovery of complex I in *Atg5*$^{+/+}$ and *Atg5*$^{-/-}$ MEFs (Figure 27C&D). In addition, siRNA against one off the main players of the MAD pathway, Vcp was used, but no significant recovery of complex I was observed (Figure 27E&F). However, antibodies to test knock-down efficiency were not available, so the knock-down might not be efficient enough and the remaining protein levels might be sufficient to degrade complex I subunits.

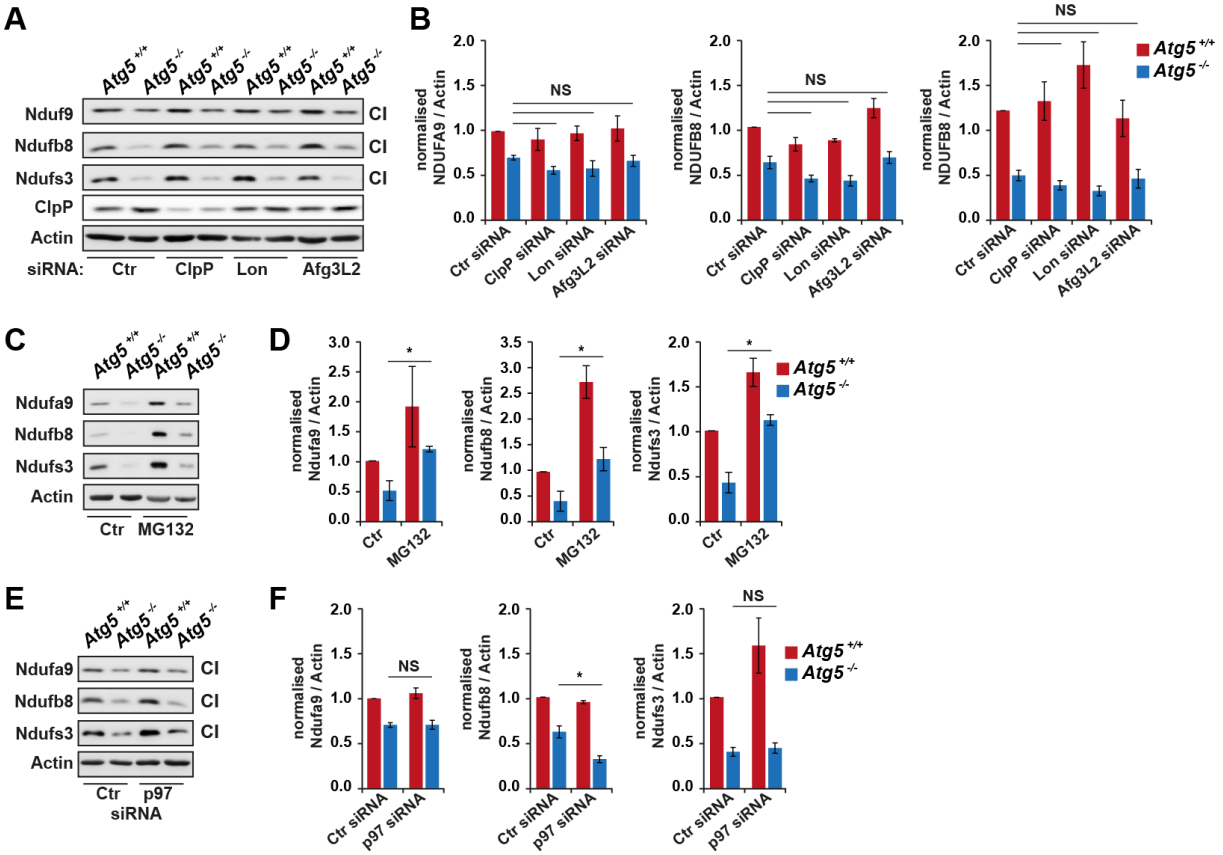

Figure 27 Knocking-down components of the MAD pathway or mitochondrial proteases with siRNA does not recover complex I subunits in *Atg5*$^{-/-}$ MEFs in glucose-based medium in.

(A) Western blot analysis of the complex I subunits: Ndufa9, Ndufb8 and Ndufs3 in *Atg5*$^{+/+}$ and *Atg5*$^{-/-}$ MEFs transfected with siRNA against *ClpP*, *Lon* and *Afg3L2*. (B) Quantification of A, the ratio to actin was normalised to *Atg5*$^{+/+}$ MEFs controls. (C) Same as A, but treated with the proteasomal inhibitor MG132 (600nM, 24 hours). (D) Quantification of C, the ratio to actin was normalised to *Atg5*$^{+/+}$ MEFs controls. (E) Western blot analysis of the complex I subunits: Ndufa9, Ndufb8 and Ndufs3 in *Atg5*$^{+/+}$ and *Atg5*$^{-/-}$ MEFs transfected with siRNA against *Vcp*. (F) Quantification of E, the ratio to actin was normalised to *Atg5*$^{+/+}$ MEFs controls. Error bars represent s.e.m., *P<0.05, NS = Not significant. (n=3).

3.1.11 Correlation between autophagy deficiency and complex I reduction in DLB, AD and FTD

To investigate if autophagy deficiency and complex I deficiency are relevant in a wider context of neurodegeneration, western blot analysis was performed to compare brain tissue from AD (temporal cortex), FTD (temporal cortex) and DLB (cingulate cortex) patients as well as age-matched control brains. In affected brain regions of AD patients, no loss of mitochondrial ETC proteins was observed (Figure 28A&B). Furthermore, LC3-II levels were unaffected and p62 did not accumulate significantly (Figure 28A&C). Thus, no clear mitochondrial phenotype, nor an autophagy deficiency was detected in AD brains.

In FTD only NDUFA9 protein levels were decreased, other complex I subunits also tended to be decreased, but this was not significant, whilst complex II (SDHA) and complex III (UQCRC2) protein levels were unaffected (Figure 28A&B). There was a tendency for less LC3 lipidation and more p62 in FTD patient brains, suggesting a potential autophagy block (Figure 28A&C).

In the cingulate cortex of DLB patients, complex I subunit NDUFB8 and complex II protein SDHA levels were significantly reduced. Similar to FTD brains, other complex I subunits showed a tendency to be down-regulated, but not complex III (UQCRC2), TOMM20 (Figure 28A&B). This correlated with a significant increase in p62 levels and a tendency for less LC3-II (Figure 28A&C).

To conclude, in FTD and DLB down-regulation of respiratory complex I and to a lesser extend complex II was observed and this correlates with a potentially impaired autophagy. Based on our data, this down-regulation can be part of a protective mechanism aiming to reduce damage from dysfunctional complex I. To draw stronger conclusions, more patient brains samples will have to be included in this study, as well as functional assays for mitochondrial ETC complexes are needed.

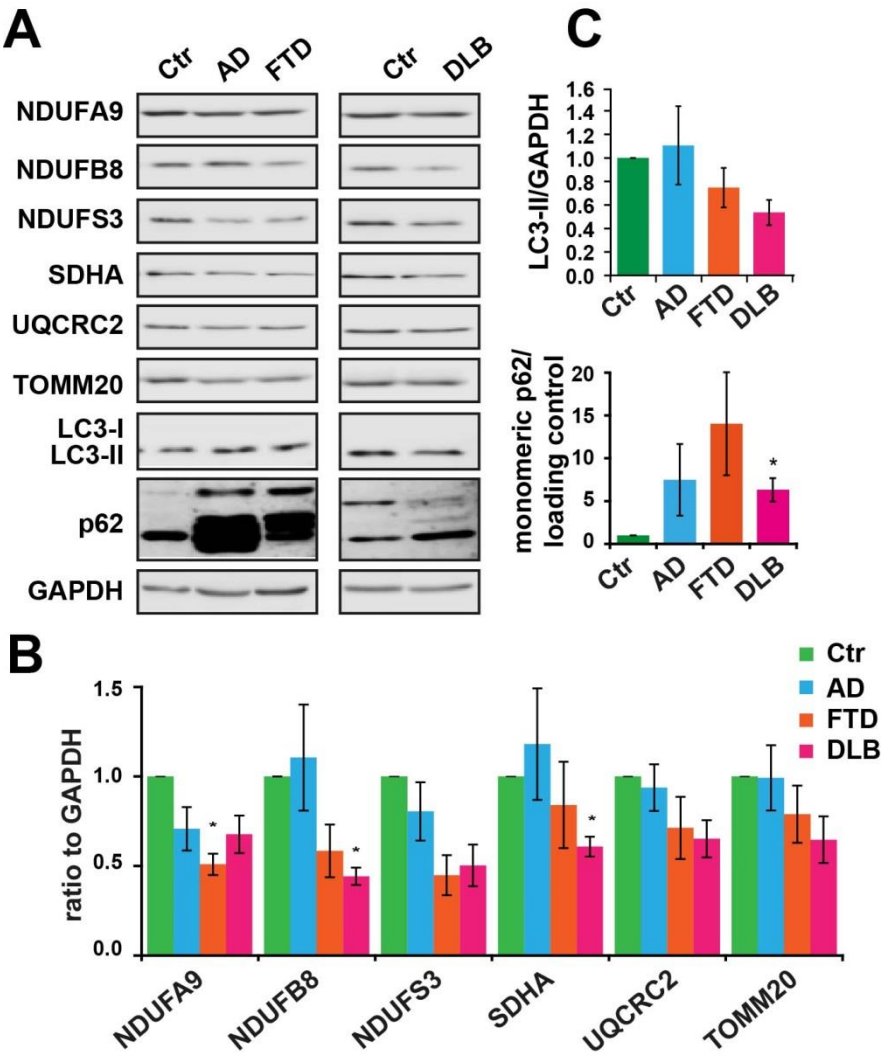

Figure 28 Autophagy deficiency correlates with reduced complex I subunits in frontotemeral dementia (FTD) and dementia with Lewy bodies (DLB).

(A) Western blot analysis of complex I subunits: NDUFA9, NDUFB8, NDUFS3, complex II: SDHA, complex III: UQCRC2, TOMM20 and autophagy markers p62 and LC3 in age-matched control brains, Alzheimer's disease (AD), frontotemporal dementia (FTD) and dementia with Lewy bodies (DLB). (B) Quantification of the different mitochondrial proteins in A. (C) Quantification of the autophagy markers in A. The ratio to actin was normalised to control brains. Error bars represent s.e.m., *P<0.05 (n=3).

3.2 Discussion

In this chapter, for the first time we have shown that autophagy dysfunction results in a striking mitochondrial phenotype, specifically an isolated down-regulation of respiratory complex I, reduced mitochondrial respiration via complex I and increased glycolysis, suggesting a metabolic rewiring. Furthermore, when cells are switched to galactose-based medium (promoting mitochondrial respiration) autophagy deficient cells die via apoptosis. Interestingly, this can be rescued by blocking ROS production via complex I and also by promoting respiration via complex II and thereby bypassing complex I. This suggests that ROS produced by complex I is causing galactose-induced cell death in autophagy deficient cells. These results open up new possibilities for targeted intervention in a wide variety of neurodegenerative diseases.

All the data shown was in Atg5 deficient MEFs, but was also confirmed in Npc1 deficient MEFs, suggesting that our results are not specific for loss of Atg5, but more general for autophagy deficiency. However, to further establish that it is indeed autophagy deficiency that result in the complex I dysfunction and subsequent galactose-induced cell death, CRISPR KO MEFs will be generated for Fip200 and Atg7. Loss of these two genes are known to result in a block in autophagy (Hara et al., 2008).

3.2.1 How are complex I subunit protein levels down-regulated in *Atg5*$^{-/-}$ MEFs in glucose-based medium?

First of all, it would be of interest to get a bigger picture of which mitochondrial ETC subunits are down-regulated in autophagy deficient MEFs using a proteomics approach like SILAC (Stable Isotope Labeling by Amino acids in Cell Culture). At the moment it is not entirely clear if it is specifically certain complex I subunits that are down-regulated, only certain complex I modules, or the entire holo-complex or even other ETC complexes. Our results suggest an isolated complex I dysfunction, as respiration via complex II was not affected, showing that complex II, III, IV and V function is not impaired.

The complex I subunits that are down-regulated in autophagy deficient cells are nuclear encoded. Thus down-regulation can have several causes, of which the most obvious potential causes could be reduced nuclear transcription, reduced cytosolic translation, reduced mitochondrial import or less efficient incorporation of the subunits into the respiratory complex. Furthermore, it could be hypothesised that the subunits

are selectively degraded within the mitochondria or via the UPS, due to oxidative damage or due to misfolding or potentially signalling events that purposefully target certain mitochondrial subunits for degradation by a post-translation modification such as ubiquitination. mRNA levels of the different mitochondrial subunits were unaltered in *Atg5*$^{-/-}$ MEFs, therefore we conclude that complex I down-regulation is not at the transcriptional level.

Interestingly, MG132, a potent proteasomal inhibitor, but also known to inhibit Lon (Granot et al., 2007), significantly recovered complex I subunits. At the moment it is not clear if this effect seen with MG132 treatment is due to inhibition of the proteasome or Lon. siRNA against Lon or Vcp did not result in the recovery of complex I subunits, however siRNA knock-down efficiency could not be tested as antibodies for the proteins were not available. Alternatively, mRNA levels could be assessed, but this has limitations, because it does not necessarily reflect the protein levels, therefore we cannot conclude if complex I is degraded by Lon or the proteasome.

The proteasome/MAD pathway (Section 1.10.4) could be an interesting pathway to asses in more detail, however this pathway is more likely to be important for the degradation of mitochondrial proteins located to the outer membrane and it is not clear how damaged inner mitochondrial proteins can be transported to the outer membrane to be presented to the proteasome. One mechanism, could involve the proteasome-dependent rupture of the OMM as was shown to occur during PINK1/Parkin mediated mitophagy (Yoshii et al., 2011, Wei et al., 2017), thereby leaving the IMM exposed to the cytosol. However, this would be expected to affect mitochondrial respiration quite drastically and is therefore not a very likely mechanism. Even though the mechanism how IMM can be presented to the cytosolic proteasome is unclear, evidence is accumulating that this pathway has the ability to degrade IMM as was nicely demonstrated for UCP2 in a cell free system (Azzu and Brand, 2010). In addition, it has been suggested that the proteasome has a higher capacity for proteolysis of mitochondrial proteins than mitochondrial proteases in basal conditions (Lau et al., 2012).

The other scenario would involve degradation via mitochondrial proteases, such as the mitochondrial matrix proteases Lon and ClpXP and the matrix-AAA and intermembrane-AAA metalloproteases, which are embedded in the IMM (Section 1.10.1). Interestingly, ClpP mRNA and protein levels were up-regulated in *Atg5*$^{-/-}$

MEFs. ClpP is a protease that degrades unfolded proteins in the mitochondrial matrix and has been implicated in the UPRmt (Haynes et al., 2007, Haynes and Ron, 2010).

The mitochondrial proteasome Lon, has been implicated in the degradation of complex I, and specifically the peripheral arm, in response to antimycin A and oligomycin treatment (Pryde et al., 2016). To further test the involvement of mitochondrial proteases, especially ClpP and Lon, these could be knocked-out in *Atg5*$^{-/-}$ MEFs using CRISPR and complex I subunits assessed. Furthermore, to avoid potential redundancy of mitochondrial proteases, multiple KO's could be created or dominant negative forms could be expressed.

To our surprise, increased *ClpP* mRNA and protein levels were not accompanied by increased expression of heat shock proteins and the transcription factor Chop10, which are normally induced upon ClpP activation. Potentially other transcription factors are activated in our conditions, such as ATF5. The UPRmt has been studied mainly in *C.elegans* and only in the last year more mechanistic data has been revealed about the mammalian UPRmt (Section 1.10.3). The regulation of the mammalian UPRmt and consequent response to mitochondrial proteotoxic stress might be more complicated than what was described in *C.elegans*. This is demonstrated by the fact that for example *Hsp70*, but not *Hsp60* was induced by accumulation of misfolded proteins in mitochondria in mammalians, suggesting that they can be regulated independently (Fiorese et al., 2016).

3.2.2 Why is specifically complex I down-regulated?

Loss of complex I has been observed with age and in neurodegenerative diseases, such as Alzheimer's and Parkinson's disease (Francis et al., 2014, Grunewald et al., 2016, Schapira, 1998, Schapira, 2010). Now, we have shown that complex I, and to a lesser extend complex II, is down-regulated in FTD and DLB, whilst in autophagy deficient cells an isolated complex I loss (protein levels and function) was observed. It is not clear why a loss of specifically complex I and to lesser extend complex II is observed, whilst complex III and IV are unaffected.

Recently the half-lives of ETC subunits in mice were determined, which showed that half-lives are very variable within the different complexes, which cannot be explained by a process like mitophagy, which is thought to degrade bigger portions of mitochondria (Karunadharma et al., 2015). It was also shown that the matrix facing subunits of complex I and II have shorter half-lives compared to the membrane-bound

subunits (Karunadharma et al., 2015), which could be caused by increased oxidative damage. Furthermore, on average complex IV subunits were shorter-lived than the others and, finally, the half-lives of the different ETC subunits correlated negatively with ubiquitin enrichment and a linear correlation between half-lives and 20S proteasome degradation susceptibility was observed (Karunadharma et al., 2015). This implies that the half-live of ETC subunits is determined by the susceptibility of being degraded via the proteasome, most likely via the MAD pathway. The half-lives of Ndufa9, Ndufb8 and Ndufs3 and Ndufv2 (CI) were not shorter than Ndufb9 (complex I), Sdha (complex II) and Uqcrc2 (complex III). On the contrary, Ndufb8 is the longest lived among these ETC subunits in control mice, CR (calory restriction) mice and rapamycin fed mice (Karunadharma et al., 2015). The latter two are models in which autophagy is induced, unfortunately no model was used in which autophagy was blocked. The half-lives of the ETC subunits could drastically change upon mitochondrial damage, as more ROS production would mainly effect complex I.

It has been suggested that the stoichiometric ratios of the respiratory chain complexes could explain an isolated loss of complex I. The ratios of the different complexes are as follows: complex I 0.8-1.3; complex II, 1.2-1.4; complex III, 3; and complex IV as 6.0-7.5 in bovine heart mitochondria (Schagger and Pfeiffer, 2001). Thus complex I, and to a lesser degree complex II, might be limited, whilst there is an excess in complex IV (Grunewald et al., 2016). If this theory is correct, complex III and complex IV would only be affected in severe conditions.

We obtained data suggesting that in autophagy deficient cells complex I is not incorporated in higher-order supercomplexes upon switching to galactose-based medium. This implies that there is an assembly defect of higher-order supercomplexes. Complex I outside of the respirasome or other supercomplexes is less stable and produces more ROS (Schagger et al., 2004, Guaras et al., 2016).

The assembly status of complex I could be assessed in more details by blue native page in the Atg5 deficient MEFs, using antibodies against different complex I subunits, which are assembled into the complex at different stages (Stroud et al., 2016). Also proteomics approach like SILAC, as suggested before, could reveal more about which complex I subunits are destabilised in the Atg5 deficient MEFs in glucose-based medium.

3.2.3 How does autophagy deficiency result in a dysfunctional mitochondrial complex I?

Now the question remains how autophagy deficiency leads to this destabilisation of complex I in glucose-based medium. First of all, autophagy dysfunction does not lead to an acute defect in complex I, as in our inducible Atg5 knock-out model (M5-7s) cells need to be treated with tetracycline (thus suppressing autophagy) for 6 weeks to observe loss of complex I and increased galactose-induced cell death. This suggests that an accumulation of autophagy substrates, or genetic/epigenetic rewiring induced by prolonged starvation is required to induce a complex I defect. Potentially, this prolonged loss of mitochondrial quality control results in mitochondrial damage, which results in mitochondrial stress and increased ROS produced at complex I. Currently, we do not know if the bulk autophagy pathway or maybe more specifically mitophagy is required for maintenance of complex I function, therefore *Pink1* KO MEFs will be generated as well, to distinguish between general autophagy and mitophagy.

Recently, it was shown that mutant TDP43 accumulates in mitochondria in ALS and FTD patients, where it binds mitochondria-transcribed messenger RNAs encoding complex I subunits ND3 and ND6 (Wang et al., 2016b). This specific down-regulation of ND3 and ND6 also resulted in the loss of other CI subunits, such as NDUFB8, but not other mitochondrial complexes and this was pathogenic (Wang et al., 2016b). Therefore, it could be that the loss of complex I we observed in brains of FTD patients was also caused by TDP43 accumulation in the mitochondria. Autophagy is important for TDP43 turnover, therefore loss of autophagy results in TDP43 accumulation, which could accumulate in mitochondria, resulting in down-regulation of complex I. It would be interesting to test if in our autophagy deficient cells TDP43 accumulates in mitochondria and inhibits ND3 and ND6 protein synthesis.

As a result of impaired autophagy, ubiquitinated proteins accumulate and could be imported into mitochondria via the MAGIC pathway (Section 1.10.2). The MAGIC pathway involves mitochondria functioning as “rubbish bins”, by clearing ubiquitinated protein aggregates (Ruan et al., 2017). It could be hypothesised that the co-import of protein aggregates by mitochondrial proteins containing a mitochondrial import signal, would interfere with the efficient import of mitochondrial proteins, such as nuclear encoded complex I subunits. Furthermore, the accumulation of cytosolic protein aggregates in mitochondria, could have a negative impact on complex I stability.

3.2.4 What causes cell death in *Atg5*$^{-/-}$ MEFs upon a switch to galactose-based medium?

Galactose-based medium lacks glucose and therefore cells grown in this medium completely rely on mitochondrial respiration for energy production. In glucose-based medium cells also mostly use mitochondria to produce ATP (Figure 18C), however they do have the option to switch to anaerobic ATP production by producing lactate. This is exactly what we observed in *Atg5*$^{-/-}$ MEFs in glucose-based medium, whilst they die in galactose-based medium, suggesting that their mitochondria are dysfunctional. We further characterised this and observed less mitochondrial respiration and less complex I-linked respiration, whereas complex II-linked respiration was unaffected.

The complex I specific superoxide inhibitor S1QEL 2.2, which prevents superoxide being formed at site I_Q and I-BET 762, which transcriptionally rewires the cell towards respiration via complex II, both rescued galactose-induced cell death in *Atg5*$^{-/-}$ MEFs, suggesting that mitochondrial ROS and, more specifically superoxide produced by complex I at site Q, is causing cell death. To further strengthen these conclusions, complex II substrates, such as succinate and fatty acids could be fed to the cells, to promote respiration of complex II and bypassing complex I-linked respiration. Furthermore, ROS measurements should be done in response to the S1QEL 2.2 and I-BET 762 treatment, to show that ROS production is reduced upon these treatments. Finally, overexpression of NDI1, a yeast NADH-quinone oxidoreductase, which mediates the electron transfer from NADH to ubiquinone and thus bypasses dysfunctional complex I (Marella et al., 2008, Seo et al., 1998). Expressing NDI1 will result in more RET, potentially leading to loss of complex I in these cells, which could rescue cell death if our hypothesis is correct.

Another interesting observation was that changing the galactose-based medium every day prevented cell death (data not shown), suggesting that the cells were starved or alternatively changing the medium functioned as an antioxidant. Autophagy is important in starvation conditions, as it recycles cytosolic components for reuse. Thus, not only ROS produced by complex I, but also starvation is involved in galactose-induced cell death, suggesting that the increased ROS production, combined with an energy and nutrient crises causes cell death. It needs to be determined how this interplay works and what the main cause is. Currently, it is not clear how increased complex I-linked ROS production, an energetic crisis and starvation can signal to induce apoptosis. Starvation is known to result in reduced mTORC1 signalling, whilst

the ADP/ATP ratio signals via the energy sensor Ampk. To disentangle how these signalling pathways might be involved in induction of apoptosis, activity of several cellular signalling pathways proceeding cell death can be investigated. Furthermore, assessing galactose-induced cell death whilst inhibiting Ampk and mTORC1 signalling, could give more information about the involvement of these signalling pathways. Interestingly, cells with hyperactive Akt signalling are more sensitive to oxidative stress by inhibiting Foxo signalling, which regulate the expression of antioxidants (Nogueira et al., 2008).

3.2.5 Could reducing the damage from complex I be a protective mechanism in neurodegenerative diseases?

Loss of complex I activity as well as altered autophagy activity is a hallmark of ageing and several neurodegenerative disorders (Section 1.12). This loss of complex I is thought to be damaging and pathogenic, however it could be speculated that loss of complex I in certain conditions (such as autophagy deficiency) is protective.

Even though our results in AD, FTD and DLB are very preliminary and more work needs to be done, we found that FTD and DLB results in loss of respiratory complex I and to a lesser extend complex II and this correlates with impaired autophagy.

In previous studies loss of complex I has been implicated in neurodegenerative diseases. For instance, in an amyloid-β protein precursor transgenic mouse model for Alzheimer's disease reduced complex I activity coincided with reduced NDUFB8 expression (Francis et al., 2014), however we did not observe this loss of NDUFB8 in the affected brain regions of Alzheimer patients. Complex I dysfunction has been heavily associated with Parkinson's disease (Schapira et al., 1989). The pesticides paraquat and rotenone that inhibit complex I activity, resulting in increased ROS production and causing Parkinson's disease (Abou-Sleiman et al., 2006), as well as mutant α-synuclein, inhibit complex I activity and result in neurodegeneration (Reeve et al., 2015). DLB also displays an isolated complex I deficiency (Navarro et al., 2009). Interestingly, autophagy deficiency also has been implicated in these diseases and our preliminary data suggested that autophagy is impaired in FTD and DLB as well.

The consensus at the moment is that isolated loss of complex I, observed in several neurodegenerative diseases, is damaging to the cell. This is mainly based on the fact that Parkinson's disease related toxins such as paraquat and rotenone inhibit complex I and result in more ROS production (Lenaz et al., 2006). In contrast, in *C.elegans* and

D.melanogaster RNAi knockdown of complex I subunits extends life span by increasing ROS levels and thereby activating stress response pathways (Hur et al., 2014, Yang and Hekimi, 2010, Yee et al., 2014, Lee et al., 2010b, Owusu-Ansah et al., 2013). Therefore, reduced complex I levels could potentially be both, beneficial and detrimental. In the case of damaged complex I, it might be beneficial to prevent damage, and down-regulate the complex.

We found that switching cells to galactose-based medium is detrimental for *Atg5*$^{-/-}$ MEFs, these conditions result in the restoration of complex I protein levels at the transcriptional and protein level. Upon a switch to galactose-based medium, *Atg5*$^{-/-}$ MEFs are forced to switch to mitochondrial respiration, resulting in cell death. We propose this cell death occurs because they are forced to up-regulate complex I, which, because quality control is lacking, produces too much ROS. Therefore, it could be hypothesised that the loss of complex I in DLB, PD and FTD is a protective mechanism to prevent aberrant ROS production at complex I and forcing respiration via complex II or produce energy via glycolysis.

3.2.6 Preventing ROS production at complex I, or bypassing respiration via complex I can be used a therapeutic target for autophagy-related neurodegenerative diseases.

It would be exciting to take our initial S1QEL 2.2 and I-BET 762 data in mammalian cells to *in vivo* autophagy mouse models. *Atg5*$^{flox/flox}$; nestin-*Cre* mice (a neuronal specific Atg5 knock-out mouse model) develop progressive motor and behavioural defects, which are often observed in neurodegenerative mouse models as well (Hara et al., 2006). Moreover, neuronal cell death and accumulation of Ub-positive cytoplasmic inclusion in neurons were observed with age in these mice (Hara et al., 2006). It was shown previously that autophagy is important for the clearance of aggregate-prone proteins (Ravikumar et al., 2002). Hara *et al*. suggest that autophagy is essential for the clearance of intracellular proteins and this is required for neuronal survival. However, mitochondrial function has not been assessed in these mice. It would be of importance to translate our cell data to this model and test if I-BET762 and S1QEL 2.2 would rescue the neurodegenerative phenotypes of the *Atg5*$^{flox/flox}$; nestin-*Cre* mice. If positive results are obtained, it would open an interesting therapeutic target for many age-related neurodegenerative diseases.

4 CHAPTER 4: OXIDATION OF p62 MEDIATES THE LINK BETWEEN REDOX STATE AND PROTEIN HOMEOSTASIS

4.1 Introduction

Ageing and age-related diseases are commonly associated with proteotoxic and oxidative stress, which can be highly damaging for cellular functioning and survival. Cells employ multiple defensive mechanisms to promote survival in these conditions. Autophagy is one of the key mechanisms to degrade toxic waste such as damaged and oxidised proteins and organelles.

Autophagy is a prosurvival pathway that has a prominent role in determining longevity in many model organisms. A number of longevity-increasing manipulations are autophagy-dependent (Madeo et al., 2015). Loss of autophagy has been associated with accelerated ageing and reduced stress resistance, whilst autophagy induction prolongs life span ((Madeo et al., 2015). In yeast for instance, different autophagy mutants have a shorter chronological life span (Matecic et al., 2010). In *C. elegans* similar observations were made, where Atg1, Atg7, Atg18 and Beclin 1 loss of function mutants have decreased life span (Toth et al., 2008) and in *D. melanogaster*, Atg1, Atg8 and Ref(2)p mutants shorten lifespan (Simonsen et al., 2008, de Castro et al., 2013). In mice, deletion of essential autophagy genes is lethal during the early postnatal period, but tissue specific loss of autophagy genes shows less dramatic phenotypes. Instead, age-related pathology is observed, such as p62 and ubiquitin positive aggregates and abnormal mitochondria accumulation (Rubinsztein et al., 2011). Furthermore, autophagy induction can extend lifespan; for example overexpression of Atg5 in mice has anti-ageing properties and extends lifespan (Pyo et al., 2013). In addition, overexpression of Atg8a or Atg1 in fly neurons prolongs lifespan (Simonsen et al., 2008, Ulgherait et al., 2014). A question we have tried to address in this chapter is if autophagy has evolved and has become more efficient in longer lived species in order to cope with the increased stress resistance.

Degradation of autophagy substrates requires autophagy receptors that can bind to the substrate and the nascent autophagosome, resulting in the delivery to the lysosome, where degradation takes place. p62 is the most studied autophagy receptor

(Section 1.3) and has been shown to be important for longevity too. Loss of p62 in mice results in late onset obesity, neurodegeneration and a decreased lifespan with increased ROS and impaired mitochondrial respiration (Ramesh Babu et al., 2008, Kwon et al., 2012).

Notably, genetic and age-related loss of efficient autophagy has been linked to age-related diseases, such as ALS (Section 1.12.3). More specifically, p62 mutations have been identified in ALS patients, which has been described in detail in section 1.4.1.

In this chapter we discovered that p62 can become oxidised, resulting in its oligomerisation and promoting autophagy. This prosurvival mechanism is evolved in vertebrates promoting oxidative stress resistance and survival. In contrast, impairment of this mechanism may cause ALS in humans.

4.2 Results

4.2.1 p62 becomes increasingly oxidised with age and forms aggregates in mouse brain

Firstly, we tested the proteostatic and autophagic status of young and old mice. In the old mouse brains, ubiquitinated proteins accumulate indicating that there is increased proteotoxic stress. This is accompanied by increased Prd-SO_3, an accepted marker for oxidative stress (figure 29A)(Wagner et al., 2002). This is in agreement with the previously described proteostatic and redox imbalance in the brain of old mice (Wagner et al., 2002, Ohtsuka et al., 1995). However, no major changes in LC3-I and LC3-II levels were observed comparing young and old mouse brains, suggesting that autophagy function is not markedly affected (Figure 29A). In addition, total levels of the autophagy substrate p62 did not increase, implying that autophagy is unperturbed. Interestingly, with age p62 DLC (Disulphide-Linked Conjugates) accumulate, these were only observed in non-reduced conditions, but were broken down in reducing conditions (Figure 29B). This suggests that they are mediated by sulfhydryl groups, such as disulphide or thioester bonds. In reduced conditions (in the presence of a reducing agent, such as β-mE, disulphide bridges within a protein or between multiple proteins are reduced, resulting in the loss of a secondary structure of a protein, or resulting in the disassembly of a multimeric protein complex (Section 1.8.3). The main p62 oligomeric species we observed is around 250 kDa, which could correspond to p62 tetramers (Figure 29B). Interestingly, when we looked in neurons (Purkinje cells) of young and old mice, we observed more accumulation of p62 aggregates in neurons of old mice, despite total p62 protein levels being unaltered (Figure 29B and C).

Next, we used mammalian cells in tissue culture to model the behaviour of p62 in response to oxidation and autophagy inhibition. After blocking autophagy with Bafilomycin A1 (Baf) or chloroquine (CQ) we observed an expected p62 accumulation, but primarily in monomeric form in non-reduced blots (Figure 29D). To induce oxidative stress we treated cells with H_2O_2 and PR-619. PR-619 is a redox cycler known to produce H_2O_2 in aqueous solutions, but it also non-specifically inhibits activity of DUBs (Redhead et al., 2015). Treating HeLa cells with H_2O_2 or PR-619 results in the formation of p62 DLC as we observed in old mouse brains (Figure 29B-D). PR-619 treatment resulted in more p62 DLC compared to H_2O_2, with the majority of protein being in DLC, whilst in response to H_2O_2 a lot of the protein is still in its monomeric

form (Figure 29D). Furthermore, both ROS treatments results in the formation of p62 aggregates similar to a block in autophagy (Figure 29E). From these results, we hypothesise that a block in autophagy results in the formation of aggregates based on non-covalent interactions, such as PB1 domain-dependent oligomerisation (Section 1.3.2), whilst there is a different, disulphide dependent oligomerisation mechanism in response to oxidation.

Thus, *in vivo* p62 is oxidised with age in mouse brains and this can be modelled in mammalian cells and this might contribute to the formation of p62 aggregates.

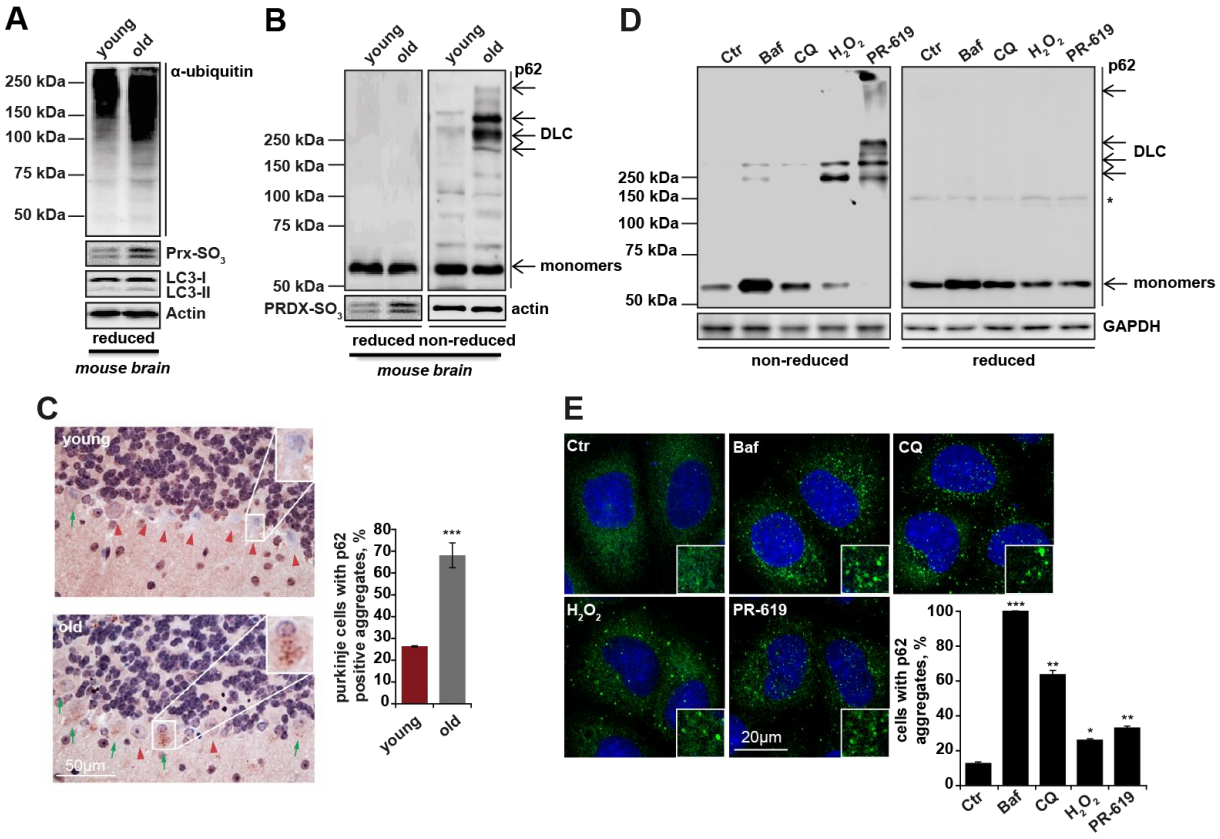

Figure 29 p62 disulphide-linked conjugates (DLC) accumulate with age in old mouse brains.

(A) Young (3 months) and old (24 months) mouse brain tissues were analysed by western blot analysis for ubiquitin, Prx-SO_3 and LC3. (B) Young and old mouse brain tissue were analysed by western blot analysis for p62 in either reducing (2.5% β-mE) or non-reducing conditions. (C) Representative images and quantification of p62 aggregates in young and old mouse Purkinje cells in the cerebellum. % of cells containing p62 positive aggregates were quantified. This experiment was performed in collaboration with Dr. Diana Jurk. (D) Effect of autophagy inhibition (bafilomycin A1 (Baf, 400nM, 4 hours) and chloroquine (CQ, 50μM, 4 hours)) and oxidative stress (H_2O_2 (3mM, 10 min) and PR-619 (5μM, 30 min)) on p62 DLC analysed by western blot analysis (E) and p62 aggregation in HeLa cells analysed by immunofluorescence staining against p62 analysed by confocal microscopy. Error bars represent s.e.m., n=3, *P<0.05, **P<0.01, ***P<0.005. Asterisk indicates a non-specific band. A, B and D were in collaboration with Dr. Diego Manni.

4.2.2 Oxidation of p62 promotes autophagy

Cysteine residues are the predominant targets to be oxidised in redox-regulated proteins. After doing multiple rounds of cysteine to alanine mutagenesis, cysteine residues 105 and 113 were identified to be required for oxidation of p62 (data not shown).

To study the significance of p62 oxidation in autophagy, *p62*$^{-/-}$ MEFs stably expressing FLAG-p62 and FLAG-C105,113Ap62 were generated (Figure 30A). FLAG-p62 and FLAG-C105,113Ap62 transgenes were expressed at slightly lower levels than the endogenous protein (Hewitt et al., 2016). The stable p62 cell lines were treated with ROS inducing agents H_2O_2 and PR-619, which both induce the formation of p62 DLC in cells expressing wild type FLAG-p62, but not in the cells expressing the FLAG-C105,113Ap62 mutant as expected (Figure 30A). These cell lines were used to investigate the role of p62 oxidation in autophagy. In addition, a cell line was generated expressing a PB1 domain oligomerisation mutant (K7A,D69A) to study the role of p62 oligomerisation in autophagy. The K7A and D69A mutations abolish the interaction surface of the PB1 domain, resulting in a loss of self-oligomerisation ability, whilst its ability to form DLC is unaffected (Lamark et al., 2003) and data not shown.

In order to understand if the formation of p62 DLC is important for autophagy and protein homeostasis, p62 cell lines were switched to serum free media (SFM) as a control, or SFM with 1mM H_2O_2 for 5 hours to induce oxidative stress and the formation of p62 DLC. In this thesis H_2O_2 treatments are always performed in SFM, because H_2O_2 becomes quenched in media containing serum. Switching cell to SFM is a starvation treatment, and thus induces autophagy. In these conditions we observed that *p62*$^{-/-}$ MEFs and *p62*$^{-/-}$ MEFs re-expressing the p62 oxidation mutant (C105,113A) or the p62 PB1-domain mutant (K7A,D69A) have decreased LC3-II levels and an accumulation of ubiquitinated proteins compared to cells expressing wild type FLAG-p62 (Figure 30B&C). This suggests that oxidation and oligomerisation of p62 is required for autophagy induction and clearance of ubiquitinated proteins. H_2O_2 treatment results in autophagy induction in cells expressing FLAG-p62, as LC3-II levels increase and wild type p62 is cleared (Figure 30B&C). In cells expressing FLAG-C105,113Ap62 or FLAG-K7AD69Ap62, autophagy is not induced to the same extend, as LC3-II levels increase less and p62 levels do not decrease significantly (Figure 30B&C). The same phenotype was observed in response to PR-619 treatment, where

increased LC3 lipidation was observed in cells expressing wild type FLAG-p62, but not in the mutants (Figure 30D&E).

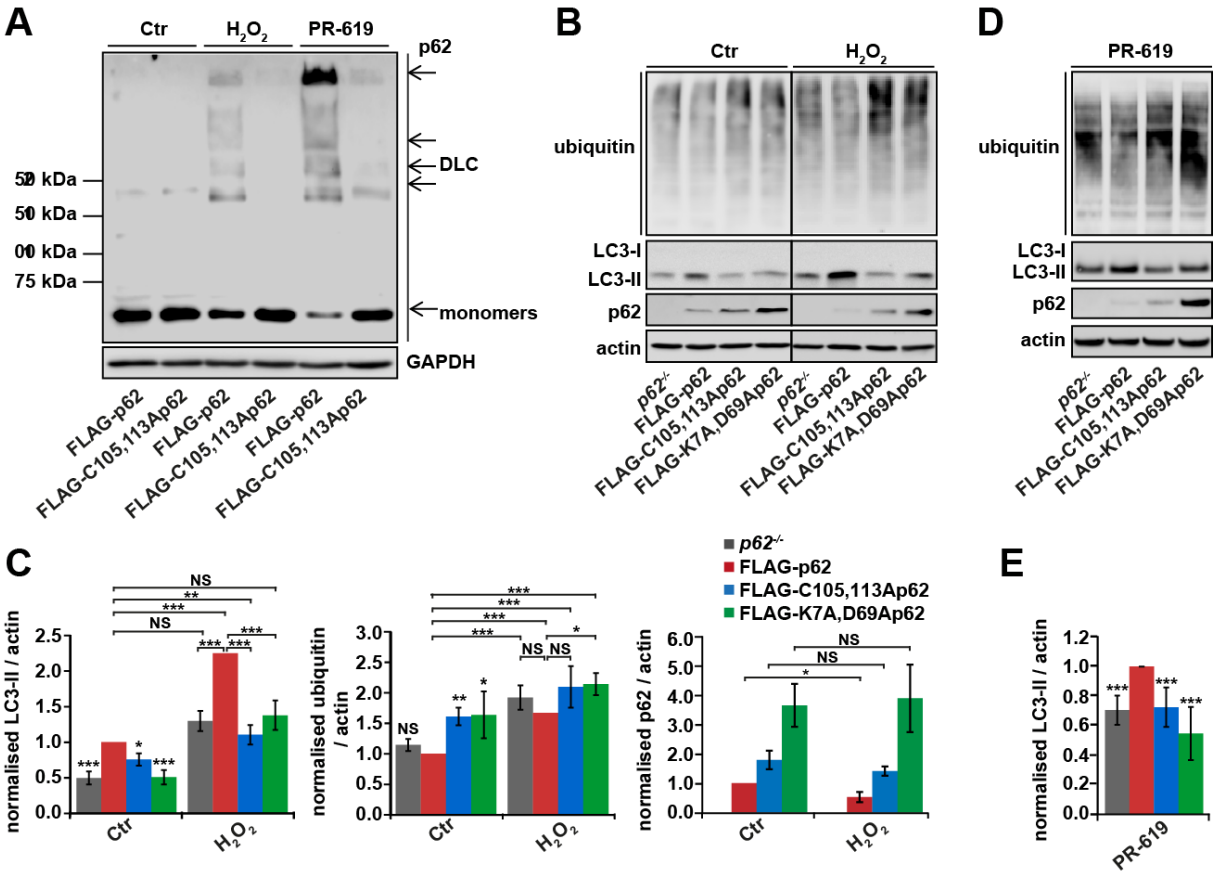

Figure 30 Oxidation of p62 promotes autophagy induction in basal and oxidative stress conditions.

(A) *p62*$^{-/-}$ MEFs stably expressing FLAG-p62 or the oxidation mutant FLAG-C105,113Ap62 were analysed by western blot analysis for p62 in non-reducing conditions in response to H_2O_2 (1mM, 1 min) or PR-619 (5μM, 10 min). (B, D) *p62*$^{-/-}$ MEFs stably expressing empty vector, FLAG-p62, FLAG-C105,113Ap62 or FLAG-K7AD69Ap62 were treated with (B) H_2O_2 (1mM, 5 hours) or (D) PR-619 (5μM, 3 hours) and subjected to western blot analysis for LC3, ubiquitin and p62. (C) Quantification of B for ubiquitin and LC3-II and p62. (E) Quantification of D for LC3-II. Quantifications were normalised to *p62*$^{-/-}$ MEFs stably expressing FLAG-p62. Error bars represent s.e.m., (n=3), *P<0.05, **P<0.01, ***P<0.005, NS= not significant.

The decrease in LC3 lipidation in the oxidation and oligomerisation mutants correlated with less autophagosomes observed by confocal microscopy (Figure 31A&B). Taken together these results suggest that autophagy induction, in particularly in oxidative stress conditions, depends on p62 oxidation and oligomerisation.

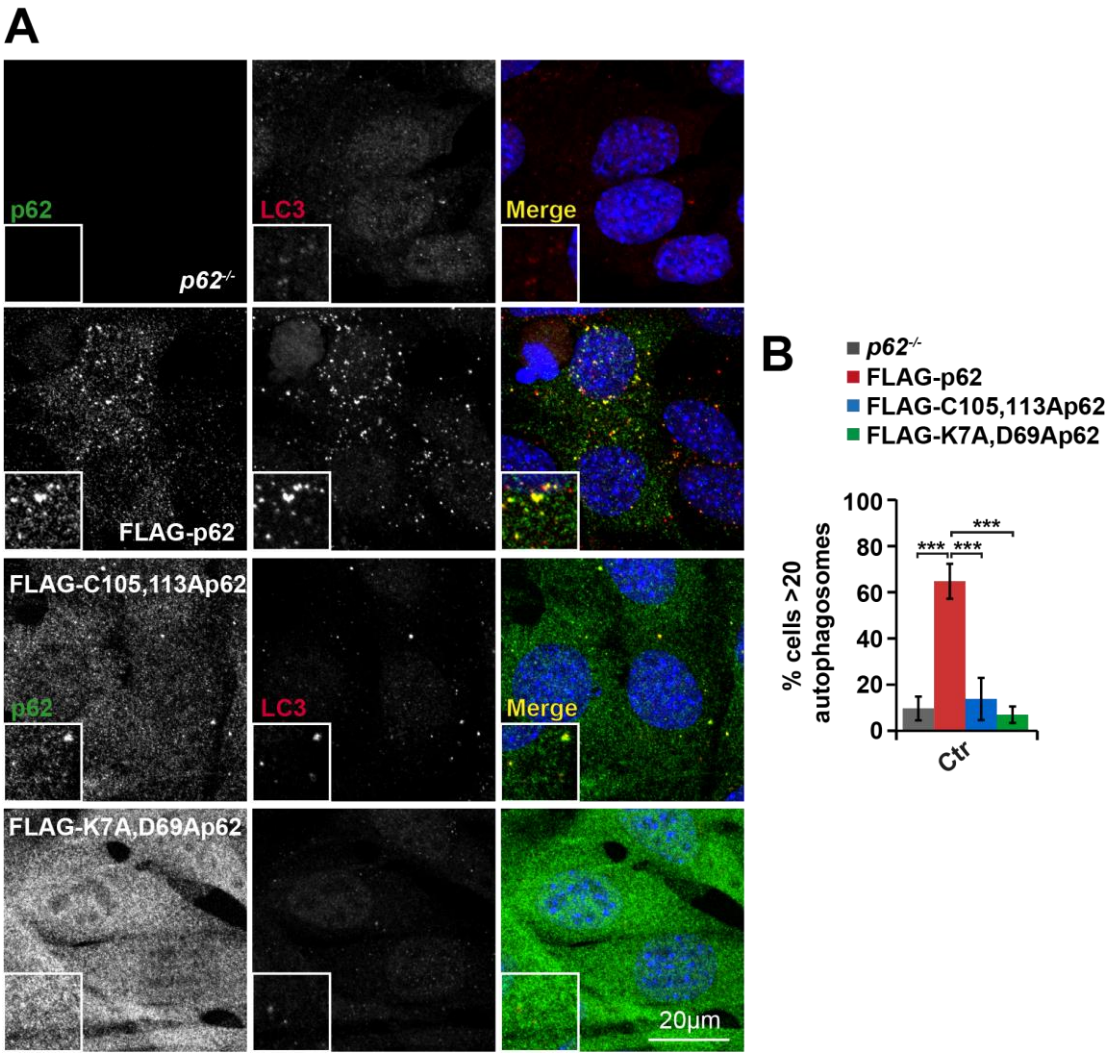

Figure 31 Oxidation of p62 promotes the formation of autophagosomes.

(A) Representative confocal microscopy images of *p62*$^{-/-}$ MEFs stably expressing empty vector, FLAG-p62, FLAG-C105,113Ap62 or FLAG-K7AD69Ap62 which were immunostained for p62 and LC3. (B) Quantification of A for percentage of cells with more than 20 autophagosomes. Error bars represent s.e.m., (n=3), ***P<0.005.

4.2.3 Oxidation of p62 is important for cell survival upon oxidative and proteotoxic stress

Autophagy is a degradation pathway that is of great importance for cell survival in oxidative and proteotoxic stress conditions. We have shown that oxidation of p62 is required to induce autophagy in basal and oxidative stress conditions and promotes clearance of poly-ubiquitinated proteins. Next, we investigated if the oxidation of p62 is important for cell survival under these circumstances. The p62 cell lines were treated with 1mM H_2O_2 for 5 hours and cell death was assessed. In *p62*$^{-/-}$ MEFs around 25% cell death was observed upon H_2O_2 treatment. In cells expressing wild type FLAG-p62 the cell death was rescued, however no rescue was observed in cells expressing the oxidation mutant (C105,113A) or the PB1 domain mutant (K7A,D69A) (Figure 32A&B).

Hence, we conclude that p62 cysteines 105 and 113 are essential for cell survival in conditions of oxidative stress. Furthermore, in response to PR-619 treatment also significantly more cell death was observed in cells expressing FLAG- C105,113Ap62 (Figure 32C). To determine if the rescue of cell death in cells expressing wild type FLAG-p62 is autophagy dependent, cells were treated with H_2O_2 in the absence or presence of autophagy inhibitors Bafilomycin A1 or chloroquine. Both autophagy inhibitors cancelled out the difference in cell survival between the two cell lines, suggesting that autophagy is the mechanism of oxidative stress resistance (Figure 32C).

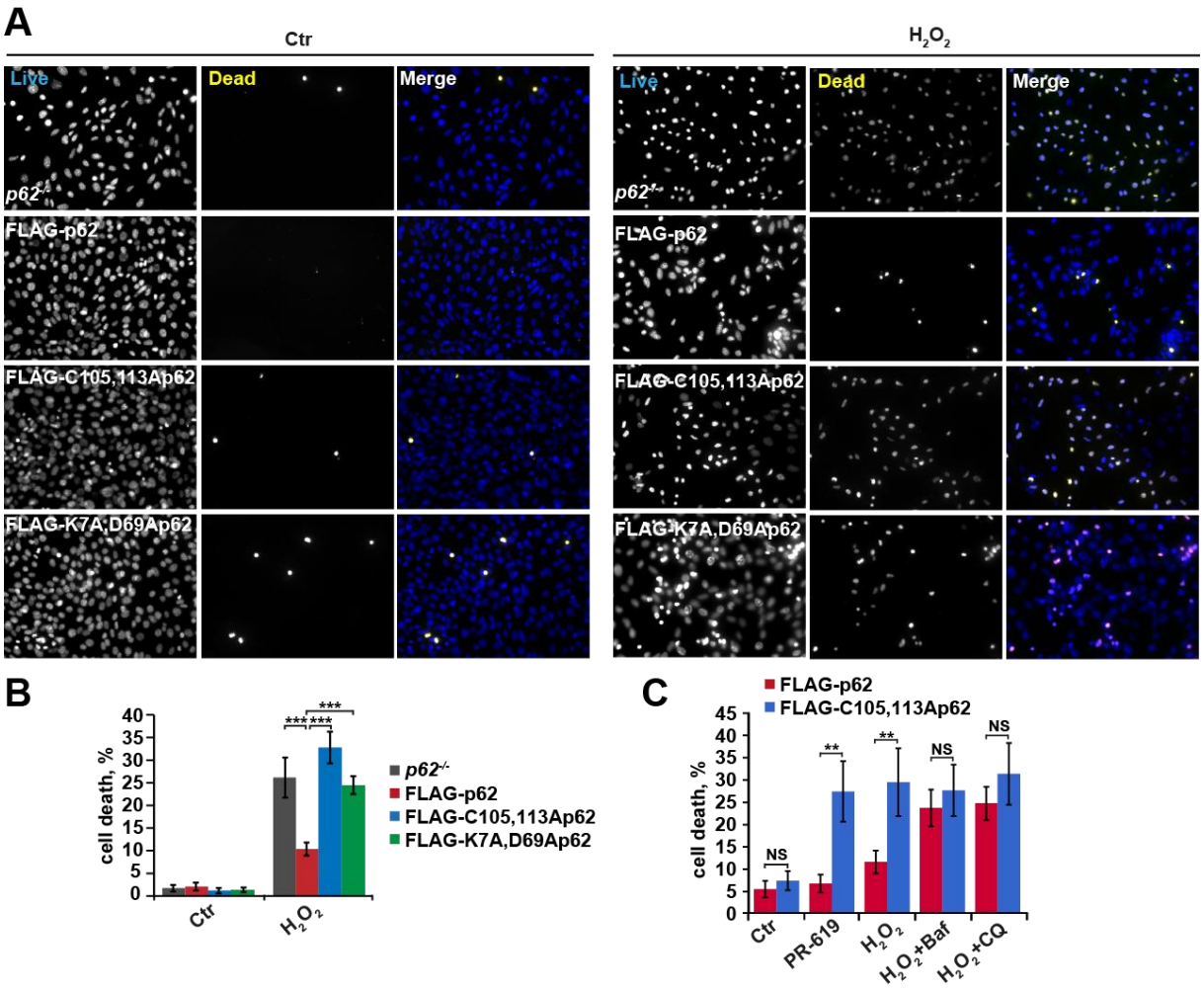

Figure 32 Oxidation of p62 promotes survival in response to oxidative stress.

(A) *p62*$^{-/-}$ MEFs stably expressing empty vector, FLAG-p62, FLAG-C105,113Ap62 or FLAG-K7AD69Ap62 were treated with H_2O_2 (1mM, 5 hours) and stained with ReadyProbes fluorescent dyes to assess cell death and quantified (B). *p62*$^{-/-}$ MEFs stably expressing FLAG-p62 or FLAG-C105,113Ap62 were treated with PR-619, H_2O_2 (1mM, 5 hours), H_2O_2 with Baf (50nM, 5 hours) or H_2O_2 with CQ (20μM, 5 hours) and stained with ReadyProbes fluorescent dyes to assess cell death and quantified. Error bars represent s.e.m., (n=3) **P<0.01, ***P<0.005, NS= not significant. These experiments were performed in collaboration with Dr. Bernadette Carroll.

4.2.4 Oxidation of p62 is not important for induction of the Nrf2 signalling pathway in response to H_2O_2 treatment

p62 has also been implicated in Nrf2 signalling, which is another well-known prosurvival pathway, especially in oxidative stress conditions (Section 1.3.8). To test if Nrf2 signalling could be an alternative mechanism of increased stress resistance in cells expressing wild type FLAG-p62 we investigated the Nrf2 response in our cell lines in response to H_2O_2 treatment. Firstly, the translocation of Nrf2 to the nucleus was assessed. Nuclear fractionations were performed and we could observe a robust Nrf2 translocation to the nucleus in response to H_2O_2, however no significant difference between *p62*$^{-/-}$ MEFs stably expressing FLAG-p62 or FLAG-C105,113Ap62 was observed (Figure 33A&B). Secondly, the induction of the Nrf2 target gene *HO-1* (Heme Oxygenase 1) as measured by qPCR was not decreased in cells expressing the p62 oxidation mutant (C105,113A) (Figure 33C). Finally, cell death was assessed in cells treated with H_2O_2 in the absence or presence of RA (Retinoic Acid, a potent Nrf2 inhibitor (Wang et al., 2007)). Inhibition of Nrf2 signalling did not cancel out the difference in cell survival between the two cell lines. Altogether, the data suggest that Nrf2 signalling is not the mechanism of oxidative stress resistance in response to oxidative stress induced by H_2O_2 (Figure 33D).

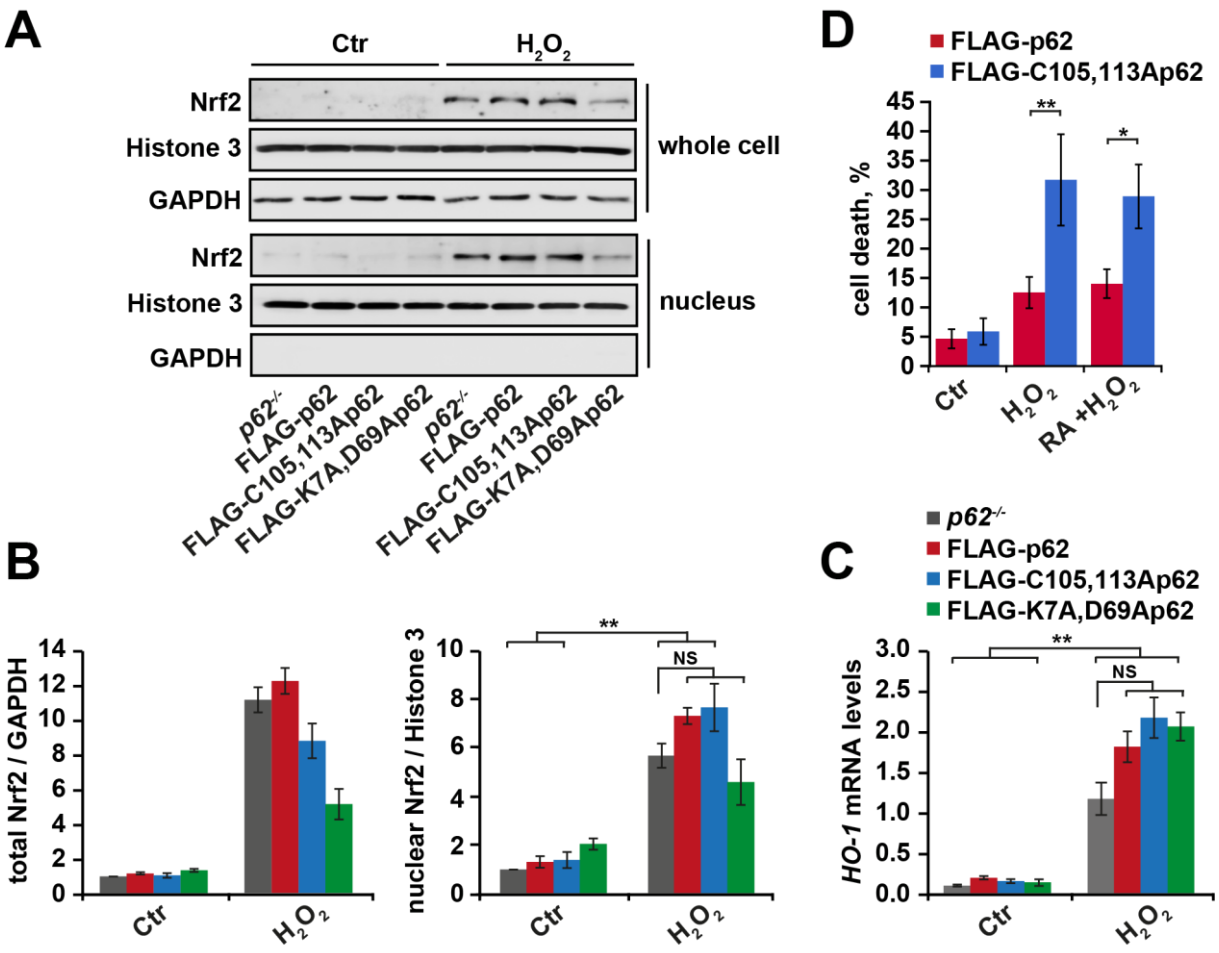

Figure 33 Oxidation of p62 is not important for induction of the Nrf2 signalling pathway in response to H_2O_2 treatment.

(A) *p62*$^{-/-}$ MEFs stably expressing FLAG-tagged wild type, C105A,C113A or K7A,D69A PB1 domain mutant p62 were treated with H_2O_2 (1mM, 5 hours) in SFM and subjected to a nuclear fractionation followed by immunoblot analysis for Nrf2, Histone 3 and GAPDH and quantified (B). (C) Cells were treated as in (A) and Nrf2 target gene *HO-1* mRNA levels were analysed by qPCR, actin was used as a loading control. This experiment was done in collaboration with Dr. Rhoda Stefanatos. (D) *p62*$^{-/-}$ MEFs stably expressing FLAG-tagged wild type or C105A,C113A mutant p62 were pre-treated with retinoic acid (RA, 30μM, 1 hour) in serum free media followed by the same treatment as in (A) with or without retinoic acid (30μM) and % cell death was analysed by ReadyProbes fluorescent dyes (Life Technologies). Error bars represent s.e.m., (n=3) *P<0.05, **P<0.01, NS= not significant.

4.2.5 Conservation of the p62 redox sensitive cysteines 105 and 113

We established that the oxidisable p62 cysteine residues are essential for the formation of p62 DLC and the subsequent degradation (Figure 30 and unpublished). Next, we were interested to determine in what time during evolution these oxidisable p62 cysteines 105 and 113 were acquired. First, we performed a multiple sequence alignment of the N-terminal fragment of p62 containing cysteine 105 and 113 in several species and found that the two cysteines have a high degree of conservation, lie in an

unstructured region ranging between amino acids 102 and 122, and are surrounded by charged residues (Figure 34). Interestingly, the two key cysteines are only acquired in vertebrates, therefore we hypothesised that oxidation of p62 is a prosurvival mechanism only acquired late in evolution.

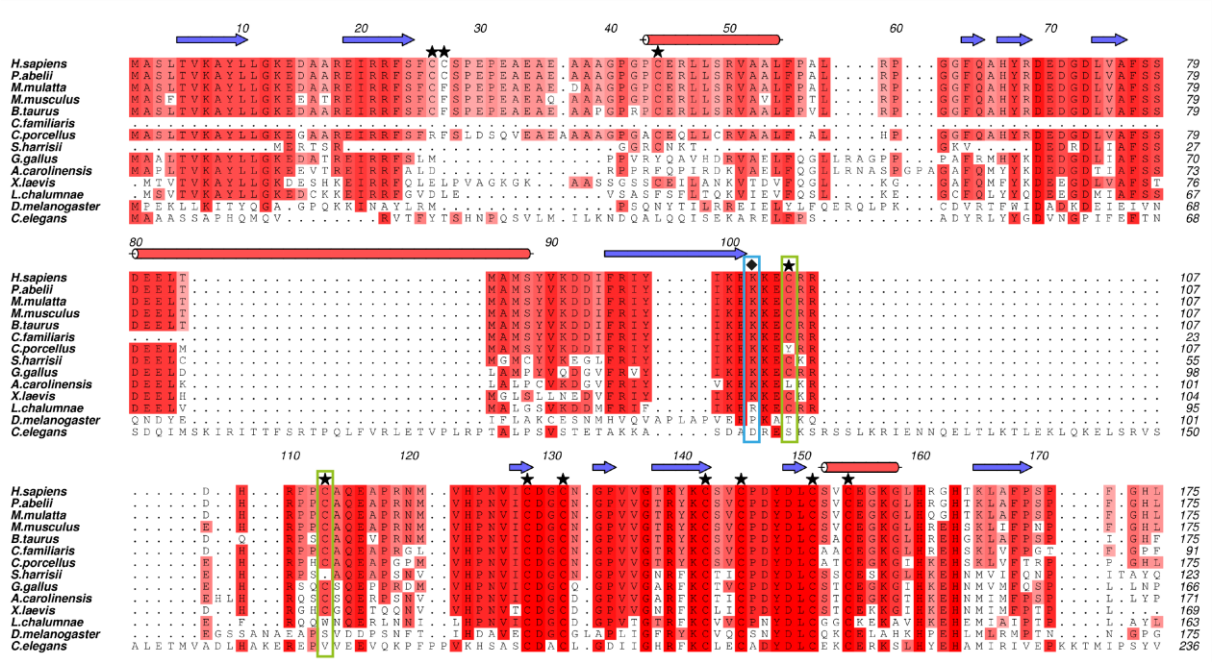

Figure 34 p62 cysteines 105 and 113 are conserved from invertebrates to humans.

Multiple alignment of p62 sequences (amino acid 1-200) in different species. Increasing conservation is shown by light-dark red; cysteine residues are indicated by stars, and a lysine residue that is mutated in a sporadic ALS-case is indicated by a diamond and a blue box. Lines above the sequence alignment indicate predicted ordered regions with β-sheets shown as blue arrows and α-helices shown as red cylinders. Cysteine 105 and 113 are marked by a green box. The alignment was performed by Dr. Graham Smith.

4.2.6 The redox insensitive *Drosophila melanogaster* p62 homolog Ref(2)P accumulates with age

Ref(2)P, which is the *Drosophila* orthologue of p62, similar to p62 has been found to be a component of protein aggregates formed during ageing in *Drosophila melanogaster* brains (Nezis et al., 2008). Ref(2)P does not contain oxidisable cysteines in between the PB1 domain and the ZZ domain and does not form p62 DLC with age (Figure 34 and 35A). Young and old flies were assessed for total Ref(2)P levels and Ref(2)P DLC. In old whole flies, Ref(2)P accumulated and no Ref(2)P DLC were observed (Figure 35A). This could suggest that indeed the missing oxidisable cysteines are required for efficient p62 degradation and that the prosurvival mechanism we identified is lacking in flies.

To test if the acquisition of redox-regulated cysteines in vertebrates is an evolutionary advantage we generated flies expressing humanised Ref(2)P using CRISPR/Cas9 genome editing. Amino-acids 91-116 of *D. melanogaster* (knock-in strain w^{1118}) Ref(2)P were replaced with amino acids 100-118 of human p62, including the oxidisable cysteine residues 105 and 113 (Figure 35B). Indeed, in response to H_2O_2, humanised Ref(2)P^{ox}, but not wild type Ref(2)P, forms DLC (Figure 35C). Therefore, these flies were used for the experiments described in the rest of this results chapter.

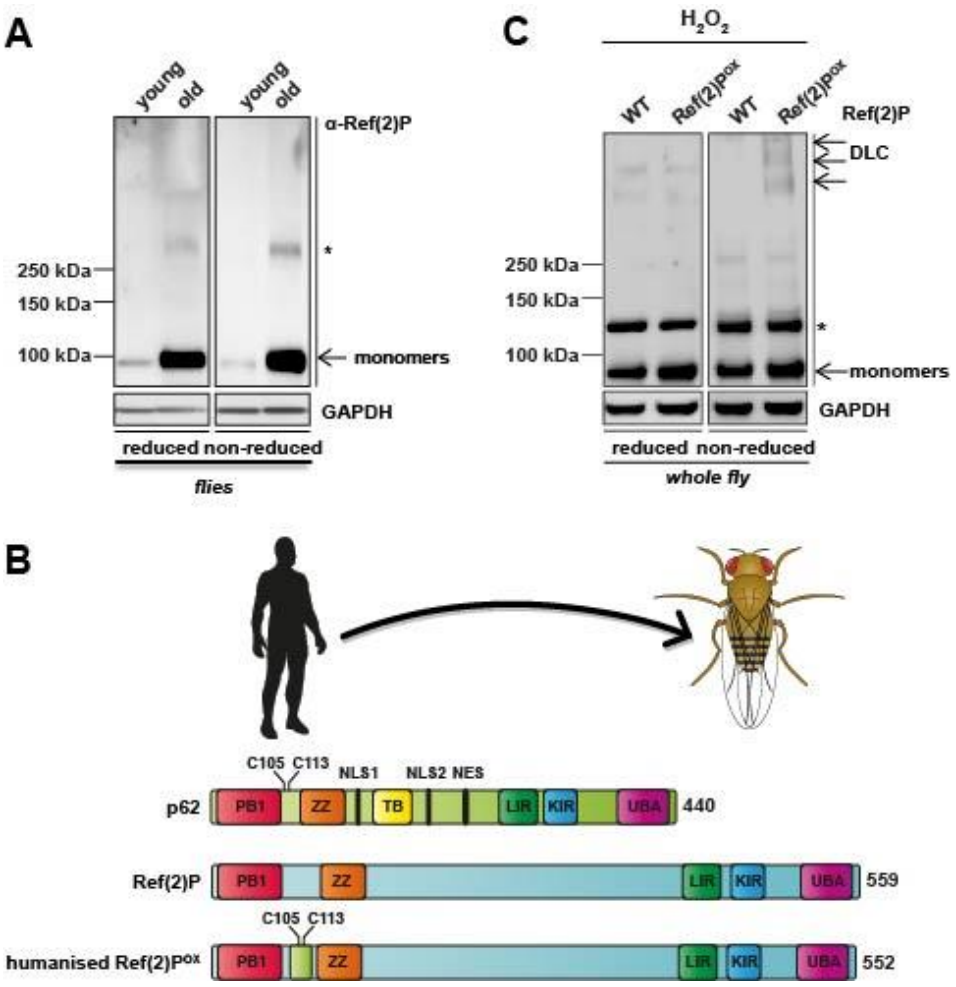

Figure 35 Ref(2)P is not oxidised and accumulates with age.

(A) Young (10 days) and old (75 days) whole flies were analysed by western blot analysis for Ref(2)P in either reducing (2.5% β-mE) or non-reducing conditions. (B) Schematic diagram showing p62 and Ref(2)P domain structure and introduction of the p62 linker region, including the oxidable cysteines, into Ref(2)P. (C) Wild type and humanised oxidisable Ref(2)P^{ox} flies treated with H_2O_2 *in vitro* (1mM, 5 min) were analysed for Ref(2)P in either reducing (2.5% β-mE) or non-reducing conditions. The asterisk indicates a non-specific band.

4.2.7 Oxidisable humanised Ref(2)P^{ox} promotes autophagy

Previously we found that in mammalian cells p62 oxidation is a mechanism to promote autophagy (Figures 30). We were interested if a similar phenotype was observed in our flies expressing Ref(2)P^{ox}. To test autophagy flux, flies were fed chloroquine for 2 days and H_2O was used as a control. Then flies were switched to 32°C for 2 days to induce proteotoxic stress (Menger et al., 2015), also in the presence of H_2O or the autophagy inhibitor chloroquine in the food. The flies expressing humanised Ref(2)P^{ox} displayed increased lipidated Atg8 (the fly homolog of LC3) levels upon autophagy inhibition compared to flies expressing wild type Ref(2)P, indicating that these humanised flies have an increased autophagic flux (Figure 36).

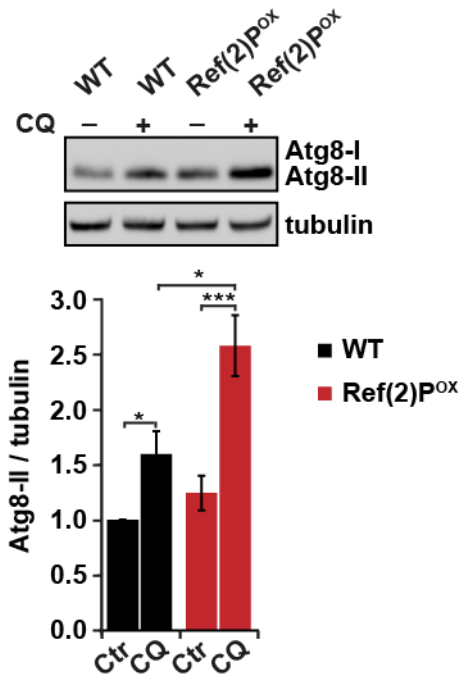

Figure 36 Oxidisable humanised Ref(2)P^{ox} promotes autophagy.

Wild type and humanised oxidisable Ref(2)P^{ox} flies were switched to 32°C for 2 days in the absence or presence of chloroquine and were analysed by western blot analysis for Atg8. Flies were pretreated with H_2O as a control or chloroquine to block autophagy for 2 days. Error bars represent s.e.m., n=3 (at least 10 flies per replicate), *P<0.05, ***P<0.005.

4.2.8 Flies carrying oxidisable humanised Ref(2)P^{ox} are more resistant to oxidative stress

Next, we evaluated if this increased autophagy flux in flies carrying oxidisable humanised Ref(2)P^{ox} also impacts on survival in stress conditions. In order to induce oxidative stress in the flies we used paraquat. This is an herbicide that is reduced within cells to increase ROS production. Flies were fed 20mM paraquat or H_2O as a control and survival of wild type flies or flies carrying Ref(2)P^{ox} was determined. We found that flies carrying Ref(2)P^{ox} lived longer, showing that these flies are more resistant to oxidative stress (Figure 37A). This was associated with decreased levels of ubiquitinated proteins and Ref(2)P, indicating that autophagy substrates are degraded more efficiently in flies carrying oxidisable Ref(2)P (37B&C).

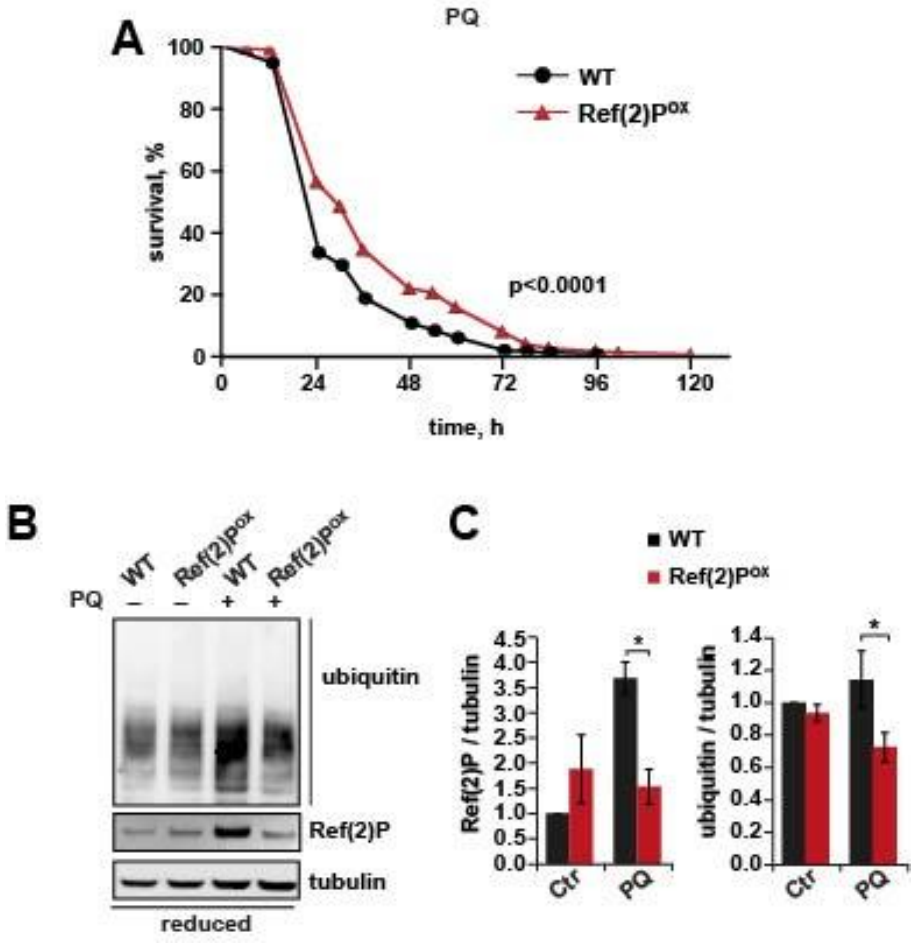

Figure 37 Oxidisable humanised Ref(2)P^{ox} protects agains oxidative stress.

(A) Survival of wild type and humanised oxidisable Ref(2)P^{ox} flies (three repeats, at least 60 flies per replicate) fed with paraquat (PQ, 20mM) and survival was assessed every 12 hours. Survival was plotted as adult life span in days. (B) Ctr (H_2O) and paraquat (20mM, 12 hours) fed wild type and humanised oxidisable Ref(2)P^{ox} flies were analysed by western blot analysis for ubiquitin and Ref(2)P. (C) Quantification of B. Error bars represent s.e.m., n=3 (at least 10 flies per replicate), *P<0.05.

We have shown that oxidisable humanised Ref(2)P^{ox} protects against oxidative stress induced by paraquat. Next, we wanted to know if this is also applicable to another oxidative stressor. In order to test this, we switched flies to 32°C after eclosing, this thermal stressor is also associated with oxidative stress (Jacobson et al., 2010) and results in a shorter life span (only around 20 days) and accumulation of ubiquitinated proteins and Ref(2)P (Figure 38A&B). Upon these conditions, flies carrying Ref(2)P^{ox} had a striking life span extension compared to wild type flies (Figure 38A). This was accompanied by a significant reduction of Ref(2)P levels, and ubiquitinated protein levels showed a trend to be decreased at 32°C as well (Figure 38B&C). Thus, oxidisable humanised Ref(2)P^{ox} protects against oxidative stress and we propose that the same mechanism as for p62 oxidation in mammalian cells can be applied here. Thus, oxidative stress promotes the formation of Ref(2)P DLC, which promotes autophagy induction, and thus degradation of itself as well as associated substrates, such as ubiquitinated proteins and this promotes survival.

We conclude that introducing the p62 linker region, including the oxidisable cysteines 105 and 113, results in a gain of function of p62. Ref(2)P^{ox} can be oxidised and form DLC, which is has a prosurvival role in oxidative stress conditions.

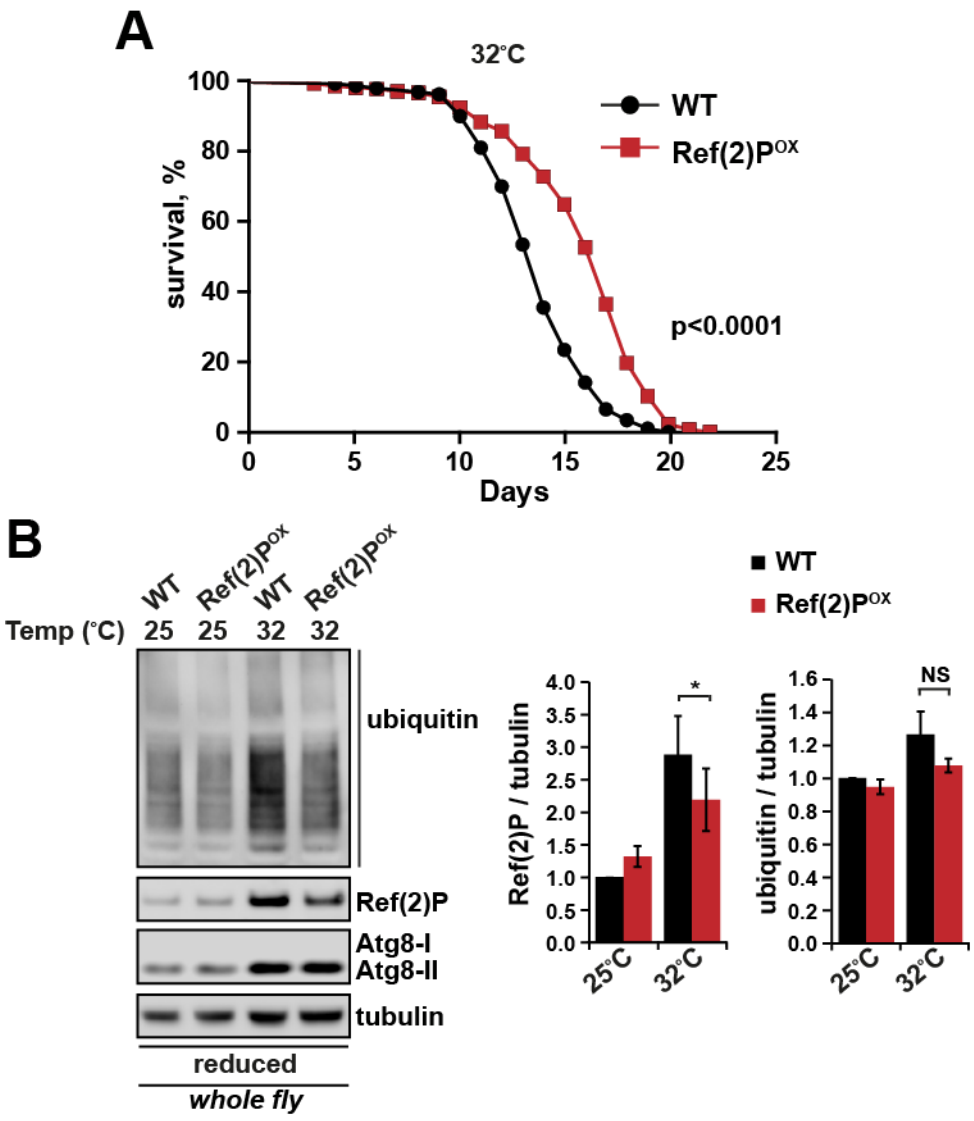

Figure 38 Oxidisable humanised Ref(2)P^{ox} extends fly lifespan upon proteotoxic stress.

(A) Combined survival data (three repeats, at least 60 flies per replicate) of wild type and humanised oxidisable Ref(2)P^{ox} flies subjected to proteotoxic stress (32°C). Survival was plotted as adult lifespan in days. (B) Two days old wild type or humanised oxidisable Ref(2)P^{ox} flies were switched to 32°C for 2 days or maintained at 25°C and were analysed by western blot for ubiquitin and Ref(2)P. Error bars represent s.e.m., n=3 (at least 10 flies per replicate), *P<0.05.

4.2.9 Oxidation of p62 is impaired in the Amyotrophic Lateral Sclerosis p62 K102E mutant

To investigate if the loss of oxidation of p62 could cause age-related diseases we looked for known mutations located close to the identified oxidisable cysteines 105 and 113. One ALS-associated mutation (K102E) was identified in the unstructured region and the mechanism of pathology is unknown (Teyssou et al., 2013). We hypothesised that the K102E mutation would interfere with degradation of p62 by impairing the ability of p62 to be oxidised and form DLC. Lysine 102 is a highly conserved residue and

locates closely to the key oxidisable cysteine 105 (Figure 39A) (Le Ber et al., 2013). *In silico* analyses predicted that the K102E mutation can interfere with the sensitivity of cysteine 105 to be oxidised by introducing an extra negative charge in the vicinity that changes the PK_a of the cysteine (Figure 39B). Reactive cysteines are known to be close to positive charged residues, such as arginine and lysine, whilst unreactive cysteines are located closely to negatively charged residues such as glutamic acid. Thus, we predict that the K102E mutation results in less reactive cysteine 105 and thereby affecting the potential of p62 to form DLC in response to ROS. Moreover, an *in silico* model of disulphide bond-mediated p62 oligomerisation of the N-terminal PB1 domain and the unstructured linker region predicted that K102 may be involved in the salt-bridge formation with E19 within the PB1 domain (Figure 39C). This salt bridge stabilises the protein, and also affects the conformation and orientation of the near C105, enabling formation of the disulphide bond between C105 and C113 from another p62 subunit (Figure 39C). The K102E mutation disrupts this stabilising interaction and results in a conformation change of the loop, making C105 inaccessible to form disulphide bonds with a neighbouring p62 molecules (Figure 39C). Thus, the K102E mutation could lead to impaired oxidation by two means; changing the electrostatic potential around C105 and changing the conformation of the flexible loop between the PB1 domain and the ZZ domain, thereby perturbing formation of disulphide bonds with neighbouring p62 molecules.

To test if this mutation indeed would preturb oxidation of p62, as predicted by our models, HeLa cells were transfected with FLAG-tagged wild type p62, FLAG-C105,113Ap62 and FLAG-K102Ep62 and treated with the ROS inducing agents, H_2O_2 and PR-619. We found that the K102E mutations resulted in a loss of DLC formation in response to H_2O_2 and PR-619, almost to the same extent as the C105,113A double mutation (4-11D&E).

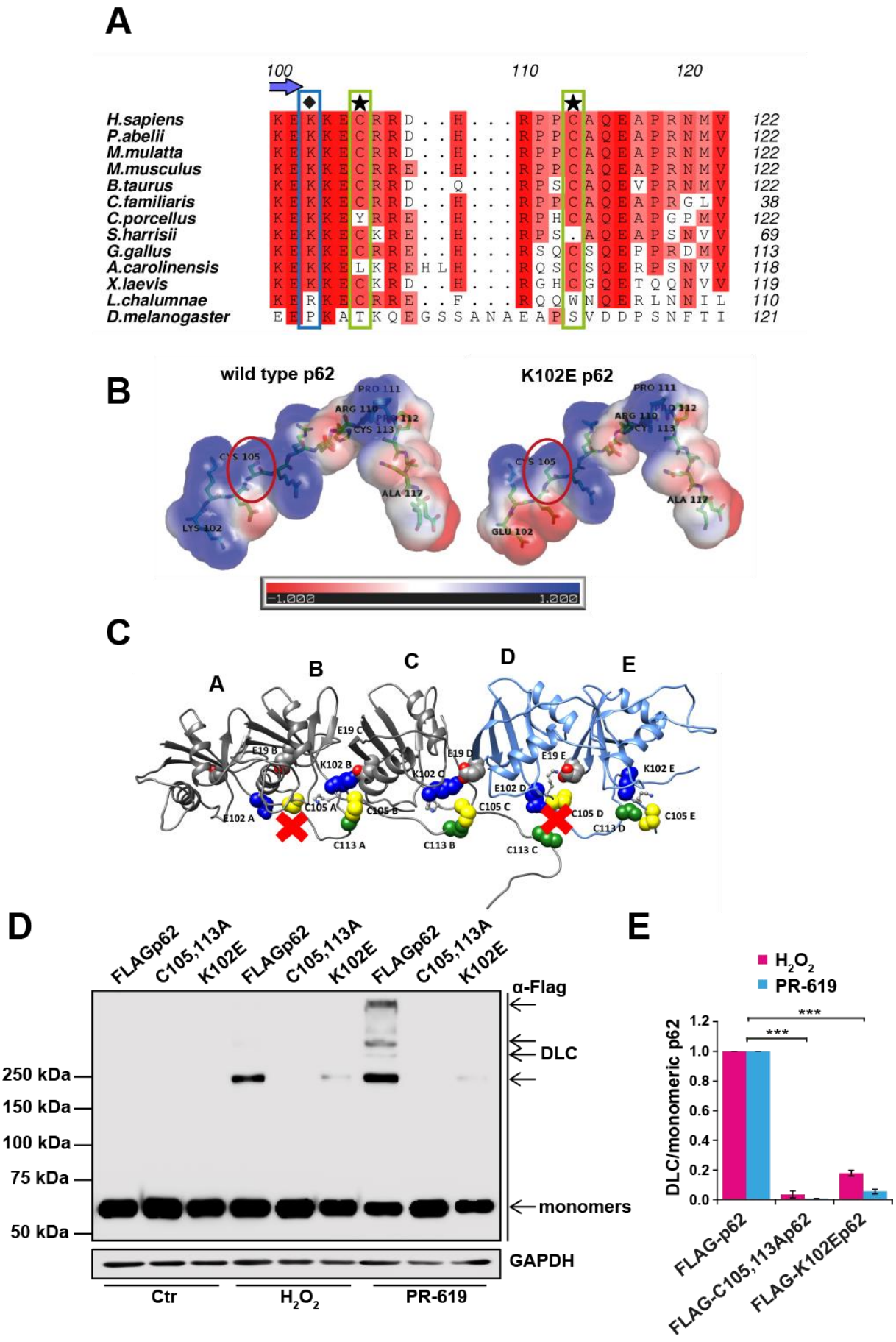

Figure 39 The ALS related mutation K102E impairs oxidation of p62.

(A) Multiple alignment of p62 sequences (amino acid 100-122) in different species. Increasing conservation is shown by light-dark red; cysteine 105 and 113 are indicated by stars and a green box, and a lysine residue that is mutated in a sporadic ALS-case is indicated by a diamond and a blue box. (B) Models of the p62 linker region (amino acids 102-117) containing cysteine residues involved in p62 oxidation of wild type and K102E mutant showing electrostatic potential between -1RT (red) and +1RT (blue) mapped to the solvent accessible surface. Cysteine 105 is marked by a red circle. (C) *In silico* analysis p62 oxidation and oligomerisation of the N-terminal PB1 domains (residues 3-125) and the potential impact the K102E has on the oxidation and oligomerisation. Two of the monomers (A and D) are K102E mutants, while monomers B, C and E are wild type. K102E mutation triggers large conformational changes locally, which affect the position and orientation of C105 residue (yellow) and impair the disulphide bond between C105 and C115 (green) from the previous monomer (e.g. K102E mutation in chain D disrupts the disulphide bond between C105 from the monomer D and C115 from the monomer C. Thus, equimolar mixture of WT and K102E mutant p62 (as would be expected in patients with heterozygous mutation) results in the covalently-linked trimers (coloured grey in the figure) and disrupts the larger oligomers. Residue K102 is coloured blue. In wild type p62 it interacts with E19 (highlighted as spheres and coloured by heteroatom). In the K102E mutant this favourable electrostatic interaction is disrupted, strong electrostatic repulsion triggers the conformational changes, and the adjacent K103 (highlighted in the monomer D and displayed as balls and sticks) moves towards E19, thus compensating for the loss of favourable interaction, while residue 102 moves outwards. (D) Western blot analysis of non-reduced samples of HeLa cells transfected with FLAG-p62, FLAG-C105,113Ap62 and FLAG-K102Ep62 treated with H_2O_2 (3mM, 1min) and PR-619 (5μM, 10 min). (D) The ratio of DLC to monomeric p62 was quantified and normalised to FLAG-p62. Error bars represent s.e.m., n=3, ***P<0.001. Alignment and models depicted in A&B and C were created by Drs. Graham Smith and Agnieszka Bronowska, respectively.

4.2.10 Oxidation of p62 is independent of the "charged bridge"

The K102, C105 and C113 locate in the "charged bridge", including many charged residues. Ciuffa at al. found that the positively charged R106 and R107 residues were important for the charged bridge, resulting in stabilisation of PB1 domain-mediated oligomers (Ciuffa et al., 2015). In order to assess if other charged residues in the linker region containing the oxidisable cysteines could affect oxidation of p62, several different mutants were generated; negatively charged to positively charged (E104K); positively charged to negatively charged (R106E, R107E); negatively charged to neutral (D108A) and positive to neutral (H109A). GFP-tagged p62 plasmids, wild type or carrying the previously described mutations, were transfected into HeLa cells and treated with the ROS inducing agent PR-619. None of the mutations affected the formation of p62 DLC (Figure 40A). This suggest that the formation of p62 DLC does not depend on the charged bridge, and that the oxidation of cysteines is dominant and potentially aligns the charged bridge. We propose that the formation of p62 DLC via the oxidisable cysteines 105 and 113 is an alternative mode for oligomerisation, which could seed oligomers.

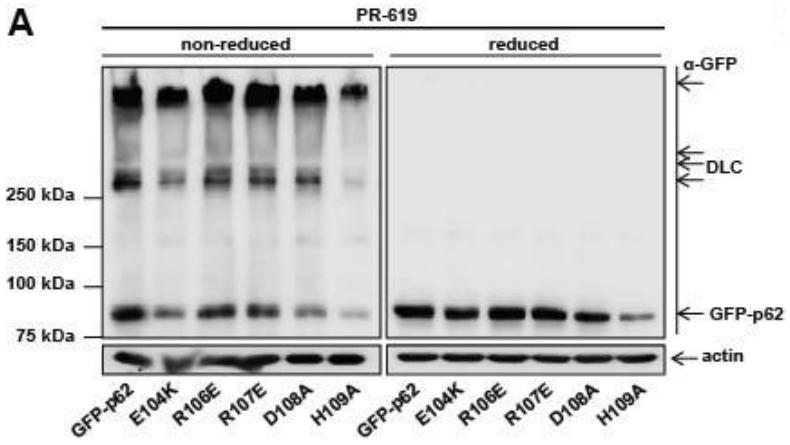

Figure 40 Mutations in the charged bridge do not affect p62 DLC formation.

(A) Western blot analysis of non-reduced samples of HeLa cells transfected with GFP-p62, GFP-E104Kp62, GFP-R106Ep62, GFP-R107Ep62, GFP-D108Ap62, GFP-H109Ap62 treated with PR-619 (10μM, 10 min).

4.2.11 The K102E mutation interferes with the ability of p62 to promote autophagy

Considering that oxidation of p62 promotes autophagy and cell survival upon oxidative stress as shown previously (Figure 30, 31 & 32), we tested if the K102E mutation interferes with autophagy induction. We observed that LC3 lipidation was reduced in *p62*$^{-/-}$ MEFs stably expressing FLAG-K102Ep62 in basal conditions and in response to H_2O_2, this coincided with increased p62 and ubiquitinated protein levels (Figure 41A). Furthermore, fewer autophagosomes were observed in *p62*$^{-/-}$ MEFs stably expressing FLAG-K102Ep62, suggesting an autophagy impairment (Figure 41B).

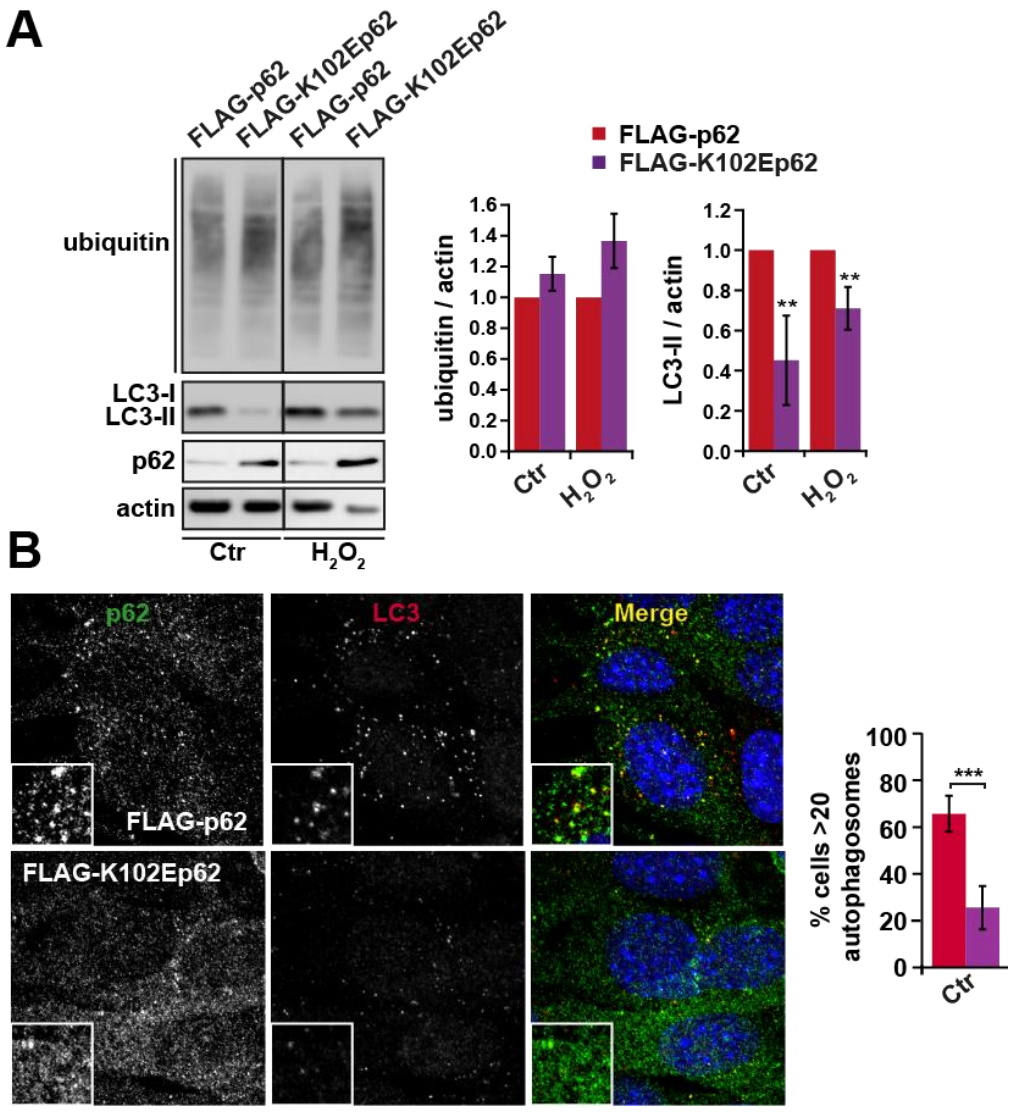

Figure 41 The K102E mutation interferes with the ability of p62 to promote autophagy.

A) *p62*$^{-/-}$ MEFs stably expressing FLAG-p62 or the ALS mutant FLAG-K102Ep62 were treated with 1mM H_2O_2 for 5 hours and subjected to western blot analyses for LC3, ubiquitin and p62. Ubiquitin and LC3-II levels were quantified and normalised to *p62*$^{-/-}$ MEFs expressing FLAG-p62. (B) Representative confocal microscopy images of *p62*$^{-/-}$ MEFs stably expressing FLAG-p62 or FLAG-K102Ep62 were immunostained for p62 and LC3. Error bars represent s.e.m., n=3, **P<0.005, ***P<0.005.

4.2.12 The ALS related K102E mutation results in impaired p62 oxidation in human spinal cord tissue

Finally, immunochemistry analysis of spinal cord tissue of the K102E patient demonstrated an increase in ubiquitin- and p62- positive inclusions compared to other sporadic ALS cases (Teyssou et al., 2013), which could be caused by impaired autophagy, similar to what we observed in the *p62*$^{-/-}$ MEFs stably expressing FLAG-K102Ep62. We analysed spinal cord tissue from a patient with ALS caused by sporadic heterozyguos K102E mutation using western blot and compared to sporadic ALS (SALS) cases without p62 mutations as well as age-matched controls. We found that

in SALS cases total p62 as well as p62 DLC tend to accumulate compared to healthy controls (Figure 42A&B), suggesting that the previously described mechanism for p62 oligomerisation in mouse and tissue culture also applies to human tissue. It also suggests that autophagy is impaired in these SALS cases, as described in the literature (Section 1.12.3).

Similar to aged mouse brains and in tissue culture, the main p62 DLC species we observe is around 250 kDa. In contrast, in the patient carrying the K102E p62 mutation, p62 DLC accumulate in a low molecular weight form, between 100 and 150 kDa, which potentially is a p62 dimer or trimer (Figure 42A). Considering that the carrier is heterozygous for the K102E mutation, it could be speculated that the K102E interacts with wild type p62, allowing the formation of p62 dimers and trimers, but surpressing the formation of higher order DLC, suggesting that the K102E mutation is dominant-negative, as was suggested by our *in silico* model (Figure 39C)

We conclude that the K102E mutation interferes with the function of p62 as a sensor of oxidation, resulting in impaired autophagy. Therefore, an impairment of the mechanism by which p62 associated proteins are degraded in response to oxidative stress could be an underlying factor in the ALS pathology caused by the K102E mutation.

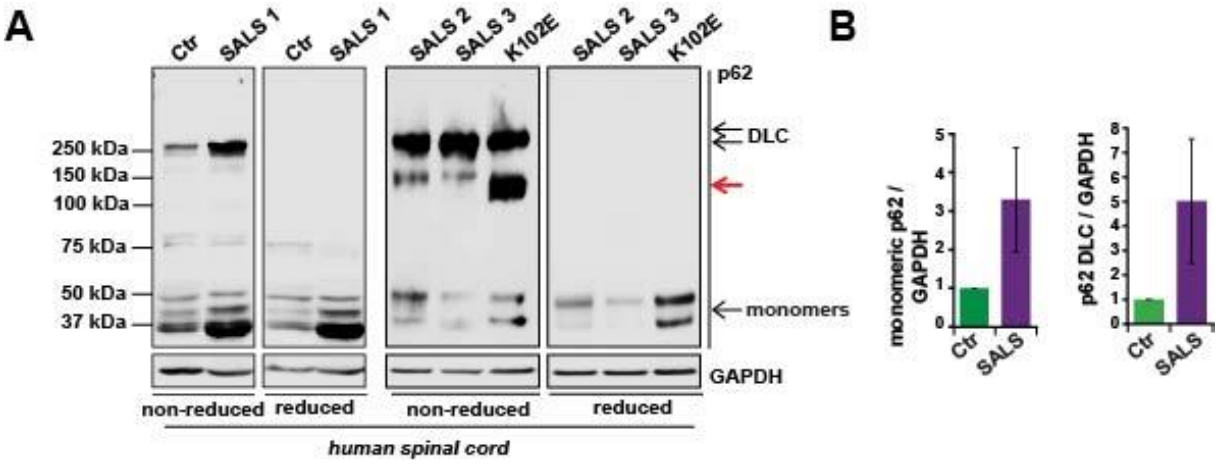

Figure 42 The ALS related K102E mutation results in impaired p62 DLC formation in human spinal cord tissue.

(A) Spinal cord tissue from ALS patients with either unknown (SALS) or K102E p62 mutation or age-matched controls (Ctr) were subjected to western blot analysis for p62 in either non-reducing or reducing (2.5% β-mE) conditions. The red arrow points to an intermediate DLC of p62 which accumulated in the K102E case. (B) Levels of monomeric p62 and DLC were quantified in SALS cases and age-matched controls (n=3).

4.3 Discussion

This is the first time that it has been shown that an autophagy receptor can be redox regulated in response to ROS. We propose that redox-regulation of p62 is a mechanism acquired during evolution of vertebrates to promote autophagy in response to oxidative stress. Lower-order species, such as *D. melanogaster,* do not have this mechanism, but we have shown that introduction of the redox-sensitive cysteines promotes fly survival in oxidative stress conditions. This mechanism might be especially relevant for longer lived species, as the ALS related K102E mutation impairs oxidation of p62 and thus may result in neurodegeneration (Figure 43).

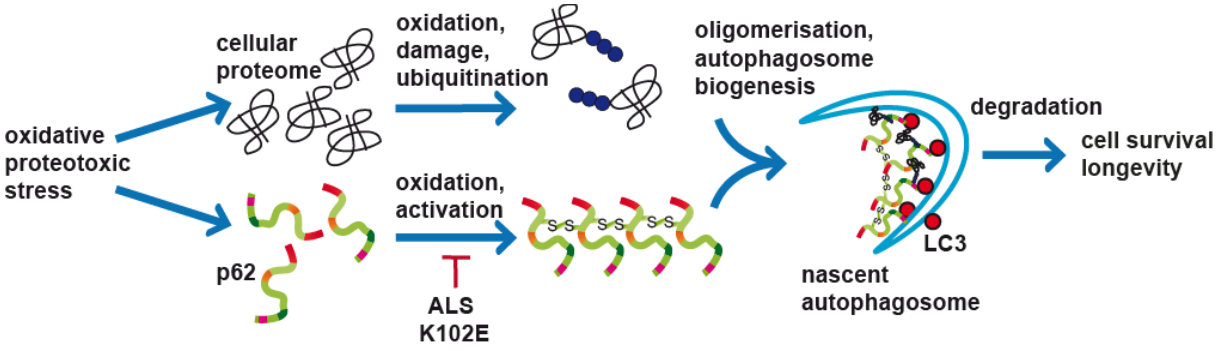

Figure 43 Diagram of the proposed role for p62 oxidation in the degradation of autophagy substrates.

Formation of p62 DLC is triggered by oxidative stress, which promotes degradation of p62 and p62 substrates (such as poly-ubiquitinated proteins) trough autophagy. The ALS associated K102E mutant impairs oxidation of p62.

We have shown that p62 is increasingly oxidised in mouse brains with age (Figure 29B), in tissue culture upon ROS treatments (Figure 30) and in human brains (Figure 42). First of all, we assume that the observed p62 DLC around 250 kDa is a tetramer of p62 molecules. However, it is also possible that other proteins interact with p62 via disulphide bonds. It would be interesting to test this and purify p62 DLC and identify the proteins in the p62 DLC by mass-spectrometry. Unfortunately, this has proven to be difficult as p62 is a very aggregate prone protein (data not shown). We propose that upon oxidation stress cysteines 105 and 113 form disulphide bonds with cysteine 105 and 113 of another p62 molecule. Even though, these two cysteines are the most important oxidisable cysteines, still a little p62 DLC formation remains in cells expressing the FLAG-C105,113p62 (Figure 30A), suggesting that other cysteines (even though they are probably less reactive) can form sulphide bonds as well.

4.3.1 How can a localised ROS signal result in the formation of p62 DLC?

Formation of DLC is triggered by ROS, such as H_2O_2 and in such conditions the prosurvival- and autophagy-promoting roles of p62 are most apparent. Interestingly, in basal conditions, a little p62 DLC is observed as well (Figures 29B, 30A, 42) and also in starvation conditions oxidation of p62 promotes autophagy (Figure 30B-D). Interestingly, Atg4, the only other identified redox-regulated protein that is involved in autophagy was also shown to be oxidised in starvation conditions, without stressing the cells with extracellular ROS (Scherz-Shouval et al., 2007). They convincingly demonstrated that starvation induces the formation of H_2O_2 (Scherz-Shouval et al., 2007), but how this H_2O_2 is produced is unclear. One possible mechanism involves the direct production of ROS via mitochondria, for example via complex I (Scherz-Shouval et al., 2007). How this could be regulated is unclear. Alternatively, local inactivation of Prxs can result in a localised ROS signal. At the plasma membrane, phosphorylation of Prx1 in response to growth factor stimulation results in its inactivation, allowing the build-up of a local H_2O_2 signal (Woo et al., 2010). Prx1 and Prx2 are cytosolic localised, whilst Prx3 and Prx4 are restricted to mitochondria and the ER respectively. As Prx1 was also able to localise to membranes (Woo et al., 2010) it cannot be excluded that these, or other Prxs are present at the site of autophagosome formation. Interestingly, Prx1, Prx 2 and Prx 6 have been shown to locate to the autophagosomal membrane (Overbye et al., 2007). It would be intriguing to assess if a similar mechanism occurs in response to autophagy stimulating conditions such as starvation, where Prxs are for example inactivated at the ER-mitochondrial contact site or at the early phagophore/autophagosome, resulting in a localised H_2O_2 signal. Recently, a computational model by Travasso *et al*. suggest that direct oxidation of redox targets (p62 in this case) by H_2O_2 is not likely to happen. Prxs have a much higher rate constants in the range of 10^7–10^8 M^{-1} s^{-1}, whilst cysteines of other redox regulated proteins range from 9−164 M^{-1} s^{-1}, and in addition Prxs are very abundant (Travasso et al., 2017). According to their model, even locally inactivating Prxs or a locally produced high H_2O_2 signal is not sufficient to directly oxidise less reactive redox targets (e.g. p62). They suggest that oxidised forms of Prx (sulfonate or disulphide forms) mediate the oxidation of redox targets (Travasso et al., 2017). Thus, it could be speculated that the autophagosomal localised Prx1, Prx 2 or Prx 6 function as redox relay proteins. The Prxs could act as initial H_2O_2 sensors and then oxidise target proteins. This would involve the formation of a transient DLC between peroxiredoxin and p62, as was suggested for Ask1-Prx1 (Jarvis et al., 2012), Stat3-Prx2 (Sobotta et

al., 2015) and Dj-1-Prx2 (Fernandez-Caggiano et al., 2016) (Figure 44). Alternatively, oxidised Prxs could oxidise Trxs, resulting in less reduction of p62 DLC by Trx (Diego Manni, data not shown).

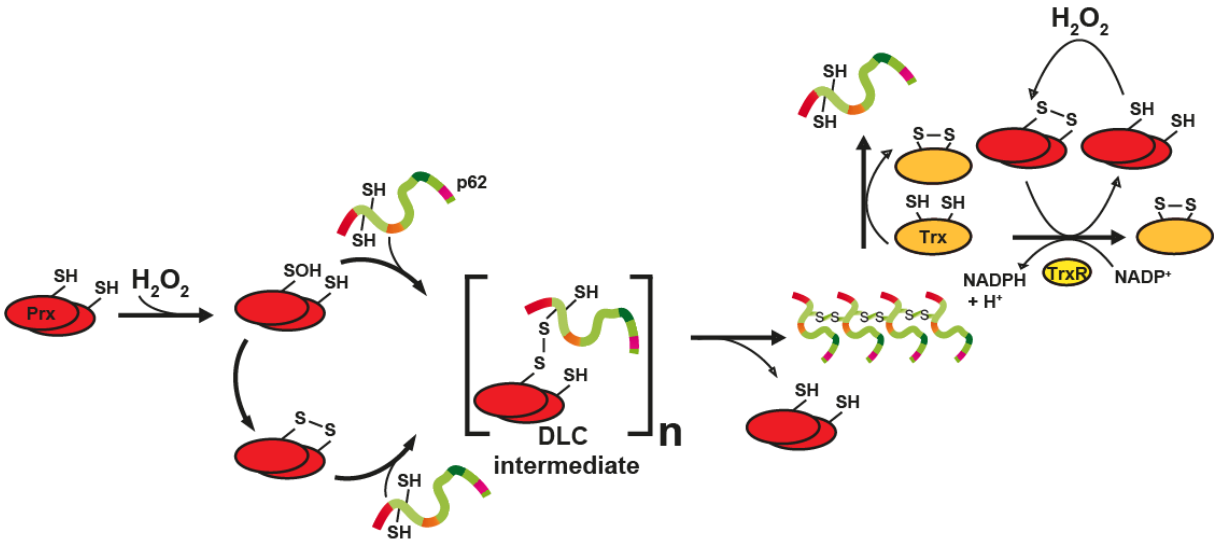

Figure 44 Schematic diagram for a proposed model for Prx-mediated p62 cysteine oxidation.

Peroxiredoxin (Prx, red) gets oxidised by H_2O_2 and forms a sulfenic acid (-SOH), which can further resolve into a Prx dimer (S-S). Oxidised Prx can then oxidise p62 via a thiol-disulphide exchange, by forming a short-lived Prx-p62 DLC intermediate (in brackets), resulting in the formation of p62 DLC. The p62 DLC can be reduced via thioredoxins (Trx, Orange). Trx can also be oxidised by oxided Prx. Thus hyperoxidation/ inactivation of Prx would most likely result in less H_2O_2 signal transduction to p62, or less oxidation of Trx and thus more reduction of p62, both leading to less p62 DLC. This figure is modified after (Sobotta et al., 2015).

4.3.2 A novel role for p62 and the formation of p62 DLC in autophagy induction

p62 is a protein with multiple functions, for example it is involved in several signalling pathways and aggregate formation. However, its function is primarily as an autophagy receptor in selective autophagy, bridging ubiquitinated cargo to LC3. Our data revealed that the formation of p62 DLC promotes autophagy induction. An increased autophagy flux (more lipidated Atg8 accumulated upon autophagy inhibition) was especially apparent in flies expressing oxidisable Ref(2)P^{ox} (Figure 36), but also in *p62*$^{-/-}$ MEFs re-expressing FLAG-C105,113Ap62 ubiquitinated proteins and p62 accumulated, whilst there was less lipidated LC3 and autophagosomes (Figure 30B-E, 31A&B). Thus, in addition to its role in the late stage of the autophagy pathway, our data suggest that p62 also functions in the early steps of autophagy induction. In Chapter 5 we will speculate in more detail how p62 could be involved in autophagy induction and what the role of ROS are during autophagy initiation.

In addition, to promoting autophagy initiation, the formation of p62 DLC could also promote the degradation of ubiquitinated cargo by increased binding to LC3-positive membranes. Previously, it has been shown that oligomerisation of p62 is important for its targeting to the nascent autophagosome (Wurzer et al., 2015, Itakura and Mizushima, 2011). It was proposed that oligomerisation of p62 stabilises its interaction with LC3 clusters on the autophagosomal membrane. It was shown that not the affinity of binding to individual LC3 molecules was affected, but upon oligomerisation the off-rate of p62, from LC3 positive vesicles was reduced (Wurzer et al., 2015). Furthermore, oligomerisation of p62 also promotes the interaction with ubiquitin and promotes specificity towards linear and K63-linked, but not K48-linked ubiquitin chains (Wurzer et al., 2015). We have shown that oxidation of p62 promotes aggregate formation (data not shown) and as oligomerisation of p62 has been shown to be important for efficient recruitment of ubiquitinated cargo to the nascent autophagosome. We propose that the formation of p62 DLC functions via the same mechanism as described by Wurzer *et al*. Thus oxidation of p62 has a dual role in autophagy, firstly it promotes autophagy initiation and secondly it promotes aggregation, resulting in efficient targeting of substrates to the autophagosome.

4.3.3 How does the formation of p62 and Ref(2)P DLC promotes oxidative stress resistance in cells and in flies?

In cells, as well as in flies, oxidation of p62 results in increases stress resistance. Upon oxidative stress less cell death was observed in *p62*$^{-/-}$ MEFs expressing wild type p62, compared to expressing the C105A,113A mutant. We introduced the human p62 linker region, including the redox-regulated cysteines into Ref(2)P, thereby creating Ref(2)P^{ox}. Flies expressing this humanised Ref(2)P^{ox} showed prolonged survival upon oxidative stress. At the moment a control, reintroducing the p62 linker region without cysteine 105 and 113 into Ref(2)P is missing and should be included in future studies.

We showed the increased stress resistance due to the formation of p62 DLC is autophagy dependent (Figure 32C) and our data suggests that Nrf2 signalling is not involved (Figure 33). Previously, it was shown that in response to arsenic (III) Nrf2 signalling is induced in a p62-dependent manner (Ichimura et al., 2013). However, we do not observe a significant p62 dependence in response to H_2O_2 (Figure 33B&C). Ichimura *et al*. used *p62*$^{+/+}$ and *p62*$^{-/-}$ MEFs and also used *HO-1* mRNA levels as a readout, similar to us. Therefore, we think that the stressor As(III) is a different, or a

more potent Nrf2 inducer and it would be interesting to test if Nrf2 signalling in response to As(III) is dependent on p62 oxidation.

As we conclude that the increased stress resistance is dependent on autophagy, questions remain, such as is there a specific cargo targeted upon p62 oxidation or is bulk autophagy induced. The clearance of damaged, misfolded proteins via autophagy has been shown to be important for cell survival (Ogata et al., 2006, Chen et al., 2017, Tyedmers et al., 2010). We have focused on the clearance of ubiquitinated proteins, but different organelles and pathogens are degraded via selective autophagy as well.

4.3.4 How does the ALS related K102E mutation prevent the formation of p62 DLC?

Lysine 102, which is located very near to cysteine 105, has been identified to be mutated into a glutamic acid in a sporadic late-onset ALS patient. Interestingly, this mutation prevents the formation of p62 DLC (Figure 39). However, mutating other positive charged residues, such as R106 and R107 do not affect p62 DLC formation (Figure 40). It is likely that these residues are less important for the reactivity of cysteine 105. Therefore, it would be interesting to test if mutating K103 into a negatively charged residue such as a glutamic acid affects oxidation as well. If this mutation does not affect p62 oxidation, it would suggest that there is something special about lysine 102. It could be speculated that not only the reactivity of the cysteines plays a role, but lysine 102 could be important for an enzymatic form of oxidation, or via for example peroxiredoxins. To test this, K102 could be mutated into neutral, negative charged residues or other positive charged residues. If only a charge reversal mutations affect the formation of p62 DLC, but not other mutations, it would suggest that positive charged lysine affects the pKa of the cysteine and the interaction with E19 (Figure 39B&C). However, if substitutions to other charged residues, or neutral residues also affect p62 DLC formation, it would suggest that this lysine affect oxidation of p62 by another means and that the cysteine is not oxidised directly by H_2O_2. Our *In silico* model of p62 oxidation (39C) could be used to test these hypotheses.

4.3.5 What is the consequence of p62 DLC perturbation?

We have shown that the formation of p62 DLC is a prosurvival mechanism that is acquired in vertebrates and it promotes autophagy induction and thus degradation of autophagy substrates during oxidative stress conditions. On the contrary, we have shown that if this mechanism is perturbed in humans (K102E mutation in ALS patient) it may result in age-related diseases such as neurodegeneration (Figure 39, 41). The

K102E mutation showed a similar phenotype to the C105A, C113A mutant, where decreased LC3-II levels coincided with increased p62 and ubiquitinated protein levels, which was especially apparent in oxidative stress conditions (Figure 41). Teyssou *et al*. performed a careful neuropathological analysis of the K102E patient. The K102E p62 mutant carrier was a female who at age 81 was diagnosed with sporadic ALS, with a bulbar disease onset and a duration of 10 months. Microscopic analysis revealed mild neuronal loss in the spinal anterior horns, in the twelfth nucleus and in the substantia nigra (without Lewy bodies). Immunohistochemistry examination showed the accumulation of ubiquitin, TDP-43 and p62 positive filamentous and rounded inclusions in spinal cord. Furthermore, motor neurons contained intracellular small ubiquitin and TDP-43 positive aggregates and increased p62 protein levels were observed, which is consistent with our findings (Teyssou et al., 2013)(Figures 41 & 42). Interestingly, the K102E mutant patient had a late disease onset. It could be speculated that subtle effects on autophagy by the ALS-related K102E mutation predispose neurons to a vulnerability, which over time, with age, or a second hit in another autophagy or UPS related protein, might be detrimental (Cuervo et al., 2005, Scotter et al., 2014). It is not clear why perturbed formation of p62 DLC primarily seem to effect motor neurons, potentially they particularly rely on protein and organelle quality control and thus are affected most.

To study the function of p62 DLC formation in more detail, our flies, including the previously suggested control (reintroducing the p62 linker region without cysteine residues 105 and 113 into Ref(2)P) and a new “ALS” fly (reintroducing the p62 linker region with the K102E mutation into Ref(2)P) could be assessed for motor function and other ALS related and neurodegenerative pathology. These flies could also be crossed with flies expressing mutant human *SOD1* or *TDP-43* to specifically study ALS (Watson et al., 2008, Diaper et al., 2013).

Promoting autophagy has been shown to prolong life span in flies (Simonsen et al., 2008, Ulgherait et al., 2014), thus it could be speculated that introducing the oxidisable cysteines in Ref(2)P also extends lifespan. It would be interesting to test this and do lifespans in normal conditions (25°C).

5 CHAPTER 5: OXIDATION OF THE AUTOPHAGY RECEPTORS NBR1, TAX1BP1, NDP52 AND OPTN

5.1 Introduction

In the previous chapter we described how p62 is oxidised and how this induces autophagy, which, as a pro-survival pathway, impacts on cell survival in oxidative stress conditions in mammalian tissue culture and in flies and how impaired p62 oxidation might be causative for late-onset ALS. In this chapter we investigated if the oxidation of autophagy receptors is a recurring theme.

In section 1.3 4 other autophagy receptors, NBR1, TAX1BP1, NDP52 and OPTN have been described in great detail. These 4 autophagy receptors were selected because they are most widely studied and contain similar functional domains as p62, such as LC3- and ubiquitin binding domains and they all can dimerise or oligomerise, even though not always to the same extent as p62. NBR1 has a PB1 domain, but this PB1 domain does not promote oligomerisation of the protein. Instead it uses the first CC domain to oligomerise (Kirkin et al., 2009). NDP52 contains a CC domain, which has been shown to promote its dimerisation (Kim et al., 2013a), whilst OPTN contains multiple CC domains, which most likely promote trimerisation (Agou et al., 2002, Gao et al., 2014). Also TAX1BP1 and NBR1 contain multiple smaller CC domains which are thought to be important for dimerization as well (Ling and Goeddel, 2000). Data published by others suggest that CC domains can be redox regulated. For example dimerization of occludin , as well as dimerization of voltage-gated H(+) (Hv) channel via its CC domain is redox dependent (Walter et al., 2009, Fujiwara et al., 2013). Disulphide bonds formed between two CC domain alpha-helices resulted in stabilisation of coiled-coil assembly. Furthermore, mutating the cysteine required for redox regulation of this CC domain in the Hv channel did not affect the secondary structure of the coiled-coil domain (Fujiwara et al., 2013). These autophagy receptors are also distinct from p62 in many other ways, which has been reviewed in section 1.4.

Oxidation of p62 was shown to be important for oligomerisation and formation of p62 aggregates (Chapter 4 and data not shown). Therefore, we hypothesise that oxidation of these other autophagy receptors promotes dimerization and oligomerisation via redox regulated CC domains. As shown in the previous chapter, the oligomerisation of p62 is important for autophagy initiation. Other autophagy receptors have been suggested to affect autophagy flux as well, although this has not been studied in much

detail (Itakura et al., 2012, Wurzer et al., 2015, Mizushima, 2007). In this results chapter, tools have been generated to study the role of receptors in regulating autophagy induction.

OPTN and NDP52 have been shown to be required for the degradation of mitochondria (mitophagy) (Section 1.5). Recently, antimycin A and oligomycin treatments have been used mostly to study PINK1/Parkin mediated mitophagy. antimycin A is a mitochondrial complex III inhibitor and results in aberrant ROS production at complex III. Oligomycin inhibits complex V (the ATPase) and thereby prevent reverse functioning of the ATPase in order to maintain Δψm. Thus, this treatment used to induce mitophagy, results in loss of Δψm and ROS production at complex III. We questioned if oxidation of autophagy receptors could be important in PINK1/Parkin mediated mitophagy.

The aim of this chapter is to assess if NBR1, TAX1BP1, NDP52 and OPTN have the ability to form DLC's and generate different tools that can be used to study the role of the formation of autophagy receptor DLC's in starvation induced autophagy and selective autophagy, especially mitophagy.

5.2 Results

5.2.1 The autophagy receptors NBR1, TAX1BP1, NDP52 and OPTN form DLC in response to oxidative stress

To assess if other autophagy receptors are oxidisable, HeLa cells were treated with the oxidants H_2O_2 and PR-619. Western blot analysis of non-reduced samples were probed for 4 autophagy receptors: NBR1, TAX1BP1, NDP52 and OPTN and p62 was included as a positive control. Interestingly, we observed that all receptors have the ability to form DLC (Figure 45). First of all, NBR1, which is structurally most comparable to p62, forms DLC almost as efficiently as p62. In response to PR-619 no monomeric species were visible, suggesting that all NBR1 protein is associated with NBR1 DLC. H_2O_2, which is a more transient ROS species, also results in the oxidation of NBR1, although slightly less as what is observed for p62. The NBR1 DLC species formed at ~230 and ~270 kDa could potentially be a trimer a tetramer, however the oligomers formed are too large to predict the size. TAX1BP1, NDP52 and OPTN also form DLC, in response to H_2O_2, DLC's are again less formed compared to p62, suggesting that these autophagy receptors are slightly less sensitive to ROS. In response to PR-619, all TAX1BP1 protein is in higher order oligomers, which could be TAX1BP1 tetramers and higher order species (Figure 45). The main NDP52 DLC species formed are ~200

kDa, most likely being a NDP52 tetramer, but also lower order species were observed. OPTN seems to form several different sized DLC's, but the main species are ~200 and ~270 kDa, which could be OPTN trimers and tetramers. To conclude, all receptors tested can form DLC and thus this could be a general mechanism that is required for their function. It is also possible that these receptors form disulphides with other proteins and this hopefully will be addressed in future experiments, but not in this thesis.

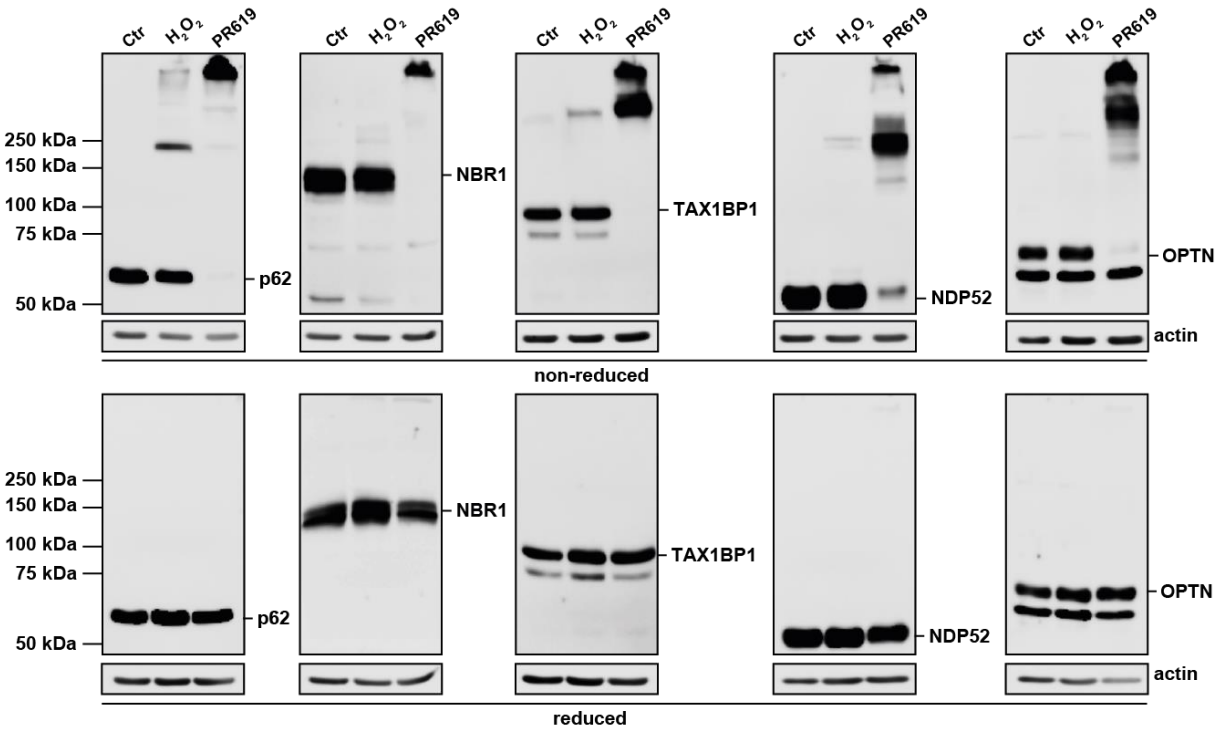

Figure 45 NBR1, TAX1BP1, NDP52 and OPTN form DLC in response to oxidative stress.

HeLa cells were treated with H_2O_2 (5mM, 1 min) or PR-619 (10μM, 10 min) and analysed by western blot for endogenous p62, NBR1, TAX1BP1, NDP52 and OPTN in either reducing (2.5% β-mE) or non-reducing conditions.

5.2.2 TAX1BP1, NDP52 and OPTN DLC are formed when TrxR is inhibited

In order to assess if the oxidation of autophagy receptors is reversible, HeLa cells were treated with 500 µM H_2O_2 for different durations. H_2O_2 treatment is sufficient to produce low levels of TAX1BP1, NDP52 and OPTN DLC (Figure 46). This is accompanied by PRX hyperoxidation (PRX-SO_3) and the formation of PRX-3 dimers (Figure 46). We observed that H_2O_2 treatment triggers a rapid (1 minute) and reversible formation of TAX1BP1, NDP52 and OPTN DLC (Figure 46). The OPTN DLC are hard to observe, suggesting again that it is less sensitive to ROS.

In addition, we tested if these DLC can be reduced by the Trx system (Section 1.8.4). We treated HeLa cells with H_2O_2 for the indicated time points in the absence or presence of TrxR inhibitors curcumin or auranofin. Curcumin is a natural occurring compound that inhibits TrxR (Cai et al., 2012), whilst auranofin is a chemically produced potent inhibitor of TrxR. Inhibition of TrxR results in the accumulation of Prx dimers and limits the formation of hyperoxidised Prx-SO_3. In the presence of curcumin, more TAX1BP1, NDP52 and OPTN DLC are formed. Upon TrxR inhibition by auranofin TAX1BP1 is all in DLC, and no monomeric band is observed. On the contrary, NDP52 and OPTN do form DLC, but most NDP52 and OPTN is in the reduced monomeric form (Figure 46). This suggests that all three receptors are reducible by thioredoxin, but TAX1BP1 seems the most redox-sensitive.

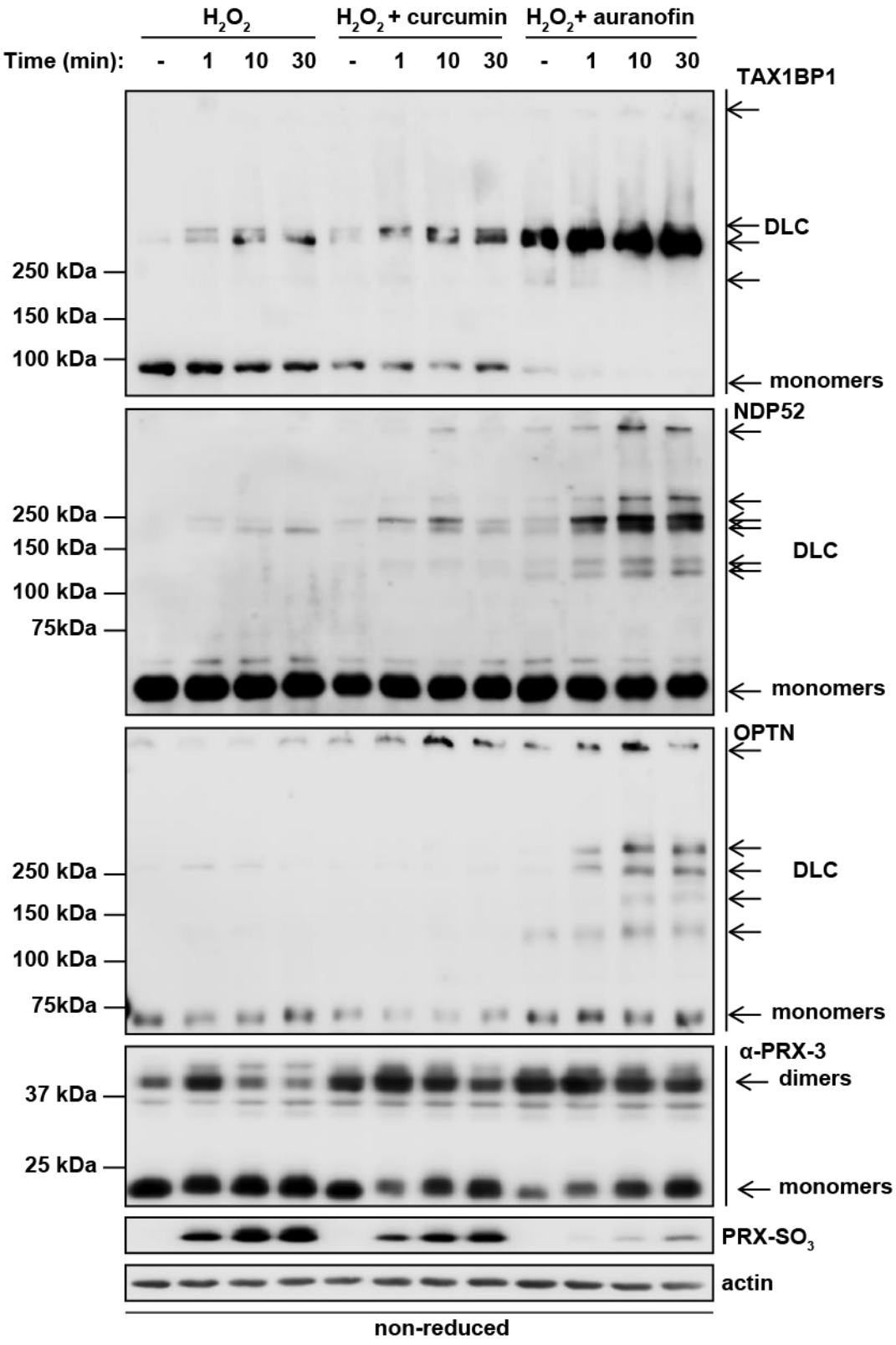

Figure 46 TAX1BP1, NDP52 and OPTN are reducible by the thioredoxin antioxidant system.

HeLa cells were pre-treated with TrxR inhibitors, curcumin (50μM) or auranofin (5μM) for 30 min, then treated with H_2O_2 (500μM) at different time points as shown. Cell were then lysed and immunoblotted in non-reduced conditions for TAX1BP1, NDP52, OPTN and PRX-3 and reduced conditions for PRX-SO_3 and actin.

5.2.3 Gibson assembly of autophagy receptors in pDEST26 backbone

Now we have established that, in addition to p62, other autophagy receptors can form DLC and that they can be reduced by the thioredoxin system. Next, we were interested which cysteines are important for this redox sensing. Furthermore, knowing which cysteines are important, gives us the opportunity to create a redox-insensitive mutant, which can be used to elucidate the function of the DLC formation by autophagy receptors.

In order to perform cysteine mutagenesis we needed plasmids with the DNA sequence of the autophagy receptors. His-tagged OPTN (human) in the pDEST26 backbone was purchased from Addgene (Plasmid #23050). This mammalian expression vector contains the neomycin resistance gene, which is useful for creating stable cell lines, therefore we cloned FLAG-tagged NDP52 into the same backbone. Gibson assembly, a cloning strategy that has been developed in the last decade, was used. This method allows to combine multiple DNA fragments with overlapping sequences.

DNA fragments with 20-40 base pair overlap were created by amplifying DNA fragments with primers with appropriate overlap using the primers in table 13 (Figure 47A). After assembly of the fragments the construct was verified by a control digestion with SacI (Figure 47B). Finally, the entire insert was sequenced. His-FLAG-NDP52 was transfected into HeLa PentaKO cells (CRISPR KO for p62, OPTN, NDP52, TAX1BP1 and NBR1) (Figure 47C) and western blot analysis was performed to assess if the protein is expressed correctly and is oxidised upon H_2O_2 and PR-619 treatment. Indeed, transient overexpressed NDP52 formed DLC, as was detected with a FLAG and NDP52 antibody (Figure 47D). The DLC sizes were similar as observed previously with endogenous NDP52 (Figure 47D).

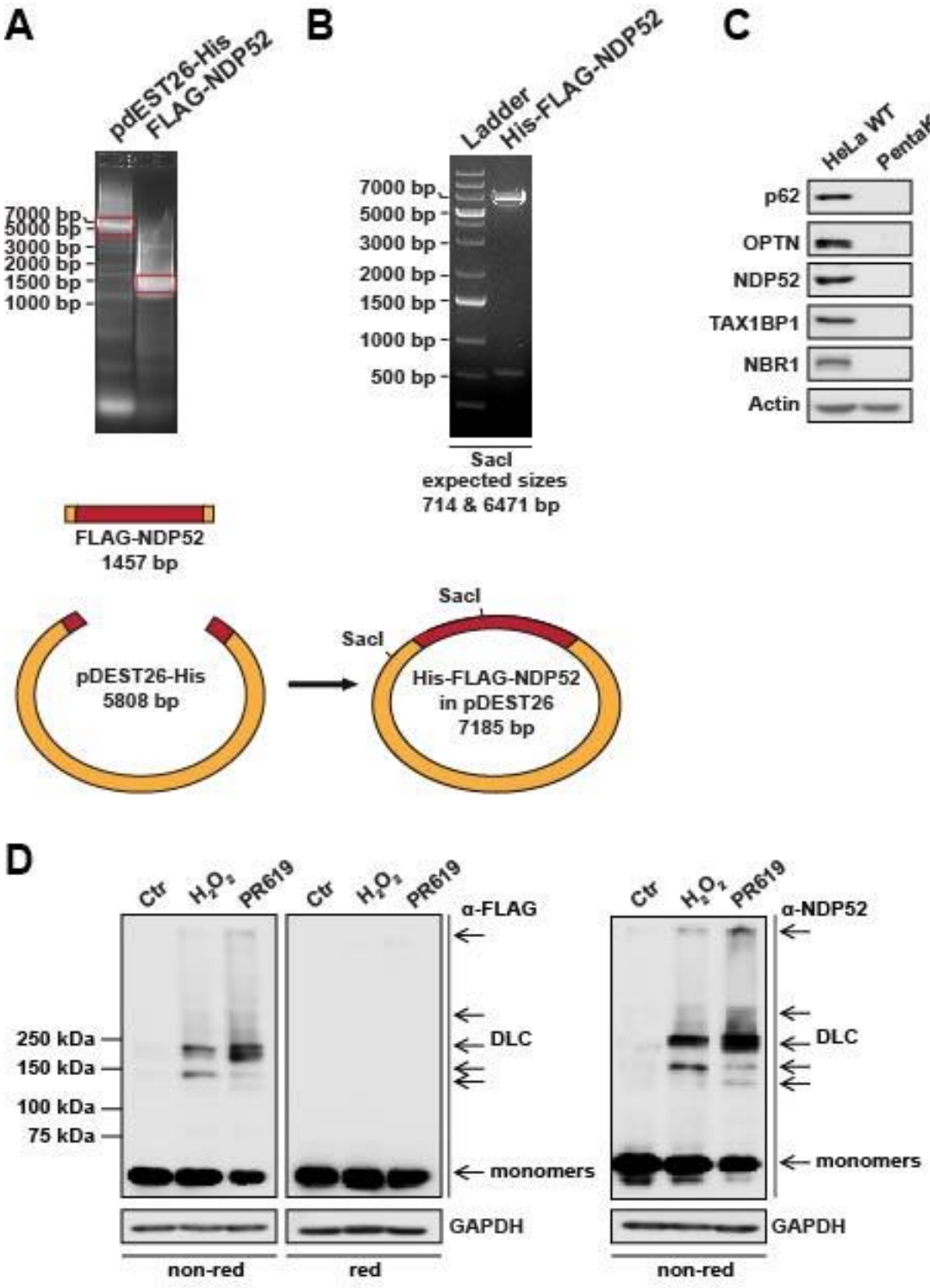

Figure 47 Gibson cloning of FLAG-NDP52 into pDEST26 (His).

(A) Agarose gel electrophoreses analysis of the PCR product for pDEST26 (His) and the insert FLAG-NDP52. The red squares represent the band that were gel-purified and used for Gibson assembly. The pDEST26 backbone and the NDP52 insert are depicted in orange and red respectively. The PCR product created contain overlapping regions with the insert and backbone. (B) Agarose gel electrophoreses analysis of the cloned His-FLAG-NDP52 plasmid digested with SacI to assess correct assembly. (C) HeLa wild type and PentaKO cells were analysed by western blot analysis for p62, OPTN, NDP52, TAX1BP1 and NBR1. (D) HeLa PentaKO cells were transfected with the His-FLAG-NDP52 plasmid and treated with 5mM and 20μM PR-619 and analysed by western blot analysis for FLAG or NDP52 in non-reducing conditions.

5.2.4 Analysis of conservation of cysteines in redox regulated autophagy receptors

In p62 we found that two cysteines were required for the formation of p62 DLC. NDP52, OPTN, TAX1BP1 and NBR1 contain 13, 7, 19 and 20 cysteines, respectively (Figure 48), of which 3, 3, 8 and 6 cysteines are part of a zinc finger and predicted to be non-essential for the formation of DLC. This prediction is based on previous data from p62 mutagenesis; mutating cysteines in the p62 ZZ domain resulted in more DLC formation, potentially because Zinc binding is lost and cysteines become available and can form disulphide bonds, or lack of zinc binding results in a conformational change that promotes oxidation of other cysteines (Diego Manni, data not shown).

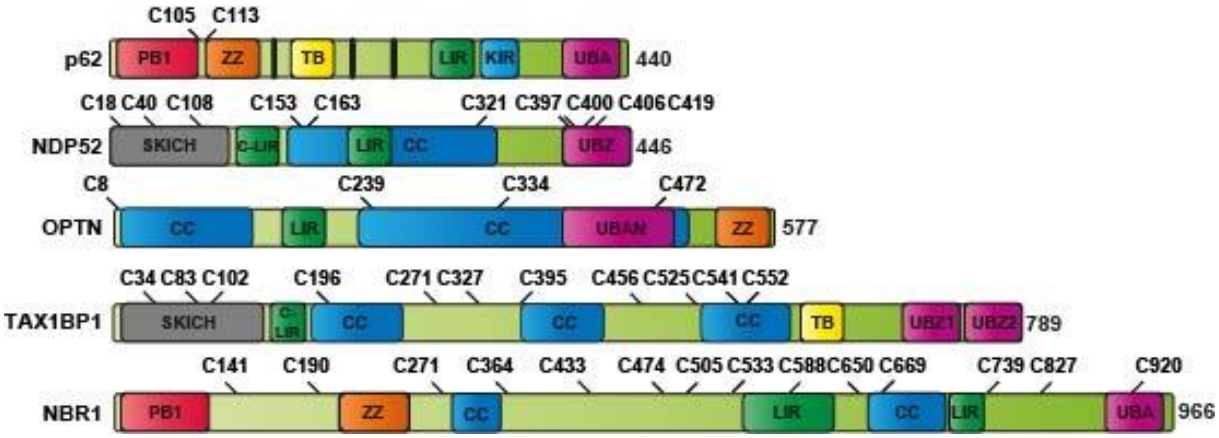

Figure 48 Schematic diagram of the domain structure of p62, NDP52, OPTN, TAX1BP1 and NBR1 including the cysteines.

p62 cysteine residues at position 105 and 113 were previously identified to be required for redox regulation of p62. Cysteines located in ZZ domains are not shown. The Ubiquitin binding domains are depicted in purple, PB1 domains in red, CC domains in blue, LC3-binding domains in green, ZZ domains in orange, KIR domain in light blue, TB domains in yellow and the SKICH domain in grey. p62 also contains nuclear localisation signals, depicted in black.

5.2.5 Cysteines at positions 8, 239, 334 and 472 are all important for the formation of OPTN DLC

First single Cys to Ala substitutions of C8, C239, C334 and C472 of OPTN were performed and revealed that C334A resulted in less of the ~270 kDa DLC, whilst the C472A mutation resulted in the loss of the ~200 kDa DLC (Figure 49A, blue boxes). To reduce the formation of OPTN DLC further, a second round of mutagenesis was carried out, using the C334A mutation as the basis. Both the C8A and the C472A mutation resulted in less DLC formation; C8A mainly affected higher order DLC species, whilst C472A again resulted in the loss of the ~200 kDa DLC (Figure 49B). Finally, a third and fourth round of mutagenesis was performed to prevent the formation

of residual OPTN DLC. Adding the C8A mutation to the C334A, C472A double mutant mainly prevented the formation of higher order DLC and mutating Cys 239 on top of the triple mutant, resulted in an almost complete loss of OPTN DLC (Figure 49C). This quadruple mutant (from now on called 4xCA OPTN) will be used for further functional studies (Figure 49D).

Furthermore, we multiple protein alignments revealed that the 4 cysteines are conserved in vertebrates (Appendix, Figure 57).

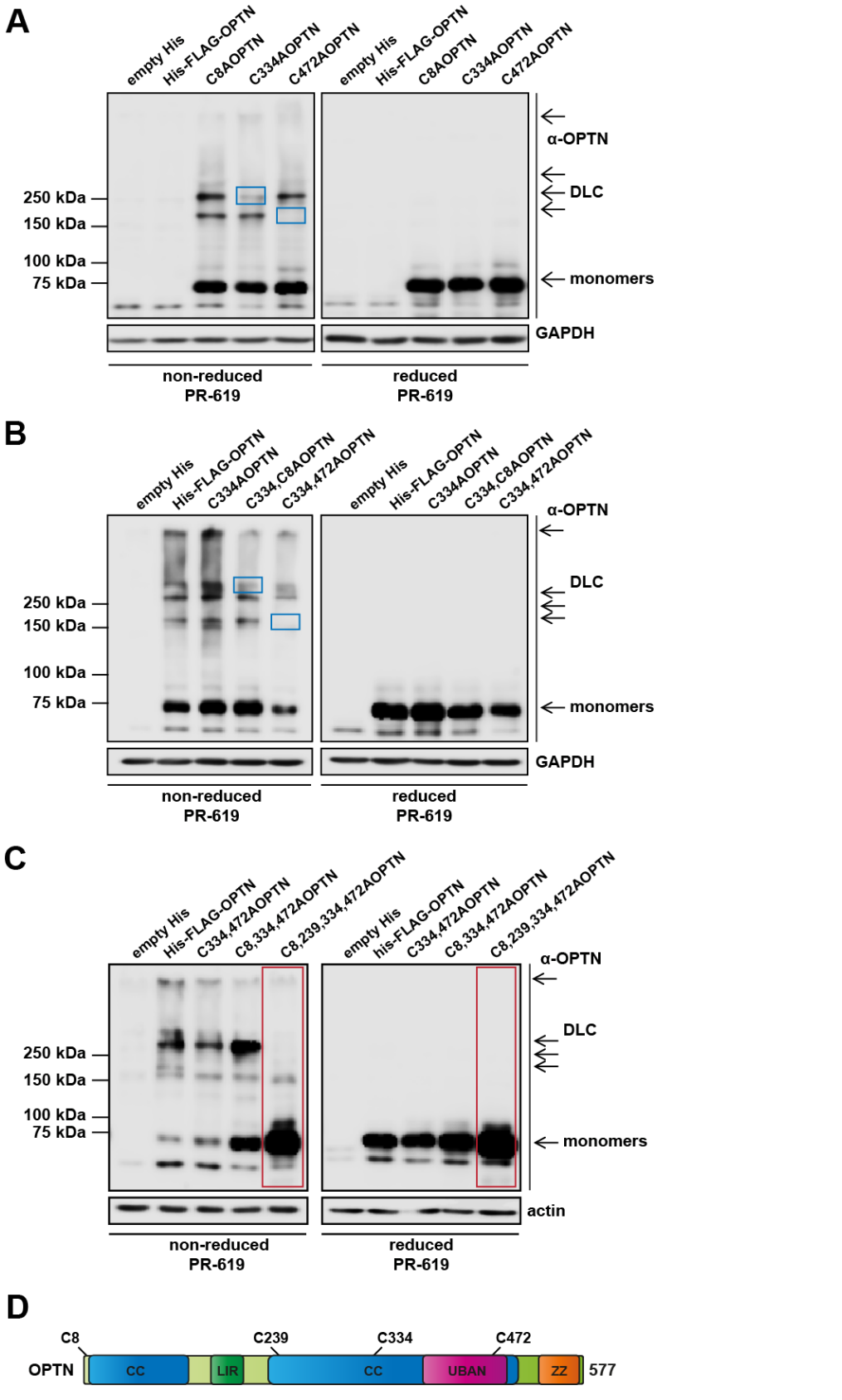

Figure 49 Cysteines at positions 8, 239, 334 and 472 are all important for the formation of OPTN DLC.

(A) Single, (B) double, (C) triple or quadruple cysteine mutant OPTN plasmids were generated and transfected in HeLa PentaKO cells. Cells were treated with 20μM PR-619 for 10 min and analysed by western blot for OPTN in either reducing (2.5% β-mE) or non-reducing conditions. (D) Schematic diagram of the OPTN structure showing the location of the redox sensitive cysteines.

5.2.6 Cysteines located in the CC domain are important for the formation of NDP52 DLC

The same approach was taken to identify cysteines required for NDP52 DLC formation. First single Cys to Ala substitutions of C18, C40, C108, C153, C163, C321, C397, C400, C406 and C419 were performed. The C153A mutation had the clearest effect on NDP52 DLC formation, especially the ~210-230 kDa DLC levels were reduced which are potentially tetramers (Figure 50A). A second round of mutagenesis, using C153A as the backbone, showed that the C153A,163A double mutation prevented NDP52 DLC formation most (Figure 50B). Therefore, this double mutant was used for a third round of mutagenesis, as there was still some residual DLC's left. The C18A mutation prevents the formation of the ~150 kDa DLC, however it results in the appearance of a different ~130 kDa DLC (Figure 50 B&C, blue boxes). It would be interesting to purify these different species to assess their composition. The C153A, C163A, C321A triple mutant resulted in an almost complete loss of NDP52 DLC formation upon oxidative stress and this NDP52 triple mutant was used to study the role of NDP52 oxidation. These three cysteines all localise to the CC domain and it would be interesting how cysteines mutations in this domain affects dimerization of NDP52 (Figure 50D). Interestingly, we found that the three cysteines we identified to be most important for oxidation of NDP52 are acquired very late in evolution and are conserved in primates (Appendix Figure 58).

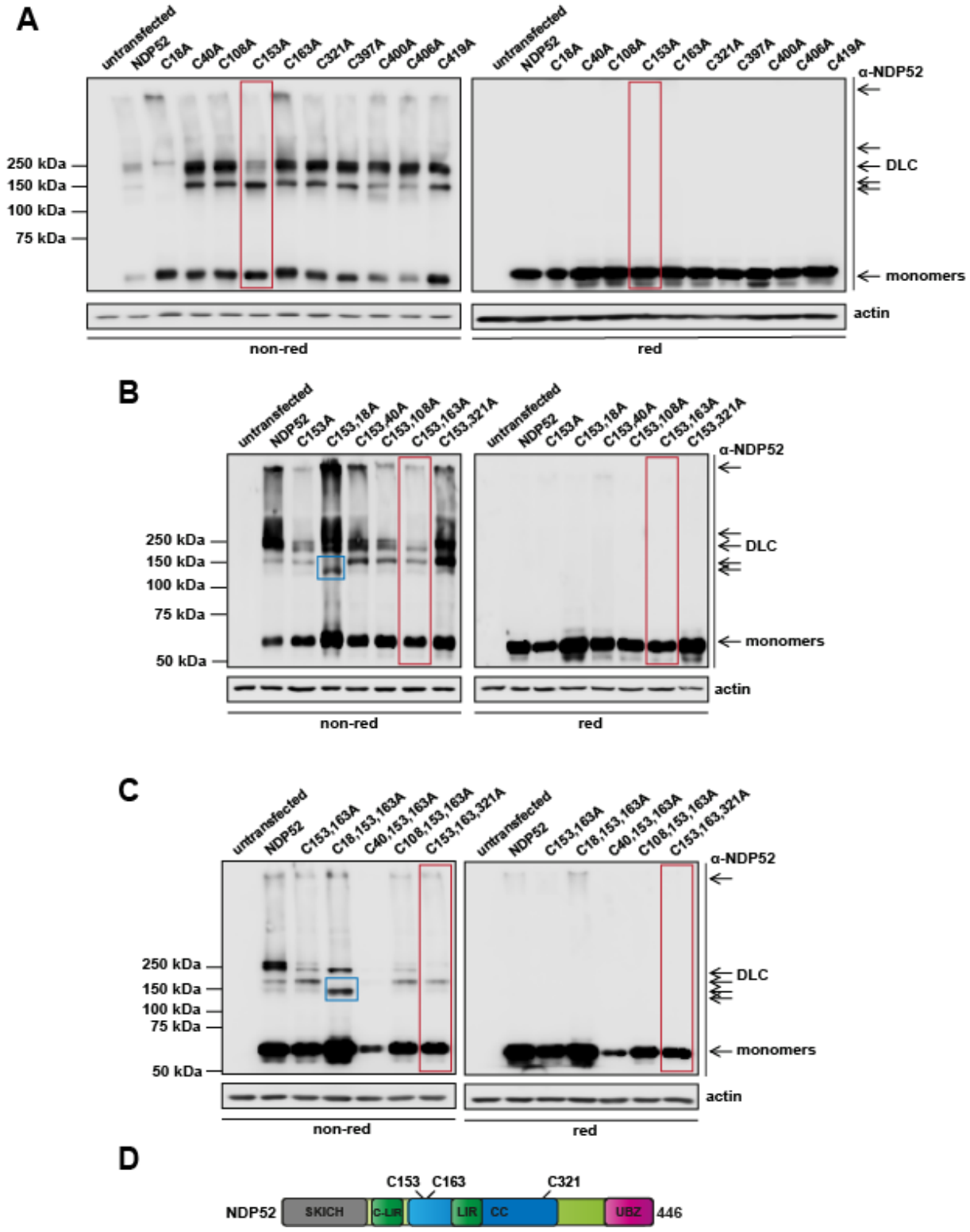

Figure 50 Cysteines at positions 153, 163 and 321 are important for the formation of NDP52 DLC.

(A) Single, (B) double and (C) triple cysteine mutant NDP52 plasmids were generated and transfected into HeLa PentaKO cells. Cells were treated with 20μM PR-619 for 10 min and analysed by western blot for NDP52 in either reducing (2.5% β-mE) or non-reducing conditions. (D) Schematic diagram of the NDP52 structure showing the location of the redox sensitive cysteines.

5.2.7 Generation of stable cell lines expressing tagged autophagy receptors in HeLa PentaKO cells

To study the role of autophagy receptors in autophagy induction, stable cell lines were generated. Because there is a lot of redundancy among the different receptors, we decided to use HeLa PentaKO cells to re-express wild type p62, NDP52 or OPTN or the respective oxidation mutants. The cysteines essential for redox regulation of NBR1 and TAX1BP1 remain to be determined and will be included in follow-up research.

NDP52 and OPTN were cloned in the lentiviral vector pLENTI6/V5-DEST, which has a blasticidin selection marker. In order to do so, Gibson assembly was used and primers were designed to PCR the pLENTI6/V5-DEST backbone (without overhang), so that it could be re-used to insert the different receptors and their mutants. The generated PCR fragments were used for Gibson assembly and control digestions were performed to test if the generated plasmid was correct (Figure 51A&B). Finally, plasmids were send for sequencing and the entire insert was sequenced.

Because HeLa cells have a good transfection efficiency, we carried out stable transfections to generate HeLa PentaKO stably expressing His-FLAG-p62, His-FLAG-C105,113Ap62, His-FLAG-OPTN, His-FLAG-4XCAOPTN, His-FLAG-NDP52 or His-FLAG-C153,163,321A-NDP52. After the transfection of HeLa pentaKO, blasticidin selection was used to select for the cells which have the plasmid integrated into the genome. To test the expression levels of the different proteins western blot analysis was performed. Expression levels of p62 and NDP52 were similar to endogenous levels and also OPTN levels were similar between wild type and the 4XCA mutant (Figure 51C).

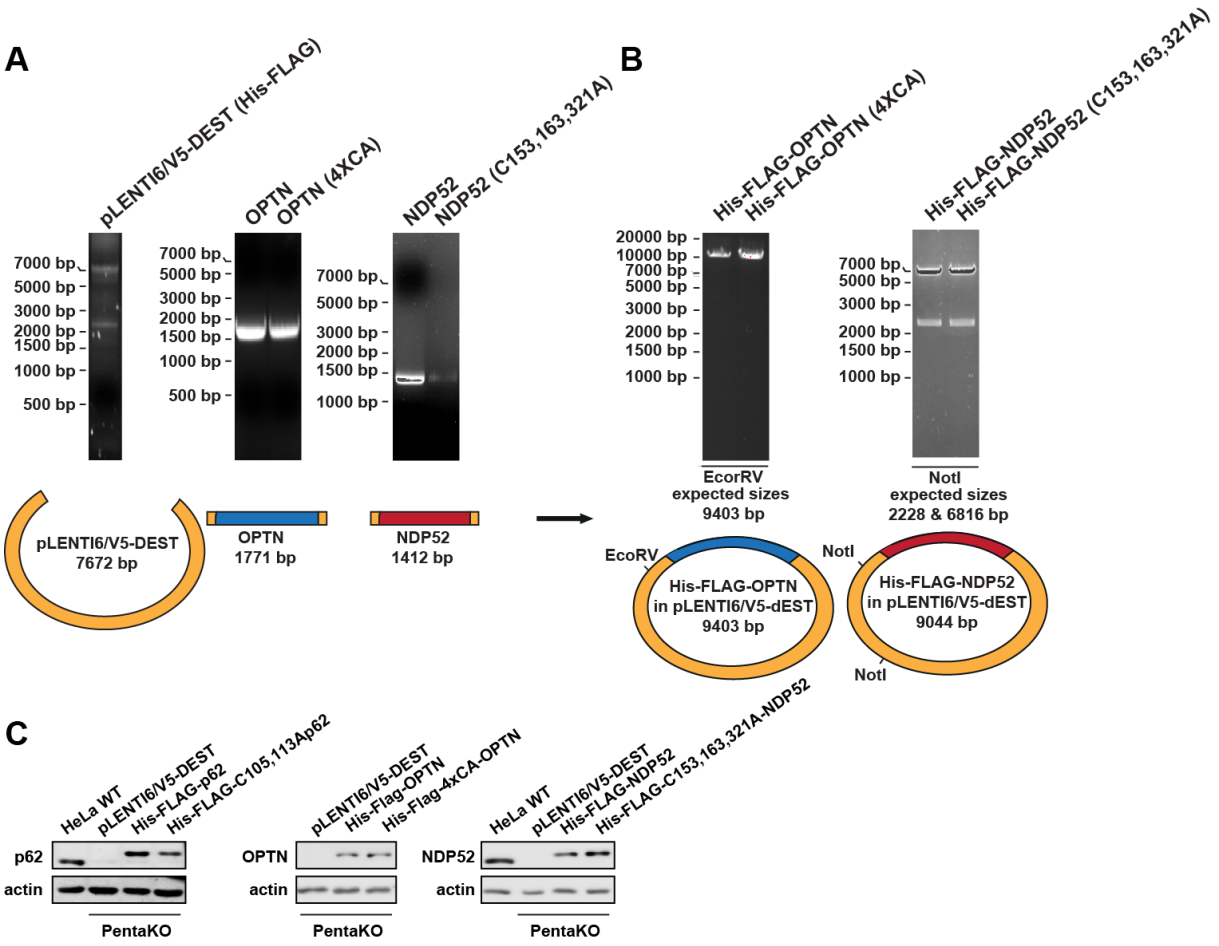

Figure 51 Cloning of OPTN and NPD52 in the lentiviral pLENTI6/V5-DEST plasmid and generation of stable cell lines.

(A) Agarose gel electrophoreses analysis of the PCR products for pLENTI6/V5-DEST (His-FLAG) backbone (orange), OPTN wild type and 4xCA mutant inserts (blue) and NDP52 wild type and C153,163,321A mutant inserts (red). (B) Agarose gel electrophoreses analysis of the cloned His-FLAG-OPTN and His-FLAG-NDP52 wildtype and mutant plasmids in the pLENTI6/V5-DEST backbone, digested with EcoRV and NotI, respectively. (C) HeLa wild type and PentaKO cells stably expressing His-FLAG-p62, His-FLAG OPTN and His-FLAG-NDP52 wildtype and mutants were analysed by western blot analysis for p62, OPTN and NDP52.

5.2.8 Autophagy receptors are required for autophagy induction

In chapter 2 we showed that oxidation of p62 regulates autophagy flux and that this is important for cell survival and stress resistance in mammalian cells and flies. Here we found that autophagy receptors are indeed important to regulate an autophagy response in basal and starvation conditions. Autophagic flux in HeLa wild type and PentaKO cells was measured in basal conditions and serum starvation conditions using Bafilomycin A1 to block autophagosome-lysosome fusion. Interestingly, this revealed that in PentaKO cells autophagy flux was decreased in basal conditions, as LC3-II accumulated less in PentaKO cells compared to wild type cells and this phenotype was even more striking in cells that were serum starved (Figure 52). The

HeLa PentaKO cells expressing p62, OPTN and NDP52 (Figure 51) can be used to rescue the autophagy defect. HeLa PentaKO cells expressing TAX1BP1 and NBR1 will need to be generated as well to complete this set. As soon as the most important receptor(s) have been identified, oxidation mutants can be tested as well.

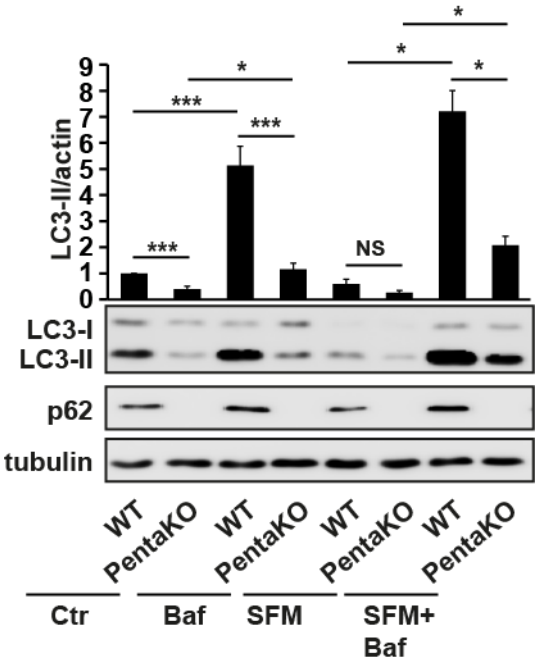

Figure 52 Autophagy receptors are required for autophagy initiation.

HeLa wild type or PentaKO cells were treated Bafilomycin A1 (Baf, 400nM, 4 hours) in either complete (Ctr) or serum free medium (SFM) and analysed by western blot for LC3 and p62. Error bars represent s.e.m., (n=3), *P<0.05, ***P<0.005, NS= not significant.

5.2.9 mtKeima can be used to measure PINK1/Parkin mediated mitophagy in HeLa PentaKO cells

p62, OPTN, NDP52, TAX1BP1 and NBR1 have been shown to recruit to damaged mitochondria and serve different roles during mitophagy (Section 1.5), however OPTN and NDP52, and to a lesser extent TAX1BP1, were shown to be required (Lazarou et al., 2015). To test if oxidation of NDP52 and OPTN is required for PINK1/Parkin mediated mitophagy we generated HeLa PentaKO stably expressing YFP-Parkin and mtKeima. mtKeima is a mitochondrial targeted pH sensitive fluorescence protein, which is protease-resistant. Upon a switch to low pH (lysosome) it changes the excitation wavelength from 458nm (visualised as green) to 561nm (visualised as red) (Figure 53A). HeLa cells and HeLa PentaKO cells stably expressing Parkin-YFP and mt-Keima were kindly created by Dr. Michael Lazarou, Monash Univeristy. To test if the cell lines can be used to define the level of mitophagy, HeLa wild type and PentaKO cells were treated for 3 hours with antimycin A and oligomycin (AO) and live cell

imaging was performed. In control conditions Parkin localised to the cytosol and no mitophagy events were observed, however upon 3h AO treatment Parkin translocated to perinuclear mitochondria. In wild type HeLa cells mitophagy events (red) were observed, in contrast to HeLa PentaKO cells (Figure 53B), showing that these cells can be used to measure mitophagy events.

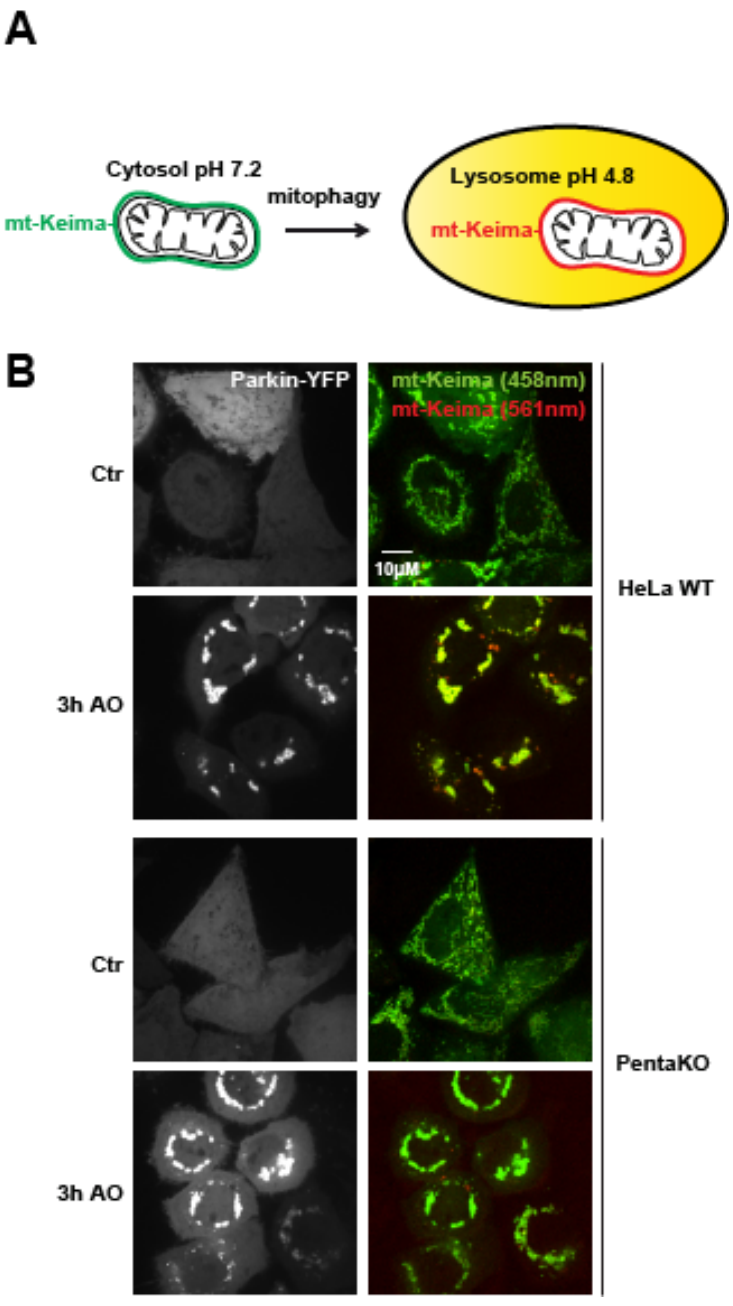

Figure 53 mtKeima can be used to measure PINK1/Parkin mediated mitophagy in HeLa PentaKO cells.

(A) Schematic diagram of the fluorescent mitochondrial targeted Keima (mtKeima). mtKeima has an excitation spectrum that is pH sensitive. In neutral pH (cytosol) the protein is predominantly excited with 458 nm, whereas in an acidic environment (lysosome) the excitation shifts to 561 nm. (B) HeLa wild type and PentaKO stably expressing YFP-Parkin and mtKeima were treated with AO (antimycin A and oligomycin) for 3 hours and analysed by confocal microscopy.

5.2.10 The C153,163,321A mutations in NDP52 impair PINK1/Parkin mediated mitophagy

HeLa PentaKO cells expressing YFP (Yellow Fluorescent Protein)-Parkin and mtKeima reintroducing His-FLAG-tagged NDP52 and OPTN and their respective oxidation mutants were generated as previously described in section 5.2.7. His-FLAG-NDP52 protein expression levels were very similar to endogenous NDP52, whilst His-FLAG-OPTN levels were higher than endogenous levels, however levels between wild type and mutant OPTN were similar (Figure 54A). These cell lines were used to test if oxidation of NDP52 and OPTN is required for PINK1/Parkin mediated mitophagy. Cells were seeded on glass bottom dishes and after 3 hours of AO treatment cells were imaged by confocal microscopy. High ratio 550/430 nm signal / cell area was calculated as an index for the mitophagy (Katayama et al., 2011). As published previously, PentaKO cells had a clear mitophagy defect (Figure 54B). Interestingly, significantly less PINK1/Parkin-mediated mitophagy was induced in cells expressing C153,163,321A NDP52 mutant compared to wild type, suggesting that oxidation-sensing properties of NDP52 are required for its function in PINK1/Parkin mediated mitophagy. In order to test if NDP52 gets recruited to mitochondria upon mitophagy induction, mitochondria were isolated in basal and upon 3h AO treatment and western blot analysis in non-reduced and reduced conditions was performed (Figure 54C). Upon 3 hours AO treatment the majority of NDP52 is degraded, mostly via autophagy, but also by the proteasome (Data not shown). We hypothesised that we could not observe NDP52 DLC upon 3h AO treatment, because they are rapidly degraded. Therefore, we co-treated cells with the proteasomal inhibitor MG132 and Bafilomycin A1 to block autophagy. In these conditions, we could see wild type NDP52 form DLC at mitochondria, whilst the C153,163,321A mutant was only able the form lower order DLC around 120 and 150 kDa (Figure 54C). Furthermore, increased ubiquitination of wild type NDP52 in response to AO treatment was observed (Figure 54C).

Together this data suggest that NDP52 forms DLC on mitochondria in response to mitophagy induction, and this is required for an efficient delivery of the damaged mitochondria to the lysosome.

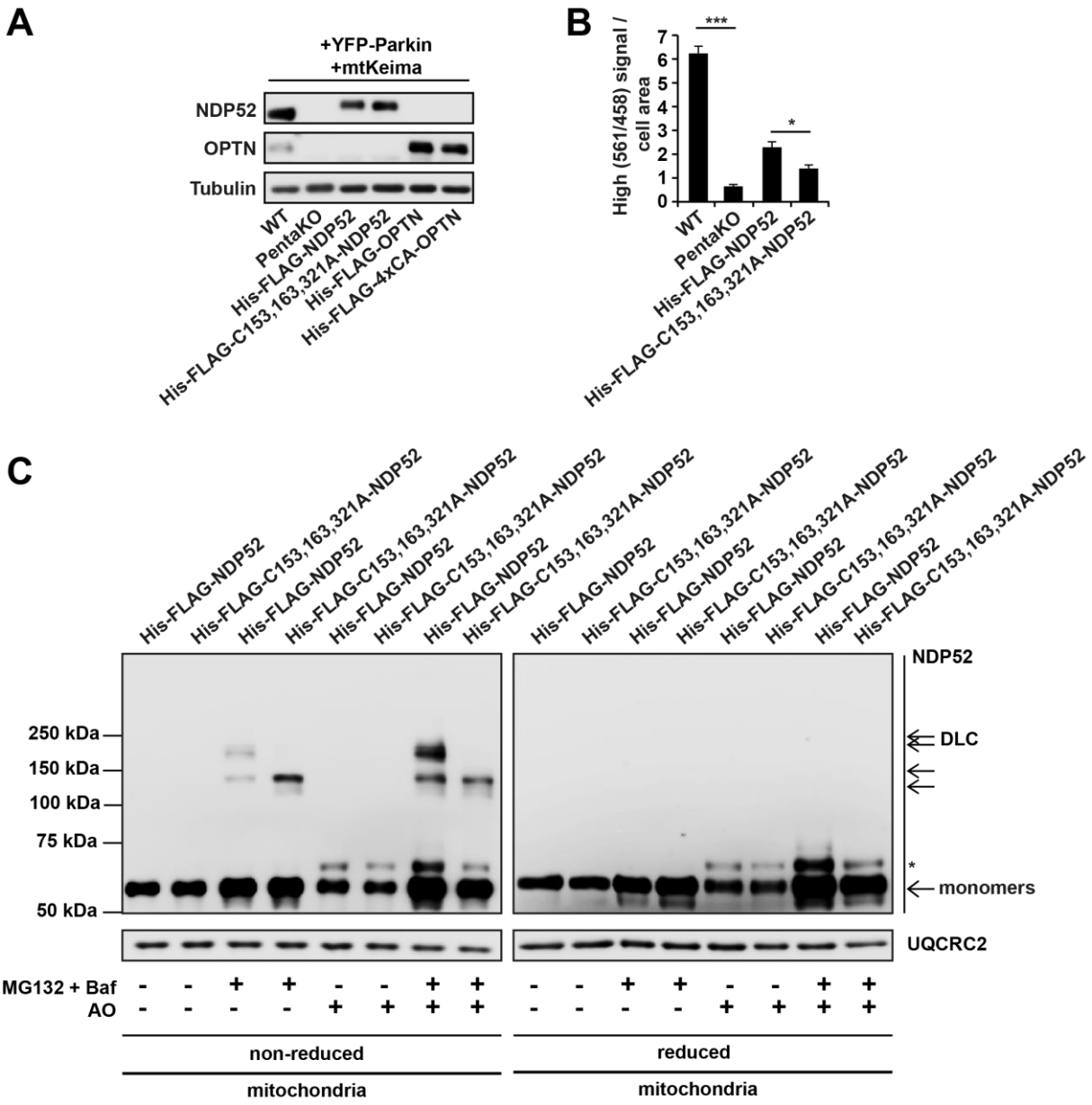

Figure 54 The C153,163,321A mutations in NDP52 impair PINK1/Parkin mediated mitophagy.

(A) HeLa wild type or PentaKO cells stably expressing YFP-Parkin, mtKeima and His-FLAG-NDP52 or His-FLAG-OPTN and their respective oxidation mutants were analysed by western blot analysis for NDP52 and OPTN to check the expression levels. (B) HeLa wild type and PentaKO stably expressing YFP-Parkin and mtKeima and His-FLAG-NDP52 or His-FLAG-C153,163,321A-NDP52 were treated with AO for 3 hours and high (561/458) signal / cell area values were obtained from confocal images. Error bars represent s.e.m., (n=3), *P<0.05, ***P<0.005. In collaboration with Dr. Yoana Rabanal Ruiz. (C) HeLa PentaKO stably expressing YFP-Parkin and mtKeima and His-FLAG-NDP52 or His-FLAG-C153,163,321A-NDP52 were treated with AO for 3 hours in the absence or presence of MG132 and Bafilomycin A1 (Baf), followed by a mitochondrial isolation and western blot analysis for NDP52 in either reducing (2.5% β-mE) or non-reducing conditions. The asterisk indicates ubiquitination of NDP52. The mitochondrial protein UQCRC2 was used as a loading control.

5.3 Discussion

For the first time, we have shown that not only p62, but also four additional autophagy receptors, being OPTN, NDP52, TAX1BP1 and NBR1 have the ability to form DLC in response to oxidative stress and that these receptors are reducible by the thioredoxin system. Three cysteines in NDP52 and four cysteines in OPTN all locating in CC domains were shown to be essential for oxidation. In addition, we found that autophagy receptors are important for autophagy induction and tools were developed to assess which receptors are important and if oxidation of these autophagy receptors is important in this process. Furthermore, we have shown that the three oxidisable cysteines we identified in NDP52 are important for its function in PINK1/Parkin mediated mitophagy.

5.3.1 Is oxidation of autophagy receptors a reoccurring theme?

The previous chapter described how oxidation of p62 promotes autophagy and cell survival upon oxidative stress conditions and how disrupting this mechanism can result in neurodegeneration. p62 is the most studied autophagy receptor, however it is not the only one. Very similar receptors with very similar domain structure and function have been identified. Autophagy receptors are poorly conserved in contrast to the core autophagy machinery. These receptors have in some cases redundant functions, but also have their own unique roles (Section 1.3). We were interested to assess if these autophagy receptors also have the ability to form DLC in response to oxidative stress. Excitingly, we indeed found that all receptors studied (OPTN, NDP52, TAX1BP1 and NBR1) had the ability to form DLC. It needs to be elucidated if DLC formation of these receptors is functional. Different OPTN DLC species were observed, which could be dimers, trimers and tetramers and higher order species. NDP52 DLC could be trimers and tetramers. TAX1BP1 and NBR1 DLC formation shows a more similar behaviour to p62, where most likely tetramers are formed. Size-exclusion chromatography could give us more information about the size of higher-order DLC, as western blot analysis only helps predicting the size up to 250 kDa.

As we first identified OPTN and NDP52 as redox regulated proteins and they are well known for their role in mitophagy, we started with a mutagenesis screen to identify essential redox regulated cysteines. Interestingly, we found that mutating certain cysteines in OPTN and NDP52 resulted in a loss of distinct DLC species and not a reduction in all DLC's as we observed for p62 previously (Diego Manni, data not shown). Purifying the different DLC species and assessing their composition could

reveal more about their function. The purification of these species was proven to be difficult for p62 (Diego Manni, not shown), however OPTN, NDP52, TAX1BP1 and NBR1 are less aggregate prone, and therefore potentially easier to purify. When purified, 2D sequential non-reducing/reducing ('diagonal') SDS-PAGE could be performed to identify proteins that are present in the DLC (Sobotta et al., 2015). Mass spectrometry of oxidised receptors (comparing wild type and oxidation mutants) could help to identify the proteins present in the DLC, whilst including single NDP52 and OPTN cysteine mutants would reveal more about what cysteines are important to form disulphide bridges with other proteins.

5.3.2 How is the oxidation status of autophagy receptors regulated?

As introduced in section 1.8, proteins can be oxidised directly by H_2O_2, but also indirectly via for example Prxs, and they can be reduced via the Trx system. We found that autophagy receptors can be reduced via Trx, as inhibiting TrxR results in the formation of OPTN, NDP52 and TAX1BP1 DLC. Especially TAX1BP1 seemed very sensitive for oxidation in those conditions, as no monomeric TAX1BP1 was observed anymore (Figure 46). To confirm if these receptors are indeed reduced by the thioredoxin system, co-immunoprecipitations of receptors with different thioredoxin and Prxs could be performed. Because these interactions are very transient and hard to observe, trapping mutants could be used.

It would be interesting to asses if the autophagy receptors get oxidised directly by H_2O_2 or indirectly via Prxs. As discussed previously in the case of p62 (Section 4.3.1), we propose that the autophagy receptors could be indirectly oxidised by H_2O_2 via Prxs; this mechanism involves a physical interaction between the Prxs and the autophagy receptors, which allows the transfer of oxidising equivalents between the two (Sobotta et al., 2015). If this is the case, hetero-oligomeric species containing for example TAX1BP1 and peroxiredoxin should be observed, especially in conditions where TrxR is inhibited. Purifying the DLC's and assessing their composition could reveal more about a potential involvement of Prxs in the formation of these DLC's.

5.3.3 How can autophagy receptors regulate autophagy?

We found that autophagy receptors not only function in targeting cargo to the autophagosome, but also regulate autophagy flux and induction in starvation (Figure 52). As we have shown in chapter 3, oxidation of p62 promotes autophagy. It would be interesting to assess if other autophagy receptors have a similar role in autophagy

initiation. Cell lines have been generated to investigate the role of individual receptors. Furthermore, it would be interesting to test in more detail how autophagy flux could be regulated by autophagy receptors. Potentially, receptors impact on upstream signalling pathways, such as growth factor signalling via AKT or mTORC1 signalling. For example, p62 has been suggested to be an integral part of the mTORC1 complex, and could affect downstream autophagy initiation (Duran et al., 2011).

Also a more direct role for in receptors in autophagy initiation could be hypothesised, as p62 and NBR1 (other receptors were not tested) have been observed at autophagosome formation sites where they form distinct puncta (Kishi-Itakura et al., 2014, Itakura and Mizushima, 2011). Interestingly, p62 oligomerisation via its PB1 domain is essential for the recruitment to the ER autophagosome formation site (Kishi-Itakura et al., 2014). In literature, a role for autophagy receptors in autophagy maturation has been proposed. For example, NDP52 was suggested to be involved in autophagosome maturation, but not initiation, as autophagosomes accumulate upon loss of NDP52 (Verlhac et al., 2015a). Tumbarello *et al*. suggested that OPTN, NDP52 and TAX1BP1 are important for autophagosome maturation by linking autophagosomes to myoxin VI, which is import for fusion with lysosomes (Verlhac et al., 2015a, Verlhac et al., 2015b, Tumbarello et al., 2012). However, they also observed that a triple knock-down of NDP52, OPTN and TAX1BP1 reduced autophagosome formation in basal and upon autophagy induction induced by proteotoxic stress and they hypothesised that the limited targeting of cargo to the autophagosomal membrane was causative (Tumbarello et al., 2012). It is not known how targeting of cargo affects autophagy flux, but it is an interesting idea that autophagy cargo and autophagy initiation come together to make selective autophagy as efficient as possible. This hypothesis is supported by work in yeast, where Atg1 (Ulk1/2 orthologue) can be activated by receptor bound cargo (protein aggregates and peroxisomes were tested) and a scaffold (Atg11) even in nutrient-rich conditions and thus locally overwriting the inhibitory mTORC1 signal (Kamber et al., 2015). Work in mammalian cells suggests that indeed cargo and receptors recruit and initiate autophagosome formation around the cargo. For example, Lazarou *et al.* showed that upon mitochondrial damage, NDP52 and OPTN, are required for the recruitment of ULK1 and DFCP1, two proteins involved in autophagosome biogenesis, to mitochondria (Lazarou et al., 2015). By using the HeLa PentaKO cells re-expressing the different autophagy receptors we can elucidate questions such as which receptors are most important for autophagy

initiation, without having problems with redundancy of other receptors and a potential role for oxidation of receptors can be investigated.

5.3.4 Does oxidation of NDP52 promote mitophagy?

As autophagy receptors function in bridging cargo and the autophagosomal machinery, it would be interesting to test if oxidation of autophagy receptors promotes cell survival by promoting degradation of distinct intracellular components. Mitochondria are one of the main sources for ROS, therefore it would be especially interesting to look into the selective degradation of these organelles. OPTN, NDP52, TAX1BP1, NBR1 and p62 all are recruited to damaged mitochondria, but only OPTN, NDP52 and, to a lesser extend TAX1BP1, were shown to be required for mitophagy (Lazarou et al., 2015). Excitingly, we found that mutating cysteines 153, 163 and 321 into alanines impacts on the role of NDP52 in PINK1/Parkin mediated mitophagy.

All the reactive cysteines identified are located in CC domains, which is important for dimerization. Potentially, the formation of disulphide bridges between NDP52 molecules result in the alignment of CC domains and triggers dimerization. Interestingly, the CC domain of occludin (a transmembrane tight junction protein) was shown to be redox sensitive, as disulphide bridges were involved in dimerization (Walter et al., 2009). Furthermore, a cysteine in the CC domain in the voltage-gated H^+ channel forms a disulphide bond which increases the thermal stability of the CC domain and promotes dimerization (Fujiwara et al., 2013), showing that CC domains can be redox regulated. We will have to rule out that our cysteine to alanine substitutions in the CC domains of NDP52 do not impact on the secondary structure of these domains. Knowing that cysteine 153, 163 and 321 are only conserved in primates, suggests that they are not important for CC domain secondary structure, because the other CC domain residues are highly conserved (Appendix, Figure 58).

In order to conclude that oxidation of NDP52 promotes mitophagy, a few issues need to be addressed. For example, it has not been elucidated if PINK1/Parkin mediated mitophagy induced by antimycin A and oligomycin is ROS-dependent instead of Δψm-dependent. In order to address this S3QEL2 can be used in our mtKeima assay. antimycin A treatment results in ROS production at respiratory complex III. S3QEL2 is an inhibitor that prevents ROS production induced upon antimycin A treatment, without affecting the Δψm or the ETC (Orr et al., 2015).

We were able to show that upon mitophagy induction NDP52 gets oxidised on mitochondria, which suggests that AO treatment does result in ROS production, and the recruitment and oxidation of NDP52.

5.3.5 How could oxidation of NDP52 promote mitophagy?

Mechanistically, it is not clear how and at what stage oxidation of NDP52 would promote mitophagy. First of all, its recruitment to mitochondria could be affected. Recruitment of NDP52 to damaged mitochondria is Ub-dependent. Therefore, it would be interesting to biochemically assess Ub binding of wild type and the NDP52 oxidation mutant, as well as their recruitment to damaged mitochondria. If binding to Ub and recruitment to damaged mitochondria is unaffected, recruitment of autophagy initiation components, such as ULK1, DFCP1, WIPI1, Atg9 or LC3 could be assessed. ULK1 and DFCP1 recruitment have been shown to be dependent on NDP52 and OPTN and would be a primary target (Lazarou et al., 2015).

In chapter 4, we showed that oxidation of p62 promotes its oligomerisation and that this promotes autophagy induction, resulting in increased oxidative stress resistance. We hypothesise that oxidation of NDP52, similarly to p62, results in oligomerisation of the protein and that this results in an increased binding avidity to autophagy proteins.

Most likely, antimycin A and oligomycin treatment would result in a ROS gradient, which could result in the formation of NDP52 DLC in the cytosol near damaged mitochondria, and this could help the assembly of the mitophagy machinery prior to the binding of receptors to mitochondria. In figure 55 a final model speculating a potential role for oxidation of NDP52 in PINK1/Parkin mediated mitophagy is presented.

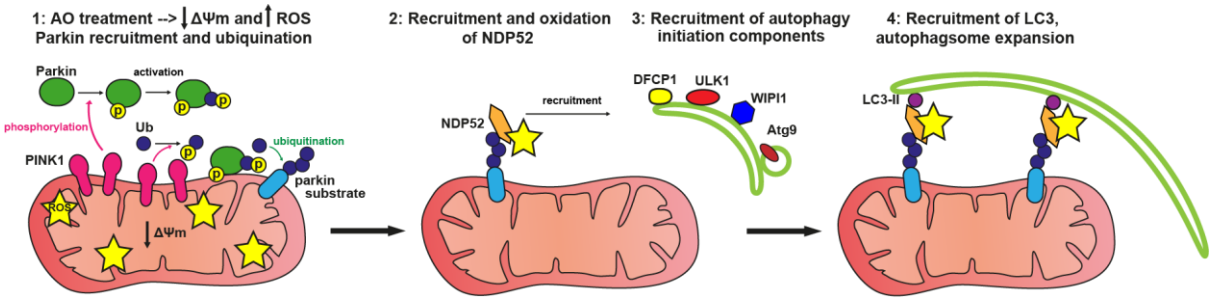

Figure 55 Model describing a potential role for oxidation of NDP52 in PINK1/Parkin mediated mitophagy.

1: Antimycin A and oligomycin treatment results in a loss of mitochondrial membrane potential (Δψm), but more importantly ROS production at respiratory complex III. This results in the accumulation of PINK1 at the mitochondrial membrane, where it phosphorylates Parkin and Ub. Parkin ubiquitinates outer mitochondrial membrane proteins, resulting in 2: the recruitment of NDP52 to the ROS producing mitochondrion, where it gets oxidised. 3: Oxidised and oligomerised NDP52 more efficiently recruits autophagy initiation components, promoting the formation of an autophagosomal membrane around the mitochondrion. 4: Finally, oxidised NDP52 recruits LC3 to promote degradation via fusion with lysosomes.

5.3.6 Could oxidation of autophagy receptors be implicated in xenophagy?

Autophagy receptors also have been heavily implicated in xenophagy (Section 1.6). It has been established that in response to an infection one of the first host responses is the production of ROS by NOXs in macrophages and neutrophils (Robinson, 2008). It was shown that *Salmonella* experiences more oxidative stress in the cytosol, compared to the vacuole (van der Heijden and Finlay, 2015). It could be speculated that this cytosolic ROS signal produced by the host cell activates autophagy and promotes autophagy receptors DLC formation. This formation of DLC potentially could more efficiently target bacteria for degradation via autophagy. Recruitment and oxidation of the receptors at the bacterial membrane could promote the formation of a signalling platform, which promotes an inflammatory response and promotes the recruitment of WIPI's and other autophagy machinery components similar to was proposed for mitophagy (Section 1.5, Figure 55). The stable cell lines we created can also be used to test if HeLa Penta KO cells re-expressing non-oxidisable autophagy receptors cope less well with a *Salmonella* infection.

Substrates of oxidation-dependent autophagy can also be identified by subjecting HeLa PentaKO cells expressing wild type or non-oxidisable autophagy receptors to a proteomics analysis. Proteins that accumulate in cells expressing non-oxidisable autophagy receptors could be verified and studied in more detail.

We hypothesise that oxidation of autophagy receptors, a mechanism acquired in vertebrates, could protect longer lived species against an increasing load of oxidative and proteotoxic stress, but also against mitochondrial dysfunction and bacterial infections. Future work will focus on characterising the redox-regulated autophagy receptors in more depth and to investigate the contribution of oxidation of autophagy receptors to cell survival, but also how perturbations of oxidation can cause disease.

6 CONCLUSIONS

In this thesis, molecular mechanisms of autophagy and the effect of autophagy dysfunction on mitochondrial function and neurodegeneration were studied.
Long lifespan of evolutionary higher organisms including humans is associated with the challenge to maintain viability of post mitotic cells, such as neurons, for many years and even decades. Autophagy is increasingly recognized as an important prosurvival pathway in oxidative and proteotoxic stress conditions. With age autophagy function declines, and is also compromised in several neurodegenerative diseases. We identified a novel role for autophagy in the maintenance of mitochondrial health, and specifically its role in the maintenance of respiratory complex I. The current consensus is that autophagy dysfunction results in proteotoxic stress and this causes disease. However, we found that cell death caused by autophagy dysfunction can be rescued by preventing ROS production at complex I or bypassing complex I-linked respiration. This raises the possibility that via a similar mechanism, autophagy decline with age or in patients suffering from autophagy-associated diseases, complex I function becomes compromised, which could contribute to the disease symptoms. This new knowledge opens up new strategies to battle neurodegeneration. I-BET 762 and S1QEL 2.2 can be tested in autophagy deficient mouse models to see if they prevent and/or delay the development of a neurodegenerative phenotype at the organism level as well.

Furthermore, we found that vertebrates have evolved mechanisms to respond and adapt to the increasing load of proteins damaged by oxidation with age. This involves the oxidation of the autophagy receptor p62, which promotes autophagy flux and the clearance of autophagy cargo, resulting in increased stress resistance in mammalian cells and in flies. Oxidation of p62 as a mechanism to promote autophagy in oxidative stress conditions is a completely new concept. In addition, we obtained data revealing an important role for redox regulated cysteines in NDP52 for the degradation of mitochondria via mitophagy and tools were created to study the role of other autophagy receptors in autophagy initiation and selective autophagy. We hypothesise that in addition to oxidation of p62, redox regulation of other autophagy receptors, also promote autophagy in a oligomerisation-dependent manner. Oligomerised autophagy receptors and cargo could function as a platform to recruit autophagy initiation components and thereby promote autophagy. Some recent findings suggest that the fate of cargo is determined by oligomerisation state of autophagy receptors, instead of

for example Ub linkage types (Lu et al., 2017). This raises the possibility that oxidation of receptors promote degradation of cargo via autophagy, whilst non-oxidised receptors favour degradation of cargo via the proteasome.

As autophagy deficiency results in neurodegeneration, we studied the effect of an ALS-related p62 mutant K102E, which affects oxidation of p62 and autophagy induction. Based on this data we put forward the idea that lacking this oxidation mechanism of p62 can result in age-related neurodegenerative disease. The evolutionary evolved oxidation of p62 is a promising therapeutic target to activate autophagy. If we could manipulate the p62 protein to function in its oxidised form without ROS being present, autophagy initiation could be promoted, which could prevent or delay ALS and potentially other age-related neurodegenerative diseases.

7 APPENDICES

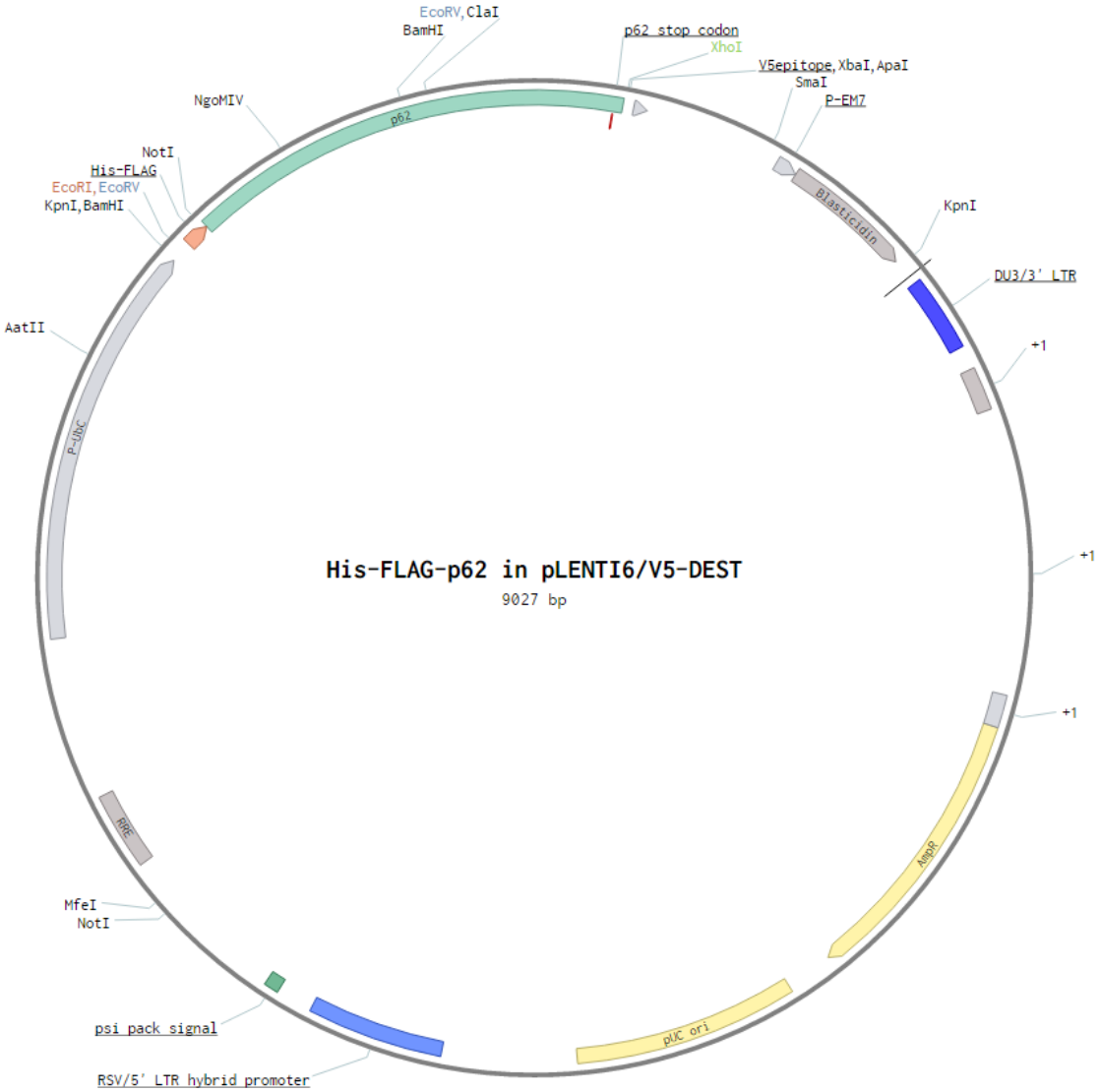

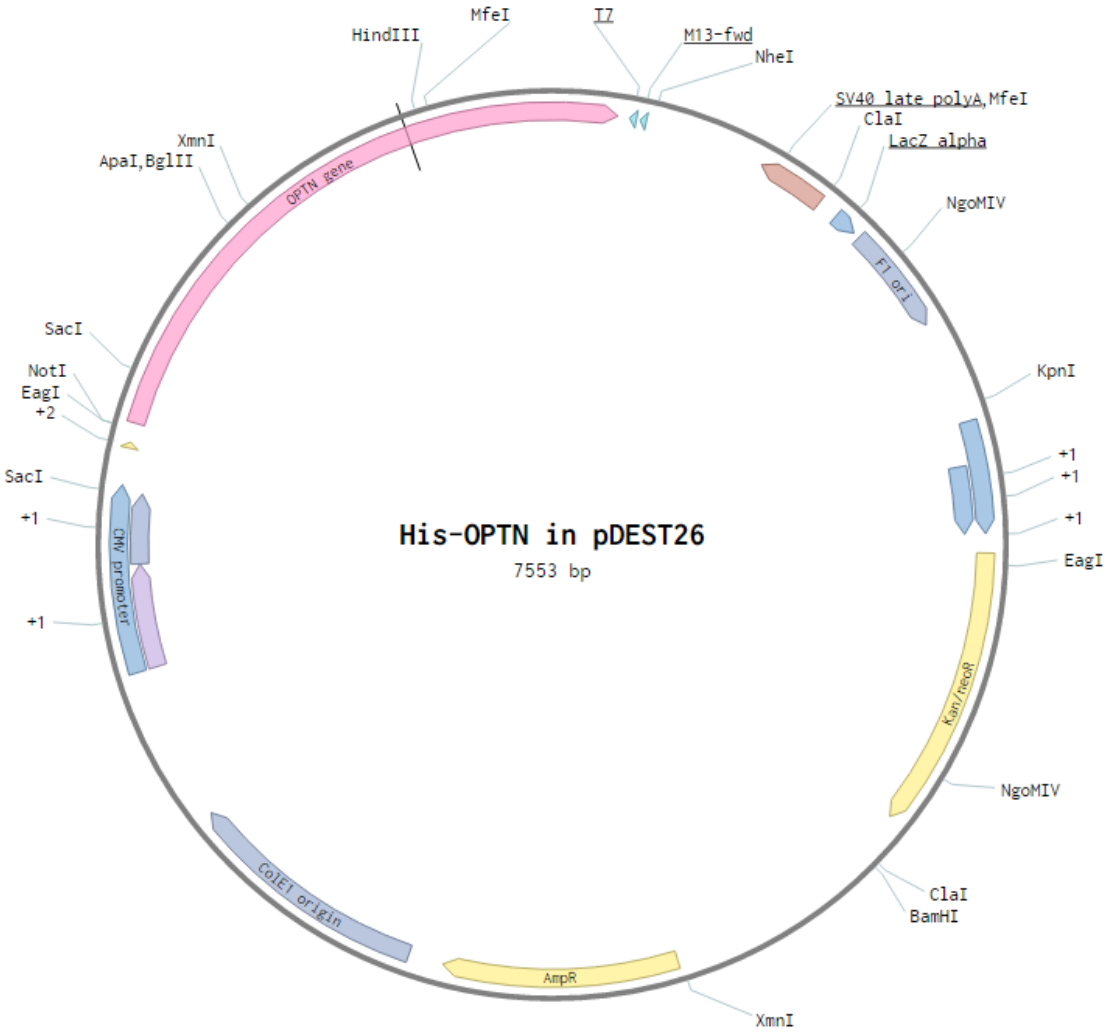
His-OPTN in pDEST26
7553 bp
HindIII
MfeI
T7
M13-fwd
NheI
SV40 late polyA,MfeI
ClaI
LacZ alpha
NgoMIV
F1 ori
KpnI
+1
+1
+1
EagI
NgoMIV
ClaI
BamHI
XmnI
AmpR
ColE1 origin
Kan/neoR
CMV promoter
+1
SacI
+1
NotI
EagI
+2
SacI
OPTN gene
XmnI
ApaI,BglII

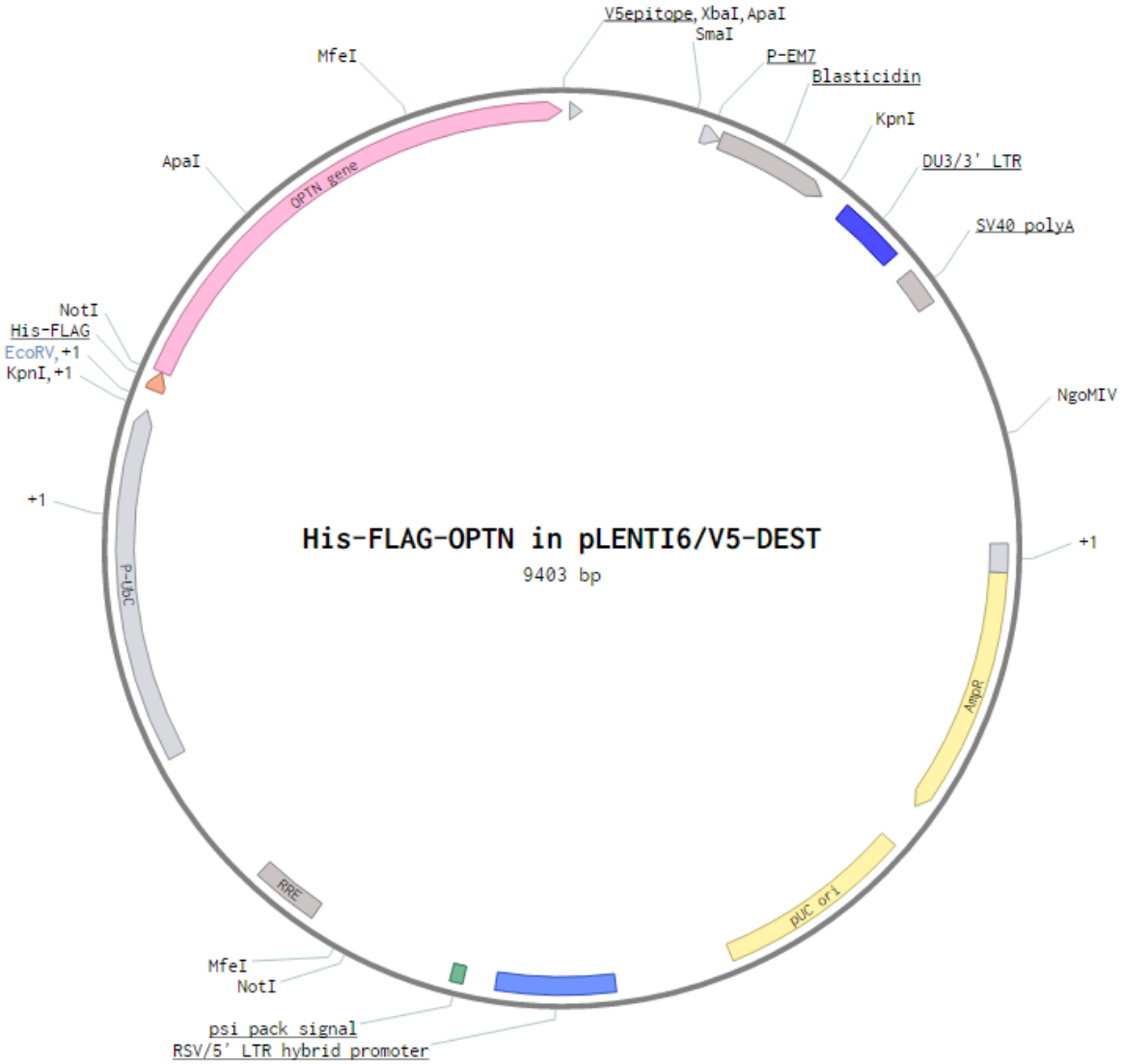
His-FLAG-OPTN in pLENTI6/V5-DEST
9403 bp
V5epitope, XbaI, ApaI
SmaI
MfeI
P-EM7
Blasticidin
KpnI
ApaI
DU3/3' LTR
SV40 polyA
NotI
His-FLAG
EcoRV, +1
KpnI, +1
NgoMIV
+1
+1
OPTN gene
P-Ubc
AmpR
RRE
pUC ori
MfeI
NotI
psi pack signal
RSV/5' LTR hybrid promoter

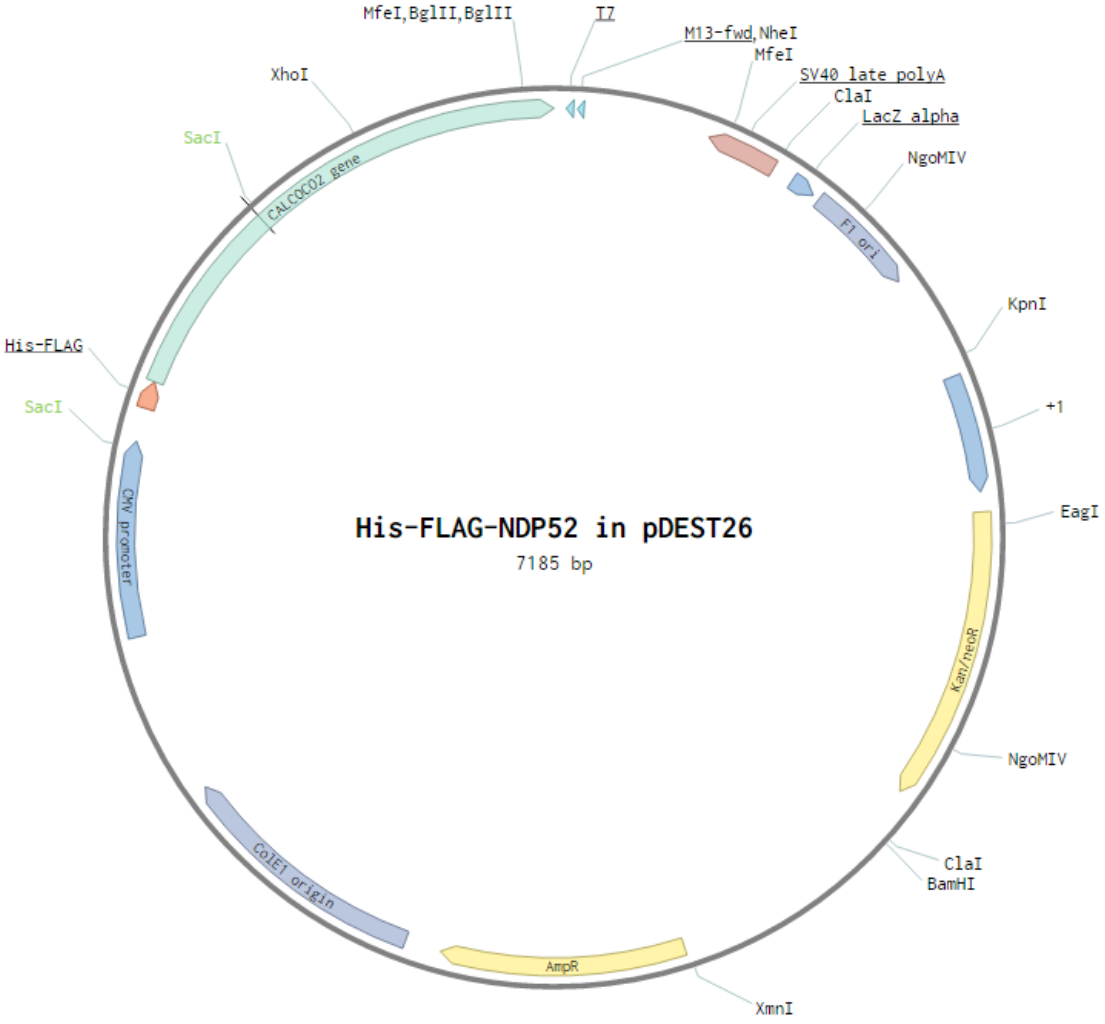
His-FLAG-NDP52 in pDEST26
7185 bp
MfeI,BglII,BglII
T7
M13-fwd,NheI
MfeI
SV40 late polyA
ClaI
LacZ alpha
NgoMIV
F1 ori
KpnI
+1
EagI
Kan/neoR
NgoMIV
ClaI
BamHI
XmnI
AmpR
ColE1 origin
CMV promoter
SacI
His-FLAG
SacI
XhoI
CALCOCO2 gene

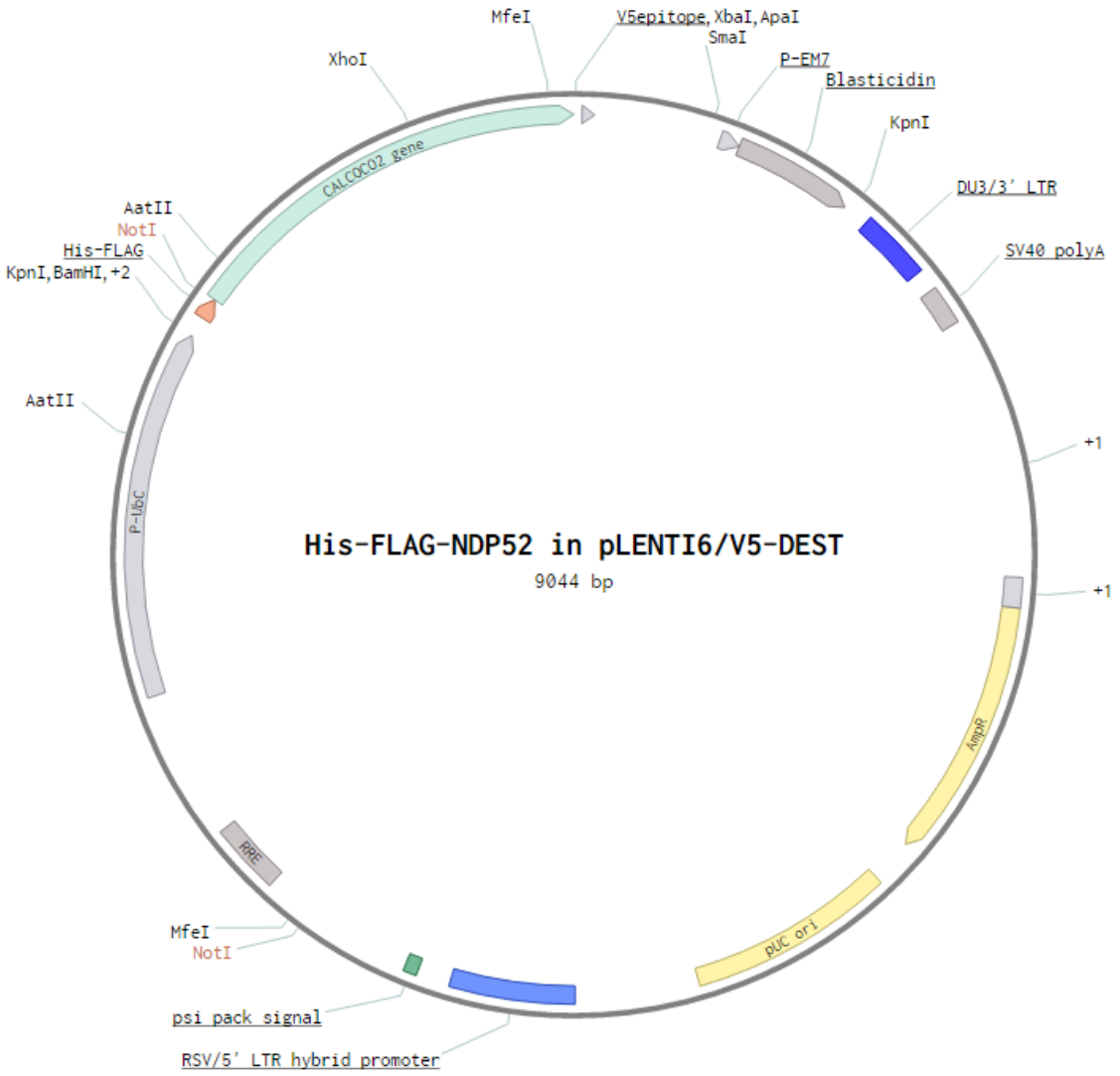
His-FLAG-NDP52 in pLENTI6/V5-DEST
9044 bp
MfeI
V5epitope, XbaI, ApaI
SmaI
XhoI
P-EM7
Blasticidin
KpnI
DU3/3' LTR
SV40 polyA
+1
+1
AmpR
pUC ori
RRE
MfeI
NotI
psi pack signal
RSV/5' LTR hybrid promoter
AatII
P-LbC
AatII
NotI
His-FLAG
KpnI, BamHI, +2
CALCOCO2 gene


BamHI
EcoRV
ClaI
1-122p62
BglII
EagI
p62
SalI,KpnI,ApaI,SmaI,BamHI
XbaI
MfeI
GFP
f1 ori
NheI
+1
GFP-p62 in pEGFP C2
6063 bp
SV40 promoter
+1
ClaI
EagI
CMV enhancer
Amp
ColE1 origin

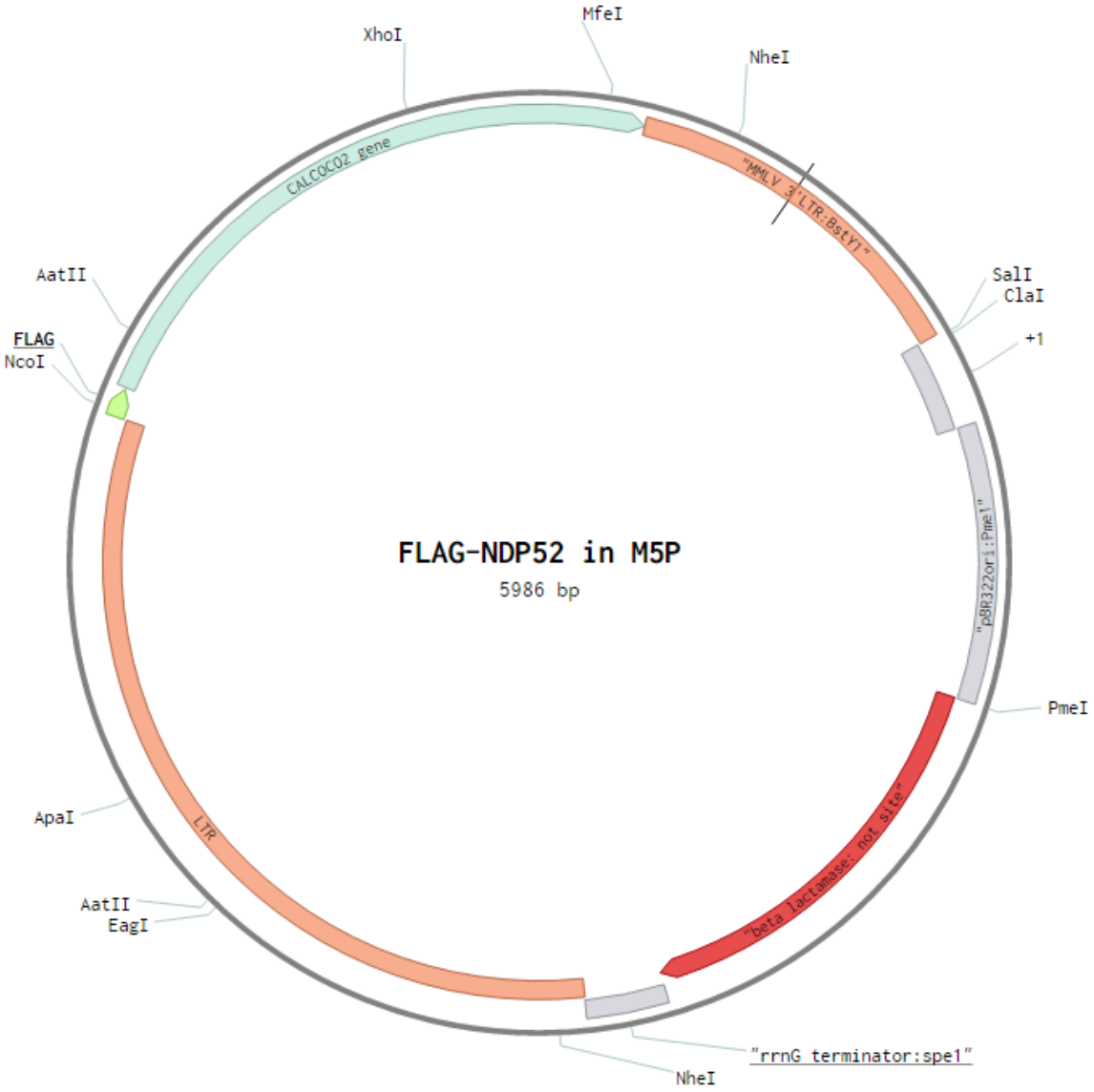

Figure 56 Plasmids used or generated in this study.

Plasmid maps are shown and restriction sites used for control digestions are indicated in different colours.

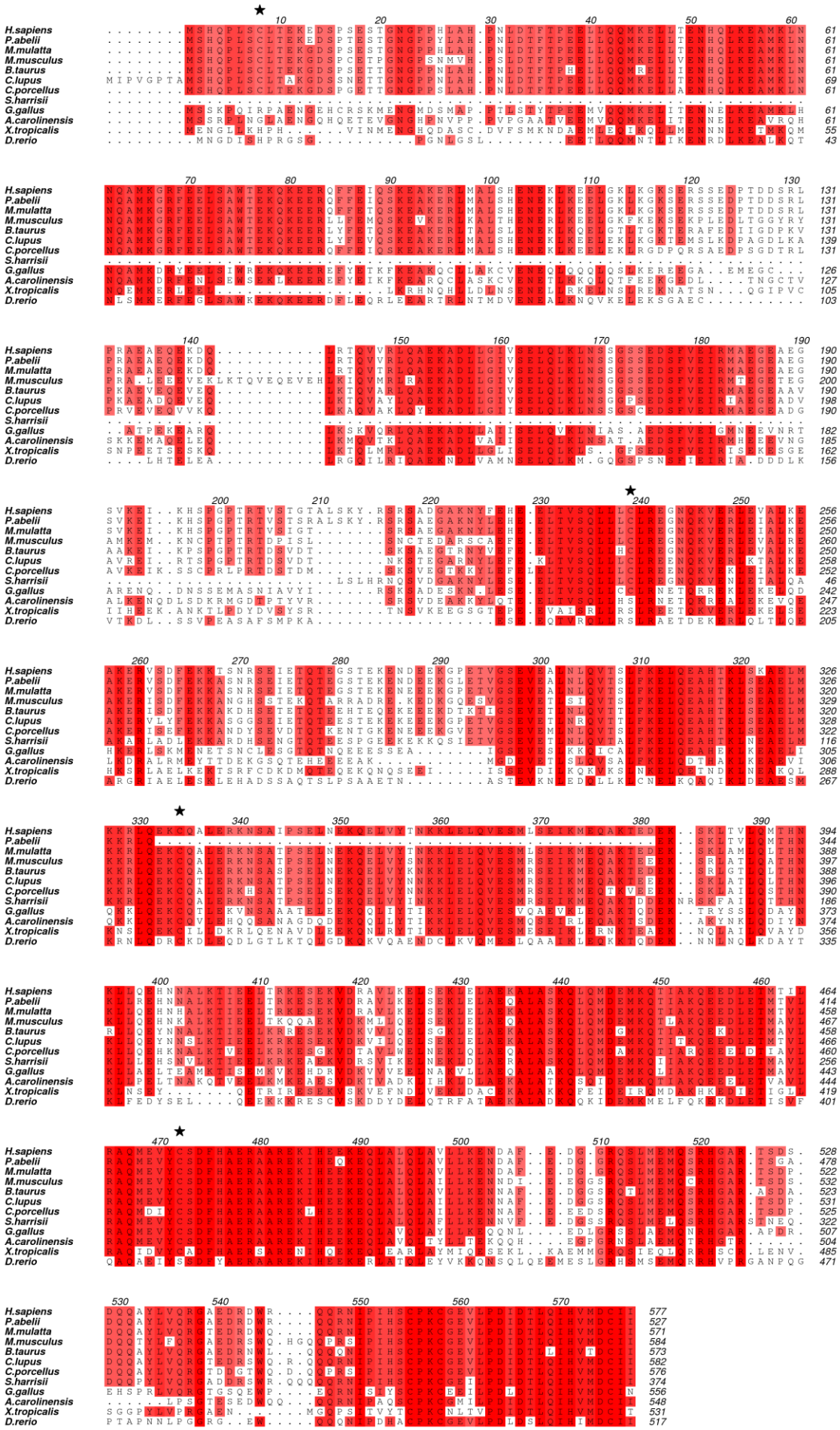
H.sapiens
P.abelii
M.mulatta
M.musculus
B.taurus
C.lupus
C.porcellus
S.harrisii
G.gallus
A.carolinensis
X.tropicalis
D.rerio

Figure 57 Protein sequence alignment of OPTN.

Multiple alignment of OPTN sequences in different species. Cysteines are indicated by a black star and have emerged in vertebrates. Increasing conservation is shown by light-dark red; cysteine residues are indicated by stars. The alignment was performed by Dr. Graham Smith.

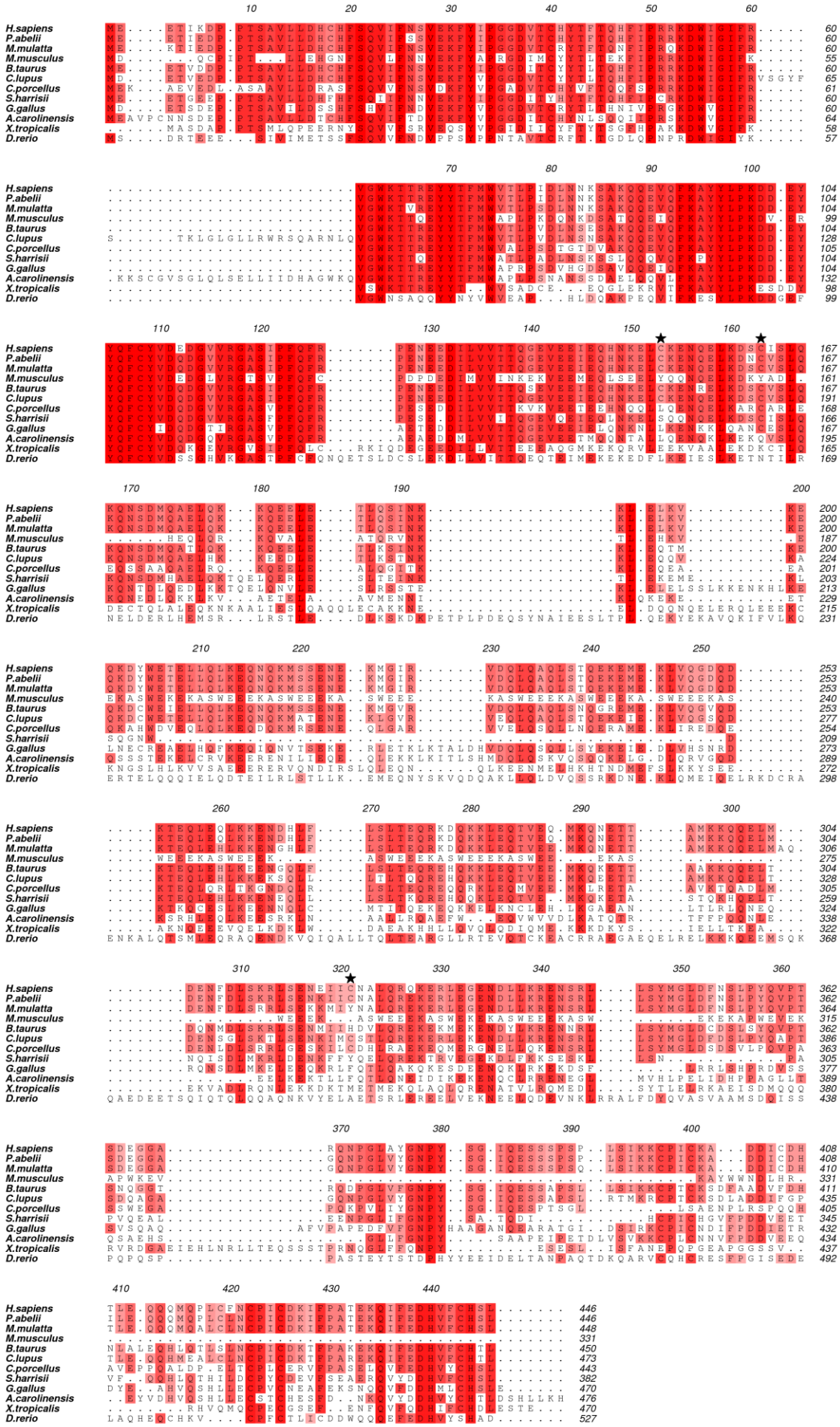
H.sapiens
P.abelii
M.mulatta
M.musculus
B.taurus
C.lupus
C.porcellus
S.harrisii
G.gallus
A.carolinensis
X.tropicalis
D.rerio

Figure 58 Protein sequence alignment of NDP52.

Multiple alignment of NDP52 sequences in different species. Increasing conservation is shown by light-dark red; cysteine residues 153,163 and 321 are indicated by black stars and these are conserved in primates.

8 REFERENCES

ABOU-SLEIMAN, P. M., MUQIT, M. M. & WOOD, N. W. 2006. Expanding insights of mitochondrial dysfunction in Parkinson's disease. *Nat Rev Neurosci,* 7**,** 207-19.

ACIN-PEREZ, R., FERNANDEZ-SILVA, P., PELEATO, M. L., PEREZ-MARTOS, A. & ENRIQUEZ, J. A. 2008. Respiratory active mitochondrial supercomplexes. *Mol Cell,* 32**,** 529-39.

AGATHOCLEOUS, M., LOVE, N. K., RANDLETT, O., HARRIS, J. J., LIU, J., MURRAY, A. J. & HARRIS, W. A. 2012. Metabolic differentiation in the embryonic retina. *Nat Cell Biol,* 14**,** 859-64.

AGOU, F., YE, F., GOFFINONT, S., COURTOIS, G., YAMAOKA, S., ISRAEL, A. & VERON, M. 2002. NEMO trimerizes through its coiled-coil C-terminal domain. *J Biol Chem,* 277**,** 17464-75.

AKUTSU, M., DIKIC, I. & BREMM, A. 2016. Ubiquitin chain diversity at a glance. *J Cell Sci,* 129**,** 875-80.

AL-FUROUKH, N., IANNI, A., NOLTE, H., HOLPER, S., KRUGER, M., WANROOIJ, S. & BRAUN, T. 2015. ClpX stimulates the mitochondrial unfolded protein response (UPRmt) in mammalian cells. *Biochim Biophys Acta,* 1853**,** 2580-91.

ALAM, N. & SCHUELER-FURMAN, O. 2017. Modeling Peptide-Protein Structure and Binding Using Monte Carlo Sampling Approaches: Rosetta FlexPepDock and FlexPepBind. *Methods Mol Biol,* 1561**,** 139-169.

ALEXANDER, A., CAI, S. L., KIM, J., NANEZ, A., SAHIN, M., MACLEAN, K. H., INOKI, K., GUAN, K. L., SHEN, J., PERSON, M. D., KUSEWITT, D., MILLS, G. B., KASTAN, M. B. & WALKER, C. L. 2010. ATM signals to TSC2 in the cytoplasm to regulate mTORC1 in response to ROS. *Proc Natl Acad Sci U S A,* 107**,** 4153-8.

ALLEN, S., HEATH, P. R., KIRBY, J., WHARTON, S. B., COOKSON, M. R., MENZIES, F. M., BANKS, R. E. & SHAW, P. J. 2003. Analysis of the cytosolic proteome in a cell culture model of familial amyotrophic lateral sclerosis reveals alterations to the proteasome, antioxidant defenses, and nitric oxide synthetic pathways. *J Biol Chem,* 278**,** 6371-83.

ANTELMANN, H. & HELMANN, J. D. 2011. Thiol-based redox switches and gene regulation. *Antioxid Redox Signal,* 14**,** 1049-63.

ATORINO, L., SILVESTRI, L., KOPPEN, M., CASSINA, L., BALLABIO, A., MARCONI, R., LANGER, T. & CASARI, G. 2003. Loss of m-AAA protease in mitochondria causes complex I deficiency and increased sensitivity to oxidative stress in hereditary spastic paraplegia. *J Cell Biol,* 163**,** 777-87.

AXE, E. L., WALKER, S. A., MANIFAVA, M., CHANDRA, P., RODERICK, H. L., HABERMANN, A., GRIFFITHS, G. & KTISTAKIS, N. T. 2008. Autophagosome formation from membrane compartments enriched in phosphatidylinositol 3-phosphate and dynamically connected to the endoplasmic reticulum. *J Cell Biol,* 182**,** 685-701.

AZZU, V. & BRAND, M. D. 2010. Degradation of an intramitochondrial protein by the cytosolic proteasome. *J Cell Sci,* 123**,** 578-85.

BAKER, M., MACKENZIE, I. R., PICKERING-BROWN, S. M., GASS, J., RADEMAKERS, R., LINDHOLM, C., SNOWDEN, J., ADAMSON, J., SADOVNICK, A. D., ROLLINSON, S., CANNON, A., DWOSH, E., NEARY, D., MELQUIST, S., RICHARDSON, A., DICKSON, D., BERGER, Z., ERIKSEN, J., ROBINSON, T., ZEHR, C., DICKEY, C. A., CROOK, R., MCGOWAN, E., MANN, D., BOEVE, B., FELDMAN, H. & HUTTON, M. 2006. Mutations in progranulin cause tau-negative frontotemporal dementia linked to chromosome 17. *Nature,* 442**,** 916-9.

BAKER, N. A., SEPT, D., JOSEPH, S., HOLST, M. J. & MCCAMMON, J. A. 2001. Electrostatics of nanosystems: application to microtubules and the ribosome. *Proc Natl Acad Sci U S A,* 98**,** 10037-41.

BANNWARTH, S., AIT-EL-MKADEM, S., CHAUSSENOT, A., GENIN, E. C., LACAS-GERVAIS, S., FRAGAKI, K., BERG-ALONSO, L., KAGEYAMA, Y., SERRE, V., MOORE, D. G., VERSCHUEREN, A., ROUZIER, C., LE BER, I., AUGE, G., COCHAUD, C., LESPINASSE, F., N'GUYEN, K., DE SEPTENVILLE, A., BRICE, A., YU-WAI-MAN, P., SESAKI, H., POUGET, J. & PAQUIS-FLUCKLINGER, V. 2014. A mitochondrial origin for frontotemporal dementia and amyotrophic lateral sclerosis through CHCHD10 involvement. *Brain,* 137**,** 2329-45.

BARROW, J. J., BALSA, E., VERDEGUER, F., TAVARES, C. D., SOUSTEK, M. S., HOLLINGSWORTH, L. R. T., JEDRYCHOWSKI, M., VOGEL, R., PAULO, J. A., SMEITINK, J., GYGI, S. P., DOENCH, J., ROOT, D. E. & PUIGSERVER, P. 2016. Bromodomain Inhibitors Correct Bioenergetic Deficiency Caused by Mitochondrial Disease Complex I Mutations. *Mol Cell,* 64**,** 163-175.

BECK, F., UNVERDORBEN, P., BOHN, S., SCHWEITZER, A., PFEIFER, G., SAKATA, E., NICKELL, S., PLITZKO, J. M., VILLA, E., BAUMEISTER, W. & FORSTER, F. 2012. Near-atomic resolution structural model of the yeast 26S proteasome. *Proc Natl Acad Sci U S A,* 109**,** 14870-5.

BENEDETTI, C., HAYNES, C. M., YANG, Y., HARDING, H. P. & RON, D. 2006. Ubiquitin-like protein 5 positively regulates chaperone gene expression in the mitochondrial unfolded protein response. *Genetics,* 174**,** 229-39.

BENJAMIN, J. L., SUMPTER, R., JR., LEVINE, B. & HOOPER, L. V. 2013. Intestinal epithelial autophagy is essential for host defense against invasive bacteria. *Cell Host Microbe,* 13**,** 723-34.

BENTO, C. F., RENNA, M., GHISLAT, G., PURI, C., ASHKENAZI, A., VICINANZA, M., MENZIES, F. M. & RUBINSZTEIN, D. C. 2016. Mammalian Autophagy: How Does It Work? *Annu Rev Biochem,* 85**,** 685-713.

BERGE, G., SANDO, S. B., RONGVE, A., AARSLAND, D. & WHITE, L. R. 2014. Apolipoprotein E epsilon2 genotype delays onset of dementia with Lewy bodies in a Norwegian cohort. *J Neurol Neurosurg Psychiatry,* 85**,** 1227-31.

BERNALES, S., MCDONALD, K. L. & WALTER, P. 2006. Autophagy counterbalances endoplasmic reticulum expansion during the unfolded protein response. *PLoS Biol,* 4**,** e423.

BINGOL, B., TEA, J. S., PHU, L., REICHELT, M., BAKALARSKI, C. E., SONG, Q., FOREMAN, O., KIRKPATRICK, D. S. & SHENG, M. 2014. The mitochondrial deubiquitinase USP30 opposes parkin-mediated mitophagy. *Nature,* 510**,** 370-5.

BIRMINGHAM, C. L., SMITH, A. C., BAKOWSKI, M. A., YOSHIMORI, T. & BRUMELL, J. H. 2006. Autophagy controls Salmonella infection in response to damage to the Salmonella-containing vacuole. *J Biol Chem,* 281**,** 11374-83.

BJORKOY, G., LAMARK, T., BRECH, A., OUTZEN, H., PERANDER, M., OVERVATN, A., STENMARK, H. & JOHANSEN, T. 2005. p62/SQSTM1 forms protein aggregates degraded by autophagy and has a protective effect on huntingtin-induced cell death. *J Cell Biol,* 171**,** 603-14.

BOLANOS, J. P. & ALMEIDA, A. 2010. The pentose-phosphate pathway in neuronal survival against nitrosative stress. *IUBMB Life,* 62**,** 14-8.

BOND, C. S. & SCHUTTELKOPF, A. W. 2009. ALINE: a WYSIWYG protein-sequence alignment editor for publication-quality alignments. *Acta Crystallogr D Biol Crystallogr,* 65**,** 510-2.

BORGHERO, G., PUGLIATTI, M., MARROSU, F., MARROSU, M. G., MURRU, M. R., FLORIS, G., CANNAS, A., OCCHINERI, P., CAU, T. B., LOI, D., TICCA, A., TRACCIS, S., MANERA, U., CANOSA, A., MOGLIA, C., CALVO, A., BARBERIS, M., BRUNETTI, M., GIBBS, J. R.,

RENTON, A. E., ERRICHIELLO, E., ZOLEDZIEWSKA, M., MULAS, A., QIAN, Y., DIN, J., PLINER, H. A., TRAYNOR, B. J. & CHIO, A. 2016. TBK1 is associated with ALS and ALS-FTD in Sardinian patients. *Neurobiol Aging,* 43**,** 180.e1-5.

BOTA, D. A. & DAVIES, K. J. 2016. Mitochondrial Lon protease in human disease and aging: Including an etiologic classification of Lon-related diseases and disorders. *Free Radic Biol Med,* 100**,** 188-198.

BOTA, D. A., VAN REMMEN, H. & DAVIES, K. J. 2002. Modulation of Lon protease activity and aconitase turnover during aging and oxidative stress. *FEBS Lett,* 532**,** 103-6.

BRADY, O. A., MENG, P., ZHENG, Y., MAO, Y. & HU, F. 2011. Regulation of TDP-43 aggregation by phosphorylation and p62/SQSTM1. *J Neurochem,* 116**,** 248-59.

BRAND, M. D. 2016. Mitochondrial generation of superoxide and hydrogen peroxide as the source of mitochondrial redox signaling. *Free Radic Biol Med,* 100**,** 14-31.

BRAND, M. D., GONCALVES, R. L., ORR, A. L., VARGAS, L., GERENCSER, A. A., BORCH JENSEN, M., WANG, Y. T., MELOV, S., TURK, C. N., MATZEN, J. T., DARDOV, V. J., PETRASSI, H. M., MEEUSEN, S. L., PEREVOSHCHIKOVA, I. V., JASPER, H., BROOKES, P. S. & AINSCOW, E. K. 2016. Suppressors of Superoxide-H2O2 Production at Site IQ of Mitochondrial Complex I Protect against Stem Cell Hyperplasia and Ischemia-Reperfusion Injury. *Cell Metab,* 24**,** 582-592.

BRAS, J., GUERREIRO, R., DARWENT, L., PARKKINEN, L., ANSORGE, O., ESCOTT-PRICE, V., HERNANDEZ, D. G., NALLS, M. A., CLARK, L. N., HONIG, L. S., MARDER, K., VAN DER FLIER, W. M., LEMSTRA, A., SCHELTENS, P., ROGAEVA, E., ST GEORGE-HYSLOP, P., LONDOS, E., ZETTERBERG, H., ORTEGA-CUBERO, S., PASTOR, P., FERMAN, T. J., GRAFF-RADFORD, N. R., ROSS, O. A., BARBER, I., BRAAE, A., BROWN, K., MORGAN, K., MAETZLER, W., BERG, D., TROAKES, C., AL-SARRAJ, S., LASHLEY, T., COMPTA, Y., REVESZ, T., LEES, A., CAIRNS, N., HALLIDAY, G. M., MANN, D., PICKERING-BROWN, S., DICKSON, D. W., SINGLETON, A. & HARDY, J. 2014. Genetic analysis implicates APOE, SNCA and suggests lysosomal dysfunction in the etiology of dementia with Lewy bodies. *Hum Mol Genet,* 23**,** 6139-46.

BRAUN, R. J., SOMMER, C., LEIBIGER, C., GENTIER, R. J., DUMIT, V. I., PADUCH, K., EISENBERG, T., HABERNIG, L., TRAUSINGER, G., MAGNES, C., PIEBER, T., SINNER, F., DENGJEL, J., VAN LEEUWEN, F. W., KROEMER, G. & MADEO, F. 2015. Accumulation of Basic Amino Acids at Mitochondria Dictates the Cytotoxicity of Aberrant Ubiquitin. *Cell Rep*.

CAI, W., ZHANG, B., DUAN, D., WU, J. & FANG, J. 2012. Curcumin targeting the thioredoxin system elevates oxidative stress in HeLa cells. *Toxicol Appl Pharmacol,* 262**,** 341-8.

CANTLEY, L. C. 2002. The phosphoinositide 3-kinase pathway. *Science,* 296**,** 1655-7.

CAO, J., SCHULTE, J., KNIGHT, A., LESLIE, N. R., ZAGOZDZON, A., BRONSON, R., MANEVICH, Y., BEESON, C. & NEUMANN, C. A. 2009. Prdx1 inhibits tumorigenesis via regulating PTEN/AKT activity. *Embo j,* 28**,** 1505-17.

CARROLL, B., MAETZEL, D., MADDOCKS, O. D., OTTEN, G., RATCLIFF, M., SMITH, G. R., DUNLOP, E. A., PASSOS, J. F., DAVIES, O. R., JAENISCH, R., TEE, A. R., SARKAR, S. & KOROLCHUK, V. I. 2016. Control of TSC2-Rheb signaling axis by arginine regulates mTORC1 activity. *Elife,* 5.

CASTREJON-JIMENEZ, N. S., LEYVA-PAREDES, K., HERNANDEZ-GONZALEZ, J. C., LUNA-HERRERA, J. & GARCIA-PEREZ, B. E. 2015. The role of autophagy in bacterial infections. *Biosci Trends,* 9**,** 149-59.

CEREGIDO, M. A., SPINOLA AMILIBIA, M., BUTS, L., RIVERA-TORRES, J., GARCIA-PINO, A., BRAVO, J. & VAN NULAND, N. A. 2014. The structure of TAX1BP1 UBZ1+2 provides insight into target specificity and adaptability. *J Mol Biol,* 426**,** 674-90.

CHA-MOLSTAD, H., SUNG, K. S., HWANG, J., KIM, K. A., YU, J. E., YOO, Y. D., JANG, J. M., HAN, D. H., MOLSTAD, M., KIM, J. G., LEE, Y. J., ZAKRZEWSKA, A., KIM, S. H., KIM, S. T., KIM, S. Y., LEE, H. G., SOUNG, N. K., AHN, J. S., CIECHANOVER, A., KIM, B. Y. & KWON, Y. T. 2015. Amino-terminal arginylation targets endoplasmic reticulum chaperone BiP for autophagy through p62 binding. *Nat Cell Biol,* 17**,** 917-29.

CHA-MOLSTAD, H., YU, J. E., LEE, S. H., KIM, J. G., SUNG, K. S., HWANG, J., YOO, Y. D., LEE, Y. J., KIM, S. T., LEE, D. H., CIECHANOVER, A., KIM, B. Y. & KWON, Y. T. 2016. Modulation of SQSTM1/p62 activity by N-terminal arginylation of the endoplasmic reticulum chaperone HSPA5/GRP78/BiP. *Autophagy,* 12**,** 426-8.

CHALASANI, M. L., KUMARI, A., RADHA, V. & SWARUP, G. 2014. E50K-OPTN-induced retinal cell death involves the Rab GTPase-activating protein, TBC1D17 mediated block in autophagy. *PLoS One,* 9**,** e95758.

CHAN, N. C., SALAZAR, A. M., PHAM, A. H., SWEREDOSKI, M. J., KOLAWA, N. J., GRAHAM, R. L., HESS, S. & CHAN, D. C. 2011. Broad activation of the ubiquitin-proteasome system by Parkin is critical for mitophagy. *Hum Mol Genet,* 20**,** 1726-37.

CHANTRANUPONG, L., SCARIA, S. M., SAXTON, R. A., GYGI, M. P., SHEN, K., WYANT, G. A., WANG, T., HARPER, J. W., GYGI, S. P. & SABATINI, D. M. 2016. The CASTOR Proteins Are Arginine Sensors for the mTORC1 Pathway. *Cell,* 165**,** 153-64.

CHAUHAN, S., MANDELL, M. A. & DERETIC, V. 2015. IRGM governs the core autophagy machinery to conduct antimicrobial defense. *Mol Cell,* 58**,** 507-21.

CHAUHAN, S., MANDELL, M. A. & DERETIC, V. 2016. Mechanism of action of the tuberculosis and Crohn disease risk factor IRGM in autophagy. *Autophagy,* 12**,** 429-31.

CHEN, L., BREWER, M. D., GUO, L., WANG, R., JIANG, P. & YANG, X. 2017. Enhanced Degradation of Misfolded Proteins Promotes Tumorigenesis. *Cell Rep,* 18**,** 3143-3154.

CHEN, Y., MCMILLAN-WARD, E., KONG, J., ISRAELS, S. J. & GIBSON, S. B. 2008. Oxidative stress induces autophagic cell death independent of apoptosis in transformed and cancer cells. *Cell Death Differ,* 15**,** 171-82.

CHORLEY, B. N., CAMPBELL, M. R., WANG, X., KARACA, M., SAMBANDAN, D., BANGURA, F., XUE, P., PI, J., KLEEBERGER, S. R. & BELL, D. A. 2012. Identification of novel NRF2-regulated genes by ChIP-Seq: influence on retinoid X receptor alpha. *Nucleic Acids Res,* 40**,** 7416-29.

CIRULLI, E. T., LASSEIGNE, B. N., PETROVSKI, S., SAPP, P. C., DION, P. A., LEBLOND, C. S., COUTHOUIS, J., LU, Y. F., WANG, Q., KRUEGER, B. J., REN, Z., KEEBLER, J., HAN, Y., LEVY, S. E., BOONE, B. E., WIMBISH, J. R., WAITE, L. L., JONES, A. L., CARULLI, J. P., DAY-WILLIAMS, A. G., STAROPOLI, J. F., XIN, W. W., CHESI, A., RAPHAEL, A. R., MCKENNA-YASEK, D., CADY, J., VIANNEY DE JONG, J. M., KENNA, K. P., SMITH, B. N., TOPP, S., MILLER, J., GKAZI, A., AL-CHALABI, A., VAN DEN BERG, L. H., VELDINK, J., SILANI, V., TICOZZI, N., SHAW, C. E., BALOH, R. H., APPEL, S., SIMPSON, E., LAGIER-TOURENNE, C., PULST, S. M., GIBSON, S., TROJANOWSKI, J. Q., ELMAN, L., MCCLUSKEY, L., GROSSMAN, M., SHNEIDER, N. A., CHUNG, W. K., RAVITS, J. M., GLASS, J. D., SIMS, K. B., VAN DEERLIN, V. M., MANIATIS, T., HAYES, S. D., ORDUREAU, A., SWARUP, S., LANDERS, J., BAAS, F., ALLEN, A. S., BEDLACK, R. S., HARPER, J. W., GITLER, A. D., ROULEAU, G. A., BROWN, R., HARMS, M. B., COOPER, G. M., HARRIS, T., MYERS, R. M. & GOLDSTEIN, D. B. 2015. Exome sequencing in amyotrophic lateral sclerosis identifies risk genes and pathways. *Science,* 347**,** 1436-41.

CIUFFA, R., LAMARK, T., TARAFDER, A. K., GUESDON, A., RYBINA, S., HAGEN, W. J., JOHANSEN, T. & SACHSE, C. 2015. The Selective Autophagy Receptor p62 Forms a Flexible Filamentous Helical Scaffold. *Cell Rep*.

CLAGUE, M. J., HERIDE, C. & URBE, S. 2015. The demographics of the ubiquitin system. *Trends Cell Biol,* 25**,** 417-26.

CLAUSEN, T. H., LAMARK, T., ISAKSON, P., FINLEY, K., LARSEN, K. B., BRECH, A., OVERVATN, A., STENMARK, H., BJORKOY, G., SIMONSEN, A. & JOHANSEN, T. 2010. p62/SQSTM1 and ALFY interact to facilitate the formation of p62 bodies/ALIS and their degradation by autophagy. *Autophagy,* 6**,** 330-44.

COHEN, M. M., LEBOUCHER, G. P., LIVNAT-LEVANON, N., GLICKMAN, M. H. & WEISSMAN, A. M. 2008. Ubiquitin-proteasome-dependent degradation of a mitofusin, a critical regulator of mitochondrial fusion. *Mol Biol Cell,* 19**,** 2457-64.

CORNELISSEN, T., HADDAD, D., WAUTERS, F., VAN HUMBEECK, C., MANDEMAKERS, W., KOENTJORO, B., SUE, C., GEVAERT, K., DE STROOPER, B., VERSTREKEN, P. & VANDENBERGHE, W. 2014. The deubiquitinase USP15 antagonizes Parkin-mediated mitochondrial ubiquitination and mitophagy. *Hum Mol Genet,* 23**,** 5227-42.

COUCH, G. S., HENDRIX, D. K. & FERRIN, T. E. 2006. Nucleic acid visualization with UCSF Chimera. *Nucleic Acids Res,* 34**,** e29.

CRUTS, M., KUMAR-SINGH, S. & VAN BROECKHOVEN, C. 2006. Progranulin mutations in ubiquitin-positive frontotemporal dementia linked to chromosome 17q21. *Curr Alzheimer Res,* 3**,** 485-91.

CUERVO, A. M., BERGAMINI, E., BRUNK, U. T., DROGE, W., FFRENCH, M. & TERMAN, A. 2005. Autophagy and aging: the importance of maintaining "clean" cells. *Autophagy,* 1**,** 131-40.

CUERVO, A. M., STEFANIS, L., FREDENBURG, R., LANSBURY, P. T. & SULZER, D. 2004. Impaired degradation of mutant alpha-synuclein by chaperone-mediated autophagy. *Science,* 305**,** 1292-5.

CUNNINGHAM, C. N., BAUGHMAN, J. M., PHU, L., TEA, J. S., YU, C., COONS, M., KIRKPATRICK, D. S., BINGOL, B. & CORN, J. E. 2015. USP30 and parkin homeostatically regulate atypical ubiquitin chains on mitochondria. *Nat Cell Biol,* 17**,** 160-9.

CUYVERS, E. & SLEEGERS, K. 2016. Genetic variations underlying Alzheimer's disease: evidence from genome-wide association studies and beyond. *Lancet Neurol,* 15**,** 857-68.

D'AMICO, E., FACTOR-LITVAK, P., SANTELLA, R. M. & MITSUMOTO, H. 2013. Clinical perspective on oxidative stress in sporadic amyotrophic lateral sclerosis. *Free Radic Biol Med,* 65**,** 509-27.

DAROSZEWSKA, A., VAN 'T HOF, R. J., ROJAS, J. A., LAYFIELD, R., LANDAO-BASONGA, E., ROSE, L., ROSE, K. & RALSTON, S. H. 2011. A point mutation in the ubiquitin-associated domain of SQSMT1 is sufficient to cause a Paget's disease-like disorder in mice. *Hum Mol Genet,* 20**,** 2734-44.

DAVID, D. C., HAUPTMANN, S., SCHERPING, I., SCHUESSEL, K., KEIL, U., RIZZU, P., RAVID, R., DROSE, S., BRANDT, U., MULLER, W. E., ECKERT, A. & GOTZ, J. 2005. Proteomic and functional analyses reveal a mitochondrial dysfunction in P301L tau transgenic mice. *J Biol Chem,* 280**,** 23802-14.

DE CASTRO, I. P., COSTA, A. C., CELARDO, I., TUFI, R., DINSDALE, D., LOH, S. H. & MARTINS, L. M. 2013. Drosophila ref(2)P is required for the parkin-mediated suppression of mitochondrial dysfunction in pink1 mutants. *Cell Death Dis,* 4**,** e873.

DE CASTRO, I. P., MARTINS, L. M. & TUFI, R. 2010. Mitochondrial quality control and neurological disease: an emerging connection. *Expert Rev Mol Med,* 12**,** e12.

DE MARCO, N., BUONO, M., TROISE, F. & DIEZ-ROUX, G. 2006. Optineurin increases cell survival and translocates to the nucleus in a Rab8-dependent manner upon an apoptotic stimulus. *J Biol Chem,* 281**,** 16147-56.

DEJESUS-HERNANDEZ, M., MACKENZIE, I. R., BOEVE, B. F., BOXER, A. L., BAKER, M., RUTHERFORD, N. J., NICHOLSON, A. M., FINCH, N. A., FLYNN, H., ADAMSON, J., KOURI, N., WOJTAS, A., SENGDY, P., HSIUNG, G. Y., KARYDAS, A., SEELEY, W. W., JOSEPHS, K. A., COPPOLA, G., GESCHWIND, D. H., WSZOLEK, Z. K., FELDMAN, H., KNOPMAN, D. S., PETERSEN, R. C., MILLER, B. L., DICKSON, D. W., BOYLAN, K. B., GRAFF-RADFORD, N. R. & RADEMAKERS, R. 2011. Expanded GGGGCC hexanucleotide repeat in noncoding region of C9ORF72 causes chromosome 9p-linked FTD and ALS. *Neuron,* 72**,** 245-56.

DENG, H. X., CHEN, W., HONG, S. T., BOYCOTT, K. M., GORRIE, G. H., SIDDIQUE, N., YANG, Y., FECTO, F., SHI, Y., ZHAI, H., JIANG, H., HIRANO, M., RAMPERSAUD, E., JANSEN, G. H., DONKERVOORT, S., BIGIO, E. H., BROOKS, B. R., AJROUD, K., SUFIT, R. L., HAINES, J. L., MUGNAINI, E., PERICAK-VANCE, M. A. & SIDDIQUE, T. 2011. Mutations in UBQLN2 cause dominant X-linked juvenile and adult-onset ALS and ALS/dementia. *Nature,* 477**,** 211-5.

DENG, H. X., ZHAI, H., BIGIO, E. H., YAN, J., FECTO, F., AJROUD, K., MISHRA, M., AJROUD-DRISS, S., HELLER, S., SUFIT, R., SIDDIQUE, N., MUGNAINI, E. & SIDDIQUE, T. 2010. FUS-immunoreactive inclusions are a common feature in sporadic and non-SOD1 familial amyotrophic lateral sclerosis. *Ann Neurol,* 67**,** 739-48.

DEPONTE, M. 2013. Glutathione catalysis and the reaction mechanisms of glutathione-dependent enzymes. *Biochim Biophys Acta,* 1830**,** 3217-66.

DERETIC, V. 2010. A master conductor for aggregate clearance by autophagy. *Dev Cell,* 18**,** 694-6.

DEVI, L., RAGHAVENDRAN, V., PRABHU, B. M., AVADHANI, N. G. & ANANDATHEERTHAVARADA, H. K. 2008. Mitochondrial import and accumulation of alpha-synuclein impair complex I in human dopaminergic neuronal cultures and Parkinson disease brain. *J Biol Chem,* 283**,** 9089-100.

DI BARTOLOMEO, S., CORAZZARI, M., NAZIO, F., OLIVERIO, S., LISI, G., ANTONIOLI, M., PAGLIARINI, V., MATTEONI, S., FUOCO, C., GIUNTA, L., D'AMELIO, M., NARDACCI, R., ROMAGNOLI, A., PIACENTINI, M., CECCONI, F. & FIMIA, G. M. 2010. The dynamic interaction of AMBRA1 with the dynein motor complex regulates mammalian autophagy. *J Cell Biol,* 191**,** 155-68.

DIAPER, D. C., ADACHI, Y., LAZAROU, L., GREENSTEIN, M., SIMOES, F. A., DI DOMENICO, A., SOLOMON, D. A., LOWE, S., ALSUBAIE, R., CHENG, D., BUCKLEY, S., HUMPHREY, D. M., SHAW, C. E. & HIRTH, F. 2013. Drosophila TDP-43 dysfunction in glia and muscle cells cause cytological and behavioural phenotypes that characterize ALS and FTLD. *Hum Mol Genet,* 22**,** 3883-93.

DIKIC, I. & DOTSCH, V. 2009. Ubiquitin linkages make a difference. *Nat Struct Mol Biol,* 16**,** 1209-10.

DILLIN, A., HSU, A. L., ARANTES-OLIVEIRA, N., LEHRER-GRAIWER, J., HSIN, H., FRASER, A. G., KAMATH, R. S., AHRINGER, J. & KENYON, C. 2002. Rates of behavior and aging specified by mitochondrial function during development. *Science,* 298**,** 2398-401.

DOI, H., ADACHI, H., KATSUNO, M., MINAMIYAMA, M., MATSUMOTO, S., KONDO, N., MIYAZAKI, Y., IIDA, M., TOHNAI, G., QIANG, Q., TANAKA, F., YANAGAWA, T., WARABI, E., ISHII, T. & SOBUE, G. 2013. p62/SQSTM1 differentially removes the toxic mutant androgen receptor via autophagy and inclusion formation in a spinal and bulbar muscular atrophy mouse model. *J Neurosci,* 33**,** 7710-27.

DOOLEY, H. C., RAZI, M., POLSON, H. E., GIRARDIN, S. E., WILSON, M. I. & TOOZE, S. A. 2014. WIPI2 links LC3 conjugation with PI3P, autophagosome formation, and pathogen clearance by recruiting Atg12-5-16L1. *Mol Cell,* 55**,** 238-52.

DURAN, A., AMANCHY, R., LINARES, J. F., JOSHI, J., ABU-BAKER, S., POROLLO, A., HANSEN, M., MOSCAT, J. & DIAZ-MECO, M. T. 2011. p62 is a key regulator of nutrient sensing in the mTORC1 pathway. *Mol Cell,* 44**,** 134-46.

DURIEUX, J., WOLFF, S. & DILLIN, A. 2011. The cell-non-autonomous nature of electron transport chain-mediated longevity. *Cell,* 144**,** 79-91.

EISELE, Y. S., MONTEIRO, C., FEARNS, C., ENCALADA, S. E., WISEMAN, R. L., POWERS, E. T. & KELLY, J. W. 2015. Targeting protein aggregation for the treatment of degenerative diseases. *Nat Rev Drug Discov,* 14**,** 759-80.

ELLINGHAUS, D., ZHANG, H., ZEISSIG, S., LIPINSKI, S., TILL, A., JIANG, T., STADE, B., BROMBERG, Y., ELLINGHAUS, E., KELLER, A., RIVAS, M. A., SKIECEVICIENE, J., DONCHEVA, N. T., LIU, X., LIU, Q., JIANG, F., FORSTER, M., MAYR, G., ALBRECHT, M., HASLER, R., BOEHM, B. O., GOODALL, J., BERZUINI, C. R., LEE, J., ANDERSEN, V., VOGEL, U., KUPCINSKAS, L., KAYSER, M., KRAWCZAK, M., NIKOLAUS, S., WEERSMA, R. K., PONSIOEN, C. Y., SANS, M., WIJMENGA, C., STRACHAN, D. P., MCARDLE, W. L., VERMEIRE, S., RUTGEERTS, P., SANDERSON, J. D., MATHEW, C. G., VATN, M. H., WANG, J., NOTHEN, M. M., DUERR, R. H., BUNING, C., BRAND, S., GLAS, J., WINKELMANN, J., ILLIG, T., LATIANO, A., ANNESE, V., HALFVARSON, J., D'AMATO, M., DALY, M. J., NOTHNAGEL, M., KARLSEN, T. H., SUBRAMANI, S., ROSENSTIEL, P., SCHREIBER, S., PARKES, M. & FRANKE, A. 2013. Association between variants of PRDM1 and NDP52 and Crohn's disease, based on exome sequencing and functional studies. *Gastroenterology,* 145**,** 339-47.

FASS, E., SHVETS, E., DEGANI, I., HIRSCHBERG, K. & ELAZAR, Z. 2006. Microtubules support production of starvation-induced autophagosomes but not their targeting and fusion with lysosomes. *J Biol Chem,* 281**,** 36303-16.

FECTO, F., YAN, J., VEMULA, S. P., LIU, E., YANG, Y., CHEN, W., ZHENG, J. G., SHI, Y., SIDDIQUE, N., ARRAT, H., DONKERVOORT, S., AJROUD-DRISS, S., SUFIT, R. L., HELLER, S. L., DENG, H. X. & SIDDIQUE, T. 2011. SQSTM1 mutations in familial and sporadic amyotrophic lateral sclerosis. *Arch Neurol,* 68**,** 1440-6.

FERNANDEZ-CAGGIANO, M., SCHRODER, E., CHO, H. J., BURGOYNE, J., BARALLOBRE-BARREIRO, J., MAYR, M. & EATON, P. 2016. Oxidant-induced Interprotein Disulfide Formation in Cardiac Protein DJ-1 Occurs via an Interaction with Peroxiredoxin 2. *J Biol Chem,* 291**,** 10399-410.

FILIMONENKO, M., STUFFERS, S., RAIBORG, C., YAMAMOTO, A., MALEROD, L., FISHER, E. M., ISAACS, A., BRECH, A., STENMARK, H. & SIMONSEN, A. 2007. Functional multivesicular bodies are required for autophagic clearance of protein aggregates associated with neurodegenerative disease. *J Cell Biol,* 179**,** 485-500.

FINGERT, J. H. 2011. Primary open-angle glaucoma genes. *Eye (Lond),* 25**,** 587-95.

FINLEY, D. 2009. Recognition and processing of ubiquitin-protein conjugates by the proteasome. *Annu Rev Biochem,* 78**,** 477-513.

FIORESE, C. J., SCHULZ, A. M., LIN, Y. F., ROSIN, N., PELLEGRINO, M. W. & HAYNES, C. M. 2016. The Transcription Factor ATF5 Mediates a Mammalian Mitochondrial UPR. *Curr Biol,* 26**,** 2037-43.

FRAKE, R. A., RICKETTS, T., MENZIES, F. M. & RUBINSZTEIN, D. C. 2015. Autophagy and neurodegeneration. *J Clin Invest,* 125**,** 65-74.

FRANCIS, B. M., YANG, J., SONG, B. J., GUPTA, S., MAJ, M., BAZINET, R. P., ROBINSON, B. & MOUNT, H. T. 2014. Reduced levels of mitochondrial complex I subunit NDUFB8 and linked complex I + III oxidoreductase activity in the TgCRND8 mouse model of Alzheimer's disease. *J Alzheimers Dis,* 39**,** 347-55.

FREISCHMIDT, A., WIELAND, T., RICHTER, B., RUF, W., SCHAEFFER, V., MULLER, K., MARROQUIN, N., NORDIN, F., HUBERS, A., WEYDT, P., PINTO, S., PRESS, R.,

MILLECAMPS, S., MOLKO, N., BERNARD, E., DESNUELLE, C., SORIANI, M. H., DORST, J., GRAF, E., NORDSTROM, U., FEILER, M. S., PUTZ, S., BOECKERS, T. M., MEYER, T., WINKLER, A. S., WINKELMAN, J., DE CARVALHO, M., THAL, D. R., OTTO, M., BRANNSTROM, T., VOLK, A. E., KURSULA, P., DANZER, K. M., LICHTNER, P., DIKIC, I., MEITINGER, T., LUDOLPH, A. C., STROM, T. M., ANDERSEN, P. M. & WEISHAUPT, J. H. 2015. Haploinsufficiency of TBK1 causes familial ALS and fronto-temporal dementia. *Nat Neurosci,* 18**,** 631-6.

FUJIWARA, Y., TAKESHITA, K., NAKAGAWA, A. & OKAMURA, Y. 2013. Structural characteristics of the redox-sensing coiled coil in the voltage-gated H+ channel. *J Biol Chem,* 288**,** 17968-75.

GAL, J., STROM, A. L., KILTY, R., ZHANG, F. & ZHU, H. 2007. p62 accumulates and enhances aggregate formation in model systems of familial amyotrophic lateral sclerosis. *J Biol Chem,* 282**,** 11068-77.

GAL, J., STROM, A. L., KWINTER, D. M., KILTY, R., ZHANG, J., SHI, P., FU, W., WOOTEN, M. W. & ZHU, H. 2009. Sequestosome 1/p62 links familial ALS mutant SOD1 to LC3 via an ubiquitin-independent mechanism. *J Neurochem,* 111**,** 1062-73.

GANLEY, I. G., LAM DU, H., WANG, J., DING, X., CHEN, S. & JIANG, X. 2009. ULK1.ATG13.FIP200 complex mediates mTOR signaling and is essential for autophagy. *J Biol Chem,* 284**,** 12297-305.

GAO, J., OHTSUBO, M., HOTTA, Y. & MINOSHIMA, S. 2014. Oligomerization of optineurin and its oxidative stress- or E50K mutation-driven covalent cross-linking: possible relationship with glaucoma pathology. *PLoS One,* 9**,** e101206.

GARCIA-ESCUDERO, V., MARTIN-MAESTRO, P., PERRY, G. & AVILA, J. 2013. Deconstructing mitochondrial dysfunction in Alzheimer disease. *Oxid Med Cell Longev,* 2013**,** 162152.

GE, L. & SCHEKMAN, R. 2014. The ER-Golgi intermediate compartment feeds the phagophore membrane. *Autophagy,* 10**,** 170-2.

GEIGER, J. T., DING, J., CRAIN, B., PLETNIKOVA, O., LETSON, C., DAWSON, T. M., ROSENTHAL, L. S., PANTELYAT, A., GIBBS, J. R., ALBERT, M. S., HERNANDEZ, D. G., HILLIS, A. E., STONE, D. J., SINGLETON, A. B., HARDY, J. A., TRONCOSO, J. C. & SCHOLZ, S. W. 2016. Next-generation sequencing reveals substantial genetic contribution to dementia with Lewy bodies. *Neurobiol Dis,* 94**,** 55-62.

GEISLER, S., HOLMSTROM, K. M., SKUJAT, D., FIESEL, F. C., ROTHFUSS, O. C., KAHLE, P. J. & SPRINGER, W. 2010. PINK1/Parkin-mediated mitophagy is dependent on VDAC1 and p62/SQSTM1. *Nat Cell Biol,* 12**,** 119-31.

GENIN, E. C., PLUTINO, M., BANNWARTH, S., VILLA, E., CISNEROS-BARROSO, E., ROY, M., ORTEGA-VILA, B., FRAGAKI, K., LESPINASSE, F., PINERO-MARTOS, E., AUGE, G., MOORE, D., BURTE, F., LACAS-GERVAIS, S., KAGEYAMA, Y., ITOH, K., YU-WAI-MAN, P., SESAKI, H., RICCI, J. E., VIVES-BAUZA, C. & PAQUIS-FLUCKLINGER, V. 2016. CHCHD10 mutations promote loss of mitochondrial cristae junctions with impaired mitochondrial genome maintenance and inhibition of apoptosis. *EMBO Mol Med,* 8**,** 58-72.

GERSCH, M., STAHL, M., POREBA, M., DAHMEN, M., DZIEDZIC, A., DRAG, M. & SIEBER, S. A. 2016. Barrel-shaped ClpP Proteases Display Attenuated Cleavage Specificities. *ACS Chem Biol,* 11**,** 389-99.

GIJSELINCK, I., VAN LANGENHOVE, T., VAN DER ZEE, J., SLEEGERS, K., PHILTJENS, S., KLEINBERGER, G., JANSSENS, J., BETTENS, K., VAN CAUWENBERGHE, C., PERESON, S., ENGELBORGHS, S., SIEBEN, A., DE JONGHE, P., VANDENBERGHE, R., SANTENS, P., DE BLEECKER, J., MAES, G., BAUMER, V., DILLEN, L., JORIS, G., CUIJT, I., CORSMIT, E., ELINCK, E., VAN DONGEN, J., VERMEULEN, S., VAN DEN BROECK, M., VAERENBERG, C., MATTHEIJSSENS, M., PEETERS, K., ROBBERECHT, W., CRAS, P., MARTIN, J. J., DE DEYN,

P. P., CRUTS, M. & VAN BROECKHOVEN, C. 2012. A C9orf72 promoter repeat expansion in a Flanders-Belgian cohort with disorders of the frontotemporal lobar degeneration-amyotrophic lateral sclerosis spectrum: a gene identification study. *Lancet Neurol,* 11**,** 54-65.

GIJSELINCK, I., VAN MOSSEVELDE, S., VAN DER ZEE, J., SIEBEN, A., PHILTJENS, S., HEEMAN, B., ENGELBORGHS, S., VANDENBULCKE, M., DE BAETS, G., BAUMER, V., CUIJT, I., VAN DEN BROECK, M., PEETERS, K., MATTHEIJSSENS, M., ROUSSEAU, F., VANDENBERGHE, R., DE JONGHE, P., CRAS, P., DE DEYN, P. P., MARTIN, J. J., CRUTS, M. & VAN BROECKHOVEN, C. 2015. Loss of TBK1 is a frequent cause of frontotemporal dementia in a Belgian cohort. *Neurology,* 85**,** 2116-25.

GOBERDHAN, D. C., WILSON, C. & HARRIS, A. L. 2016. Amino Acid Sensing by mTORC1: Intracellular Transporters Mark the Spot. *Cell Metab,* 23**,** 580-9.

GOMES, L. C. & DIKIC, I. 2014. Autophagy in antimicrobial immunity. *Mol Cell,* 54**,** 224-33.

GOODE, A., BUTLER, K., LONG, J., CAVEY, J., SCOTT, D., SHAW, B., SOLLENBERGER, J., GELL, C., JOHANSEN, T., OLDHAM, N. J., SEARLE, M. S. & LAYFIELD, R. 2016. Defective recognition of LC3B by mutant SQSTM1/p62 implicates impairment of autophagy as a pathogenic mechanism in ALS-FTLD. *Autophagy,* 12**,** 1094-104.

GOWANS, G. J., HAWLEY, S. A., ROSS, F. A. & HARDIE, D. G. 2013. AMP is a true physiological regulator of AMP-activated protein kinase by both allosteric activation and enhancing net phosphorylation. *Cell Metab,* 18**,** 556-66.

GRANOT, Z., KOBILER, O., MELAMED-BOOK, N., EIMERL, S., BAHAT, A., LU, B., BRAUN, S., MAURIZI, M. R., SUZUKI, C. K., OPPENHEIM, A. B. & ORLY, J. 2007. Turnover of mitochondrial steroidogenic acute regulatory (StAR) protein by Lon protease: the unexpected effect of proteasome inhibitors. *Mol Endocrinol,* 21**,** 2164-77.

GRIMM, A., BILIOURIS, E. E., LANG, U. E., GOTZ, J., MENSAH-NYAGAN, A. G. & ECKERT, A. 2016. Sex hormone-related neurosteroids differentially rescue bioenergetic deficits induced by amyloid-beta or hyperphosphorylated tau protein. *Cell Mol Life Sci,* 73**,** 201-15.

GRUNEWALD, A., RYGIEL, K. A., HEPPLEWHITE, P. D., MORRIS, C. M., PICARD, M. & TURNBULL, D. M. 2016. Mitochondrial DNA Depletion in Respiratory Chain-Deficient Parkinson Disease Neurons. *Ann Neurol,* 79**,** 366-78.

GU, J., WU, M., GUO, R., YAN, K., LEI, J., GAO, N. & YANG, M. 2016. The architecture of the mammalian respirasome. *Nature,* 537**,** 639-43.

GUARAS, A., PERALES-CLEMENTE, E., CALVO, E., ACIN-PEREZ, R., LOUREIRO-LOPEZ, M., PUJOL, C., MARTINEZ-CARRASCOSO, I., NUNEZ, E., GARCIA-MARQUES, F., RODRIGUEZ-HERNANDEZ, M. A., CORTES, A., DIAZ, F., PEREZ-MARTOS, A., MORAES, C. T., FERNANDEZ-SILVA, P., TRIFUNOVIC, A., NAVAS, P., VAZQUEZ, J. & ENRIQUEZ, J. A. 2016. The CoQH2/CoQ Ratio Serves as a Sensor of Respiratory Chain Efficiency. *Cell Rep,* 15**,** 197-209.

GUERREIRO, R., ESCOTT-PRICE, V., DARWENT, L., PARKKINEN, L., ANSORGE, O., HERNANDEZ, D. G., NALLS, M. A., CLARK, L., HONIG, L., MARDER, K., VAN DER FLIER, W., HOLSTEGE, H., LOUWERSHEIMER, E., LEMSTRA, A., SCHELTENS, P., ROGAEVA, E., ST GEORGE-HYSLOP, P., LONDOS, E., ZETTERBERG, H., ORTEGA-CUBERO, S., PASTOR, P., FERMAN, T. J., GRAFF-RADFORD, N. R., ROSS, O. A., BARBER, I., BRAAE, A., BROWN, K., MORGAN, K., MAETZLER, W., BERG, D., TROAKES, C., AL-SARRAJ, S., LASHLEY, T., COMPTA, Y., REVESZ, T., LEES, A., CAIRNS, N. J., HALLIDAY, G. M., MANN, D., PICKERING-BROWN, S., POWELL, J., LUNNON, K., LUPTON, M. K., DICKSON, D., HARDY, J., SINGLETON, A. & BRAS, J. 2016. Genome-wide analysis of genetic correlation in dementia with Lewy bodies, Parkinson's and Alzheimer's diseases. *Neurobiol Aging,* 38**,** 214.e7-214.e10.

GURUNG, R., TAN, A., OOMS, L. M., MCGRATH, M. J., HUYSMANS, R. D., MUNDAY, A. D., PRESCOTT, M., WHISSTOCK, J. C. & MITCHELL, C. A. 2003. Identification of a novel domain in two mammalian inositol-polyphosphate 5-phosphatases that mediates membrane ruffle localization. The inositol 5-phosphatase skip localizes to the endoplasmic reticulum and translocates to membrane ruffles following epidermal growth factor stimulation. *J Biol Chem,* 278**,** 11376-85.

GUTIERREZ, M. G., MASTER, S. S., SINGH, S. B., TAYLOR, G. A., COLOMBO, M. I. & DERETIC, V. 2004. Autophagy is a defense mechanism inhibiting BCG and Mycobacterium tuberculosis survival in infected macrophages. *Cell,* 119**,** 753-66.

GUTTERIDGE, J. M. & HALLIWELL, B. 2000. Free radicals and antioxidants in the year 2000. A historical look to the future. *Ann N Y Acad Sci,* 899**,** 136-47.

HAILEY, D. W., RAMBOLD, A. S., SATPUTE-KRISHNAN, P., MITRA, K., SOUGRAT, R., KIM, P. K. & LIPPINCOTT-SCHWARTZ, J. 2010. Mitochondria supply membranes for autophagosome biogenesis during starvation. *Cell,* 141**,** 656-67.

HALLIWELL, B. 2007. Biochemistry of oxidative stress. *Biochem Soc Trans,* 35**,** 1147-50.

HALLIWELL, B. & CROSS, C. E. 1994. Oxygen-derived species: their relation to human disease and environmental stress. *Environ Health Perspect,* 102 Suppl 10**,** 5-12.

HAMASAKI, M., FURUTA, N., MATSUDA, A., NEZU, A., YAMAMOTO, A., FUJITA, N., OOMORI, H., NODA, T., HARAGUCHI, T., HIRAOKA, Y., AMANO, A. & YOSHIMORI, T. 2013. Autophagosomes form at ER-mitochondria contact sites. *Nature,* 495**,** 389-93.

HANADA, T., NODA, N. N., SATOMI, Y., ICHIMURA, Y., FUJIOKA, Y., TAKAO, T., INAGAKI, F. & OHSUMI, Y. 2007. The Atg12-Atg5 conjugate has a novel E3-like activity for protein lipidation in autophagy. *J Biol Chem,* 282**,** 37298-302.

HANSEN, R. E., ROTH, D. & WINTHER, J. R. 2009. Quantifying the global cellular thiol-disulfide status. *Proc Natl Acad Sci U S A,* 106**,** 422-7.

HARA, T., NAKAMURA, K., MATSUI, M., YAMAMOTO, A., NAKAHARA, Y., SUZUKI-MIGISHIMA, R., YOKOYAMA, M., MISHIMA, K., SAITO, I., OKANO, H. & MIZUSHIMA, N. 2006. Suppression of basal autophagy in neural cells causes neurodegenerative disease in mice. *Nature,* 441**,** 885-9.

HARA, T., TAKAMURA, A., KISHI, C., IEMURA, S., NATSUME, T., GUAN, J. L. & MIZUSHIMA, N. 2008. FIP200, a ULK-interacting protein, is required for autophagosome formation in mammalian cells. *J Cell Biol,* 181**,** 497-510.

HASEGAWA, J., IWAMOTO, R., OTOMO, T., NEZU, A., HAMASAKI, M. & YOSHIMORI, T. 2016. Autophagosome-lysosome fusion in neurons requires INPP5E, a protein associated with Joubert syndrome. *Embo j,* 35**,** 1853-67.

HAYASHI-NISHINO, M., FUJITA, N., NODA, T., YAMAGUCHI, A., YOSHIMORI, T. & YAMAMOTO, A. 2009. A subdomain of the endoplasmic reticulum forms a cradle for autophagosome formation. *Nat Cell Biol,* 11**,** 1433-7.

HAYNES, C. M., PETROVA, K., BENEDETTI, C., YANG, Y. & RON, D. 2007. ClpP mediates activation of a mitochondrial unfolded protein response in C. elegans. *Dev Cell,* 13**,** 467-80.

HAYNES, C. M. & RON, D. 2010. The mitochondrial UPR - protecting organelle protein homeostasis. *J Cell Sci,* 123**,** 3849-55.

HENCKAERTS, L., CLEYNEN, I., BRINAR, M., JOHN, J. M., VAN STEEN, K., RUTGEERTS, P. & VERMEIRE, S. 2011. Genetic variation in the autophagy gene ULK1 and risk of Crohn's disease. *Inflamm Bowel Dis,* 17**,** 1392-7.

HEO, J. M., LIVNAT-LEVANON, N., TAYLOR, E. B., JONES, K. T., DEPHOURE, N., RING, J., XIE, J., BRODSKY, J. L., MADEO, F., GYGI, S. P., ASHRAFI, K., GLICKMAN, M. H. & RUTTER, J.

2010. A stress-responsive system for mitochondrial protein degradation. *Mol Cell,* 40**,** 465-80.

HEO, J. M., ORDUREAU, A., PAULO, J. A., RINEHART, J. & HARPER, J. W. 2015. The PINK1-PARKIN Mitochondrial Ubiquitylation Pathway Drives a Program of OPTN/NDP52 Recruitment and TBK1 Activation to Promote Mitophagy. *Mol Cell,* 60**,** 7-20.

HEWITT, G., CARROLL, B., SARALLAH, R., CORREIA-MELO, C., OGRODNIK, M., NELSON, G., OTTEN, E. G., MANNI, D., ANTROBUS, R., MORGAN, B. A., VON ZGLINICKI, T., JURK, D., SELUANOV, A., GORBUNOVA, V., JOHANSEN, T., PASSOS, J. F. & KOROLCHUK, V. I. 2016. SQSTM1/p62 mediates crosstalk between autophagy and the UPS in DNA repair. *Autophagy,* 12**,** 1917-1930.

HIRAI, K., ALIEV, G., NUNOMURA, A., FUJIOKA, H., RUSSELL, R. L., ATWOOD, C. S., JOHNSON, A. B., KRESS, Y., VINTERS, H. V., TABATON, M., SHIMOHAMA, S., CASH, A. D., SIEDLAK, S. L., HARRIS, P. L., JONES, P. K., PETERSEN, R. B., PERRY, G. & SMITH, M. A. 2001. Mitochondrial abnormalities in Alzheimer's disease. *J Neurosci,* 21**,** 3017-23.

HIRANO, S., UEMURA, T., ANNOH, H., FUJITA, N., WAGURI, S., ITOH, T. & FUKUDA, M. 2016. Differing susceptibility to autophagic degradation of two LC3-binding proteins: SQSTM1/p62 and TBC1D25/OATL1. *Autophagy,* 12**,** 312-26.

HJERPE, R., BETT, J. S., KEUSS, M. J., SOLOVYOVA, A., MCWILLIAMS, T. G., JOHNSON, C., SAHU, I., VARGHESE, J., WOOD, N., WIGHTMAN, M., OSBORNE, G., BATES, G. P., GLICKMAN, M. H., TROST, M., KNEBEL, A., MARCHESI, F. & KURZ, T. 2016. UBQLN2 Mediates Autophagy-Independent Protein Aggregate Clearance by the Proteasome. *Cell,* 166**,** 935-49.

HORTOBAGYI, T., TROAKES, C., NISHIMURA, A. L., VANCE, C., VAN SWIETEN, J. C., SEELAAR, H., KING, A., AL-SARRAJ, S., ROGELJ, B. & SHAW, C. E. 2011. Optineurin inclusions occur in a minority of TDP-43 positive ALS and FTLD-TDP cases and are rarely observed in other neurodegenerative disorders. *Acta Neuropathol,* 121**,** 519-27.

HOSOKAWA, N., HARA, T., KAIZUKA, T., KISHI, C., TAKAMURA, A., MIURA, Y., IEMURA, S., NATSUME, T., TAKEHANA, K., YAMADA, N., GUAN, J. L., OSHIRO, N. & MIZUSHIMA, N. 2009. Nutrient-dependent mTORC1 association with the ULK1-Atg13-FIP200 complex required for autophagy. *Mol Biol Cell,* 20**,** 1981-91.

HOSOKAWA, N., HARA, Y. & MIZUSHIMA, N. 2007. Generation of cell lines with tetracycline-regulated autophagy and a role for autophagy in controlling cell size. *FEBS Lett,* 581**,** 2623-9.

HOUTEN, S. M. & WANDERS, R. J. 2010. A general introduction to the biochemistry of mitochondrial fatty acid beta-oxidation. *J Inherit Metab Dis,* 33**,** 469-77.

HOUTKOOPER, R. H., MOUCHIROUD, L., RYU, D., MOULLAN, N., KATSYUBA, E., KNOTT, G., WILLIAMS, R. W. & AUWERX, J. 2013. Mitonuclear protein imbalance as a conserved longevity mechanism. *Nature,* 497**,** 451-7.

HSU, L. J., SAGARA, Y., ARROYO, A., ROCKENSTEIN, E., SISK, A., MALLORY, M., WONG, J., TAKENOUCHI, T., HASHIMOTO, M. & MASLIAH, E. 2000. alpha-synuclein promotes mitochondrial deficit and oxidative stress. *Am J Pathol,* 157**,** 401-10.

HU, G., MCQUISTON, T., BERNARD, A., PARK, Y. D., QIU, J., VURAL, A., ZHANG, N., WATERMAN, S. R., BLEWETT, N. H., MYERS, T. G., MARAIA, R. J., KEHRL, J. H., UZEL, G., KLIONSKY, D. J. & WILLIAMSON, P. R. 2015. A conserved mechanism of TOR-dependent RCK-mediated mRNA degradation regulates autophagy. *Nat Cell Biol,* 17**,** 930-42.

HUANG, R., XU, Y., WAN, W., SHOU, X., QIAN, J., YOU, Z., LIU, B., CHANG, C., ZHOU, T., LIPPINCOTT-SCHWARTZ, J. & LIU, W. 2015. Deacetylation of nuclear LC3 drives autophagy initiation under starvation. *Mol Cell,* 57**,** 456-66.

HUETT, A., HEATH, R. J., BEGUN, J., SASSI, S. O., BAXT, L. A., VYAS, J. M., GOLDBERG, M. B. & XAVIER, R. J. 2012. The LRR and RING domain protein LRSAM1 is an E3 ligase crucial for ubiquitin-dependent autophagy of intracellular Salmonella Typhimurium. *Cell Host Microbe,* 12**,** 778-90.

HUNTE, C., ZICKERMANN, V. & BRANDT, U. 2010. Functional modules and structural basis of conformational coupling in mitochondrial complex I. *Science,* 329**,** 448-51.

HUOTARI, J. & HELENIUS, A. 2011. Endosome maturation. *Embo j,* 30**,** 3481-500.

HUR, J. H., STORK, D. A. & WALKER, D. W. 2014. Complex-I-ty in aging. *J Bioenerg Biomembr,* 46**,** 329-35.

HUSNJAK, K. & DIKIC, I. 2012. Ubiquitin-binding proteins: decoders of ubiquitin-mediated cellular functions. *Annu Rev Biochem,* 81**,** 291-322.

HUTTON, M., LENDON, C. L., RIZZU, P., BAKER, M., FROELICH, S., HOULDEN, H., PICKERING-BROWN, S., CHAKRAVERTY, S., ISAACS, A., GROVER, A., HACKETT, J., ADAMSON, J., LINCOLN, S., DICKSON, D., DAVIES, P., PETERSEN, R. C., STEVENS, M., DE GRAAFF, E., WAUTERS, E., VAN BAREN, J., HILLEBRAND, M., JOOSSE, M., KWON, J. M., NOWOTNY, P., CHE, L. K., NORTON, J., MORRIS, J. C., REED, L. A., TROJANOWSKI, J., BASUN, H., LANNFELT, L., NEYSTAT, M., FAHN, S., DARK, F., TANNENBERG, T., DODD, P. R., HAYWARD, N., KWOK, J. B., SCHOFIELD, P. R., ANDREADIS, A., SNOWDEN, J., CRAUFURD, D., NEARY, D., OWEN, F., OOSTRA, B. A., HARDY, J., GOATE, A., VAN SWIETEN, J., MANN, D., LYNCH, T. & HEUTINK, P. 1998. Association of missense and 5'-splice-site mutations in tau with the inherited dementia FTDP-17. *Nature,* 393**,** 702-5.

HYTTINEN, J. M., AMADIO, M., VIIRI, J., PASCALE, A., SALMINEN, A. & KAARNIRANTA, K. 2014. Clearance of misfolded and aggregated proteins by aggrephagy and implications for aggregation diseases. *Ageing Res Rev,* 18**,** 16-28.

HYTTINEN, J. M., NIITTYKOSKI, M., SALMINEN, A. & KAARNIRANTA, K. 2013. Maturation of autophagosomes and endosomes: a key role for Rab7. *Biochim Biophys Acta,* 1833**,** 503-10.

ICHIMURA, Y., KUMANOMIDOU, T., SOU, Y. S., MIZUSHIMA, T., EZAKI, J., UENO, T., KOMINAMI, E., YAMANE, T., TANAKA, K. & KOMATSU, M. 2008. Structural basis for sorting mechanism of p62 in selective autophagy. *J Biol Chem,* 283**,** 22847-57.

ICHIMURA, Y., WAGURI, S., SOU, Y. S., KAGEYAMA, S., HASEGAWA, J., ISHIMURA, R., SAITO, T., YANG, Y., KOUNO, T., FUKUTOMI, T., HOSHII, T., HIRAO, A., TAKAGI, K., MIZUSHIMA, T., MOTOHASHI, H., LEE, M. S., YOSHIMORI, T., TANAKA, K., YAMAMOTO, M. & KOMATSU, M. 2013. Phosphorylation of p62 Activates the Keap1-Nrf2 Pathway during Selective Autophagy. *Mol Cell,* 51**,** 618-31.

IGUCHI, Y., KATSUNO, M., IKENAKA, K., ISHIGAKI, S. & SOBUE, G. 2013. Amyotrophic lateral sclerosis: an update on recent genetic insights. *J Neurol,* 260**,** 2917-27.

IMARISIO, S., CARMICHAEL, J., KOROLCHUK, V., CHEN, C. W., SAIKI, S., ROSE, C., KRISHNA, G., DAVIES, J. E., TTOFI, E., UNDERWOOD, B. R. & RUBINSZTEIN, D. C. 2008. Huntington's disease: from pathology and genetics to potential therapies. *Biochem J,* 412**,** 191-209.

INOKI, K., LI, Y., ZHU, T., WU, J. & GUAN, K. L. 2002. TSC2 is phosphorylated and inhibited by Akt and suppresses mTOR signalling. *Nat Cell Biol,* 4**,** 648-57.

INOUE, Y. & KLIONSKY, D. J. 2010. Regulation of macroautophagy in Saccharomyces cerevisiae. *Semin Cell Dev Biol,* 21**,** 664-70.

ITAKURA, E., KISHI-ITAKURA, C., KOYAMA-HONDA, I. & MIZUSHIMA, N. 2012. Structures containing Atg9A and the ULK1 complex independently target depolarized mitochondria at initial stages of Parkin-mediated mitophagy. *J Cell Sci,* 125**,** 1488-99.

ITAKURA, E. & MIZUSHIMA, N. 2011. p62 Targeting to the autophagosome formation site requires self-oligomerization but not LC3 binding. *J Cell Biol,* 192**,** 17-27.

ITOH, K., CHIBA, T., TAKAHASHI, S., ISHII, T., IGARASHI, K., KATOH, Y., OYAKE, T., HAYASHI, N., SATOH, K., HATAYAMA, I., YAMAMOTO, M. & NABESHIMA, Y. 1997. An Nrf2/small Maf heterodimer mediates the induction of phase II detoxifying enzyme genes through antioxidant response elements. *Biochem Biophys Res Commun,* 236**,** 313-22.

JACOBSON, J., LAMBERT, A. J., PORTERO-OTIN, M., PAMPLONA, R., MAGWERE, T., MIWA, S., DRIEGE, Y., BRAND, M. D. & PARTRIDGE, L. 2010. Biomarkers of aging in Drosophila. *Aging Cell,* 9**,** 466-77.

JAGER, S., BUCCI, C., TANIDA, I., UENO, T., KOMINAMI, E., SAFTIG, P. & ESKELINEN, E. L. 2004. Role for Rab7 in maturation of late autophagic vacuoles. *J Cell Sci,* 117**,** 4837-48.

JAHREISS, L., MENZIES, F. M. & RUBINSZTEIN, D. C. 2008. The itinerary of autophagosomes: from peripheral formation to kiss-and-run fusion with lysosomes. *Traffic,* 9**,** 574-87.

JAIN, A., LAMARK, T., SJOTTEM, E., LARSEN, K. B., AWUH, J. A., OVERVATN, A., MCMAHON, M., HAYES, J. D. & JOHANSEN, T. 2010. p62/SQSTM1 is a target gene for transcription factor NRF2 and creates a positive feedback loop by inducing antioxidant response element-driven gene transcription. *J Biol Chem,* 285**,** 22576-91.

JARVIS, R. M., HUGHES, S. M. & LEDGERWOOD, E. C. 2012. Peroxiredoxin 1 functions as a signal peroxidase to receive, transduce, and transmit peroxide signals in mammalian cells. *Free Radic Biol Med,* 53**,** 1522-30.

JI, Z. S., MIRANDA, R. D., NEWHOUSE, Y. M., WEISGRABER, K. H., HUANG, Y. & MAHLEY, R. W. 2002. Apolipoprotein E4 potentiates amyloid beta peptide-induced lysosomal leakage and apoptosis in neuronal cells. *J Biol Chem,* 277**,** 21821-8.

JI, Z. S., MULLENDORFF, K., CHENG, I. H., MIRANDA, R. D., HUANG, Y. & MAHLEY, R. W. 2006. Reactivity of apolipoprotein E4 and amyloid beta peptide: lysosomal stability and neurodegeneration. *J Biol Chem,* 281**,** 2683-92.

JIN, S., TIAN, S., CHEN, Y., ZHANG, C., XIE, W., XIA, X., CUI, J. & WANG, R. F. 2016. USP19 modulates autophagy and antiviral immune responses by deubiquitinating Beclin-1. *Embo j,* 35**,** 866-80.

JO, C., GUNDEMIR, S., PRITCHARD, S., JIN, Y. N., RAHMAN, I. & JOHNSON, G. V. 2014. Nrf2 reduces levels of phosphorylated tau protein by inducing autophagy adaptor protein NDP52. *Nat Commun,* 5**,** 3496.

JOHANSEN, T. & LAMARK, T. 2011. Selective autophagy mediated by autophagic adapter proteins. *Autophagy,* 7**,** 279-96.

JOHNSON, J. O., MANDRIOLI, J., BENATAR, M., ABRAMZON, Y., VAN DEERLIN, V. M., TROJANOWSKI, J. Q., GIBBS, J. R., BRUNETTI, M., GRONKA, S., WUU, J., DING, J., MCCLUSKEY, L., MARTINEZ-LAGE, M., FALCONE, D., HERNANDEZ, D. G., AREPALLI, S., CHONG, S., SCHYMICK, J. C., ROTHSTEIN, J., LANDI, F., WANG, Y. D., CALVO, A., MORA, G., SABATELLI, M., MONSURRO, M. R., BATTISTINI, S., SALVI, F., SPATARO, R., SOLA, P., BORGHERO, G., GALASSI, G., SCHOLZ, S. W., TAYLOR, J. P., RESTAGNO, G., CHIO, A. & TRAYNOR, B. J. 2010. Exome sequencing reveals VCP mutations as a cause of familial ALS. *Neuron,* 68**,** 857-64.

JOHNSTON, A. J., HOOGENRAAD, J., DOUGAN, D. A., TRUSCOTT, K. N., YANO, M., MORI, M., HOOGENRAAD, N. J. & RYAN, M. T. 2002. Insertion and assembly of human tom7 into the preprotein translocase complex of the outer mitochondrial membrane. *J Biol Chem,* 277**,** 42197-204.

JUNG, C. H., JUN, C. B., RO, S. H., KIM, Y. M., OTTO, N. M., CAO, J., KUNDU, M. & KIM, D. H. 2009. ULK-Atg13-FIP200 complexes mediate mTOR signaling to the autophagy machinery. *Mol Biol Cell,* 20**,** 1992-2003.

KABEYA, Y., MIZUSHIMA, N., UENO, T., YAMAMOTO, A., KIRISAKO, T., NODA, T., KOMINAMI, E., OHSUMI, Y. & YOSHIMORI, T. 2000. LC3, a mammalian homologue of yeast Apg8p, is localized in autophagosome membranes after processing. *EMBO J,* 19**,** 5720-8.

KABEYA, Y., MIZUSHIMA, N., YAMAMOTO, A., OSHITANI-OKAMOTO, S., OHSUMI, Y. & YOSHIMORI, T. 2004. LC3, GABARAP and GATE16 localize to autophagosomal membrane depending on form-II formation. *J Cell Sci,* 117**,** 2805-12.

KAMBER, R. A., SHOEMAKER, C. J. & DENIC, V. 2015. Receptor-Bound Targets of Selective Autophagy Use a Scaffold Protein to Activate the Atg1 Kinase. *Mol Cell,* 59**,** 372-81.

KANE, L. A., LAZAROU, M., FOGEL, A. I., LI, Y., YAMANO, K., SARRAF, S. A., BANERJEE, S. & YOULE, R. J. 2014. PINK1 phosphorylates ubiquitin to activate Parkin E3 ubiquitin ligase activity. *J Cell Biol,* 205**,** 143-53.

KANG, R., ZEH, H. J., LOTZE, M. T. & TANG, D. 2011. The Beclin 1 network regulates autophagy and apoptosis. *Cell Death Differ,* 18**,** 571-80.

KARBOWSKI, M. & YOULE, R. J. 2011. Regulating mitochondrial outer membrane proteins by ubiquitination and proteasomal degradation. *Curr Opin Cell Biol,* 23**,** 476-82.

KARUNADHARMA, P. P., BASISTY, N., DAI, D. F., CHIAO, Y. A., QUARLES, E. K., HSIEH, E. J., CRISPIN, D., BIELAS, J. H., ERICSON, N. G., BEYER, R. P., MACKAY, V. L., MACCOSS, M. J. & RABINOVITCH, P. S. 2015. Subacute calorie restriction and rapamycin discordantly alter mouse liver proteome homeostasis and reverse aging effects. *Aging Cell,* 14**,** 547-57.

KATAYAMA, H., KOGURE, T., MIZUSHIMA, N., YOSHIMORI, T. & MIYAWAKI, A. 2011. A sensitive and quantitative technique for detecting autophagic events based on lysosomal delivery. *Chem Biol,* 18**,** 1042-52.

KAZLAUSKAITE, A., KONDAPALLI, C., GOURLAY, R., CAMPBELL, D. G., RITORTO, M. S., HOFMANN, K., ALESSI, D. R., KNEBEL, A., TROST, M. & MUQIT, M. M. 2014. Parkin is activated by PINK1-dependent phosphorylation of ubiquitin at Ser65. *Biochem J,* 460**,** 127-39.

KELSO, G. F., PORTEOUS, C. M., COULTER, C. V., HUGHES, G., PORTEOUS, W. K., LEDGERWOOD, E. C., SMITH, R. A. & MURPHY, M. P. 2001. Selective targeting of a redox-active ubiquinone to mitochondria within cells: antioxidant and antiapoptotic properties. *J Biol Chem,* 276**,** 4588-96.

KIM, B. W., HONG, S. B., KIM, J. H., KWON, D. H. & SONG, H. K. 2013a. Structural basis for recognition of autophagic receptor NDP52 by the sugar receptor galectin-8. *Nat Commun,* 4**,** 1613.

KIM, J., KUNDU, M., VIOLLET, B. & GUAN, K. L. 2011. AMPK and mTOR regulate autophagy through direct phosphorylation of Ulk1. *Nat Cell Biol,* 13**,** 132-41.

KIM, P. K., HAILEY, D. W., MULLEN, R. T. & LIPPINCOTT-SCHWARTZ, J. 2008. Ubiquitin signals autophagic degradation of cytosolic proteins and peroxisomes. *Proc Natl Acad Sci U S A,* 105**,** 20567-74.

KIM, S., LEE, D., SONG, J. C., CHO, S. J., YUN, S. M., KOH, Y. H., SONG, J., JOHNSON, G. V. & JO, C. 2014. NDP52 associates with phosphorylated tau in brains of an Alzheimer disease mouse model. *Biochem Biophys Res Commun,* 454**,** 196-201.

KIM, Y. E., HIPP, M. S., BRACHER, A., HAYER-HARTL, M. & HARTL, F. U. 2013b. Molecular chaperone functions in protein folding and proteostasis. *Annu Rev Biochem,* 82**,** 323-55.

KIM, Y. M., PARK, J. M., GRUNWALD, D. & KIM, D. H. 2016. An expanded role for mTORC1 in autophagy. *Mol Cell Oncol,* 3**,** e1010958.

KIRBY, D. M., RENNIE, K. J., SMULDERS-SRINIVASAN, T. K., ACIN-PEREZ, R., WHITTINGTON, M., ENRIQUEZ, J. A., TREVELYAN, A. J., TURNBULL, D. M. & LIGHTOWLERS, R. N. 2009.

Transmitochondrial embryonic stem cells containing pathogenic mtDNA mutations are compromised in neuronal differentiation. *Cell Prolif,* 42**,** 413-24.

KIRISAKO, T., ICHIMURA, Y., OKADA, H., KABEYA, Y., MIZUSHIMA, N., YOSHIMORI, T., OHSUMI, M., TAKAO, T., NODA, T. & OHSUMI, Y. 2000. The reversible modification regulates the membrane-binding state of Apg8/Aut7 essential for autophagy and the cytoplasm to vacuole targeting pathway. *J Cell Biol,* 151**,** 263-76.

KIRKIN, V., LAMARK, T., SOU, Y. S., BJORKOY, G., NUNN, J. L., BRUUN, J. A., SHVETS, E., MCEWAN, D. G., CLAUSEN, T. H., WILD, P., BILUSIC, I., THEURILLAT, J. P., OVERVATN, A., ISHII, T., ELAZAR, Z., KOMATSU, M., DIKIC, I. & JOHANSEN, T. 2009. A role for NBR1 in autophagosomal degradation of ubiquitinated substrates. *Mol Cell,* 33**,** 505-16.

KISHI-ITAKURA, C., KOYAMA-HONDA, I., ITAKURA, E. & MIZUSHIMA, N. 2014. Ultrastructural analysis of autophagosome organization using mammalian autophagy-deficient cells. *J Cell Sci,* 127**,** 4089-102.

KITADA, T., ASAKAWA, S., HATTORI, N., MATSUMINE, H., YAMAMURA, Y., MINOSHIMA, S., YOKOCHI, M., MIZUNO, Y. & SHIMIZU, N. 1998. Mutations in the parkin gene cause autosomal recessive juvenile parkinsonism. *Nature,* 392**,** 605-8.

KLIONSKY, D. J. 2007. Autophagy: from phenomenology to molecular understanding in less than a decade. *Nat Rev Mol Cell Biol,* 8**,** 931-7.

KMITA, K. & ZICKERMANN, V. 2013. Accessory subunits of mitochondrial complex I. *Biochem Soc Trans,* 41**,** 1272-9.

KOBAYASHI, A., KANG, M. I., WATAI, Y., TONG, K. I., SHIBATA, T., UCHIDA, K. & YAMAMOTO, M. 2006. Oxidative and electrophilic stresses activate Nrf2 through inhibition of ubiquitination activity of Keap1. *Mol Cell Biol,* 26**,** 221-9.

KOMATSU, M., KUROKAWA, H., WAGURI, S., TAGUCHI, K., KOBAYASHI, A., ICHIMURA, Y., SOU, Y. S., UENO, I., SAKAMOTO, A., TONG, K. I., KIM, M., NISHITO, Y., IEMURA, S., NATSUME, T., UENO, T., KOMINAMI, E., MOTOHASHI, H., TANAKA, K. & YAMAMOTO, M. 2010. The selective autophagy substrate p62 activates the stress responsive transcription factor Nrf2 through inactivation of Keap1. *Nat Cell Biol,* 12**,** 213-23.

KOMATSU, M., WAGURI, S., CHIBA, T., MURATA, S., IWATA, J., TANIDA, I., UENO, T., KOIKE, M., UCHIYAMA, Y., KOMINAMI, E. & TANAKA, K. 2006. Loss of autophagy in the central nervous system causes neurodegeneration in mice. *Nature,* 441**,** 880-4.

KOMATSU, M., WAGURI, S., KOIKE, M., SOU, Y. S., UENO, T., HARA, T., MIZUSHIMA, N., IWATA, J., EZAKI, J., MURATA, S., HAMAZAKI, J., NISHITO, Y., IEMURA, S., NATSUME, T., YANAGAWA, T., UWAYAMA, J., WARABI, E., YOSHIDA, H., ISHII, T., KOBAYASHI, A., YAMAMOTO, M., YUE, Z., UCHIYAMA, Y., KOMINAMI, E. & TANAKA, K. 2007. Homeostatic levels of p62 control cytoplasmic inclusion body formation in autophagy-deficient mice. *Cell,* 131**,** 1149-63.

KOMATSU, M., WAGURI, S., UENO, T., IWATA, J., MURATA, S., TANIDA, I., EZAKI, J., MIZUSHIMA, N., OHSUMI, Y., UCHIYAMA, Y., KOMINAMI, E., TANAKA, K. & CHIBA, T. 2005. Impairment of starvation-induced and constitutive autophagy in Atg7-deficient mice. *J Cell Biol,* 169**,** 425-34.

KONDAPALLI, C., KAZLAUSKAITE, A., ZHANG, N., WOODROOF, H. I., CAMPBELL, D. G., GOURLAY, R., BURCHELL, L., WALDEN, H., MACARTNEY, T. J., DEAK, M., KNEBEL, A., ALESSI, D. R. & MUQIT, M. M. 2012. PINK1 is activated by mitochondrial membrane potential depolarization and stimulates Parkin E3 ligase activity by phosphorylating Serine 65. *Open Biol,* 2**,** 120080.

KONG, J. & XU, Z. 1998. Massive mitochondrial degeneration in motor neurons triggers the onset of amyotrophic lateral sclerosis in mice expressing a mutant SOD1. *J Neurosci,* 18**,** 3241-50.

KOPITO, R. R. 2000. Aggresomes, inclusion bodies and protein aggregation. *Trends Cell Biol,* 10**,** 524-30.

KORAC, J., SCHAEFFER, V., KOVACEVIC, I., CLEMENT, A. M., JUNGBLUT, B., BEHL, C., TERZIC, J. & DIKIC, I. 2013. Ubiquitin-independent function of optineurin in autophagic clearance of protein aggregates. *J Cell Sci,* 126**,** 580-92.

KOROLCHUK, V. I., SAIKI, S., LICHTENBERG, M., SIDDIQI, F. H., ROBERTS, E. A., IMARISIO, S., JAHREISS, L., SARKAR, S., FUTTER, M., MENZIES, F. M., O'KANE, C. J., DERETIC, V. & RUBINSZTEIN, D. C. 2011. Lysosomal positioning coordinates cellular nutrient responses. *Nat Cell Biol,* 13**,** 453-60.

KOYANO, F., OKATSU, K., KOSAKO, H., TAMURA, Y., GO, E., KIMURA, M., KIMURA, Y., TSUCHIYA, H., YOSHIHARA, H., HIROKAWA, T., ENDO, T., FON, E. A., TREMPE, J. F., SAEKI, Y., TANAKA, K. & MATSUDA, N. 2014. Ubiquitin is phosphorylated by PINK1 to activate parkin. *Nature,* 510**,** 162-6.

KRAFT, L. J., DOWLER, J., MANRAL, P. & KENWORTHY, A. K. 2016. Size, organization, and dynamics of soluble SQSTM1 and LC3-SQSTM1 complexes in living cells. *Autophagy,* 12**,** 1660-74.

KUMA, A., HATANO, M., MATSUI, M., YAMAMOTO, A., NAKAYA, H., YOSHIMORI, T., OHSUMI, Y., TOKUHISA, T. & MIZUSHIMA, N. 2004. The role of autophagy during the early neonatal starvation period. *Nature,* 432**,** 1032-6.

KUMA, A., MIZUSHIMA, N., ISHIHARA, N. & OHSUMI, Y. 2002. Formation of the approximately 350-kDa Apg12-Apg5.Apg16 multimeric complex, mediated by Apg16 oligomerization, is essential for autophagy in yeast. *J Biol Chem,* 277**,** 18619-25.

KUUSISTO, E., SALMINEN, A. & ALAFUZOFF, I. 2001. Ubiquitin-binding protein p62 is present in neuronal and glial inclusions in human tauopathies and synucleinopathies. *Neuroreport,* 12**,** 2085-90.

KWON, J., HAN, E., BUI, C. B., SHIN, W., LEE, J., LEE, S., CHOI, Y. B., LEE, A. H., LEE, K. H., PARK, C., OBIN, M. S., PARK, S. K., SEO, Y. J., OH, G. T., LEE, H. W. & SHIN, J. 2012. Assurance of mitochondrial integrity and mammalian longevity by the p62-Keap1-Nrf2-Nqo1 cascade. *EMBO Rep,* 13**,** 150-6.

KYOSTILA, K., SYRJA, P., JAGANNATHAN, V., CHANDRASEKAR, G., JOKINEN, T. S., SEPPALA, E. H., BECKER, D., DROGEMULLER, M., DIETSCHI, E., DROGEMULLER, C., LANG, J., STEFFEN, F., ROHDIN, C., JADERLUND, K. H., LAPPALAINEN, A. K., HAHN, K., WOHLSEIN, P., BAUMGARTNER, W., HENKE, D., OEVERMANN, A., KERE, J., LOHI, H. & LEEB, T. 2015. A missense change in the ATG4D gene links aberrant autophagy to a neurodegenerative vacuolar storage disease. *PLoS Genet,* 11**,** e1005169.

LAI, A. Y. & MCLAURIN, J. 2012. Inhibition of amyloid-beta peptide aggregation rescues the autophagic deficits in the TgCRND8 mouse model of Alzheimer disease. *Biochim Biophys Acta,* 1822**,** 1629-37.

LAMARK, T., PERANDER, M., OUTZEN, H., KRISTIANSEN, K., OVERVATN, A., MICHAELSEN, E., BJORKOY, G. & JOHANSEN, T. 2003. Interaction codes within the family of mammalian Phox and Bem1p domain-containing proteins. *J Biol Chem,* 278**,** 34568-81.

LAMB, C. A., YOSHIMORI, T. & TOOZE, S. A. 2013. The autophagosome: origins unknown, biogenesis complex. *Nat Rev Mol Cell Biol,* 14**,** 759-74.

LAPLANTE, M., HORVAT, S., FESTUCCIA, W. T., BIRSOY, K., PREVORSEK, Z., EFEYAN, A. & SABATINI, D. M. 2012. DEPTOR cell-autonomously promotes adipogenesis, and its expression is associated with obesity. *Cell Metab,* 16**,** 202-12.

LAPLANTE, M. & SABATINI, D. M. 2012. mTOR signaling in growth control and disease. *Cell,* 149**,** 274-93.

LAPUENTE-BRUN, E., MORENO-LOSHUERTOS, R., ACIN-PEREZ, R., LATORRE-PELLICER, A., COLAS, C., BALSA, E., PERALES-CLEMENTE, E., QUIROS, P. M., CALVO, E., RODRIGUEZ-HERNANDEZ, M. A., NAVAS, P., CRUZ, R., CARRACEDO, A., LOPEZ-OTIN, C., PEREZ-MARTOS, A., FERNANDEZ-SILVA, P., FERNANDEZ-VIZARRA, E. & ENRIQUEZ, J. A. 2013. Supercomplex assembly determines electron flux in the mitochondrial electron transport chain. *Science,* 340**,** 1567-70.

LATIMER, H. R. & VEAL, E. A. 2016. Peroxiredoxins in Regulation of MAPK Signalling Pathways; Sensors and Barriers to Signal Transduction. *Mol Cells,* 39**,** 40-5.

LAU, E., WANG, D., ZHANG, J., YU, H., LAM, M. P., LIANG, X., ZONG, N., KIM, T. Y. & PING, P. 2012. Substrate- and isoform-specific proteome stability in normal and stressed cardiac mitochondria. *Circ Res,* 110**,** 1174-8.

LAZAROU, M., SLITER, D. A., KANE, L. A., SARRAF, S. A., WANG, C., BURMAN, J. L., SIDERIS, D. P., FOGEL, A. I. & YOULE, R. J. 2015. The ubiquitin kinase PINK1 recruits autophagy receptors to induce mitophagy. *Nature,* 524**,** 309-14.

LE BER, I., CAMUZAT, A., GUERREIRO, R., BOUYA-AHMED, K., BRAS, J., NICOLAS, G., GABELLE, A., DIDIC, M., DE SEPTENVILLE, A., MILLECAMPS, S., LENGLET, T., LATOUCHE, M., KABASHI, E., CAMPION, D., HANNEQUIN, D., HARDY, J., BRICE, A., FRENCH, C. & GENETIC RESEARCH NETWORK ON, F. F.-A. 2013. SQSTM1 mutations in French patients with frontotemporal dementia or frontotemporal dementia with amyotrophic lateral sclerosis. *JAMA Neurol,* 70**,** 1403-10.

LE BER, I., DE SEPTENVILLE, A., MILLECAMPS, S., CAMUZAT, A., CAROPPO, P., COURATIER, P., BLANC, F., LACOMBLEZ, L., SELLAL, F., FLEURY, M. C., MEININGER, V., CAZENEUVE, C., CLOT, F., FLABEAU, O., LEGUERN, E. & BRICE, A. 2015. TBK1 mutation frequencies in French frontotemporal dementia and amyotrophic lateral sclerosis cohorts. *Neurobiol Aging,* 36**,** 3116.e5-8.

LEE, E. J. & TOURNIER, C. 2011. The requirement of uncoordinated 51-like kinase 1 (ULK1) and ULK2 in the regulation of autophagy. *Autophagy,* 7**,** 689-95.

LEE, J. Y., NAGANO, Y., TAYLOR, J. P., LIM, K. L. & YAO, T. P. 2010a. Disease-causing mutations in parkin impair mitochondrial ubiquitination, aggregation, and HDAC6-dependent mitophagy. *J Cell Biol,* 189**,** 671-9.

LEE, S., KIM, S. M. & LEE, R. T. 2013. Thioredoxin and thioredoxin target proteins: from molecular mechanisms to functional significance. *Antioxid Redox Signal,* 18**,** 1165-207.

LEE, S. J., HWANG, A. B. & KENYON, C. 2010b. Inhibition of respiration extends C. elegans life span via reactive oxygen species that increase HIF-1 activity. *Curr Biol,* 20**,** 2131-6.

LEE, Y., STEVENS, D. A., KANG, S. U., JIANG, H., LEE, Y. I., KO, H. S., SCARFFE, L. A., UMANAH, G. E., KANG, H., HAM, S., KAM, T. I., ALLEN, K., BRAHMACHARI, S., KIM, J. W., NEIFERT, S., YUN, S. P., FIESEL, F. C., SPRINGER, W., DAWSON, V. L., SHIN, J. H. & DAWSON, T. M. 2017. PINK1 Primes Parkin-Mediated Ubiquitination of PARIS in Dopaminergic Neuronal Survival. *Cell Rep,* 18**,** 918-932.

LENAZ, G., BARACCA, A., FATO, R., GENOVA, M. L. & SOLAINI, G. 2006. New insights into structure and function of mitochondria and their role in aging and disease. *Antioxid Redox Signal,* 8**,** 417-37.

LETTS, J. A., FIEDORCZUK, K. & SAZANOV, L. A. 2016. The architecture of respiratory supercomplexes. *Nature,* 537**,** 644-648.

LEUNER, K., SCHUTT, T., KURZ, C., ECKERT, S. H., SCHILLER, C., OCCHIPINTI, A., MAI, S., JENDRACH, M., ECKERT, G. P., KRUSE, S. E., PALMITER, R. D., BRANDT, U., DROSE, S., WITTIG, I., WILLEM, M., HAASS, C., REICHERT, A. S. & MULLER, W. E. 2012. Mitochondrion-derived reactive oxygen species lead to enhanced amyloid beta formation. *Antioxid Redox Signal,* 16**,** 1421-33.

LEVYTSKYY, R. M., GERMANY, E. M. & KHALIMONCHUK, O. 2016. Mitochondrial Quality Control Proteases in Neuronal Welfare. *J Neuroimmune Pharmacol,* 11**,** 629-644.

LI, W. W., YANG, R., GUO, J. C., REN, H. M., ZHA, X. L., CHENG, J. S. & CAI, D. F. 2007. Localization of alpha-synuclein to mitochondria within midbrain of mice. *Neuroreport,* 18**,** 1543-6.

LI, X., RYDZEWSKI, N., HIDER, A., ZHANG, X., YANG, J., WANG, W., GAO, Q., CHENG, X. & XU, H. 2016. A molecular mechanism to regulate lysosome motility for lysosome positioning and tubulation. *Nat Cell Biol,* 18**,** 404-17.

LINDORFF-LARSEN, K., PIANA, S., PALMO, K., MARAGAKIS, P., KLEPEIS, J. L., DROR, R. O. & SHAW, D. E. 2010. Improved side-chain torsion potentials for the Amber ff99SB protein force field. *Proteins,* 78**,** 1950-8.

LING, L. & GOEDDEL, D. V. 2000. T6BP, a TRAF6-interacting protein involved in IL-1 signaling. *Proc Natl Acad Sci U S A,* 97**,** 9567-72.

LING, S. C., POLYMENIDOU, M. & CLEVELAND, D. W. 2013. Converging mechanisms in ALS and FTD: disrupted RNA and protein homeostasis. *Neuron,* 79**,** 416-38.

LIVNEH, I., COHEN-KAPLAN, V., COHEN-ROSENZWEIG, C., AVNI, N. & CIECHANOVER, A. 2016. The life cycle of the 26S proteasome: from birth, through regulation and function, and onto its death. *Cell Res,* 26**,** 869-85.

LOMEN-HOERTH, C., ANDERSON, T. & MILLER, B. 2002. The overlap of amyotrophic lateral sclerosis and frontotemporal dementia. *Neurology,* 59**,** 1077-9.

LOPEZ-FABUEL, I., LE DOUCE, J., LOGAN, A., JAMES, A. M., BONVENTO, G., MURPHY, M. P., ALMEIDA, A. & BOLANOS, J. P. 2016. Complex I assembly into supercomplexes determines differential mitochondrial ROS production in neurons and astrocytes. *Proc Natl Acad Sci U S A,* 113**,** 13063-13068.

LOPEZ-OTIN, C., BLASCO, M. A., PARTRIDGE, L., SERRANO, M. & KROEMER, G. 2013. The hallmarks of aging. *Cell,* 153**,** 1194-217.

LU, K., DEN BRAVE, F. & JENTSCH, S. 2017. Receptor oligomerization guides pathway choice between proteasomal and autophagic degradation. *Nat Cell Biol,* 19**,** 732-739.

LU, K., PSAKHYE, I. & JENTSCH, S. 2014. Autophagic Clearance of PolyQ Proteins Mediated by Ubiquitin-Atg8 Adaptors of the Conserved CUET Protein Family. *Cell*.

LUTOLF, M. P., TIRELLI, N., CERRITELLI, S., CAVALLI, L. & HUBBELL, J. A. 2001. Systematic modulation of Michael-type reactivity of thiols through the use of charged amino acids. *Bioconjug Chem,* 12**,** 1051-6.

MA, T., LI, J., XU, Y., YU, C., XU, T., WANG, H., LIU, K., CAO, N., NIE, B. M., ZHU, S. Y., XU, S., LI, K., WEI, W. G., WU, Y., GUAN, K. L. & DING, S. 2015. Atg5-independent autophagy regulates mitochondrial clearance and is essential for iPSC reprogramming. *Nat Cell Biol,* 17**,** 1379-87.

MADEO, F., ZIMMERMANN, A., MAIURI, M. C. & KROEMER, G. 2015. Essential role for autophagy in life span extension. *J Clin Invest,* 125**,** 85-93.

MAOR, G., CABASSO, O., KRIVORUK, O., RODRIGUEZ, J., STELLER, H., SEGAL, D. & HOROWITZ, M. 2016. The contribution of mutant GBA to the development of Parkinson disease in Drosophila. *Hum Mol Genet,* 25**,** 2712-2727.

MARANZANA, E., BARBERO, G., FALASCA, A. I., LENAZ, G. & GENOVA, M. L. 2013. Mitochondrial respiratory supercomplex association limits production of reactive oxygen species from complex I. *Antioxid Redox Signal,* 19**,** 1469-80.

MARELLA, M., SEO, B. B., NAKAMARU-OGISO, E., GREENAMYRE, J. T., MATSUNO-YAGI, A. & YAGI, T. 2008. Protection by the NDI1 gene against neurodegeneration in a rotenone rat model of Parkinson's disease. *PLoS One,* 3**,** e1433.

MARI, M., GRIFFITH, J., RIETER, E., KRISHNAPPA, L., KLIONSKY, D. J. & REGGIORI, F. 2010. An Atg9-containing compartment that functions in the early steps of autophagosome biogenesis. *J Cell Biol,* 190**,** 1005-22.

MARINO, S. M. & GLADYSHEV, V. N. 2010. Cysteine function governs its conservation and degeneration and restricts its utilization on protein surfaces. *J Mol Biol,* 404**,** 902-16.

MARTINA, J. A., CHEN, Y., GUCEK, M. & PUERTOLLANO, R. 2012. MTORC1 functions as a transcriptional regulator of autophagy by preventing nuclear transport of TFEB. *Autophagy,* 8**,** 903-14.

MARTINUS, R. D., GARTH, G. P., WEBSTER, T. L., CARTWRIGHT, P., NAYLOR, D. J., HOJ, P. B. & HOOGENRAAD, N. J. 1996. Selective induction of mitochondrial chaperones in response to loss of the mitochondrial genome. *Eur J Biochem,* 240**,** 98-103.

MARUYAMA, H., MORINO, H., ITO, H., IZUMI, Y., KATO, H., WATANABE, Y., KINOSHITA, Y., KAMADA, M., NODERA, H., SUZUKI, H., KOMURE, O., MATSUURA, S., KOBATAKE, K., MORIMOTO, N., ABE, K., SUZUKI, N., AOKI, M., KAWATA, A., HIRAI, T., KATO, T., OGASAWARA, K., HIRANO, A., TAKUMI, T., KUSAKA, H., HAGIWARA, K., KAJI, R. & KAWAKAMI, H. 2010. Mutations of optineurin in amyotrophic lateral sclerosis. *Nature,* 465**,** 223-6.

MASSEY, A., KIFFIN, R. & CUERVO, A. M. 2004. Pathophysiology of chaperone-mediated autophagy. *Int J Biochem Cell Biol,* 36**,** 2420-34.

MASSEY, D. C. & PARKES, M. 2007. Genome-wide association scanning highlights two autophagy genes, ATG16L1 and IRGM, as being significantly associated with Crohn's disease. *Autophagy,* 3**,** 649-51.

MATECIC, M., SMITH, D. L., PAN, X., MAQANI, N., BEKIRANOV, S., BOEKE, J. D. & SMITH, J. S. 2010. A microarray-based genetic screen for yeast chronological aging factors. *PLoS Genet,* 6**,** e1000921.

MATSUMOTO, G., SHIMOGORI, T., HATTORI, N. & NUKINA, N. 2015. TBK1 controls autophagosomal engulfment of polyubiquitinated mitochondria through p62/SQSTM1 phosphorylation. *Hum Mol Genet,* 24**,** 4429-42.

MATSUMOTO, G., WADA, K., OKUNO, M., KUROSAWA, M. & NUKINA, N. 2011. Serine 403 phosphorylation of p62/SQSTM1 regulates selective autophagic clearance of ubiquitinated proteins. *Mol Cell,* 44**,** 279-89.

MCEWAN, D. G. & DIKIC, I. 2015. PLEKHM1: Adapting to life at the lysosome. *Autophagy,* 11**,** 720-2.

MCEWAN, D. G., POPOVIC, D., GUBAS, A., TERAWAKI, S., SUZUKI, H., STADEL, D., COXON, F. P., MIRANDA DE STEGMANN, D., BHOGARAJU, S., MADDI, K., KIRCHOF, A., GATTI, E., HELFRICH, M. H., WAKATSUKI, S., BEHRENDS, C., PIERRE, P. & DIKIC, I. 2015. PLEKHM1 regulates autophagosome-lysosome fusion through HOPS complex and LC3/GABARAP proteins. *Mol Cell,* 57**,** 39-54.

MCKEITH, I., MINTZER, J., AARSLAND, D., BURN, D., CHIU, H., COHEN-MANSFIELD, J., DICKSON, D., DUBOIS, B., DUDA, J. E., FELDMAN, H., GAUTHIER, S., HALLIDAY, G., LAWLOR, B., LIPPA, C., LOPEZ, O. L., CARLOS MACHADO, J., O'BRIEN, J., PLAYFER, J. & REID, W. 2004. Dementia with Lewy bodies. *Lancet Neurol,* 3**,** 19-28.

MCKEITH, I. G., DICKSON, D. W., LOWE, J., EMRE, M., O'BRIEN, J. T., FELDMAN, H., CUMMINGS, J., DUDA, J. E., LIPPA, C., PERRY, E. K., AARSLAND, D., ARAI, H., BALLARD, C. G., BOEVE, B., BURN, D. J., COSTA, D., DEL SER, T., DUBOIS, B., GALASKO, D., GAUTHIER, S., GOETZ, C. G., GOMEZ-TORTOSA, E., HALLIDAY, G., HANSEN, L. A., HARDY, J., IWATSUBO, T., KALARIA, R. N., KAUFER, D., KENNY, R. A., KORCZYN, A., KOSAKA, K., LEE, V. M., LEES, A., LITVAN, I., LONDOS, E., LOPEZ, O. L., MINOSHIMA, S., MIZUNO, Y., MOLINA, J. A., MUKAETOVA-LADINSKA, E. B., PASQUIER, F., PERRY, R. H., SCHULZ, J. B.,

TROJANOWSKI, J. Q. & YAMADA, M. 2005. Diagnosis and management of dementia with Lewy bodies: third report of the DLB Consortium. *Neurology,* 65**,** 1863-72.

MENGER, K. E., JAMES, A. M., COCHEME, H. M., HARBOUR, M. E., CHOUCHANI, E. T., DING, S., FEARNLEY, I. M., PARTRIDGE, L. & MURPHY, M. P. 2015. Fasting, but Not Aging, Dramatically Alters the Redox Status of Cysteine Residues on Proteins in Drosophila melanogaster. *Cell Rep,* 11**,** 1856-65.

MENZIES, F. M., FLEMING, A., CARICASOLE, A., BENTO, C. F., ANDREWS, S. P., ASHKENAZI, A., FULLGRABE, J., JACKSON, A., JIMENEZ SANCHEZ, M., KARABIYIK, C., LICITRA, F., LOPEZ RAMIREZ, A., PAVEL, M., PURI, C., RENNA, M., RICKETTS, T., SCHLOTAWA, L., VICINANZA, M., WON, H., ZHU, Y., SKIDMORE, J. & RUBINSZTEIN, D. C. 2017. Autophagy and Neurodegeneration: Pathogenic Mechanisms and Therapeutic Opportunities. *Neuron,* 93**,** 1015-1034.

METHNER, C., CHOUCHANI, E. T., BUONINCONTRI, G., PELL, V. R., SAWIAK, S. J., MURPHY, M. P. & KRIEG, T. 2014. Mitochondria selective S-nitrosation by mitochondria-targeted S-nitrosothiol protects against post-infarct heart failure in mouse hearts. *Eur J Heart Fail,* 16**,** 712-7.

MIJALJICA, D., PRESCOTT, M. & DEVENISH, R. J. 2011. Microautophagy in mammalian cells: revisiting a 40-year-old conundrum. *Autophagy,* 7**,** 673-82.

MILLER, L., ROLLINSON, S., CALLISTER, J. B., YOUNG, K., HARRIS, J., GERHARD, A., NEARY, D., RICHARDSON, A., SNOWDEN, J., MANN, D. M. & PICKERING-BROWN, S. M. 2015. p62/SQSTM1 analysis in frontotemporal lobar degeneration. *Neurobiol Aging,* 36**,** 1603.e5-9.

MINEGISHI, Y., IEJIMA, D., KOBAYASHI, H., CHI, Z. L., KAWASE, K., YAMAMOTO, T., SEKI, T., YUASA, S., FUKUDA, K. & IWATA, T. 2013. Enhanced optineurin E50K-TBK1 interaction evokes protein insolubility and initiates familial primary open-angle glaucoma. *Hum Mol Genet,* 22**,** 3559-67.

MIZUNO, Y., AMARI, M., TAKATAMA, M., AIZAWA, H., MIHARA, B. & OKAMOTO, K. 2006. Immunoreactivities of p62, an ubiqutin-binding protein, in the spinal anterior horn cells of patients with amyotrophic lateral sclerosis. *J Neurol Sci,* 249**,** 13-8.

MIZUSHIMA, N. 2007. Autophagy: process and function. *Genes Dev,* 21**,** 2861-73.

MIZUSHIMA, N., YAMAMOTO, A., HATANO, M., KOBAYASHI, Y., KABEYA, Y., SUZUKI, K., TOKUHISA, T., OHSUMI, Y. & YOSHIMORI, T. 2001. Dissection of autophagosome formation using Apg5-deficient mouse embryonic stem cells. *J Cell Biol,* 152**,** 657-68.

MOCHIDA, K., OIKAWA, Y., KIMURA, Y., KIRISAKO, H., HIRANO, H., OHSUMI, Y. & NAKATOGAWA, H. 2015. Receptor-mediated selective autophagy degrades the endoplasmic reticulum and the nucleus. *Nature,* 522**,** 359-62.

MONASTYRSKA, I., RIETER, E., KLIONSKY, D. J. & REGGIORI, F. 2009. Multiple roles of the cytoskeleton in autophagy. *Biol Rev Camb Philos Soc,* 84**,** 431-48.

MOOKERJEE, S. A., GONCALVES, R. L., GERENCSER, A. A., NICHOLLS, D. G. & BRAND, M. D. 2015. The contributions of respiration and glycolysis to extracellular acid production. *Biochim Biophys Acta,* 1847**,** 171-81.

MOORE, A. S. & HOLZBAUR, E. L. 2016. Dynamic recruitment and activation of ALS-associated TBK1 with its target optineurin are required for efficient mitophagy. *Proc Natl Acad Sci U S A,* 113**,** E3349-58.

MORRISWOOD, B., RYZHAKOV, G., PURI, C., ARDEN, S. D., ROBERTS, R., DENDROU, C., KENDRICK-JONES, J. & BUSS, F. 2007. T6BP and NDP52 are myosin VI binding partners with potential roles in cytokine signalling and cell adhesion. *J Cell Sci,* 120**,** 2574-85.

MUNCH, C. & HARPER, J. W. 2016. Mitochondrial unfolded protein response controls matrix pre-RNA processing and translation. *Nature,* 534**,** 710-3.

MURPHY, M. P. 2009. How mitochondria produce reactive oxygen species. *Biochem J,* 417**,** 1-13.

NAGABHUSHANA, A., CHALASANI, M. L., JAIN, N., RADHA, V., RANGARAJ, N., BALASUBRAMANIAN, D. & SWARUP, G. 2010. Regulation of endocytic trafficking of transferrin receptor by optineurin and its impairment by a glaucoma-associated mutant. *BMC Cell Biol,* 11**,** 4.

NAKAGAWA, I., AMANO, A., MIZUSHIMA, N., YAMAMOTO, A., YAMAGUCHI, H., KAMIMOTO, T., NARA, A., FUNAO, J., NAKATA, M., TSUDA, K., HAMADA, S. & YOSHIMORI, T. 2004. Autophagy defends cells against invading group A Streptococcus. *Science,* 306**,** 1037-40.

NAKAI, A., YAMAGUCHI, O., TAKEDA, T., HIGUCHI, Y., HIKOSO, S., TANIIKE, M., OMIYA, S., MIZOTE, I., MATSUMURA, Y., ASAHI, M., NISHIDA, K., HORI, M., MIZUSHIMA, N. & OTSU, K. 2007. The role of autophagy in cardiomyocytes in the basal state and in response to hemodynamic stress. *Nat Med,* 13**,** 619-24.

NAKAMURA, K., KIMPLE, A. J., SIDEROVSKI, D. P. & JOHNSON, G. L. 2010. PB1 domain interaction of p62/sequestosome 1 and MEKK3 regulates NF-kappaB activation. *J Biol Chem,* 285**,** 2077-89.

NAKATOGAWA, H., ISHII, J., ASAI, E. & OHSUMI, Y. 2012. Atg4 recycles inappropriately lipidated Atg8 to promote autophagosome biogenesis. *Autophagy,* 8**,** 177-86.

NALLS, M. A., DURAN, R., LOPEZ, G., KURZAWA-AKANBI, M., MCKEITH, I. G., CHINNERY, P. F., MORRIS, C. M., THEUNS, J., CROSIERS, D., CRAS, P., ENGELBORGHS, S., DE DEYN, P. P., VAN BROECKHOVEN, C., MANN, D. M., SNOWDEN, J., PICKERING-BROWN, S., HALLIWELL, N., DAVIDSON, Y., GIBBONS, L., HARRIS, J., SHEERIN, U. M., BRAS, J., HARDY, J., CLARK, L., MARDER, K., HONIG, L. S., BERG, D., MAETZLER, W., BROCKMANN, K., GASSER, T., NOVELLINO, F., QUATTRONE, A., ANNESI, G., DE MARCO, E. V., ROGAEVA, E., MASELLIS, M., BLACK, S. E., BILBAO, J. M., FOROUD, T., GHETTI, B., NICHOLS, W. C., PANKRATZ, N., HALLIDAY, G., LESAGE, S., KLEBE, S., DURR, A., DUYCKAERTS, C., BRICE, A., GIASSON, B. I., TROJANOWSKI, J. Q., HURTIG, H. I., TAYEBI, N., LANDAZABAL, C., KNIGHT, M. A., KELLER, M., SINGLETON, A. B., WOLFSBERG, T. G. & SIDRANSKY, E. 2013. A multicenter study of glucocerebrosidase mutations in dementia with Lewy bodies. *JAMA Neurol,* 70**,** 727-35.

NARENDRA, D., KANE, L. A., HAUSER, D. N., FEARNLEY, I. M. & YOULE, R. J. 2010. p62/SQSTM1 is required for Parkin-induced mitochondrial clustering but not mitophagy; VDAC1 is dispensable for both. *Autophagy,* 6**,** 1090-106.

NARGUND, A. M., FIORESE, C. J., PELLEGRINO, M. W., DENG, P. & HAYNES, C. M. 2015. Mitochondrial and nuclear accumulation of the transcription factor ATFS-1 promotes OXPHOS recovery during the UPR(mt). *Mol Cell,* 58**,** 123-33.

NARGUND, A. M., PELLEGRINO, M. W., FIORESE, C. J., BAKER, B. M. & HAYNES, C. M. 2012. Mitochondrial import efficiency of ATFS-1 regulates mitochondrial UPR activation. *Science,* 337**,** 587-90.

NASSIF, M., VALENZUELA, V., ROJAS-RIVERA, D., VIDAL, R., MATUS, S., CASTILLO, K., FUENTEALBA, Y., KROEMER, G., LEVINE, B. & HETZ, C. 2014. Pathogenic role of BECN1/Beclin 1 in the development of amyotrophic lateral sclerosis. *Autophagy,* 10**,** 1256-71.

NATHAN, C. 2003. Specificity of a third kind: reactive oxygen and nitrogen intermediates in cell signaling. *J Clin Invest,* 111**,** 769-78.

NAVARRO, A., BOVERIS, A., BANDEZ, M. J., SANCHEZ-PINO, M. J., GOMEZ, C., MUNTANE, G. & FERRER, I. 2009. Human brain cortex: mitochondrial oxidative damage and adaptive

response in Parkinson disease and in dementia with Lewy bodies. *Free Radic Biol Med,* 46**,** 1574-80.

NEZIS, I. P., SIMONSEN, A., SAGONA, A. P., FINLEY, K., GAUMER, S., CONTAMINE, D., RUSTEN, T. E., STENMARK, H. & BRECH, A. 2008. Ref(2)P, the Drosophila melanogaster homologue of mammalian p62, is required for the formation of protein aggregates in adult brain. *J Cell Biol,* 180**,** 1065-71.

NGUYEN, T. N., PADMAN, B. S. & LAZAROU, M. 2016a. Deciphering the Molecular Signals of PINK1/Parkin Mitophagy. *Trends Cell Biol,* 26**,** 733-44.

NGUYEN, T. N., PADMAN, B. S., USHER, J., OORSCHOT, V., RAMM, G. & LAZAROU, M. 2016b. Atg8 family LC3/GABARAP proteins are crucial for autophagosome-lysosome fusion but not autophagosome formation during PINK1/Parkin mitophagy and starvation. *J Cell Biol,* 215**,** 857-874.

NIXON, R. A., WEGIEL, J., KUMAR, A., YU, W. H., PETERHOFF, C., CATALDO, A. & CUERVO, A. M. 2005. Extensive involvement of autophagy in Alzheimer disease: an immuno-electron microscopy study. *J Neuropathol Exp Neurol,* 64**,** 113-22.

NODA, T. & OHSUMI, Y. 1998. Tor, a phosphatidylinositol kinase homologue, controls autophagy in yeast. *J Biol Chem,* 273**,** 3963-6.

NOGUEIRA, V., PARK, Y., CHEN, C. C., XU, P. Z., CHEN, M. L., TONIC, I., UNTERMAN, T. & HAY, N. 2008. Akt determines replicative senescence and oxidative or oncogenic premature senescence and sensitizes cells to oxidative apoptosis. *Cancer Cell,* 14**,** 458-70.

NOVAK, I. & DIKIC, I. 2011. Autophagy receptors in developmental clearance of mitochondria. *Autophagy,* 7**,** 301-3.

NUNNARI, J. & SUOMALAINEN, A. 2012. Mitochondria: in sickness and in health. *Cell,* 148**,** 1145-59.

OGATA, M., HINO, S., SAITO, A., MORIKAWA, K., KONDO, S., KANEMOTO, S., MURAKAMI, T., TANIGUCHI, M., TANII, I., YOSHINAGA, K., SHIOSAKA, S., HAMMARBACK, J. A., URANO, F. & IMAIZUMI, K. 2006. Autophagy is activated for cell survival after endoplasmic reticulum stress. *Mol Cell Biol,* 26**,** 9220-31.

OHTSUKA, H., TAKAHASHI, R. & GOTO, S. 1995. Age-related accumulation of high-molecular-weight ubiquitin protein conjugates in mouse brains. *J Gerontol A Biol Sci Med Sci,* 50**,** B277-81.

OKATSU, K., KOYANO, F., KIMURA, M., KOSAKO, H., SAEKI, Y., TANAKA, K. & MATSUDA, N. 2015. Phosphorylated ubiquitin chain is the genuine Parkin receptor. *J Cell Biol,* 209**,** 111-28.

OKUNO, D., IINO, R. & NOJI, H. 2011. Rotation and structure of FoF1-ATP synthase. *J Biochem,* 149**,** 655-64.

OLAHOVA, M., TAYLOR, S. R., KHAZAIPOUL, S., WANG, J., MORGAN, B. A., MATSUMOTO, K., BLACKWELL, T. K. & VEAL, E. A. 2008. A redox-sensitive peroxiredoxin that is important for longevity has tissue- and stress-specific roles in stress resistance. *Proc Natl Acad Sci U S A,* 105**,** 19839-44.

ORDUREAU, A., HEO, J. M., DUDA, D. M., PAULO, J. A., OLSZEWSKI, J. L., YANISHEVSKI, D., RINEHART, J., SCHULMAN, B. A. & HARPER, J. W. 2015. Defining roles of PARKIN and ubiquitin phosphorylation by PINK1 in mitochondrial quality control using a ubiquitin replacement strategy. *Proc Natl Acad Sci U S A,* 112**,** 6637-42.

ORDUREAU, A., SARRAF, S. A., DUDA, D. M., HEO, J. M., JEDRYCHOWSKI, M. P., SVIDERSKIY, V. O., OLSZEWSKI, J. L., KOERBER, J. T., XIE, T., BEAUSOLEIL, S. A., WELLS, J. A., GYGI, S. P., SCHULMAN, B. A. & HARPER, J. W. 2014. Quantitative proteomics reveal a feedforward mechanism for mitochondrial PARKIN translocation and ubiquitin chain synthesis. *Mol Cell,* 56**,** 360-75.

ORR, A. L., VARGAS, L., TURK, C. N., BAATEN, J. E., MATZEN, J. T., DARDOV, V. J., ATTLE, S. J., LI, J., QUACKENBUSH, D. C., GONCALVES, R. L., PEREVOSHCHIKOVA, I. V., PETRASSI, H. M., MEEUSEN, S. L., AINSCOW, E. K. & BRAND, M. D. 2015. Suppressors of superoxide production from mitochondrial complex III. *Nat Chem Biol,* 11**,** 834-6.

ORVEDAHL, A., MACPHERSON, S., SUMPTER, R., JR., TALLOCZY, Z., ZOU, Z. & LEVINE, B. 2010. Autophagy protects against Sindbis virus infection of the central nervous system. *Cell Host Microbe,* 7**,** 115-27.

OSAWA, T., MIZUNO, Y., FUJITA, Y., TAKATAMA, M., NAKAZATO, Y. & OKAMOTO, K. 2011. Optineurin in neurodegenerative diseases. *Neuropathology,* 31**,** 569-74.

OVERBYE, A., FENGSRUD, M. & SEGLEN, P. O. 2007. Proteomic analysis of membrane-associated proteins from rat liver autophagosomes. *Autophagy,* 3**,** 300-22.

OWUSU-ANSAH, E., SONG, W. & PERRIMON, N. 2013. Muscle mitohormesis promotes longevity via systemic repression of insulin signaling. *Cell,* 155**,** 699-712.

PANKIV, S., CLAUSEN, T. H., LAMARK, T., BRECH, A., BRUUN, J. A., OUTZEN, H., OVERVATN, A., BJORKOY, G. & JOHANSEN, T. 2007. p62/SQSTM1 binds directly to Atg8/LC3 to facilitate degradation of ubiquitinated protein aggregates by autophagy. *J Biol Chem,* 282**,** 24131-45.

PANKIV, S., LAMARK, T., BRUUN, J. A., OVERVATN, A., BJORKOY, G. & JOHANSEN, T. 2010. Nucleocytoplasmic shuttling of p62/SQSTM1 and its role in recruitment of nuclear polyubiquitinated proteins to promyelocytic leukemia bodies. *J Biol Chem,* 285**,** 5941-53.

PAPA, L. & GERMAIN, D. 2011. Estrogen receptor mediates a distinct mitochondrial unfolded protein response. *J Cell Sci,* 124**,** 1396-402.

PAPINSKI, D. & KRAFT, C. 2016. Regulation of Autophagy By Signaling Through the Atg1/ULK1 Complex. *J Mol Biol,* 428**,** 1725-41.

PAPINSKI, D., SCHUSCHNIG, M., REITER, W., WILHELM, L., BARNES, C. A., MAIOLICA, A., HANSMANN, I., PFAFFENWIMMER, T., KIJANSKA, M., STOFFEL, I., LEE, S. S., BREZOVICH, A., LOU, J. H., TURK, B. E., AEBERSOLD, R., AMMERER, G., PETER, M. & KRAFT, C. 2014. Early steps in autophagy depend on direct phosphorylation of Atg9 by the Atg1 kinase. *Mol Cell,* 53**,** 471-83.

PARK, B., YING, H., SHEN, X., PARK, J. S., QIU, Y., SHYAM, R. & YUE, B. Y. 2010. Impairment of protein trafficking upon overexpression and mutation of optineurin. *PLoS One,* 5**,** e11547.

PARK, J. M., JUNG, C. H., SEO, M., OTTO, N. M., GRUNWALD, D., KIM, K. H., MORIARITY, B., KIM, Y. M., STARKER, C., NHO, R. S., VOYTAS, D. & KIM, D. H. 2016. The ULK1 complex mediates MTORC1 signaling to the autophagy initiation machinery via binding and phosphorylating ATG14. *Autophagy,* 12**,** 547-64.

PARKINSON, N., INCE, P. G., SMITH, M. O., HIGHLEY, R., SKIBINSKI, G., ANDERSEN, P. M., MORRISON, K. E., PALL, H. S., HARDIMAN, O., COLLINGE, J., SHAW, P. J. & FISHER, E. M. 2006. ALS phenotypes with mutations in CHMP2B (charged multivesicular body protein 2B). *Neurology,* 67**,** 1074-7.

PAULSEN, C. E. & CARROLL, K. S. 2013. Cysteine-mediated redox signaling: chemistry, biology, and tools for discovery. *Chem Rev,* 113**,** 4633-79.

PETERS, O. M., GHASEMI, M. & BROWN, R. H., JR. 2015. Emerging mechanisms of molecular pathology in ALS. *J Clin Invest,* 125**,** 2548.

PETIOT, A., OGIER-DENIS, E., BLOMMAART, E. F., MEIJER, A. J. & CODOGNO, P. 2000. Distinct classes of phosphatidylinositol 3'-kinases are involved in signaling pathways that control macroautophagy in HT-29 cells. *J Biol Chem,* 275**,** 992-8.

PICKFORD, F., MASLIAH, E., BRITSCHGI, M., LUCIN, K., NARASIMHAN, R., JAEGER, P. A., SMALL, S., SPENCER, B., ROCKENSTEIN, E., LEVINE, B. & WYSS-CORAY, T. 2008. The autophagy-related protein beclin 1 shows reduced expression in early Alzheimer disease and regulates amyloid beta accumulation in mice. *J Clin Invest,* 118**,** 2190-9.

PIKKARAINEN, M., HARTIKAINEN, P., SOININEN, H. & ALAFUZOFF, I. 2011. Distribution and pattern of pathology in subjects with familial or sporadic late-onset cerebellar ataxia as assessed by p62/sequestosome immunohistochemistry. *Cerebellum,* 10**,** 720-31.

PIMENTA DE CASTRO, I., COSTA, A. C., LAM, D., TUFI, R., FEDELE, V., MOISOI, N., DINSDALE, D., DEAS, E., LOH, S. H. & MARTINS, L. M. 2012. Genetic analysis of mitochondrial protein misfolding in Drosophila melanogaster. *Cell Death Differ,* 19**,** 1308-16.

PIWKO, W. & JENTSCH, S. 2006. Proteasome-mediated protein processing by bidirectional degradation initiated from an internal site. *Nat Struct Mol Biol,* 13**,** 691-7.

POOLE, L. B. 2015. The basics of thiols and cysteines in redox biology and chemistry. *Free Radic Biol Med,* 80**,** 148-57.

POTENZA, E., DI DOMENICO, T., WALSH, I. & TOSATTO, S. C. 2015. MobiDB 2.0: an improved database of intrinsically disordered and mobile proteins. *Nucleic Acids Res,* 43**,** D315-20.

POTTIER, C., BIENIEK, K. F., FINCH, N., VAN DE VORST, M., BAKER, M., PERKERSEN, R., BROWN, P., RAVENSCROFT, T., VAN BLITTERSWIJK, M., NICHOLSON, A. M., DETURE, M., KNOPMAN, D. S., JOSEPHS, K. A., PARISI, J. E., PETERSEN, R. C., BOYLAN, K. B., BOEVE, B. F., GRAFF-RADFORD, N. R., VELTMAN, J. A., GILISSEN, C., MURRAY, M. E., DICKSON, D. W. & RADEMAKERS, R. 2015. Whole-genome sequencing reveals important role for TBK1 and OPTN mutations in frontotemporal lobar degeneration without motor neuron disease. *Acta Neuropathol,* 130**,** 77-92.

POTTING, C., WILMES, C., ENGMANN, T., OSMAN, C. & LANGER, T. 2010. Regulation of mitochondrial phospholipids by Ups1/PRELI-like proteins depends on proteolysis and Mdm35. *Embo j,* 29**,** 2888-98.

PRYDE, K. R., TAANMAN, J. W. & SCHAPIRA, A. H. 2016. A LON-ClpP Proteolytic Axis Degrades Complex I to Extinguish ROS Production in Depolarized Mitochondria. *Cell Rep,* 17**,** 2522-2531.

PY, B. F., LIPINSKI, M. M. & YUAN, J. 2007. Autophagy limits Listeria monocytogenes intracellular growth in the early phase of primary infection. *Autophagy,* 3**,** 117-25.

PYO, J. O., YOO, S. M., AHN, H. H., NAH, J., HONG, S. H., KAM, T. I., JUNG, S. & JUNG, Y. K. 2013. Overexpression of Atg5 in mice activates autophagy and extends lifespan. *Nat Commun,* 4**,** 2300.

QUIROS, P. M., LANGER, T. & LOPEZ-OTIN, C. 2015. New roles for mitochondrial proteases in health, ageing and disease. *Nat Rev Mol Cell Biol,* 16**,** 345-59.

RADKE, S., CHANDER, H., SCHAFER, P., MEISS, G., KRUGER, R., SCHULZ, J. B. & GERMAIN, D. 2008. Mitochondrial protein quality control by the proteasome involves ubiquitination and the protease Omi. *J Biol Chem,* 283**,** 12681-5.

RADTKE, A. L., DELBRIDGE, L. M., BALACHANDRAN, S., BARBER, G. N. & O'RIORDAN, M. X. 2007. TBK1 protects vacuolar integrity during intracellular bacterial infection. *PLoS Pathog,* 3**,** e29.

RAHIGHI, S. & DIKIC, I. 2012. Selectivity of the ubiquitin-binding modules. *FEBS Lett,* 586**,** 2705-10.

RAHIGHI, S., IKEDA, F., KAWASAKI, M., AKUTSU, M., SUZUKI, N., KATO, R., KENSCHE, T., UEJIMA, T., BLOOR, S., KOMANDER, D., RANDOW, F., WAKATSUKI, S. & DIKIC, I. 2009. Specific recognition of linear ubiquitin chains by NEMO is important for NF-kappaB activation. *Cell,* 136**,** 1098-109.

RAMESH BABU, J., LAMAR SEIBENHENER, M., PENG, J., STROM, A. L., KEMPPAINEN, R., COX, N., ZHU, H., WOOTEN, M. C., DIAZ-MECO, M. T., MOSCAT, J. & WOOTEN, M. W. 2008. Genetic inactivation of p62 leads to accumulation of hyperphosphorylated tau and neurodegeneration. *J Neurochem,* 106**,** 107-20.

RANDOW, F. & YOULE, R. J. 2014. Self and nonself: how autophagy targets mitochondria and bacteria. *Cell Host Microbe,* 15**,** 403-11.

RAO, Y., PERNA, M. G., HOFMANN, B., BEIER, V. & WOLLERT, T. 2016. The Atg1-kinase complex tethers Atg9-vesicles to initiate autophagy. *Nat Commun,* 7**,** 10338.

RAVID, T. & HOCHSTRASSER, M. 2008. Diversity of degradation signals in the ubiquitin-proteasome system. *Nat Rev Mol Cell Biol,* 9**,** 679-90.

RAVIKUMAR, B., DUDEN, R. & RUBINSZTEIN, D. C. 2002. Aggregate-prone proteins with polyglutamine and polyalanine expansions are degraded by autophagy. *Hum Mol Genet,* 11**,** 1107-17.

REA, S. L., MAJCHER, V., SEARLE, M. S. & LAYFIELD, R. 2014. SQSTM1 mutations--bridging Paget disease of bone and ALS/FTLD. *Exp Cell Res,* 325**,** 27-37.

REA, S. L., WALSH, J. P., LAYFIELD, R., RATAJCZAK, T. & XU, J. 2013. New Insights Into the Role of Sequestosome 1/p62 Mutant Proteins in the Pathogenesis of Paget's Disease of Bone. *Endocr Rev*.

REA, S. L., WALSH, J. P., WARD, L., MAGNO, A. L., WARD, B. K., SHAW, B., LAYFIELD, R., KENT, G. N., XU, J. & RATAJCZAK, T. 2009. Sequestosome 1 mutations in Paget's disease of bone in Australia: prevalence, genotype/phenotype correlation, and a novel non-UBA domain mutation (P364S) associated with increased NF-kappaB signaling without loss of ubiquitin binding. *J Bone Miner Res,* 24**,** 1216-23.

REDHEAD, M., SATCHELL, R., MORKUNAITE, V., SWIFT, D., PETRAUSKAS, V., GOLDING, E., ONIONS, S., MATULIS, D. & UNITT, J. 2015. A combinatorial biophysical approach; FTSA and SPR for identifying small molecule ligands and PAINs. *Anal Biochem,* 479**,** 63-73.

REEVE, A. K., LUDTMANN, M. H., ANGELOVA, P. R., SIMCOX, E. M., HORROCKS, M. H., KLENERMAN, D., GANDHI, S., TURNBULL, D. M. & ABRAMOV, A. Y. 2015. Aggregated alpha-synuclein and complex I deficiency: exploration of their relationship in differentiated neurons. *Cell Death Dis,* 6**,** e1820.

RENTON, A. E., MAJOUNIE, E., WAITE, A., SIMON-SANCHEZ, J., ROLLINSON, S., GIBBS, J. R., SCHYMICK, J. C., LAAKSOVIRTA, H., VAN SWIETEN, J. C., MYLLYKANGAS, L., KALIMO, H., PAETAU, A., ABRAMZON, Y., REMES, A. M., KAGANOVICH, A., SCHOLZ, S. W., DUCKWORTH, J., DING, J., HARMER, D. W., HERNANDEZ, D. G., JOHNSON, J. O., MOK, K., RYTEN, M., TRABZUNI, D., GUERREIRO, R. J., ORRELL, R. W., NEAL, J., MURRAY, A., PEARSON, J., JANSEN, I. E., SONDERVAN, D., SEELAAR, H., BLAKE, D., YOUNG, K., HALLIWELL, N., CALLISTER, J. B., TOULSON, G., RICHARDSON, A., GERHARD, A., SNOWDEN, J., MANN, D., NEARY, D., NALLS, M. A., PEURALINNA, T., JANSSON, L., ISOVIITA, V. M., KAIVORINNE, A. L., HOLTTA-VUORI, M., IKONEN, E., SULKAVA, R., BENATAR, M., WUU, J., CHIO, A., RESTAGNO, G., BORGHERO, G., SABATELLI, M., HECKERMAN, D., ROGAEVA, E., ZINMAN, L., ROTHSTEIN, J. D., SENDTNER, M., DREPPER, C., EICHLER, E. E., ALKAN, C., ABDULLAEV, Z., PACK, S. D., DUTRA, A., PAK, E., HARDY, J., SINGLETON, A., WILLIAMS, N. M., HEUTINK, P., PICKERING-BROWN, S., MORRIS, H. R., TIENARI, P. J. & TRAYNOR, B. J. 2011. A hexanucleotide repeat expansion in C9ORF72 is the cause of chromosome 9p21-linked ALS-FTD. *Neuron,* 72**,** 257-68.

REZAIE, T., CHILD, A., HITCHINGS, R., BRICE, G., MILLER, L., COCA-PRADOS, M., HEON, E., KRUPIN, T., RITCH, R., KREUTZER, D., CRICK, R. P. & SARFARAZI, M. 2002. Adult-onset

primary open-angle glaucoma caused by mutations in optineurin. *Science,* 295**,** 1077-9.

RHEE, S. G., KANG, S. W., CHANG, T. S., JEONG, W. & KIM, K. 2001. Peroxiredoxin, a novel family of peroxidases. *IUBMB Life,* 52**,** 35-41.

RHEIN, V., BAYSANG, G., RAO, S., MEIER, F., BONERT, A., MULLER-SPAHN, F. & ECKERT, A. 2009. Amyloid-beta leads to impaired cellular respiration, energy production and mitochondrial electron chain complex activities in human neuroblastoma cells. *Cell Mol Neurobiol,* 29**,** 1063-71.

RICHTER, B., SLITER, D. A., HERHAUS, L., STOLZ, A., WANG, C., BELI, P., ZAFFAGNINI, G., WILD, P., MARTENS, S., WAGNER, S. A., YOULE, R. J. & DIKIC, I. 2016. Phosphorylation of OPTN by TBK1 enhances its binding to Ub chains and promotes selective autophagy of damaged mitochondria. *Proc Natl Acad Sci U S A,* 113**,** 4039-44.

ROBINSON, B. H., PETROVA-BENEDICT, R., BUNCIC, J. R. & WALLACE, D. C. 1992. Nonviability of cells with oxidative defects in galactose medium: a screening test for affected patient fibroblasts. *Biochem Med Metab Biol,* 48**,** 122-6.

ROBINSON, J. M. 2008. Reactive oxygen species in phagocytic leukocytes. *Histochemistry and Cell Biology,* 130**,** 281-297.

ROGOV, V. V., STOLZ, A., RAVICAHANDRAN, A. C., RIOS-SZWED, D. O., SUZUKI, H., KNISS, A., LOHR, F., WAKATSUKI, S., DOTSCH, V., DIKIC, I., DOBSON, R. C. & MCEWAN, D. G. 2017. Structural and functional analysis of the GABARAP interaction motif (GIM). *EMBO Rep*.

ROLLINSON, S., BENNION, J., TOULSON, G., HALLIWELL, N., USHER, S., SNOWDEN, J., RICHARDSON, A., NEARY, D., MANN, D. & PICKERING-BROWN, S. M. 2012. Analysis of optineurin in frontotemporal lobar degeneration. *Neurobiol Aging,* 33**,** 425.e1-2.

ROSEN, D. R., SIDDIQUE, T., PATTERSON, D., FIGLEWICZ, D. A., SAPP, P., HENTATI, A., DONALDSON, D., GOTO, J., O'REGAN, J. P., DENG, H. X. & ET AL. 1993. Mutations in Cu/Zn superoxide dismutase gene are associated with familial amyotrophic lateral sclerosis. *Nature,* 362**,** 59-62.

ROSS, C. A. & POIRIER, M. A. 2005. Opinion: What is the role of protein aggregation in neurodegeneration? *Nat Rev Mol Cell Biol,* 6**,** 891-8.

ROSSIGNOL, R., GILKERSON, R., AGGELER, R., YAMAGATA, K., REMINGTON, S. J. & CAPALDI, R. A. 2004. Energy substrate modulates mitochondrial structure and oxidative capacity in cancer cells. *Cancer Res,* 64**,** 985-93.

RUAN, L., ZHOU, C., JIN, E., KUCHARAVY, A., ZHANG, Y., WEN, Z., FLORENS, L. & LI, R. 2017. Cytosolic proteostasis through importing of misfolded proteins into mitochondria. *Nature,* 543**,** 443-446.

RUBINO, E., RAINERO, I., CHIO, A., ROGAEVA, E., GALIMBERTI, D., FENOGLIO, P., GRINBERG, Y., ISAIA, G., CALVO, A., GENTILE, S., BRUNI, A. C., ST GEORGE-HYSLOP, P. H., SCARPINI, E., GALLONE, S. & PINESSI, L. 2012. SQSTM1 mutations in frontotemporal lobar degeneration and amyotrophic lateral sclerosis. *Neurology,* 79**,** 1556-62.

RUBINSZTEIN, D. C., CODOGNO, P. & LEVINE, B. 2012. Autophagy modulation as a potential therapeutic target for diverse diseases. *Nat Rev Drug Discov,* 11**,** 709-30.

RUBINSZTEIN, D. C., DIFIGLIA, M., HEINTZ, N., NIXON, R. A., QIN, Z. H., RAVIKUMAR, B., STEFANIS, L. & TOLKOVSKY, A. 2005. Autophagy and its possible roles in nervous system diseases, damage and repair. *Autophagy,* 1**,** 11-22.

RUBINSZTEIN, D. C., MARINO, G. & KROEMER, G. 2011. Autophagy and aging. *Cell,* 146**,** 682-95.

RUSSELL, R. C., TIAN, Y., YUAN, H., PARK, H. W., CHANG, Y. Y., KIM, J., KIM, H., NEUFELD, T. P., DILLIN, A. & GUAN, K. L. 2013. ULK1 induces autophagy by phosphorylating Beclin-1 and activating VPS34 lipid kinase. *Nat Cell Biol,* 15**,** 741-50.

SAITOH, Y., FUJIKAKE, N., OKAMOTO, Y., POPIEL, H. A., HATANAKA, Y., UEYAMA, M., SUZUKI, M., GAUMER, S., MURATA, M., WADA, K. & NAGAI, Y. 2015. p62 Plays a Protective Role in the Autophagic Degradation of Polyglutamine Protein Oligomers in Polyglutamine Disease Model Flies. *J Biol Chem,* 290**,** 1442-53.

SALAWU, F. K., UMAR, J. T. & OLOKOBA, A. B. 2011. Alzheimer's disease: a review of recent developments. *Ann Afr Med,* 10**,** 73-9.

SANZ, L., DIAZ-MECO, M. T., NAKANO, H. & MOSCAT, J. 2000. The atypical PKC-interacting protein p62 channels NF-kappaB activation by the IL-1-TRAF6 pathway. *EMBO J,* 19**,** 1576-86.

SARKAR, S., CARROLL, B., BUGANIM, Y., MAETZEL, D., NG, A. H., CASSADY, J. P., COHEN, M. A., CHAKRABORTY, S., WANG, H., SPOONER, E., PLOEGH, H., GSPONER, J., KOROLCHUK, V. I. & JAENISCH, R. 2013. Impaired autophagy in the lipid-storage disorder Niemann-Pick type C1 disease. *Cell Rep,* 5**,** 1302-15.

SARRAF, S. A., RAMAN, M., GUARANI-PEREIRA, V., SOWA, M. E., HUTTLIN, E. L., GYGI, S. P. & HARPER, J. W. 2013. Landscape of the PARKIN-dependent ubiquitylome in response to mitochondrial depolarization. *Nature,* 496**,** 372-6.

SAXTON, R. A., KNOCKENHAUER, K. E., WOLFSON, R. L., CHANTRANUPONG, L., PACOLD, M. E., WANG, T., SCHWARTZ, T. U. & SABATINI, D. M. 2016. Structural basis for leucine sensing by the Sestrin2-mTORC1 pathway. *Science,* 351**,** 53-8.

SAZANOV, L. A. 2015. A giant molecular proton pump: structure and mechanism of respiratory complex I. *Nat Rev Mol Cell Biol,* 16**,** 375-88.

SCHAGGER, H., DE COO, R., BAUER, M. F., HOFMANN, S., GODINOT, C. & BRANDT, U. 2004. Significance of respirasomes for the assembly/stability of human respiratory chain complex I. *J Biol Chem,* 279**,** 36349-53.

SCHAGGER, H. & PFEIFFER, K. 2001. The ratio of oxidative phosphorylation complexes I-V in bovine heart mitochondria and the composition of respiratory chain supercomplexes. *J Biol Chem,* 276**,** 37861-7.

SCHAPANSKY, J., NARDOZZI, J. D., FELIZIA, F. & LAVOIE, M. J. 2014. Membrane recruitment of endogenous LRRK2 precedes its potent regulation of autophagy. *Hum Mol Genet,* 23**,** 4201-14.

SCHAPANSKY, J., NARDOZZI, J. D. & LAVOIE, M. J. 2015. The complex relationships between microglia, alpha-synuclein, and LRRK2 in Parkinson's disease. *Neuroscience,* 302**,** 74-88.

SCHAPIRA, A. H. 1998. Human complex I defects in neurodegenerative diseases. *Biochim Biophys Acta,* 1364**,** 261-70.

SCHAPIRA, A. H. 2010. Complex I: inhibitors, inhibition and neurodegeneration. *Exp Neurol,* 224**,** 331-5.

SCHAPIRA, A. H. 2012. Mitochondrial diseases. *Lancet,* 379**,** 1825-34.

SCHAPIRA, A. H., COOPER, J. M., DEXTER, D., JENNER, P., CLARK, J. B. & MARSDEN, C. D. 1989. Mitochondrial complex I deficiency in Parkinson's disease. *Lancet,* 1**,** 1269.

SCHARFENBERG, F., SEREK-HEUBERGER, J., COLES, M., HARTMANN, M. D., HABECK, M., MARTIN, J., LUPAS, A. N. & ALVA, V. 2015. Structure and evolution of N-domains in AAA metalloproteases. *J Mol Biol,* 427**,** 910-23.

SCHERZ-SHOUVAL, R., SHVETS, E., FASS, E., SHORER, H., GIL, L. & ELAZAR, Z. 2007. Reactive oxygen species are essential for autophagy and specifically regulate the activity of Atg4. *EMBO J,* 26**,** 1749-60.

SCHNEIDMAN-DUHOVNY, D., INBAR, Y., NUSSINOV, R. & WOLFSON, H. J. 2005. PatchDock and SymmDock: servers for rigid and symmetric docking. *Nucleic Acids Res,* 33**,** W363-7.

SCIALO, F., SRIRAM, A., FERNANDEZ-AYALA, D., GUBINA, N., LOHMUS, M., NELSON, G., LOGAN, A., COOPER, H. M., NAVAS, P., ENRIQUEZ, J. A., MURPHY, M. P. & SANZ, A. 2016. Mitochondrial ROS Produced via Reverse Electron Transport Extend Animal Lifespan. *Cell Metab,* 23**,** 725-34.

SCOTT, R. C., SCHULDINER, O. & NEUFELD, T. P. 2004. Role and regulation of starvation-induced autophagy in the Drosophila fat body. *Dev Cell,* 7**,** 167-78.

SCOTTER, E. L., VANCE, C., NISHIMURA, A. L., LEE, Y. B., CHEN, H. J., URWIN, H., SARDONE, V., MITCHELL, J. C., ROGELJ, B., RUBINSZTEIN, D. C. & SHAW, C. E. 2014. Differential roles of the ubiquitin proteasome system and autophagy in the clearance of soluble and aggregated TDP-43 species. *J Cell Sci,* 127**,** 1263-78.

SEGREF, A., KEVEI, E., POKRZYWA, W., SCHMEISSER, K., MANSFELD, J., LIVNAT-LEVANON, N., ENSENAUER, R., GLICKMAN, M. H., RISTOW, M. & HOPPE, T. 2014. Pathogenesis of human mitochondrial diseases is modulated by reduced activity of the ubiquitin/proteasome system. *Cell Metab,* 19**,** 642-52.

SEO, B. B., KITAJIMA-IHARA, T., CHAN, E. K., SCHEFFLER, I. E., MATSUNO-YAGI, A. & YAGI, T. 1998. Molecular remedy of complex I defects: rotenone-insensitive internal NADH-quinone oxidoreductase of Saccharomyces cerevisiae mitochondria restores the NADH oxidase activity of complex I-deficient mammalian cells. *Proc Natl Acad Sci U S A,* 95**,** 9167-71.

SHIBA-FUKUSHIMA, K., INOSHITA, T., HATTORI, N. & IMAI, Y. 2014. PINK1-mediated phosphorylation of Parkin boosts Parkin activity in Drosophila. *PLoS Genet,* 10**,** e1004391.

SHIMIZU, Y., TARABORRELLI, L. & WALCZAK, H. 2015. Linear ubiquitination in immunity. *Immunol Rev,* 266**,** 190-207.

SHIN, J. H., KO, H. S., KANG, H., LEE, Y., LEE, Y. I., PLETINKOVA, O., TROCONSO, J. C., DAWSON, V. L. & DAWSON, T. M. 2011. PARIS (ZNF746) repression of PGC-1alpha contributes to neurodegeneration in Parkinson's disease. *Cell,* 144**,** 689-702.

SIES, H. 2017. Hydrogen peroxide as a central redox signaling molecule in physiological oxidative stress: Oxidative eustress. *Redox Biol,* 11**,** 613-619.

SIMONSEN, A., CUMMING, R. C., BRECH, A., ISAKSON, P., SCHUBERT, D. R. & FINLEY, K. D. 2008. Promoting basal levels of autophagy in the nervous system enhances longevity and oxidant resistance in adult Drosophila. *Autophagy,* 4**,** 176-84.

SIROHI, K. & SWARUP, G. 2016. Defects in autophagy caused by glaucoma-associated mutations in optineurin. *Exp Eye Res,* 144**,** 54-63.

SKIBINSKI, G., PARKINSON, N. J., BROWN, J. M., CHAKRABARTI, L., LLOYD, S. L., HUMMERICH, H., NIELSEN, J. E., HODGES, J. R., SPILLANTINI, M. G., THUSGAARD, T., BRANDNER, S., BRUN, A., ROSSOR, M. N., GADE, A., JOHANNSEN, P., SORENSEN, S. A., GYDESEN, S., FISHER, E. M. & COLLINGE, J. 2005. Mutations in the endosomal ESCRTIII-complex subunit CHMP2B in frontotemporal dementia. *Nat Genet,* 37**,** 806-8.

SOBOTTA, M. C., LIOU, W., STOCKER, S., TALWAR, D., OEHLER, M., RUPPERT, T., SCHARF, A. N. & DICK, T. P. 2015. Peroxiredoxin-2 and STAT3 form a redox relay for H2O2 signaling. *Nat Chem Biol,* 11**,** 64-70.

SONG, Z., CHEN, H., FIKET, M., ALEXANDER, C. & CHAN, D. C. 2007. OPA1 processing controls mitochondrial fusion and is regulated by mRNA splicing, membrane potential, and Yme1L. *J Cell Biol,* 178**,** 749-55.

SPILLANTINI, M. G., SCHMIDT, M. L., LEE, V. M., TROJANOWSKI, J. Q., JAKES, R. & GOEDERT, M. 1997. Alpha-synuclein in Lewy bodies. *Nature,* 388**,** 839-40.

STEFANI, M. & DOBSON, C. M. 2003. Protein aggregation and aggregate toxicity: new insights into protein folding, misfolding diseases and biological evolution. *J Mol Med (Berl),* 81**,** 678-99.

STEGLICH, G., NEUPERT, W. & LANGER, T. 1999. Prohibitins regulate membrane protein degradation by the m-AAA protease in mitochondria. *Mol Cell Biol,* 19**,** 3435-42.

STEVENS, D. A., LEE, Y., KANG, H. C., LEE, B. D., LEE, Y. I., BOWER, A., JIANG, H., KANG, S. U., ANDRABI, S. A., DAWSON, V. L., SHIN, J. H. & DAWSON, T. M. 2015. Parkin loss leads to PARIS-dependent declines in mitochondrial mass and respiration. *Proc Natl Acad Sci U S A,* 112**,** 11696-701.

STIBUREK, L., CESNEKOVA, J., KOSTKOVA, O., FORNUSKOVA, D., VINSOVA, K., WENCHICH, L., HOUSTEK, J. & ZEMAN, J. 2012. YME1L controls the accumulation of respiratory chain subunits and is required for apoptotic resistance, cristae morphogenesis, and cell proliferation. *Mol Biol Cell,* 23**,** 1010-23.

STROUD, D. A., SURGENOR, E. E., FORMOSA, L. E., RELJIC, B., FRAZIER, A. E., DIBLEY, M. G., OSELLAME, L. D., STAIT, T., BEILHARZ, T. H., THORBURN, D. R., SALIM, A. & RYAN, M. T. 2016. Accessory subunits are integral for assembly and function of human mitochondrial complex I. *Nature,* 538**,** 123-126.

SUN, N., YOULE, R. J. & FINKEL, T. 2016. The Mitochondrial Basis of Aging. *Mol Cell,* 61**,** 654-66.

SUZUKI, S. W., YAMAMOTO, H., OIKAWA, Y., KONDO-KAKUTA, C., KIMURA, Y., HIRANO, H. & OHSUMI, Y. 2015. Atg13 HORMA domain recruits Atg9 vesicles during autophagosome formation. *Proc Natl Acad Sci U S A,* 112**,** 3350-5.

TAFURI, F., RONCHI, D., MAGRI, F., COMI, G. P. & CORTI, S. 2015. SOD1 misplacing and mitochondrial dysfunction in amyotrophic lateral sclerosis pathogenesis. *Front Cell Neurosci,* 9**,** 336.

TAGUCHI, K., FUJIKAWA, N., KOMATSU, M., ISHII, T., UNNO, M., AKAIKE, T., MOTOHASHI, H. & YAMAMOTO, M. 2012. Keap1 degradation by autophagy for the maintenance of redox homeostasis. *Proc Natl Acad Sci U S A,* 109**,** 13561-6.

TAN, J. M., WONG, E. S., KIRKPATRICK, D. S., PLETNIKOVA, O., KO, H. S., TAY, S. P., HO, M. W., TRONCOSO, J., GYGI, S. P., LEE, M. K., DAWSON, V. L., DAWSON, T. M. & LIM, K. L. 2008. Lysine 63-linked ubiquitination promotes the formation and autophagic clearance of protein inclusions associated with neurodegenerative diseases. *Hum Mol Genet,* 17**,** 431-9.

TANAKA, A., CLELAND, M. M., XU, S., NARENDRA, D. P., SUEN, D. F., KARBOWSKI, M. & YOULE, R. J. 2010. Proteasome and p97 mediate mitophagy and degradation of mitofusins induced by Parkin. *J Cell Biol,* 191**,** 1367-80.

TANIDA, I., SOU, Y. S., EZAKI, J., MINEMATSU-IKEGUCHI, N., UENO, T. & KOMINAMI, E. 2004. HsAtg4B/HsApg4B/autophagin-1 cleaves the carboxyl termini of three human Atg8 homologues and delipidates microtubule-associated protein light chain 3- and GABAA receptor-associated protein-phospholipid conjugates. *J Biol Chem,* 279**,** 36268-76.

TAYLOR, E. B. & RUTTER, J. 2011. Mitochondrial quality control by the ubiquitin-proteasome system. *Biochem Soc Trans,* 39**,** 1509-13.

TEYSSOU, E., TAKEDA, T., LEBON, V., BOILLEE, S., DOUKOURE, B., BATAILLON, G., SAZDOVITCH, V., CAZENEUVE, C., MEININGER, V., LEGUERN, E., SALACHAS, F., SEILHEAN, D. & MILLECAMPS, S. 2013. Mutations in SQSTM1 encoding p62 in amyotrophic lateral sclerosis: genetics and neuropathology. *Acta Neuropathol,* 125**,** 511-22.

THIMMULAPPA, R. K., MAI, K. H., SRISUMA, S., KENSLER, T. W., YAMAMOTO, M. & BISWAL, S. 2002. Identification of Nrf2-regulated genes induced by the chemopreventive agent sulforaphane by oligonucleotide microarray. *Cancer Res,* 62**,** 5196-203.

THURSTON, T. L., BOYLE, K. B., ALLEN, M., RAVENHILL, B. J., KARPIYEVICH, M., BLOOR, S., KAUL, A., NOAD, J., FOEGLEIN, A., MATTHEWS, S. A., KOMANDER, D., BYCROFT, M. & RANDOW, F. 2016. Recruitment of TBK1 to cytosol-invading Salmonella induces WIPI2-dependent antibacterial autophagy. *Embo j,* 35**,** 1779-92.

THURSTON, T. L., RYZHAKOV, G., BLOOR, S., VON MUHLINEN, N. & RANDOW, F. 2009. The TBK1 adaptor and autophagy receptor NDP52 restricts the proliferation of ubiquitin-coated bacteria. *Nat Immunol,* 10**,** 1215-21.

THURSTON, T. L., WANDEL, M. P., VON MUHLINEN, N., FOEGLEIN, A. & RANDOW, F. 2012. Galectin 8 targets damaged vesicles for autophagy to defend cells against bacterial invasion. *Nature,* 482**,** 414-8.

TILL, A., SAITO, R., MERKURJEV, D., LIU, J. J., SYED, G. H., KOLNIK, M., SIDDIQUI, A., GLAS, M., SCHEFFLER, B., IDEKER, T. & SUBRAMANI, S. 2015. Evolutionary trends and functional anatomy of the human expanded autophagy network. *Autophagy,* 11**,** 1652-67.

TOTH, M. L., SIGMOND, T., BORSOS, E., BARNA, J., ERDELYI, P., TAKACS-VELLAI, K., OROSZ, L., KOVACS, A. L., CSIKOS, G., SASS, M. & VELLAI, T. 2008. Longevity pathways converge on autophagy genes to regulate life span in Caenorhabditis elegans. *Autophagy,* 4**,** 330-8.

TRAVASSO, R. D., SAMPAIO DOS AIDOS, F., BAYANI, A., ABRANCHES, P. & SALVADOR, A. 2017. Localized redox relays as a privileged mode of cytoplasmic hydrogen peroxide signaling. *Redox Biol,* 12**,** 233-245.

TSUBOYAMA, K., KOYAMA-HONDA, I., SAKAMAKI, Y., KOIKE, M., MORISHITA, H. & MIZUSHIMA, N. 2016. The ATG conjugation systems are important for degradation of the inner autophagosomal membrane. *Science,* 354**,** 1036-1041.

TUMBARELLO, D. A., MANNA, P. T., ALLEN, M., BYCROFT, M., ARDEN, S. D., KENDRICK-JONES, J. & BUSS, F. 2015. The Autophagy Receptor TAX1BP1 and the Molecular Motor Myosin VI Are Required for Clearance of Salmonella Typhimurium by Autophagy. *PLoS Pathog,* 11**,** e1005174.

TUMBARELLO, D. A., WAXSE, B. J., ARDEN, S. D., BRIGHT, N. A., KENDRICK-JONES, J. & BUSS, F. 2012. Autophagy receptors link myosin VI to autophagosomes to mediate Tom1-dependent autophagosome maturation and fusion with the lysosome. *Nat Cell Biol,* 14**,** 1024-35.

TURNER-IVEY, B., MANEVICH, Y., SCHULTE, J., KISTNER-GRIFFIN, E., JEZIERSKA-DRUTEL, A., LIU, Y. & NEUMANN, C. A. 2013. Role for Prdx1 as a specific sensor in redox-regulated senescence in breast cancer. *Oncogene,* 32**,** 5302-14.

TYEDMERS, J., MOGK, A. & BUKAU, B. 2010. Cellular strategies for controlling protein aggregation. *Nat Rev Mol Cell Biol,* 11**,** 777-88.

ULGHERAIT, M., RANA, A., RERA, M., GRANIEL, J. & WALKER, D. W. 2014. AMPK modulates tissue and organismal aging in a non-cell-autonomous manner. *Cell Rep,* 8**,** 1767-80.

UTTARA, B., SINGH, A. V., ZAMBONI, P. & MAHAJAN, R. T. 2009. Oxidative stress and neurodegenerative diseases: a review of upstream and downstream antioxidant therapeutic options. *Curr Neuropharmacol,* 7**,** 65-74.

VAFAI, S. B. & MOOTHA, V. K. 2012. Mitochondrial disorders as windows into an ancient organelle. *Nature,* 491**,** 374-83.

VALENTE, E. M., SALVI, S., IALONGO, T., MARONGIU, R., ELIA, A. E., CAPUTO, V., ROMITO, L., ALBANESE, A., DALLAPICCOLA, B. & BENTIVOGLIO, A. R. 2004. PINK1 mutations are associated with sporadic early-onset parkinsonism. *Ann Neurol,* 56**,** 336-41.

VAN BLITTERSWIJK, M., VAN VUGHT, P. W., VAN ES, M. A., SCHELHAAS, H. J., VAN DER KOOI, A. J., DE VISSER, M., VELDINK, J. H. & VAN DEN BERG, L. H. 2012. Novel optineurin

mutations in sporadic amyotrophic lateral sclerosis patients. *Neurobiol Aging,* 33**,** 1016.e1-7.

VAN DER HEIJDEN, J. & FINLAY, B. B. 2015. In vitro Real-time Measurement of the Intra-bacterial Redox Potential. *Bio Protoc,* 5**,** 1-9.

VAN DER SPOEL, D., LINDAHL, E., HESS, B., GROENHOF, G., MARK, A. E. & BERENDSEN, H. J. 2005. GROMACS: fast, flexible, and free. *J Comput Chem,* 26**,** 1701-18.

VEAL, E. & DAY, A. 2011. Hydrogen peroxide as a signaling molecule. *Antioxid Redox Signal,* 15**,** 147-51.

VEHVILAINEN, P., KOISTINAHO, J. & GUNDARS, G. 2014. Mechanisms of mutant SOD1 induced mitochondrial toxicity in amyotrophic lateral sclerosis. *Front Cell Neurosci,* 8**,** 126.

VELIKKAKATH, A. K., NISHIMURA, T., OITA, E., ISHIHARA, N. & MIZUSHIMA, N. 2012. Mammalian Atg2 proteins are essential for autophagosome formation and important for regulation of size and distribution of lipid droplets. *Mol Biol Cell,* 23**,** 896-909.

VERLHAC, P., GREGOIRE, I. P., AZOCAR, O., PETKOVA, D. S., BAGUET, J., VIRET, C. & FAURE, M. 2015a. Autophagy receptor NDP52 regulates pathogen-containing autophagosome maturation. *Cell Host Microbe,* 17**,** 515-25.

VERLHAC, P., VIRET, C. & FAURE, M. 2015b. Dual function of CALCOCO2/NDP52 during xenophagy. *Autophagy,* 11**,** 965-6.

VIJAYVERGIYA, C., BEAL, M. F., BUCK, J. & MANFREDI, G. 2005. Mutant superoxide dismutase 1 forms aggregates in the brain mitochondrial matrix of amyotrophic lateral sclerosis mice. *J Neurosci,* 25**,** 2463-70.

VINCOW, E. S., MERRIHEW, G., THOMAS, R. E., SHULMAN, N. J., BEYER, R. P., MACCOSS, M. J. & PALLANCK, L. J. 2013. The PINK1-Parkin pathway promotes both mitophagy and selective respiratory chain turnover in vivo. *Proc Natl Acad Sci U S A,* 110**,** 6400-5.

VINOTHKUMAR, K. R., ZHU, J. & HIRST, J. 2014. Architecture of mammalian respiratory complex I. *Nature,* 515**,** 80-4.

VISCOMI, C., BOTTANI, E. & ZEVIANI, M. 2015. Emerging concepts in the therapy of mitochondrial disease. *Biochim Biophys Acta,* 1847**,** 544-57.

VON MUHLINEN, N., AKUTSU, M., RAVENHILL, B. J., FOEGLEIN, A., BLOOR, S., RUTHERFORD, T. J., FREUND, S. M., KOMANDER, D. & RANDOW, F. 2012. LC3C, bound selectively by a noncanonical LIR motif in NDP52, is required for antibacterial autophagy. *Mol Cell,* 48**,** 329-42.

VOOS, W. 2009. Mitochondrial protein homeostasis: the cooperative roles of chaperones and proteases. *Res Microbiol,* 160**,** 718-25.

VOOS, W., WARD, L. A. & TRUSCOTT, K. N. 2013. The role of AAA+ proteases in mitochondrial protein biogenesis, homeostasis and activity control. *Subcell Biochem,* 66**,** 223-63.

WAGNER, E., LUCHE, S., PENNA, L., CHEVALLET, M., VAN DORSSELAER, A., LEIZE-WAGNER, E. & RABILLOUD, T. 2002. A method for detection of overoxidation of cysteines: peroxiredoxins are oxidized in vivo at the active-site cysteine during oxidative stress. *Biochem J,* 366**,** 777-85.

WAGNER, S., CARPENTIER, I., ROGOV, V., KREIKE, M., IKEDA, F., LOHR, F., WU, C. J., ASHWELL, J. D., DOTSCH, V., DIKIC, I. & BEYAERT, R. 2008. Ubiquitin binding mediates the NF-kappaB inhibitory potential of ABIN proteins. *Oncogene,* 27**,** 3739-45.

WALINDA, E., MORIMOTO, D., SUGASE, K., KONUMA, T., TOCHIO, H. & SHIRAKAWA, M. 2014. Solution structure of the ubiquitin-associated (UBA) domain of human autophagy receptor NBR1 and its interaction with ubiquitin and polyubiquitin. *J Biol Chem,* 289**,** 13890-902.

WALKER, Z., MORENO, E., THOMAS, A., INGLIS, F., TABET, N., STEVENS, T., WHITFIELD, T., AARSLAND, D., RAINER, M. & PADOVANI, A. 2016. Evolution of clinical features in possible DLB depending on FP-CIT SPECT result. *Neurology,* 87**,** 1045-51.

WALTER, J. K., RUECKERT, C., VOSS, M., MUELLER, S. L., PIONTEK, J., GAST, K. & BLASIG, I. E. 2009. The oligomerization of the coiled coil-domain of occludin is redox sensitive. *Ann N Y Acad Sci,* 1165**,** 19-27.

WANG, M. D., LITTLE, J., GOMES, J., CASHMAN, N. R. & KREWSKI, D. 2016a. Identification of risk factors associated with onset and progression of amyotrophic lateral sclerosis using systematic review and meta-analysis. *Neurotoxicology*.

WANG, S., TSUN, Z. Y., WOLFSON, R. L., SHEN, K., WYANT, G. A., PLOVANICH, M. E., YUAN, E. D., JONES, T. D., CHANTRANUPONG, L., COMB, W., WANG, T., BAR-PELED, L., ZONCU, R., STRAUB, C., KIM, C., PARK, J., SABATINI, B. L. & SABATINI, D. M. 2015. Metabolism. Lysosomal amino acid transporter SLC38A9 signals arginine sufficiency to mTORC1. *Science,* 347**,** 188-94.

WANG, W., WANG, L., LU, J., SIEDLAK, S. L., FUJIOKA, H., LIANG, J., JIANG, S., MA, X., JIANG, Z., DA ROCHA, E. L., SHENG, M., CHOI, H., LEROU, P. H., LI, H. & WANG, X. 2016b. The inhibition of TDP-43 mitochondrial localization blocks its neuronal toxicity. *Nat Med,* 22**,** 869-78.

WANG, X., YAN, R., LI, J. & SONG, J. 2016c. SOHPRED: a new bioinformatics tool for the characterization and prediction of human S-sulfenylation sites. *Mol Biosyst,* 12**,** 2849-58.

WANG, X. J., HAYES, J. D., HENDERSON, C. J. & WOLF, C. R. 2007. Identification of retinoic acid as an inhibitor of transcription factor Nrf2 through activation of retinoic acid receptor alpha. *Proc Natl Acad Sci U S A,* 104**,** 19589-94.

WANG, Y., LI, L., HOU, C., LAI, Y., LONG, J., LIU, J., ZHONG, Q. & DIAO, J. 2016d. SNARE-mediated membrane fusion in autophagy. *Semin Cell Dev Biol,* 60**,** 97-104.

WATSON, M. R., LAGOW, R. D., XU, K., ZHANG, B. & BONINI, N. M. 2008. A drosophila model for amyotrophic lateral sclerosis reveals motor neuron damage by human SOD1. *J Biol Chem,* 283**,** 24972-81.

WATT, I. N., MONTGOMERY, M. G., RUNSWICK, M. J., LESLIE, A. G. & WALKER, J. E. 2010. Bioenergetic cost of making an adenosine triphosphate molecule in animal mitochondria. *Proc Natl Acad Sci U S A,* 107**,** 16823-7.

WATTS, G. D., THOMASOVA, D., RAMDEEN, S. K., FULCHIERO, E. C., MEHTA, S. G., DRACHMAN, D. A., WEIHL, C. C., JAMROZIK, Z., KWIECINSKI, H., KAMINSKA, A. & KIMONIS, V. E. 2007. Novel VCP mutations in inclusion body myopathy associated with Paget disease of bone and frontotemporal dementia. *Clin Genet,* 72**,** 420-6.

WAUER, T., SIMICEK, M., SCHUBERT, A. & KOMANDER, D. 2015. Mechanism of phospho-ubiquitin-induced PARKIN activation. *Nature,* 524**,** 370-4.

WEBB, B. & SALI, A. 2016. Comparative Protein Structure Modeling Using MODELLER. *Curr Protoc Protein Sci,* 86**,** 2 9 1-2 9 37.

WEI, Y., CHIANG, W. C., SUMPTER, R., JR., MISHRA, P. & LEVINE, B. 2017. Prohibitin 2 Is an Inner Mitochondrial Membrane Mitophagy Receptor. *Cell,* 168**,** 224-238.e10.

WEISHAUPT, J. H., HYMAN, T. & DIKIC, I. 2016. Common Molecular Pathways in Amyotrophic Lateral Sclerosis and Frontotemporal Dementia. *Trends Mol Med,* 22**,** 769-83.

WICKLIFFE, K. E., LORENZ, S., WEMMER, D. E., KURIYAN, J. & RAPE, M. 2011. The mechanism of linkage-specific ubiquitin chain elongation by a single-subunit E2. *Cell,* 144**,** 769-81.

WILD, P., FARHAN, H., MCEWAN, D. G., WAGNER, S., ROGOV, V. V., BRADY, N. R., RICHTER, B., KORAC, J., WAIDMANN, O., CHOUDHARY, C., DOTSCH, V., BUMANN, D. & DIKIC, I. 2011.

Phosphorylation of the autophagy receptor optineurin restricts Salmonella growth. *Science,* 333**,** 228-33.

WILLIAMS, A., JAHREISS, L., SARKAR, S., SAIKI, S., MENZIES, F. M., RAVIKUMAR, B. & RUBINSZTEIN, D. C. 2006. Aggregate-prone proteins are cleared from the cytosol by autophagy: therapeutic implications. *Curr Top Dev Biol,* 76**,** 89-101.

WINSLOW, A. R., CHEN, C. W., CORROCHANO, S., ACEVEDO-AROZENA, A., GORDON, D. E., PEDEN, A. A., LICHTENBERG, M., MENZIES, F. M., RAVIKUMAR, B., IMARISIO, S., BROWN, S., O'KANE, C. J. & RUBINSZTEIN, D. C. 2010. alpha-Synuclein impairs macroautophagy: implications for Parkinson's disease. *J Cell Biol,* 190**,** 1023-37.

WINTERBOURN, C. C. 2008. Reconciling the chemistry and biology of reactive oxygen species. *Nat Chem Biol,* 4**,** 278-86.

WIRTH, C., BRANDT, U., HUNTE, C. & ZICKERMANN, V. 2016. Structure and function of mitochondrial complex I. *Biochim Biophys Acta,* 1857**,** 902-14.

WONG, Y. C. & HOLZBAUR, E. L. 2014. Optineurin is an autophagy receptor for damaged mitochondria in parkin-mediated mitophagy that is disrupted by an ALS-linked mutation. *Proc Natl Acad Sci U S A,* 111**,** E4439-48.

WOO, H. A., YIM, S. H., SHIN, D. H., KANG, D., YU, D. Y. & RHEE, S. G. 2010. Inactivation of peroxiredoxin I by phosphorylation allows localized H(2)O(2) accumulation for cell signaling. *Cell,* 140**,** 517-28.

WOOD, Z. A., SCHRODER, E., ROBIN HARRIS, J. & POOLE, L. B. 2003. Structure, mechanism and regulation of peroxiredoxins. *Trends Biochem Sci,* 28**,** 32-40.

WOOLFSON, D. N., BARTLETT, G. J., BRUNING, M. & THOMSON, A. R. 2012. New currency for old rope: from coiled-coil assemblies to alpha-helical barrels. *Curr Opin Struct Biol,* 22**,** 432-41.

WOOTEN, M. W., GEETHA, T., BABU, J. R., SEIBENHENER, M. L., PENG, J., COX, N., DIAZ-MECO, M. T. & MOSCAT, J. 2008. Essential role of sequestosome 1/p62 in regulating accumulation of Lys63-ubiquitinated proteins. *J Biol Chem,* 283**,** 6783-9.

WROBEL, L., TOPF, U., BRAGOSZEWSKI, P., WIESE, S., SZTOLSZTENER, M. E., OELJEKLAUS, S., VARABYOVA, A., LIRSKI, M., CHROSCICKI, P., MROCZEK, S., JANUSZEWICZ, E., DZIEMBOWSKI, A., KOBLOWSKA, M., WARSCHEID, B. & CHACINSKA, A. 2015. Mistargeted mitochondrial proteins activate a proteostatic response in the cytosol. *Nature,* 524**,** 485-8.

WU, M., GU, J., GUO, R., HUANG, Y. & YANG, M. 2016a. Structure of Mammalian Respiratory Supercomplex I1III2IV1. *Cell,* 167**,** 1598-1609.e10.

WU, X., LI, L. & JIANG, H. 2016b. Doa1 targets ubiquitinated substrates for mitochondria-associated degradation. *J Cell Biol,* 213**,** 49-63.

WURZER, B., ZAFFAGNINI, G., FRACCHIOLLA, D., TURCO, E., ABERT, C., ROMANOV, J. & MARTENS, S. 2015. Oligomerization of p62 allows for selection of ubiquitinated cargo and isolation membrane during selective autophagy. *Elife,* 4.

WYSS-CORAY, T. 2016. Ageing, neurodegeneration and brain rejuvenation. *Nature,* 539**,** 180-186.

XIE, X., LI, F., WANG, Y., WANG, Y., LIN, Z., CHENG, X., LIU, J., CHEN, C. & PAN, L. 2015. Molecular basis of ubiquitin recognition by the autophagy receptor CALCOCO2. *Autophagy,* 11**,** 1775-89.

YANG, W. & HEKIMI, S. 2010. A mitochondrial superoxide signal triggers increased longevity in Caenorhabditis elegans. *PLoS Biol,* 8**,** e1000556.

YANG, Y., TANG, L., ZHANG, N., PAN, L., HADANO, S. & FAN, D. 2015. Six SQSTM1 mutations in a Chinese amyotrophic lateral sclerosis cohort. *Amyotroph Lateral Scler Frontotemporal Degener,* 16**,** 378-84.

YANG, Y., WANG, G., HUANG, X. & DU, Z. 2014. Expression, purification and crystallization of the SKICH domain of human TAX1BP1. *Acta Crystallogr F Struct Biol Commun,* 70**,** 619-23.

YEE, C., YANG, W. & HEKIMI, S. 2014. The intrinsic apoptosis pathway mediates the pro-longevity response to mitochondrial ROS in C. elegans. *Cell,* 157**,** 897-909.

YLA-ANTTILA, P., VIHINEN, H., JOKITALO, E. & ESKELINEN, E. L. 2009. 3D tomography reveals connections between the phagophore and endoplasmic reticulum. *Autophagy,* 5**,** 1180-5.

YONEDA, T., BENEDETTI, C., URANO, F., CLARK, S. G., HARDING, H. P. & RON, D. 2004. Compartment-specific perturbation of protein handling activates genes encoding mitochondrial chaperones. *J Cell Sci,* 117**,** 4055-66.

YOSHIDA, S., HONG, S., SUZUKI, T., NADA, S., MANNAN, A. M., WANG, J., OKADA, M., GUAN, K. L. & INOKI, K. 2011. Redox regulates mammalian target of rapamycin complex 1 (mTORC1) activity by modulating the TSC1/TSC2-Rheb GTPase pathway. *J Biol Chem,* 286**,** 32651-60.

YOSHII, S. R., KISHI, C., ISHIHARA, N. & MIZUSHIMA, N. 2011. Parkin mediates proteasome-dependent protein degradation and rupture of the outer mitochondrial membrane. *J Biol Chem,* 286**,** 19630-40.

YU, W. H., CUERVO, A. M., KUMAR, A., PETERHOFF, C. M., SCHMIDT, S. D., LEE, J. H., MOHAN, P. S., MERCKEN, M., FARMERY, M. R., TJERNBERG, L. O., JIANG, Y., DUFF, K., UCHIYAMA, Y., NASLUND, J., MATHEWS, P. M., CATALDO, A. M. & NIXON, R. A. 2005. Macroautophagy--a novel Beta-amyloid peptide-generating pathway activated in Alzheimer's disease. *J Cell Biol,* 171**,** 87-98.

ZATLOUKAL, K., STUMPTNER, C., FUCHSBICHLER, A., HEID, H., SCHNOELZER, M., KENNER, L., KLEINERT, R., PRINZ, M., AGUZZI, A. & DENK, H. 2002. p62 Is a common component of cytoplasmic inclusions in protein aggregation diseases. *Am J Pathol,* 160**,** 255-63.

ZHANG, D., WANG, W., SUN, X., XU, D., WANG, C., ZHANG, Q., WANG, H., LUO, W., CHEN, Y., CHEN, H. & LIU, Z. 2016. AMPK regulates autophagy by phosphorylating BECN1 at threonine 388. *Autophagy,* 12**,** 1447-59.

ZHANG, D. D., LO, S. C., CROSS, J. V., TEMPLETON, D. J. & HANNINK, M. 2004. Keap1 is a redox-regulated substrate adaptor protein for a Cul3-dependent ubiquitin ligase complex. *Mol Cell Biol,* 24**,** 10941-53.

ZHANG, Y., GAO, X., SAUCEDO, L. J., RU, B., EDGAR, B. A. & PAN, D. 2003. Rheb is a direct target of the tuberous sclerosis tumour suppressor proteins. *Nat Cell Biol,* 5**,** 578-81.

ZHAO, Q., WANG, J., LEVICHKIN, I. V., STASINOPOULOS, S., RYAN, M. T. & HOOGENRAAD, N. J. 2002. A mitochondrial specific stress response in mammalian cells. *Embo j,* 21**,** 4411-9.

ZHENG, X., BOYER, L., JIN, M., MERTENS, J., KIM, Y., MA, L., MA, L., HAMM, M., GAGE, F. H. & HUNTER, T. 2016. Metabolic reprogramming during neuronal differentiation from aerobic glycolysis to neuronal oxidative phosphorylation. *Elife,* 5.

ZHENG, Y. T., SHAHNAZARI, S., BRECH, A., LAMARK, T., JOHANSEN, T. & BRUMELL, J. H. 2009. The adaptor protein p62/SQSTM1 targets invading bacteria to the autophagy pathway. *J Immunol,* 183**,** 5909-16.

ZHONG, Y., WANG, Q. J., LI, X., YAN, Y., BACKER, J. M., CHAIT, B. T., HEINTZ, N. & YUE, Z. 2009. Distinct regulation of autophagic activity by Atg14L and Rubicon associated with Beclin 1-phosphatidylinositol-3-kinase complex. *Nat Cell Biol,* 11**,** 468-76.

ZHU, J., KING, M. S., YU, M., KLIPCAN, L., LESLIE, A. G. & HIRST, J. 2015. Structure of subcomplex Ibeta of mammalian respiratory complex I leads to new supernumerary subunit assignments. *Proc Natl Acad Sci U S A,* 112**,** 12087-92.